State of Oregon
Oregon Department of Geology and Mineral Industries
Ruarri J. Day-Stirrat, State Geologist

GEOLOGIC MAP 128

GEOLOGIC MAP OF THE MILL CREEK AREA, HOOD RIVER AND WASCO COUNTIES, OREGON

by Jason D. McClaughry[1,3], Clark A. Niewendorp[2], Carlie J.M. Azzopardi[3], Heather H. Herinckx[4], and Brian M. Webb[5]

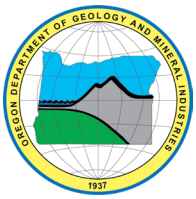

2024

[1] Oregon Department of Geology and Mineral Industries, Baker City Field Office, Baker County Courthouse, 1995 3rd Street, Suite 130, Baker City, OR 97814
[2] Retired, formerly at Oregon Department of Geology and Mineral Industries, 800 NE Oregon Street, Ste. 965 Portland, OR 97232
[3] Oregon Department of Geology and Mineral Industries, 800 NE Oregon Street, Suite 965 Portland, OR 97232
[4] Shannon & Wilson Inc., 3400 Sutton Park Drive S, Suite 1401, Jacksonville, FL 32224, formerly at Oregon Department of Geology and Mineral Industries, 800 NE Oregon Street, Ste. 965 Portland, OR 97232
[5] AECOM, 888 SW 5th Ave Ste 600, Portland, OR 97204, formerly at Oregon Department of Geology and Mineral Industries, 800 NE Oregon Street, Ste. 965 Portland, OR 97232

NOTICE

WHAT'S IN THIS REPORT?

This publication provides an updated and spatially accurate geologic framework as of 2024 for the Brown Creek, Ketchum Reservoir, Fivemile Butte 7.5' quadrangles as well as the northern part of the Flag Point 7.5' quadrangle. This framework is part of a multiyear study of the geology of the larger Middle Columbia Basin. Geologic data in the publication provide significant new details about the volcanic and structural geologic history of the area and the geologic conditions controlling the distribution of water resources, aggregate and other mineral resources, and geologic hazards.

Cover photograph: View southwest toward Mount Hood from upper Chenoweth Creek (45.62265, -121.28671 WGS84 geographic coordinates). Photo credit: Clark Niewendorp, 2016.

Expires: 12/1/2025

Oregon Department of Geology and Mineral Industries Geologic Map Series GMS-128
Published in conformance with ORS 516.030.

For additional information:
Administrative Offices
800 NE Oregon Street, Suite 965
Portland, OR 97232
Telephone (971) 673-1555
Fax (971) 673-1562
https://www.oregon.gov/dogami

TABLE OF CONTENTS

LIST OF FIGURES

LIST OF TABLES

GEODATABASES

BC2024.gdb
KR2024.gdb
FBFP2024.gdb

*See the **Appendix** for geodatabase description. See the digital publication folder for files. Geodatabases are Esri® version 10.7 format. Metadata is embedded in the geodatabases and shapefiles and is also provided as separate .xml format files.*

SHAPEFILES AND SPREADSHEETS

BC2024-open folder: Shapefiles

Cross Section Lines: GM_CartographicLines.shp
Contacts and Faults: GM_ContactsAndFaults
Reference map: GM_DataSourcePolys.shp
Geochemistry: GM_GeochemPoints.shp
Geochronology: GM_GeochronPoints.shp
Geologic Lines: GM_GeologicLines
Magnetics: GM_MagneticPoints.shp
Map Unit Labels: GM_MapUnitPolyLabelPoints
Map Units: GM_MapUnitPolys
Orientation Points: GM_OrientationPoints.shp
Wells: GM_WellPoints.shp

Spreadsheets (Microsoft® Excel®)

DataSources
DescriptionOfMapUnits
GeoMaterialDict
Glossary

KR2024-open folder: Shapefiles

Cross Section Lines: GM_CartographicLines.shp
Contacts and Faults: GM_ContactsAndFaults
Reference map: GM_DataSourcePolys.shp
Geochemistry: GM_GeochemPoints.shp
Geologic Lines: GM_GeologicLines
Magnetics: GM_MagneticPoints.shp
Map Unit Labels: GM_MapUnitPolyLabelPoints
Map Units: GM_MapUnitPolys
Orientation Points: GM_OrientationPoints.shp
Wells: GM_WellPoints.shp

Spreadsheets (Microsoft® Excel®)

DataSources
DescriptionOfMapUnits
GeoMaterialDict
Glossary

FBFP2024-open folder: Shapefiles

Cross Section Lines: GM_CartographicLines.shp
Contacts and Faults: GM_ContactsAndFaults
Reference map: GM_DataSourcePolys.shp
Geochemistry: GM_GeochemPoints.shp
Geochronology: GM_GeochronPoints.shp
Geologic Lines: GM_GeologicLines
Magnetics: GM_MagneticPoints.shp
Map Unit Labels: GM_MapUnitPolyLabelPoints
Map Units: GM_MapUnitPolys
Orientation Points: GM_OrientationPoints.shp
Wells: GM_WellPoints.shp

Spreadsheets (Microsoft® Excel®)

DataSources
DescriptionOfMapUnits
GeoMaterialDict
Glossary

MAP PLATES

Plate 1. Geologic map of the Brown Creek 7.5’ quadrangle, Wasco County, Oregon

Plate 2. Geologic map of the Ketchum Reservoir 7.5’ quadrangle, Hood River and Wasco counties, Oregon

Plate 3. Geologic map of the Fivemile Butte 7.5’ and northern part of the Flag Point 7.5’ quadrangles, Hood River and Wasco counties, Oregon

1.0 INTRODUCTION

The Fivemile Butte, Ketchum Reservoir, and Brown Creek 7.5′ quadrangles along with the northern part of the Flag Point 7.5′ quadrangle in Hood River and Wasco counties, Oregon (herein referred to as the Mill Creek area) encompass an area of 435 km^2 (168 mi^2) in the Middle Columbia Basin. The Mill Creek area is located along the eastern slopes of the northern Oregon Cascade Range, ~25 km (15 mi) ENE of Mount Hood volcano (**Figure 1-1**; Plates 1, 2, and 3). The oldest rocks cropping out in the map area are part of the Columbia River Basalt Group (CRBG), the youngest flood basalt province in the world (Reidel and others, 2013a). Upper Miocene and lower Pleistocene volcanic rocks unconformably overlie the CRBG in the map area, recording part of the volcano-tectonic development of the northern Oregon Cascade Range over the past 9 million years (McClaughry and others, 2020a, 2021).

Beginning in 2011, the Oregon Department of Geology and Mineral Industries (DOGAMI) has sought to provide an updated and spatially accurate geologic framework for the Mill Creek area as part of a multiyear study of the geology of the larger Middle Columbia Basin (**Figure 1-1**, **Figure 1-2**). Additional key objectives of this study are to: 1) determine the geologic history of volcanic rocks in this part of northern Oregon's Cascade Range; 2) provide significant new details about the structure and fault history of the Yakima Fold Belt and eastern slopes of northern Oregon's Cascade Range; 3) characterize the stratigraphic framework and geologic conditions controlling the distribution of water resources; 4) determine the distribution of potential aggregate sources and other mineral resources; and 5) describe the nature of geologic hazard. New detailed geologic data presented here also provides a basis for future geologic, geohydrologic, and geohazard studies in the Middle Columbia Basin (**Figure 1-1**).The core products of this study are this report, accompanying geologic maps and cross sections (Plates 1, 2, and 3), Esri ArcGIS™ geodatabases, and Microsoft Excel® spreadsheets tabulating point data. The geodatabases present new geologic mapping in a digital format consistent with the Level 3 standard USGS National Cooperative Geologic Mapping Program Geologic Map Schema (GeMS Level 3)(U.S. Geological Survey National Cooperative Geologic Mapping Program, 2020). They contain spatial information, including geologic polygons, contacts, structures, geochemistry, geochronology, magnetic observation, orientation points, field stations, and well data. The geodatabases also contain data about each geologic unit such as age, lithology, mineralogy, and structure. Geodata Digitization at scales of 1:8,000 or better was accomplished using a combination of high-resolution lidar topography and imagery. Surficial and bedrock geologic units in the geodatabase are depicted on Plates 1, 2, and 3 at a scale of 1:24,000. Both the geodatabases and geologic maps are supported by this report describing the geology in detail.

Detailed geologic mapping in this part of the Middle Columbia Basin is a high priority of the Oregon Geologic Map Advisory Committee, supported in part by grants from the STATEMAP component of the U.S. Geological Survey (USGS) National Cooperative Geologic Mapping Program under cooperative agreement numbers G15AC00180, G16AC00179, and G21AC00647. Additional funds were provided by the state of Oregon through DOGAMI.

Figure 1-1. Location of the Mill Creek map area, shown by a black outline, in the Middle Columbia Basin of north-central Oregon. The solid orange line corresponds to the watershed boundary of the Middle Columbia Basin. The Columbia River, flowing from east to west, in the upper part of the figure, separates Oregon on the south from Washington on the north. The Deschutes River marks the boundary between Wasco County on the west and Sherman County on the east.

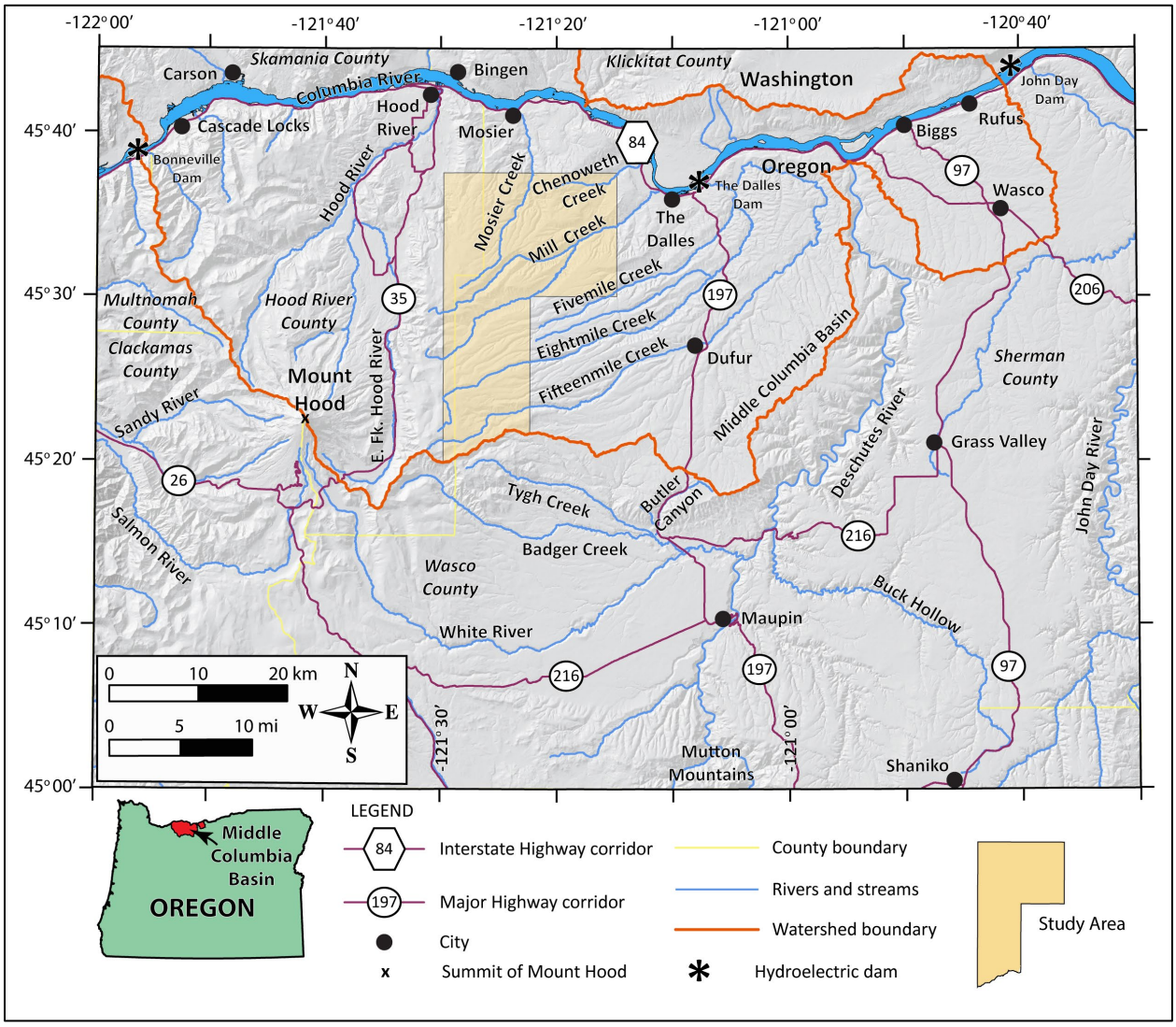

Figure 1-2. Status map of geologic mapping completed, in progress, and planned in the Middle Columbia Basin. The yellow-shaded area encompasses geologic mapping in the Mill Creek area completed for this report. Orange-shaded quadrangles include areas that have been mapped and published by DOGAMI with funding from OWRD and STATEMAP between 2011 and 2021. Blue-shaded quadrangles include areas of USGS (FEDMAP) geologic mapping. Purple-shaded quadrangles include targets of future geologic mapping by DOGAMI. Label abbreviations are as follows: B—Bingen; BC—Butler Canyon; BD—Bonneville Dam; C—Carson; CL—Cascade Locks; D—Dufur; GV—Grass Valley; HR—Hood River; JDD—John Day Dam; R—Rufus; TD—The Dalles; TDD—The Dalles Dam; W—Wasco. Dashed line running diagonally through the Ketchum Reservoir 7.5' quadrangle is the southeast boundary of the geologic map of the Hood River area by McClaughry and others (2012).

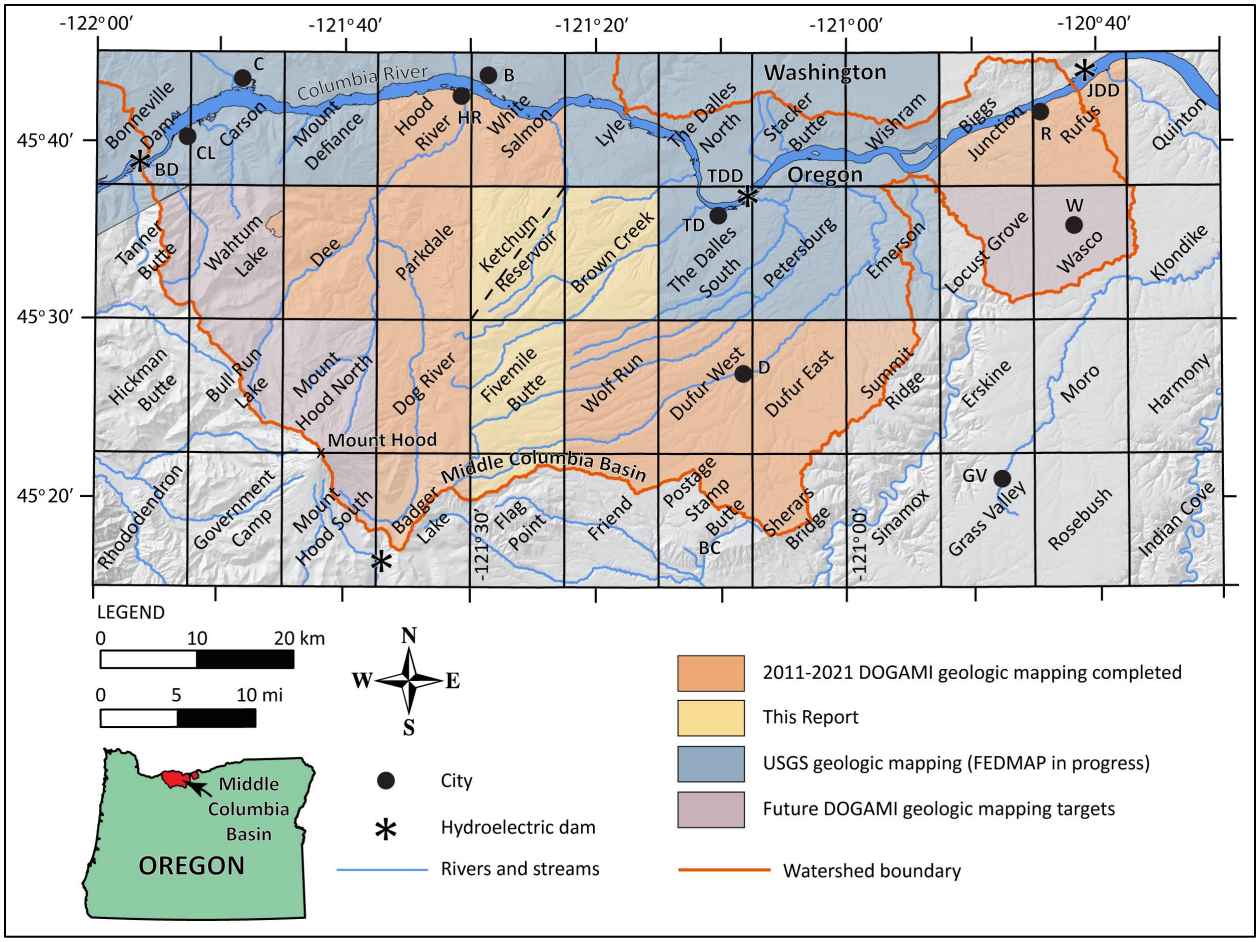

2.0 GEOGRAPHY

The Middle Columbia Basin extends from around the city of Wasco and John Day Dam on the east, to near Mount Hood and Bonneville Dam on the west and to near Butler Canyon on the south. The northern part of the basin is bound by the Columbia River Gorge. Major tributaries to the Columbia River include the Hood River, Mosier Creek, Mill Creek, Fivemile Creek, Eightmile Creek, Fifteenmile Creek, and Deschutes River (**Figure 1-1**, **Figure 1-2**).

This part of north-central Oregon is typically rugged, transitioning from the steep mountainous terrain of the Cascade Range on the west to more subdued broad plateaus and ridges incised by deep canyons on the east. Topographic relief in the Middle Columbia Basin is substantial, ranging from 3,428 m (11,246 ft) at the summit of Mount Hood along the crest of the Cascade Range to 23 m (75 ft) at the Columbia River at Bonneville Dam (**Figure 1-1**). In the map area, elevations range from 1,775 m (5,823 ft) south of Oval Lake to 195 m (640 ft) along Mosier Creek and 122 m (400 ft) along Chenoweth Creek as the drainages exit the northern part of the Mill Creek area.

Climate varies across the Middle Columbia Basin due to its transitional location between the wet marine airflow-dominated Cascade Range and the semiarid continental climate of eastern Oregon. The upland and western parts of the basin have a relatively wet climate, averaging ~77 cm (30 in) of precipitation annually (NOAA, 2020). The rain shadow of the Cascade Range reduces annual precipitation eastward sharply to <40 cm (~16 in) across the semiarid eastern part of the Middle Columbia Basin (NOAA, 2020; **Figure 1-1**).

Most of the map area is public land of the Mount Hood National Forest, managed by the U.S. Forest Service (USFS). The northern part of the Ketchum Reservoir and eastern parts of the Fivemile Butte and Brown Creek 7.5′ quadrangles are privately held rangeland and agricultural land. The Mill Creek area is accessed by number of local paved and graveled roads.

3.0 METHODOLOGY

The suite of CRBG and Cascade Range volcanic rocks mapped in the Mill Creek area is stratigraphically complex, reflecting the variable processes of deposition and reworking of volcanic and volcaniclastic units adjacent to a structurally active volcanic arc environment. Thus, reliable map correlations, even of similar-appearing stratigraphic sequences, benefit greatly from the use of detailed digital lidar-based geologic mapping, combined with numerous direct field observations.

Conventional lithologic criteria, in combination with geochemical analyses, corroborating isotopic ages, and measurements of natural remanent magnetization were used to assign rocks and deposits to geologic map units. Comparative visual analysis of unanalyzed rocks with analyzed rocks, in the context of stratigraphic position, allowed for wider correlation of map units.

Mapping presented in this report was collected digitally using a GPS-enabled Apple® iPad® 4, loaded with Esri™ Collector, following standard DOGAMI procedures outlined in Duda and others (2018, 2019). Detailed field mapping used 1-m lidar digital elevation models (DEMs; 8 pts/m^2), USGS digital raster graphics (DRGs) of traditional topographic maps, and digital Esri™ imagery as basemaps. Fieldwork conducted during this study consisted of data collection along main roads and secondary forest roads, combined with numerous traverses across private and public lands to map lithologic contacts and faults.

Geologic linework portrayed on this report's geologic maps upon our detailed observations at more than 950 field stations we visited between 2011 and 2018. We obtained supplementary lithologic information from comparison of more than 350 rock samples collected from field sites. Our lithologic map

correlations also rely on 249 new and 24 compiled X-ray fluorescence (XRF) whole-rock geochemical analyses, six compiled K-Ar isotopic ages, petrographic analysis of 59 thin sections, 93 field measurements of natural remanent magnetization, and 1,195 field and remotely collected orientation measurements (Plates 1, 2, and 3; **Appendix**).

In this report, volcanic rocks with fine-grained (<1 mm [0.04 in]) average crystal or particle size in the groundmass are characterized in the following manner (Mackenzie and others, 1997; Le Maitre and others, 2002):

- As coarse groundmass if the average crystal or particle size is <1 mm (0.04 in) and can be determined using the naked eye (>~0.5 mm [0.02 in]).
- As medium groundmass if crystals of average size cannot be determined by eye but can be distinguished by using a hand lens (>~0.05 mm [0.002 in]).
- As fine groundmass if crystals or grains of average size can be determined only by using a microscope, or by recognition when viewing through a hand lens of a sparkle or sheen in reflected light (indicating the presence of crystalline groundmass).
- As glassy groundmass if the groundmass has (fresh) or originally had (altered) the characteristics of glass (e.g., conchoidal fracture; sharp, transparent edges; vitreous luster).
- As intersertal if the groundmass has mixtures of crystalline and glassy characteristics; ratios of glass to crystalline materials may be indicated by textural terms including holocrystalline, hypocrystalline, hyalophitic, hyalopilitic, and holohyaline.
- As containing microphenocrysts if crystals observed are larger than the overall groundmass and <1 mm across (0.04).

The grain size of clastic sedimentary rocks is described above following the Wentworth (1922) scale. We compared hand samples of unconsolidated sediments and clastic sedimentary rocks in the field and/or in the laboratory to graphical representations (comparators) of the Wentworth scale to determine average representative grain size in various parts of a respective sedimentary geologic unit.

Whole-rock XRF geochemical data are essential for separating difficult-to-distinguish lava flows and pyroclastic rocks into eruptive units in the volcanic-dominated terrain of the Mill Creek area. Many lava flows were too fine-grained and glassy to be adequately characterized by mineralogical criteria alone. What's more, texturally and mineralogically similar-appearing units may have meaningfully different chemical signatures. In this report, we based descriptive rock unit names for volcanic rocks in part on the online British Geological Survey classification schemes (Gillespie and Styles, 1999; Robertson, 1999; Hallsworth and Knox, 1999), as well as on normalized major element analyses plotted on the total alkali ($Na_2O + K_2O$) versus silica (SiO_2) diagram (TAS) of Le Bas and others (1986), Le Bas and Streckeisen (1991), and Le Maitre and others (1989, 2002).

Whole-rock geochemical samples from the Mill Creek area were prepared and analyzed by XRF at the Washington State University GeoAnalytical Lab, Pullman, Washington, and at the Department of Geosciences, Franklin and Marshall College, Lancaster, Pennsylvania (see **Appendix**). Analytical procedures for the Washington State University GeoAnalytical Lab are described by Johnson and others (1999) and are available online at https://environment.wsu.edu/facilities/geoanalytical-lab/technical-notes/. Analytical procedures for the Franklin and Marshall X-ray laboratory are described by Boyd and Mertzman (1987) and Mertzman (2000), and are available online at http://www.fandm.edu/earth-environment/laboratory-facilities/xrf-and-xrd-lab. Major element determinations are normalized to a 100-percent total on a volatile-free basis and recalculated with total iron expressed as FeO*. Further details of this process are described in the **Appendix** under the heading *Geochemical Analytical Methods*.

Individual CRBG lava flows can be difficult to identify with certainty in the field, but can be distinguished on the basis of a multicriteria mapping approach using stratigraphic position and thickness, geochemistry, magnetic polarity, paleomagnetic analysis of oriented core samples, and petrography following the work of Swanson and others (1979a,b), Reidel and others (1989), Beeson and others (1985, 1989), Wells and others (1989, 2009), and Hooper (2000)(**Figure 5-7**, **Figure 5-10**). The primary uncertainties in accurately mapping these lava flows arise from: 1) poor exposure and recognition of flow contacts; 2) intraflow chemical variation; and 3) the effect of weathering on chemical composition (Wells and others, 2009; Sawlan, 2017). Where Grande Ronde and Wanapum Basalt lava flows are correlated chemically, we follow the work of Wells and others (2009) and use FeOTotal <11 weight percent as an indicator of weathered samples (**Appendix**). In areas of isolated outcrops, or where additional analytical techniques could not be applied, we used a textural approach to mapping these units by comparing outcrop samples to hand sample standards obtained from detailed and stratigraphically continuous reference sections in at Hood River and Butler Canyon.

Six K-Ar ages shown on this report's geologic maps in the Mill Creek area come from publications by Bela (1982), Bunker and others (1982), Fiebelkorn and others (1983), Anderson (1987), Sherrod and Scott (1995), Conrey and others (1996), and Gray and others (1996)(Plates 1 and 3; **Appendix**). Numerical ages assigned to dated units are described in this report using standard conventions for providing ages, e.g. in in terms of mega-annum (abbreviated Ma) for units > 1 million years old; for units < 1 million years old, ages are reported in thousands of years ago (kilo-annum, abbreviated ka). Further details of age dates are described in the **Appendix** under the heading *Geochronology Analytical Methods*.

The magnetic polarity of strongly magnetized lava flows was determined at numerous outcrops in the Mill Creek area using a handheld digital fluxgate magnetometer (see **Appendix**). Magnetic polarity reversals, commonly preserved by volcanic rocks and readily measured in the field, provide for: 1) distinguishing between flow units with normal and reversed magnetic polarity; 2) a check on the permissible age of isotopically dated samples, when compared to the paleomagnetic time scale (Cande and Kent, 1992); and 3) another means to constrain possible depositional ages for some undated strata. Further details of this process are described in the **Appendix** under the heading *Natural Remanent Magnetization Methods*.

Orientation measurements of geological planes (e.g., inclined bedding) were obtained in the field area by traditional compass and clinometer methods, and compiled from previous publications. Additional bedding measurements were generated using a routine and model developed by DOGAMI in Esri ArcGIS™ Model Builder to calculate three-point solutions from lidar bare-earth DEMs (Duda and others, 2018, 2019). Further details of this process are described in the **Appendix** under the heading *Orientation Points Methods*.

Subsurface geology that we show in geologic cross sections incorporates lithologic interpretations from water-well drill records available through the Oregon Water Resources Department (OWRD) GRID system (Plate 1; **Appendix**). We made an attempt to locate water wells and other drill holes that have well logs archived by OWRD. We estimated approximate locations using a combination of sources, including internal OWRD databases of located wells, Google Earth™, tax lot maps, street addresses, and aerial photographs. The accuracy of the locations ranges widely, from errors up to 0.8 km (0.5 mi) for wells located only by Township/Range/Section (2.6 km^2 [1 mi^2]) and plotted at the section centroid, to a few tens of meters for wells located by address or tax lot number on a city lot with bearing and distance from a corner. For each well, the number of the well log is indicated in the database. This number can be combined with the first four letters of the county name (e.g., WASC 50922), to retrieve an image of the well log from the OWRD website (http://apps.wrd.state.or.us/apps/gw/well_log/). Water wells in the

map area are sparse; the geodatabases include 145 located water-well logs with interpreted subsurface geologic units. Further details of our water well compilation process are described in the **Appendix** under the heading *Water Wells Methods*.

Microsoft Excel® spreadsheets tabulating geochemical and geochronological analyses, magnetic polarity, orientation measurements, and well points are provided as part of this publication. The **Appendix** contains a more detailed summary of data collection methods and a list of the data fields for the spreadsheets mentioned above.

Our new mapping was compiled with published and unpublished data and converted into digital format using Esri ArcGIS™ ArcMAP™ GIS software. On-screen digitizing was performed through heads-up digitizing using georeferenced 1-m lidar DEMs, 1:24,000-scale USGS digital raster images (DRGs) of traditional topographic maps, hillshade derivative of USGS 10-m DEMs, and National Agriculture Imagery Program digital orthophotos from 2014 and 2018.

We improved the locations of both contacts and faults through the use of enhanced 1-m lidar DEMs, processed using the Sky-View Factor computation tool (Zakšek and others, 2011). The Sky-View Factor computation tool is part of the Relief Visualization Toolbox (RVT), open-source processing software produced by the Institute of Anthropological and Spatial Studies at the Research Center of the Slovenian Academy of Sciences and Arts (ZRCSAZU), to help visualize raster elevation model datasets (https://iaps.zrc-sazu.si/en). Sky-View visualizes hillshade models using diffuse illumination, overcoming the common problem of direct illumination, which can obscure linear objects that lie parallel to the direction of the light source and saturation of shadow areas.

Surficial units in the Mill Creek area were delineated on the basis of geomorphology as interpreted from a combination of field observations, 1-m lidar DEMs, National Agriculture Imagery Program orthophotos from 2014 and 2018, USGS 7.5' topographic maps, and Natural Resources Conservation Service soils maps (Green, 1982). We completed digitization and the final digital Esri ArcGIS™ format geodatabase at a minimum scale of 1:8,000, supported by 3D visualization of lidar topographic data in Quick Terrain Modeler™ (Duda and others, 2018, 2019). The geologic time scale used is the 2023 (v2023/06), version of the International Stratigraphic Commission on chronostratigraphic chart (https://stratigraphy.org/chart) revised from Gradstein and others (2004), Ogg and others (2008), and Cohen and others (2013). Colors given for hand sample descriptions are from the Geological Society of America Rock-Color Chart Committee (1991).

We provide geographic map coordinates (decimal degree, datum = WGS84) for outcrop photographs shown for report figures, allowing the interested reader to visit these sites in the field or to remotely visualize the area using online mapping applications.

4.0 PREVIOUS WORK

We mapped the Mill Creek area as part of a larger effort to construct an updated geologic framework for the Middle Columbia Basin (**Figure 1-1**, **Figure 1-2**). The index map shown in **Figure 4-1** graphically summarizes the sources of mapping reviewed for our geologic depiction, as well as other sources consulted during the preparation of this report. **Table 4-1** shows a list of previous regional geologic investigations reviewed during the current geologic study. Reports listed in **Table 4-1** are organized in chronological order; those shown in bold are geologic maps that lie across the Mill Creek area.

Earlier geologic maps and reports displaying the bedrock geology in the Mill Creek area include those by Piper (1932), Waters (1968), Swanson and others (1981), Bela (1982), Sherrod and Scott (1995), and Sherrod and Smith (2000). We locally used county soil surveys produced for Hood River and Wasco

counties by the Soil Conservation Service and the Natural Resources Conservation Service to interpret the distribution of surficial units (Green, 1981, 1982; https://www.nrcs.usda.gov/conservation-basics/natural-resource-concerns/soil/soil-surveys-by-state).

Figure 4-1. Sources of regional geologic mapping reviewed and consulted during the preparation of the Mill Creek area geologic maps and this report. See DataSourcePolys feature class in the geodatabases. The Mill Creek area is shown by a white outline.

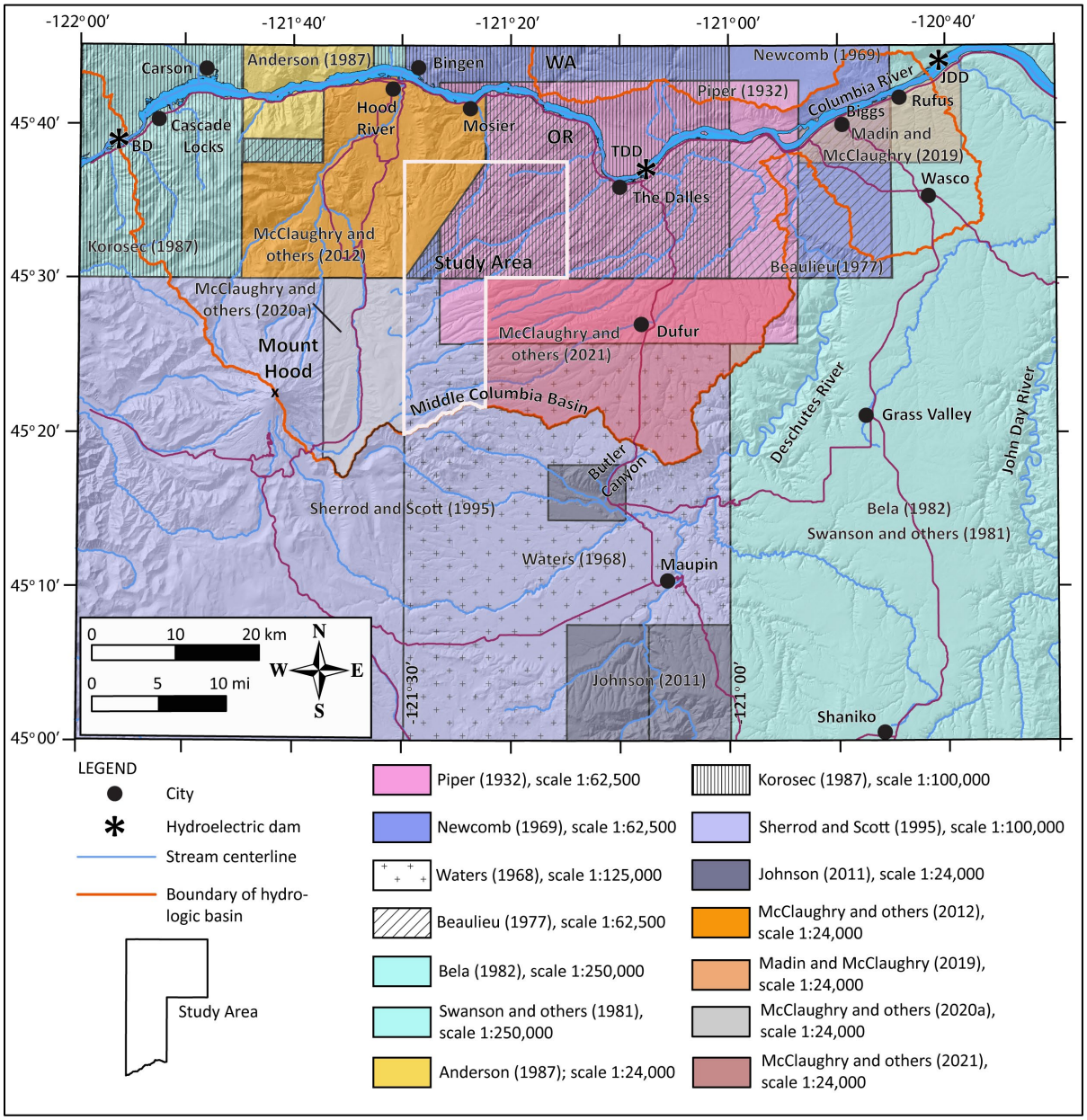

Table 4-1. Partial chronological listing of maps and reports on which this study builds. Maps shown in boldface are totally or partially within the Mill Creek area.

Author	Year	Subject	Scale
Piper	**1932**	**Geology and groundwater resources of The Dalles region**	**1:62,500**
Waters	**1968**	**Geologic map of the Dufur Quadrangle**	**1:62,500**
Newcomb	1969	Tectonic structure/groundwater Mosier area	1:62,500
Shannon and Wilson	1973	Boardman Nuclear Project	1:250,000
Beaulieu	1977	Geologic Hazards of Parts of Northern Wasco County	1:62,500
Swanson and others	**1981**	**Regional geologic map of the Columbia River Basalt Group**	**1:250,000**
Beeson and others	1982	Geologic map and geothermal potential Hood River area	
Bela	**1982**	**Geologic map Dalles 1- × 2-degree quadrangle**	**1:250,000**
Green	**1981**	**Soil Survey Hood River County**	**GIS**
Green	**1982**	**Soil Survey Wasco County**	**GIS**
Beeson and others	1985	Frenchman Springs Member Columbia River Basalt	
Korosec	1987	Geologic map Hood River 30 X 60-minute quadrangle	1:100,000
Anderson	1987	Geologic map Columbia River Gorge area	1:24,000
Lite and Grondin	1988	Groundwater/geology Mosier area	1:24,000
Sherrod and Scott	**1995**	**Geologic map Mount Hood 30 x 60-minute quadrangle**	**1:100,000**
Conrey and others	1996	Isotopic ages Hood River/Mount Hood area	
Gray and others	1996	Isotopic ages Hood River/Mount Hood area	
Conrey and others	1997	Petrology Cascade arc	
Sherrod and Smith	**2000**	**Geologic map of the Cascade Range in Oregon**	**1:500,000**
Tolan and others	2002	Evolution of the Columbia River	
Wells and others	1989	Columbia River Basalt, Columbia River Gorge	
Wells and others	2009	Columbia River Basalt, Columbia River Gorge	
Johnson	2011	Geologic map of Tygh Ridge and Dant areas	1:24,000
McClaughry and others	**2012**	**Geologic map of the Hood River Valley**	**1:36,000**
Burns and others	2012	Evaluation of basalt aquifers near Mosier	GIS
Martin and others	2013	Revisions to the stratigraphy of the Frenchman Springs Member	
Reidel and Tolan	2013	The Grande Ronde Basalt, Columbia River Basalt Group	
Lite	2013	Hydrogeology of the Mosier area	
McClaughry and others	2020a	Geologic map of the Dog River/Badger Lake 7.5’ quadrangles	1:24,000
McClaughry and others	2021	Geologic map of the Dufur area	1:24,000

5.0 GEOLOGIC AND TECTONIC SETTING

The Mill Creek area lies along the eastern side of the Cascade Range in northern Oregon, ~25 km (16 mi) ENE of Mount Hood volcano (**Figure 1-1**; Plates 1, 2, and 3). The Cascade Range is a north-south-trending volcanic arc stretching for ~1,300 km (800 mi) between northern California and southern British Columbia (**Figure 5-1**). Volcanoes making up the range and their eroded remnants are the observable magmatic expression of oblique convergence since ~40 Ma along the Cascadia subduction zone, where the offshore Juan de Fuca tectonic plate is subducted beneath North America (**Figure 5-1**; Lux, 1982; Phillips and others, 1986; Verplanck and Duncan, 1987; Conrey and others, 2002; Sherrod, 2019). The Cascade Range in Oregon is traditionally separated into two subprovinces on the basis of this ~40-million-year geologic history: the Western Cascades and High Cascades (**Figure 5-2**; Dicken, 1965). The Western Cascades subprovince is a deeply eroded terrane of Eocene to Pliocene volcanic and sedimentary rocks, while the High Cascades encompasses the late Miocene to Holocene active volcanic arc, including major young volcanoes (e.g., Mount Hood).

Figure 5-1. Tectonic setting of the northwestern United States and southwestern Canada showing regional plate boundaries, the Cascadia Subduction Zone, volcanoes of the Cascade Range, and the location of the Mill Creek area in north-central Oregon. The deformation front (red line) is defined by bathymetry where the abyssal plain meets the continental slope and is inferred to represent the surface projection of the Cascadia megathrust.). Label abbreviations are as follows: MBA—Mount Baker; GP—Glacier Peak; MR—Mount Rainier; MSH—Mount Saint Helens; MH—Mount Hood; MJ—Mount Jefferson; TS—Three Sisters; MB—Mount Bachelor; NV—Newberry Volcano; MCB—Middle Columbia Basin.

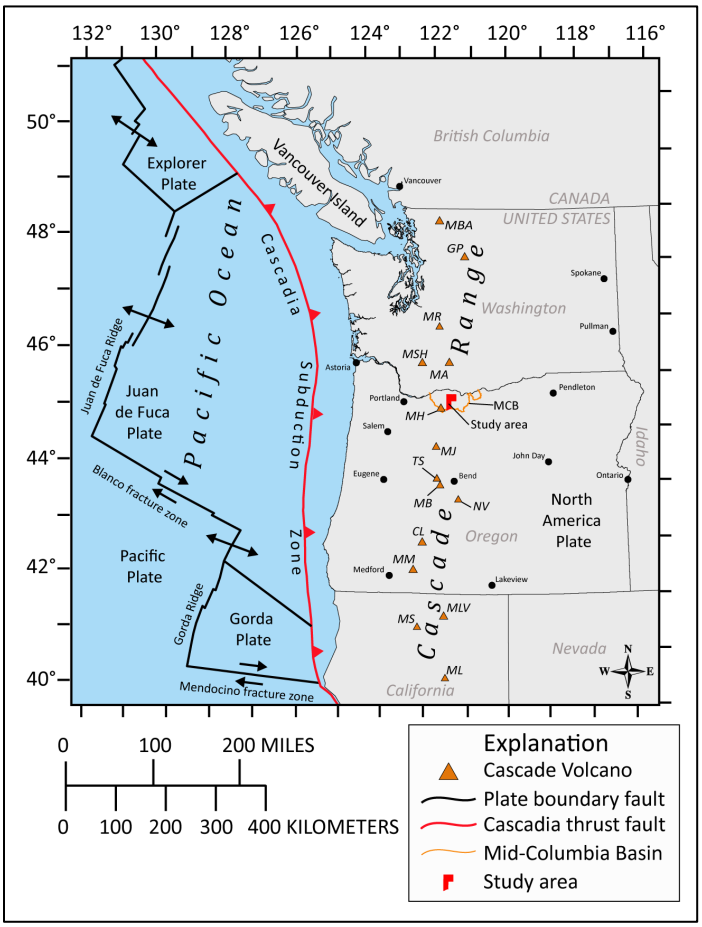

Figure 5-2. Map of the Cascade Range in the Pacific Northwest showing geographic locations, approximate extent of the Western Cascades (tan) and High Cascades (purple) in Oregon and the relationships of some major structural features of Oregon. The Mill Creek area is shown by a red polygon in north-central Oregon. Numerals 1,2, and 3 refer to the three segments of the High Cascades graben from south to north: 1) southern segment, 2) central segment, and 3) Hood River graben. Labels: BG – Baker graben; BV – Boring Volcanic Field; HRF – Hood River fault zone; HCF – Horse Creek fault zone; HFS – Hite fault System; GCF – Gales Creek fault; GRF – Green Ridge fault zone; PB – Portland Basin; PHF – Portland Hills fault; MCB – Middle Columbia Basin (orange outline); MHFZ – Mount Hood fault zone; LG – La Grande graben; OIG – Oregon-Idaho graben; SV – Simcoe Mountains; TB – Tualatin Basin; WFZ – Wallula fault zone. Labeled physiographic provinces are outlined by gray lines. Oregon physiographic provinces after Dicken (1965). Washington physiographic provinces are from Washington Department of Natural Resources (https://www.dnr.wa.gov/programs-and-services/geology/explore-popular-geology/geologic-provinces-washington). Figure modified from McClaughry and others (2020a).

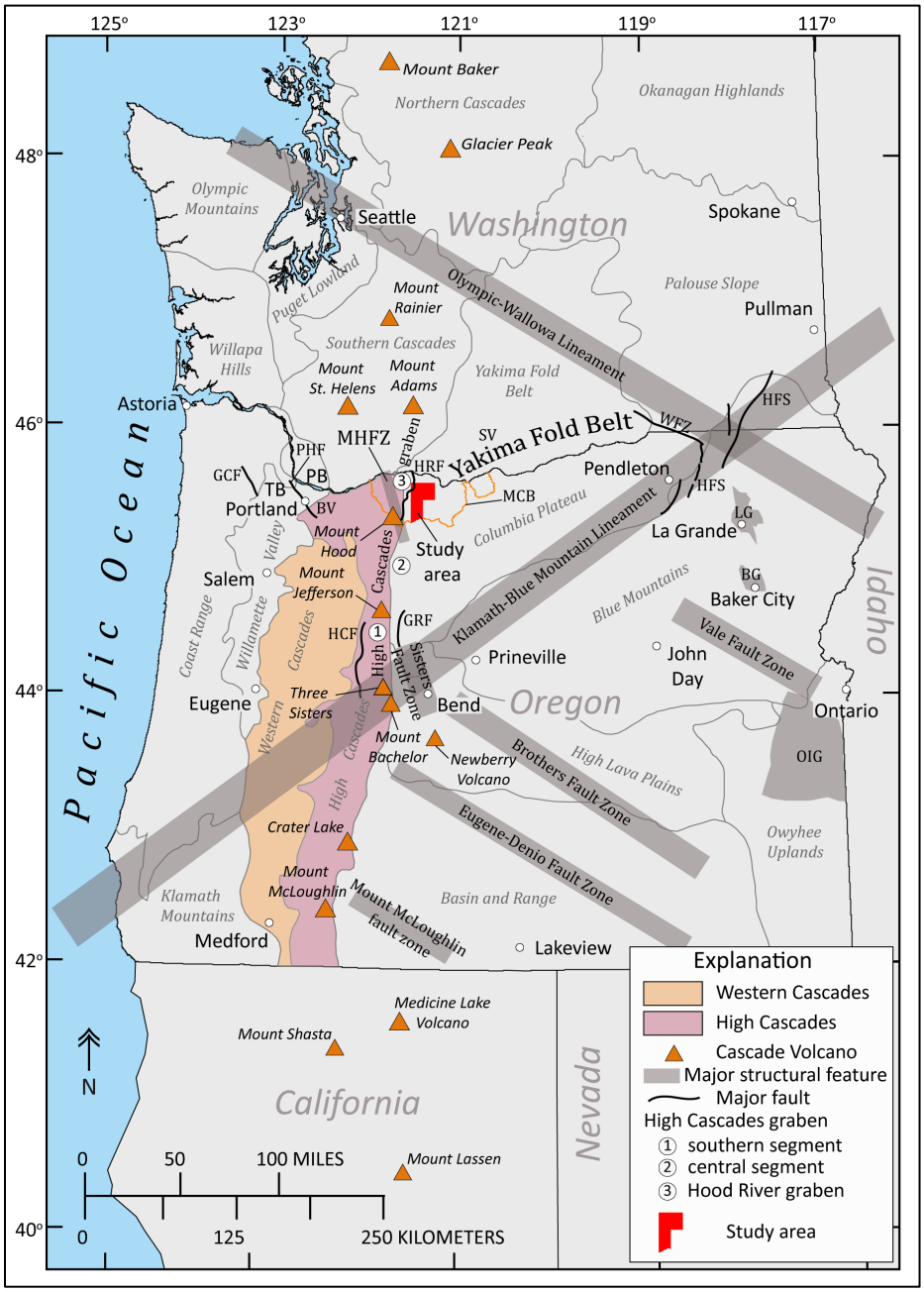

5.1 Yakima Fold Belt

The axis of the High Cascades in north-central Oregon is superimposed across the Yakima Fold Belt, a series of NE-SW-trending, asymmetric, locally overturned and faulted anticlinal ridges separated by broad synclinal valleys (**Figure 5-2**; Swanson and others, 1979a, 1981; Anderson, 1987; Watters, 1989; Reidel and Campbell, 1989; Tolan and Reidel, 1989; Anderson and others, 2013). The Yakima Fold Belt deforms much of the western and west-central Columbia Plateau of Oregon and Washington and continues westward through the Cascade Range (**Figure 5-2**; Tolan and others, 2009a).

Folds in the Yakima Fold Belt are generally ENE-trending across eastern Oregon and Washington. By contrast, across the Cascade Range, fold axes are more northeast in trend (Swanson and others, 1981; Bela, 1982; Reidel and others, 1989; Tolan and others, 2009a). ENE-directed folds in the Yakima Fold Belt east of the Cascade Range are inferred to have formed in response to a general north-south compressional regime (Reidel and others, 1989; Beeson and Tolan, 1990), while northeast-directed folds in the northern Oregon Cascade Range indicate a stress regime with the major compressive stress oriented NW-SE (Venkatakrishnan and others, 1980; Williams and others, 1982). NE-trending folds between the Dufur area and the Cascade Range are locally segmented by NNW-striking cross faults (N20°W to N30°W; **Figure 5-3**). Previous workers in the Columbia River Gorge and on the Columbia Plateau have referred to these faults as wrench faults (Anderson, 1987).

Deformation in the Yakima Fold Belt has persisted since at least the early to middle Miocene, with most of the present structural relief developing since ~10.5 Ma (Reidel and others, 1989; Tolan and others, 2009a). Structural warping in the western part of the Yakima Fold Belt during the middle Miocene is inferred to have increasingly restricted the distribution of the younger parts of the Grande Ronde, Wanapum, and Saddle Mountains basalts to structural lows in the Columbia River Gorge and Willamette Valley (Vogt, 1981; Beeson and others, 1985; Anderson and Tolan, 1986). Successively younger lava flows, most notably lava flows in the Priest Rapids and Pomona members, were partially or wholly confined to paleocanyons, possibly structurally controlled by the Yakima Fold Belt. The thickness and distribution of these CRBG units through the Columbia River Gorge locally show evidence of restricted distribution and thinning across anticlines, although these ancient channel remnants do not precisely correspond to present-day structural highs and lows (Anderson, 1987; Anderson and Vogt, 1987; Beeson and Tolan, 1990).

Folds continued to develop in post-CRBG time, as large accumulations of volcaniclastic and sedimentary detritus shed from the late Miocene Cascades (e.g., Dalles Formation) preferentially accumulated in basins along synclinal troughs. Thrust faults associated with the growth of anticlinal ridges in the Yakima Fold Belt regionally remained active following deposition of the ~9 to 5 Ma Dalles Formation. Regional thrust faults in this part of the Middle Columbia Basin include the Tygh Ridge thrust fault (southeast of the Mill Creek area), North Fork Mill Creek thrust fault, and Hellroaring Creek thrust fault (southwest of the Mill Creek area; McClaughry and others, 2020a)(**Figure 5-3**). Compressional deformation in the Middle Columbia Basin continued into the Pliocene and Pleistocene. Lava flows as young as 3.05 Ma are broadly folded and are structurally dismembered by fold-associated, NNW-striking strike-slip or oblique-slip faults in the Hood River Valley (**Figure 5-3**; McClaughry and others, 2012). Similarly oriented normal or oblique-slip faults in what is known as the Dog River-Mill Creek Divide fault zone along the East Fork Hood River show significant lateral and vertical offset of geologic units as young as 1.87 Ma (McClaughry and others, 2020a). Other evidence for recent activity on NNW-striking faults in the wider Middle Columbia Basin is found where these structures are redirecting modern stream drainages (McClaughry and others, 2012). Spatial and crosscutting relationships between folds, thrust

faults, and strike-slip faults indicate a mutual development of all three components during progressive deformational phases that occurred in the Yakima Fold Belt from the early to middle Miocene to late Pliocene (Anderson, 1987).

Figure 5-3. Physiographic map of the Mill Creek area and greater Mount Hood region, highlighting structural features. Red outline is the Mill Creek area. The solid yellow line corresponds to the watershed boundary of the Middle Columbia Basin. Mapped faults are shown as black lines. Fold axes are shown as magenta lines. Label abbreviations are as follows: BB – Badger Butte; BH – Booth Hill; BR – Bluegrass Ridge; BRFZ – Blue Ridge fault zone; CCT – Cat Creek thrust fault; CF – Chenoweth (Reverse) fault; CL – Clear Lake; DRMF – Dog River-Mill Creek Divide fault zone; EF – East Fork Hood River; FM – Fifteenmile Creek; GCWF – Gate Creek-Wyeth fault; GP – Grasshopper Point; GPF – Gibson Prairie fault; HCT – Hellroaring Creek thrust fault; HRF – Hood River fault zone; HRV –Hood River Valley; MCFZ – Mays Canyon Creek fault; MM – Middle Mountain; MMF – Multorpor Mountain fault; MT – North Fork Mill Creek thrust fault; PL – Parkdale Lava; PFZ – Pine Creek fault zone; PCFZ – Pocket Creek fault zone; RPF – Rocky Prairie thrust fault; TLF – Twin Lakes fault; UHRV – Upper Hood River Valley; WCF – Whiskey Creek thrust fault. Question mark over dashed line identifies the location of an inferred concealed thrust fault underlying the Upper Hood River Valley.

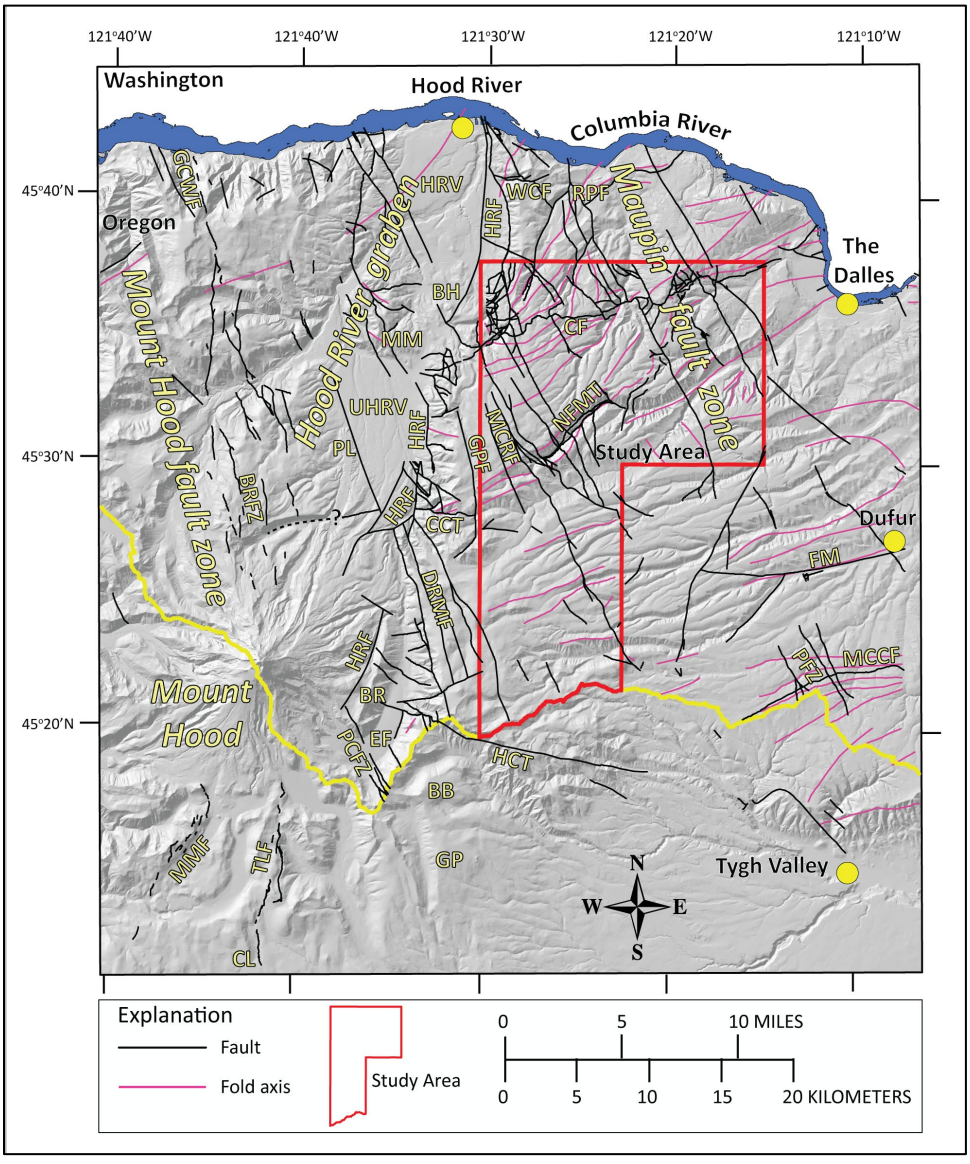

5.2 High Cascades Graben

Since ~3.7 Ma, compressional deformation in the north-central Oregon part of the Yakima Fold Belt has been accompanied by and overprinted by extension and intra-arc graben formation along the axis of the High Cascades (**Figure 5-1**, **Figure 5-2**; McClaughry and others, 2020a). The High Cascades intra-arc graben is a segmented and structurally discontinuous, ~20-to 30-km-wide (12 to 18 mi), arc-parallel graben system running for ~150 km (93 mi) along the crest of the Oregon Cascade Range, from the Three Sisters of Central Oregon north across the Columbia River and into southern Washington (**Figure 5-2**; Allen, 1966; Taylor, 1981; Williams and others, 1982; Smith and Taylor, 1983; Smith and others, 1987; Conrey and others, 2002; McClaughry and others, 2012, 2013, 2020a). This graben system is segmented into three northward-younging parts by NNW-striking faults: a southern segment between the Three Sisters and Mount Jefferson, a central segment between Mount Jefferson and Mount Hood, and a northern segment between Mount Hood and Mount Adams known as the Hood River graben (the respective segments are numbered 1 through 3 in **Figure 5-2**; Conrey and others, 2002; McClaughry and others, 2012, 2020a; Conrey and others, 2019). Older rocks, which along strike are foundered within the graben, crop out near the Cascade Range crest in the vicinity of Mount Jefferson and Mount Hood, thus precluding the presence of a significant through-going rift or graben as originally proposed by Allen (1966). All segments of the High Cascades graben are defined by significant offset along normal faults on the eastern boundary and asymmetric uplift of the western graben margin. Paleodrainages west of the graben are elevated 600 to 800 m (1,969 to 2,625 ft) above modern base levels, suggesting broad uplift of the Western Cascades concurrent with rifting (Conrey and others, 2019). Tilted fault blocks invariably dip eastward off the structural high.

The High Cascades intra-arc graben records a regional northward younging pattern for both the eruption of low-K_2O tholeiitic basalt (LKT) and the related onset of extensional faulting. Broadly, this pattern is as follows: 8 to 5 Ma at the latitude of the Three Sisters, 6 to 4 Ma near Mount Jefferson, 4 to 2 Ma in the Hood River graben, and about 1 Ma and younger in the Indian Heaven volcanic field in southern Washington (Conrey and others, 2004; Hildreth and Fierstein, 1995, 2015). Geothermal drill-core data suggest a total subsidence of 3 km (2 mi) in the southern segment and 1 km (0.6 mi) in the central segment (Conrey and others, 2002); geologic mapping and cross sections indicate subsidence of <1.2 km (0.7 mi) in the Hood River graben (**Figure 5-2**; McClaughry and others, 2012, 2013, 2020a). Subsidence developed along each graben segment as volcanism declined, typically after ~2 million years of elevated eruption rates. Volcanism immediately preceding graben formation is notable for the association of LKT basalt, Fe-rich andesite, and rhyolite lava flows, and rhyolitic ash-flow tuffs (Conrey and others, 2002; McClaughry and others, 2012; Conrey and others, 2019; McClaughry and others, 2020a). The High Cascades graben corresponds to the area with the greatest production of Quaternary volcanic material in the Cascade Range of California, Oregon, and Washington (Williams and others, 1982).

5.3 Hood River Graben

The Hood River graben is the northernmost segment of the High Cascades intra-arc graben, forming the complex tectonic depressions of the Hood River and Upper Hood River valleys (**Figure 5-2**, **Figure 5-3**; McClaughry and others, 2012, 2013, 2020a). The graben occurs from an area just south of Mount Hood, north ~50 km (31 mi) at least to Underwood Mountain along the north side of the Columbia River in Washington. Situated between the NNW-striking Mount Hood fault zone on the west and the NNW-striking Maupin fault zone on the east, the graben is defined by a 20- to 25-km-wide (12 to 16 mi) complex

network of distributed N-striking normal faults and NNW-striking right-lateral normal oblique faults (**Figure 5-3**; McClaughry and others, 2012; 2020a). Middle Mountain, a structural block of the CRBG bounded by NNW-striking oblique-slip(?) faults, divides the graben into two rhombohedral-shaped segments, known as the Hood River and Upper Hood River valleys (**Figure 5-3**; McClaughry and others, 2012).

The timing of initial graben formation in the Hood River area was contemporaneous with a major pulse of LKT volcanism in the northern Oregon Cascade Range between 4.4 and 2.1 Ma (Conrey and others, 1996; Gray and others, 1996; McClaughry and others, 2012, 2013, 2020a). This pulse of mafic volcanism was distinctly younger than a similar episode that had culminated in the southern segment of the High Cascades graben of Central Oregon by ~5 Ma (**Figure 5-2**). It contrasts with the preceding 10 million years, when andesitic eruptions dominated the northern Oregon Cascade Range (~14 to 5 Ma; Wise, 1969; Priest and others, 1983; Keith and others, 1985; Conrey and others, 1996). The south-to-north time-transgressive pattern observed along the High Cascades intra-arc graben is also observed at the scale of the Hood River graben (Conrey and others, 2002). Normal faulting along the Hood River fault zone at Mount Hood is chiefly post–3.7 Ma; normal faulting along the Hood River fault zone is chiefly post–3.05 Ma at the Columbia River (**Figure 5-3**; McClaughry and others, 2012, 2013, 2020a, 2022).

Development of the Hood River graben is related to a long history of regional clockwise tectonic rotation and northwest translation of crustal blocks along NNW-striking fault systems in the upper plate of the Cascadia subduction zone (**Figure 5-1**, **Figure 5-2**, **Figure 5-3**; McClaughry and others, 2022). NNW-striking dextral-oblique fault systems appear to be kinematically linked with N-striking normal faults to collectively accommodate right-lateral shear and east-west extension across the axis of the High Cascades volcanic arc to form the Hood River graben as a transtensional pull-apart basin (**Figure 5-3**; Bennett and others, 2019; McClaughry and others, 2020a, 2022). The stress fields, in the form of regional clockwise tectonic rotation, appear to have been relatively steady over the past 10 to 15 million years across the northern Oregon Cascade Range (McCaffrey and others, 2007). Thus, changes in the dominant style of deformation from Yakima-style folding to NW-trending transtension at roughly 4 to 3 Ma may be related to the arrival of a major pulse of LKT volcanism as the High Cascades rift propagated northward to the latitude of the Columbia River. Intra-arc rifting in the Hood River graben may have been enhanced where NW-striking right-lateral structures pass through the arc (McClaughry and others, 2022).

5.3.1 Hood River graben, eastern boundary

The eastern structural margin of the Hood River graben is the prominent west-facing escarpment of the Hood River fault zone, mapped for ~50 km (31 mi) along the eastern flank of Mount Hood to the Columbia River (**Figure 5-3**; McClaughry and others, 2012, 2013, 2020a, 2022). The fault zone may continue farther south from Mount Hood where it joins more southern strands of the eastern boundary fault of the more extensive High Cascades graben, but its presence and/or precise location in that area are not well constrained (Sherrod and Pickthorn, 1989).

The Hood River fault zone is a 1- to 3-km-wide (0.6 to 2 mi) zone of generally north-striking and west-dipping normal faults that are segmented by (and are possibly linked to) the NNW-striking right-lateral normal oblique slip faults (McClaughry and others, 2020a). Near the Columbia River, the northern end of the Hood River fault zone appears to merge with the Maupin fault zone; near Mount Hood, the southern end of the Hood River fault zone may merge with the Mount Hood fault zone (**Figure 5-3**). North-south-striking fault strands occur as discontinuous right-stepping en echelon faults that progressively shift the location of the Hood River fault zone to the east, moving north from Mount Hood to the Columbia River

(e.g., the East Fork Hood River at the mouth of Crystal Springs Creek; Booth Hill area)(**Figure 5-3**; McClaughry and others, 2012, 2020a). The Hood River fault zone has accommodated hundreds of meters of vertical offset along the eastern graben margin after 3.7 Ma, with cumulative displacement greater than 1,220 m (4,003 ft) on the south at Mount Hood decreasing northward to ~130 m (427 ft) at the Columbia River (McClaughry and others, 2012, 2020a).

5.3.2 Hood River graben, western boundary

The western structural boundary of the graben is more diffuse and less topographically obvious than the eastern boundary. It is defined by the ~55-km-long (35 mi), NNW-striking Mount Hood fault zone, a fault system extending from the Columbia River south through the summit of Mount Hood volcano to Clear Lake (**Figure 5-3**). The Mount Hood fault zone consists of multiple fault segments, including the Multorpor Mountain, Blue Ridge, and Gate Creek faults (**Figure 5-3**; Madin and others, 2017, 2021). Many of these fault segments are demonstrably pure dip slip, but a few NNW-striking faults record subtle evidence for a minor right-lateral component (Bennett and others, 2019; Madin and others, 2021a). Post-Miocene east-side-down vertical fault offset at the northern end of the Mount Hood fault zone may exceed 200 m in the CRBG exposed in the Oregon cliffs of the Columbia River Gorge, with similar offsets observed in overlying upper Pliocene LKT basalt cropping out at the top of these cliffs (Bennett and others, 2019; Madin and others, 2021a). Holocene activity has been documented in recent paleoseismic trench excavations on several of these faults, including the west-dipping Blue Ridge fault (Madin and others, 2017), the east-dipping Gate Creek fault (Bennett and others, 2021), and the west-dipping Twin Lakes fault (A. Streig, Portland State University, oral communication, 2020), where they all offset Late Pleistocene glacial till or post-glacial Holocene deposits (**Figure 5-3**). Radiocarbon ages (^{14}C) obtained from organic material within the Blue Ridge fault zone shows evidence for a single earthquake event which occurred between ~13,540 and 9,835 years before present (Madin and others, 2017).

5.4 Stratigraphic and Structural Synopsis

The following synopsis summarizes the distribution, composition, lithology, and age of map units and structural development of the Mill Creek area. The Mill Creek area is characterized by a broadly folded and generally shallow north-dipping (~1° to 3°) section of Neogene volcanic and sedimentary rocks and Quaternary surficial deposits that provide a partial record of the volcanic, depositional, and deformational history in north-central Oregon since the early Miocene (**Figure 5-4**). The synopsis is divided on the basis of the broad periods of time used in the Explanation of Map Units starting on page 40 and shown in **Figure 5-5** and on Plates 1, 2, and 3. From oldest to youngest, broad geologic units in the Mill Creek area include: (a) the ~16.2 to ~15.9 Ma CRBG; (b) ~9 to 5 Ma Dalles Formation; (c) ~3.8 to 3 Ma Pliocene volcanics; (d) ~2.6 to 1.87 Ma products of regional volcanoes; and (e) Late Pleistocene and Holocene surficial deposits.

Figure 5-4. Generalized geology of north-central Oregon. Geology is from OGDC-6, compiled by Smith and Roe (2015). Mill Creek area is shown by black outline. Solid white line corresponds to the watershed hydrologic boundary of the Middle Columbia Basin. Label abbreviations are as follows: BD—Bonneville Dam; JDD—John Day Dam; TDD—The Dalles Dam.

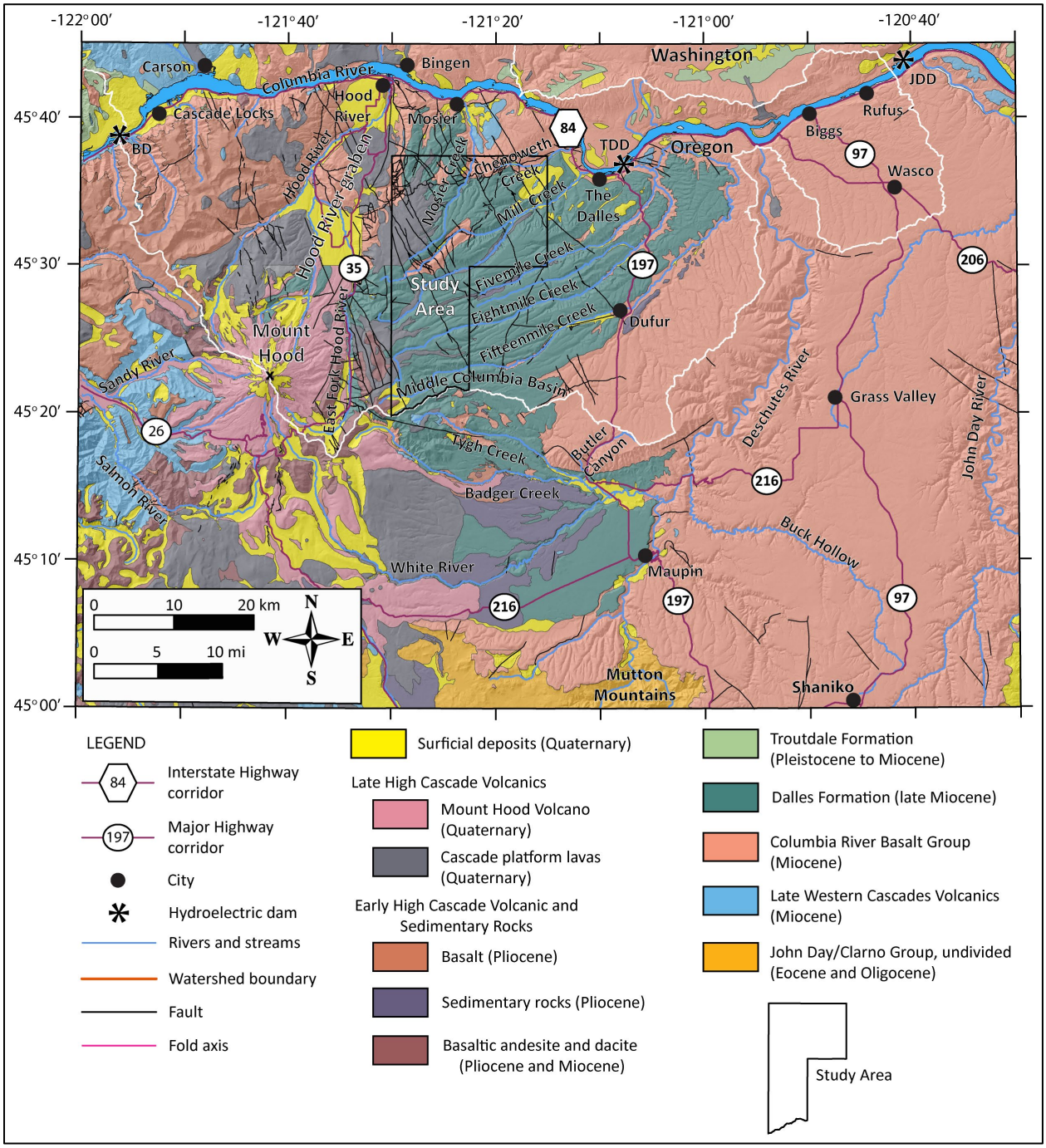

Figure 5-5. Distribution of the simplified geologic units mapped in the Mill Creek area. From oldest to youngest, these geologic units include: (a) Columbia River Basalt Group; (b) Dalles Formation; (c) Pliocene volcanics; (d) Late Pliocene and Quaternary regional volcanoes; (e) Surficial deposits.

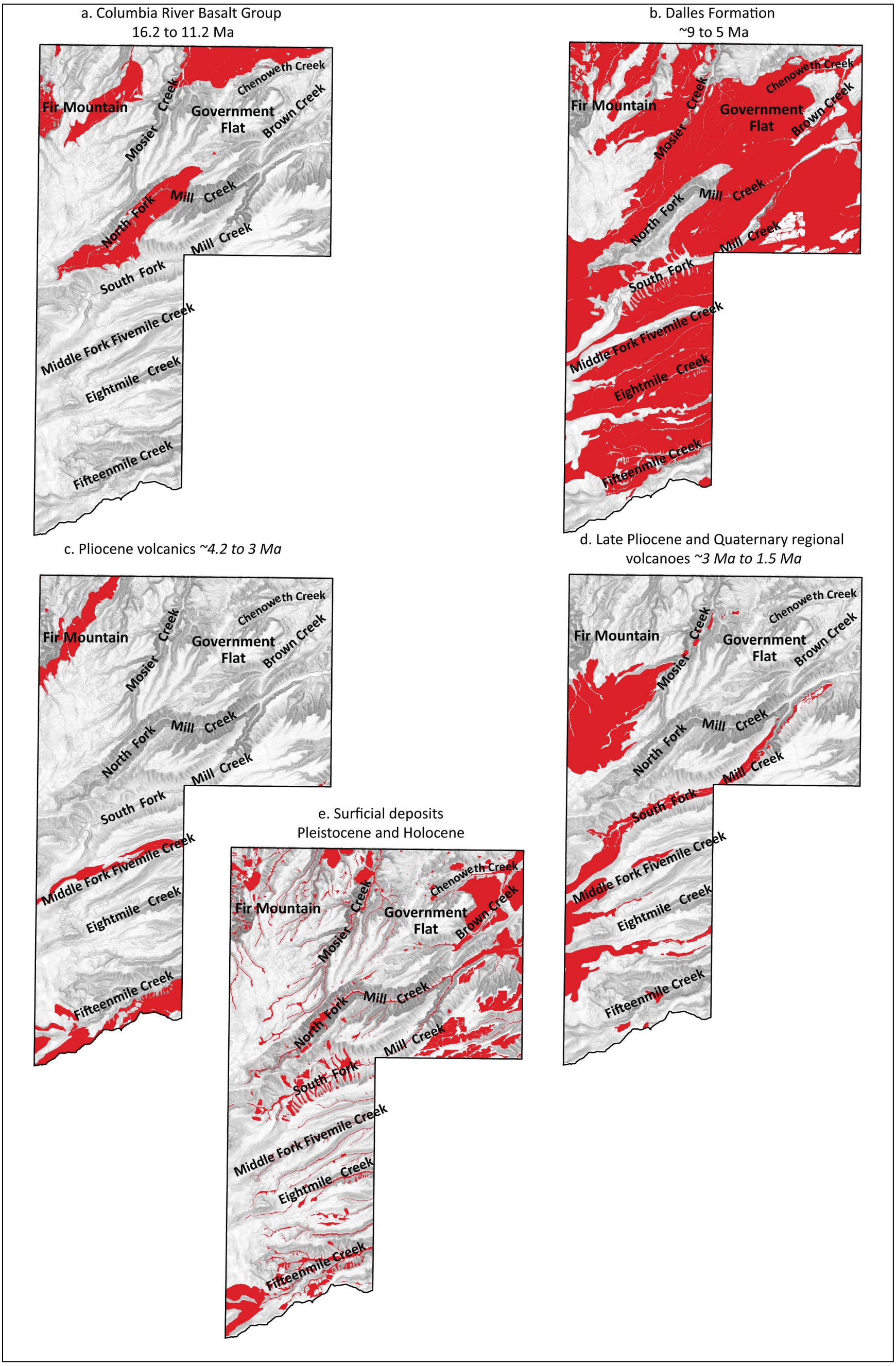

5.4.1 Middle to Lower Miocene volcanic rocks

5.4.1.1 Columbia River Basalt Group

5.4.1.1.1 *Distribution, composition, and lithology*

The oldest exposed rocks in the Mill Creek area are part of the lower to middle Miocene CRBG, an extensive succession of tholeiitic basalt and basaltic andesite lava flows that cover more than 210,000 km^2 (130,488 mi^2) in parts of Washington, Oregon, and Idaho (**Figure 5-4**, **Figure 5-5**, **Figure 5-6**, **Figure 5-7**, **Figure 5-8**, **Figure 5-9**; **Figure 5-10**; Tolan and others, 1989; Reidel and others, 2013a). Members of the CRBG cropping out in the map area include the Pomona Member of the Saddle Mountains Basalt, Priest Rapids Member (**Twpl**, **Twpr**) and Frenchman Springs Member (**Twfs, Twfh, Twfg**) of the Wanapum Basalt and Sentinel Bluffs (**Tgsb**), Winter Water (**Tgww**), Ortley (**Tgo**), and Grouse Creek (**Tggc**) members of the Grande Ronde Basalt (**Figure 5-7**, **Figure 5-10**; Plates 1, 2, and 3). Thin (<2 m [7 ft]) and discontinuous horizons of fragmental sedimentary rock or paleosols are locally found separating individual lava flows. CRBG units commonly form distinctive bench and slope topography, resulting from differential erosion within and between flows. More easily erodible interflow zones are often marked by bands of trees, while more resistant flow interiors typically form continuous cliffs with grass-topped benches. Aggregate thickness of the CRBG in the map area is as much as 550 m (1,800 ft).

CRBG lava flows were erupted from NNW-striking linear fissure systems in the eastern part of the Columbia Plateau at ~16 Ma and flowed west through the Columbia trans-arc lowland toward the low-relief topography of western Oregon and Washington (**Figure 5-6**; Tolan and Beeson, 1984; Beeson and others, 1985, 1989; Tolan and others, 1989; Wells and others, 1989, 2009; Kasbohm and Schoene, 2018). The Columbia trans-arc lowland was a generally ~60-km-wide (37 mi) valley crossing directed SW to NE, laying across the ancestral Cascade Range during the early to middle Miocene (**Figure 5-6**; Beeson and others, 1989; Beeson and Tolan, 1990). The lowland was likely structural in origin and related to fold-deformation of Eocene to middle Miocene rocks underlying north-central Oregon; it was likely not related to the development of the early Cascades volcanic arc (Beeson and Tolan, 1990). The position of the lowland, however, may have influenced later development and growth of the volcanic arc in this area (Beeson and Tolan, 1990).

Geochemical analyses of CRBG lava flows across the Middle Columbia Basin indicate tholeiitic basalt, basaltic andesite, and basaltic trachyandesite (SiO_2 = 48.6 to 57.6 weight percent), with an enrichment in iron (FeO* = 10.23 to 16.86 weight percent; *n* = 588 analyses) (**Figure 5-8**, **Figure 5-9**). Older early Miocene Grande Ronde lava flows are basaltic andesite and basaltic trachyandesite (SiO_2 = 52.99 to 57.6 weight percent; *n* = 70 analyses), with magnesium contents ranging between 3.10 and 5.22 weight percent MgO and titanium contents between 1.71 and 2.19 weight percent TiO_2. By contrast, younger lava flows making up the Wanapum Basalt have basaltic compositions (SiO_2 = 48.6 to 52.88 weight percent; *n* = 500 analyses), with magnesium content ranging between 2.60 and 5.67 weight percent MgO and distinctly higher amounts of titanium (2.77 to 4.13 weight percent TiO_2), relative to Grande Ronde Basalt (**Figure 5-8**, **Figure 5-10**a). Lava flows in both the Wanapum and Grande Ronde Basalt can be distinguished on the basis of small but analytically significant variations in TiO_2, P_2O_5, MgO, CaO, Cr, Zr, and Ba (**Figure 5-10**). Mineralogy of the CRBG includes plagioclase and pyroxene; olivine is sparse. Grande Ronde Basalt is generally aphyric and non-distinctive, while the Wanapum Basalt contains widely scattered to locally abundant plagioclase phenocrysts up to 3 cm (1.2 in) across.

Figure 5-6. Map showing the outcrop distribution of the CRBG (orange fill). The distribution includes areas from which the lava flows have been eroded, in addition to areas where lava flows are concealed by younger units. Modified from Reidel and others (2013a) and Ferns and McClaughry (2013). Label abbreviations are as follows: CJD – Chief Joseph Dike Swarm; MCB – Middle Columbia Basin; PDG – Picture Gorge Dike Swarm; SD – Steens Dike Swarm; SM – Strawberry Mountain; ST – Steens Mountain.

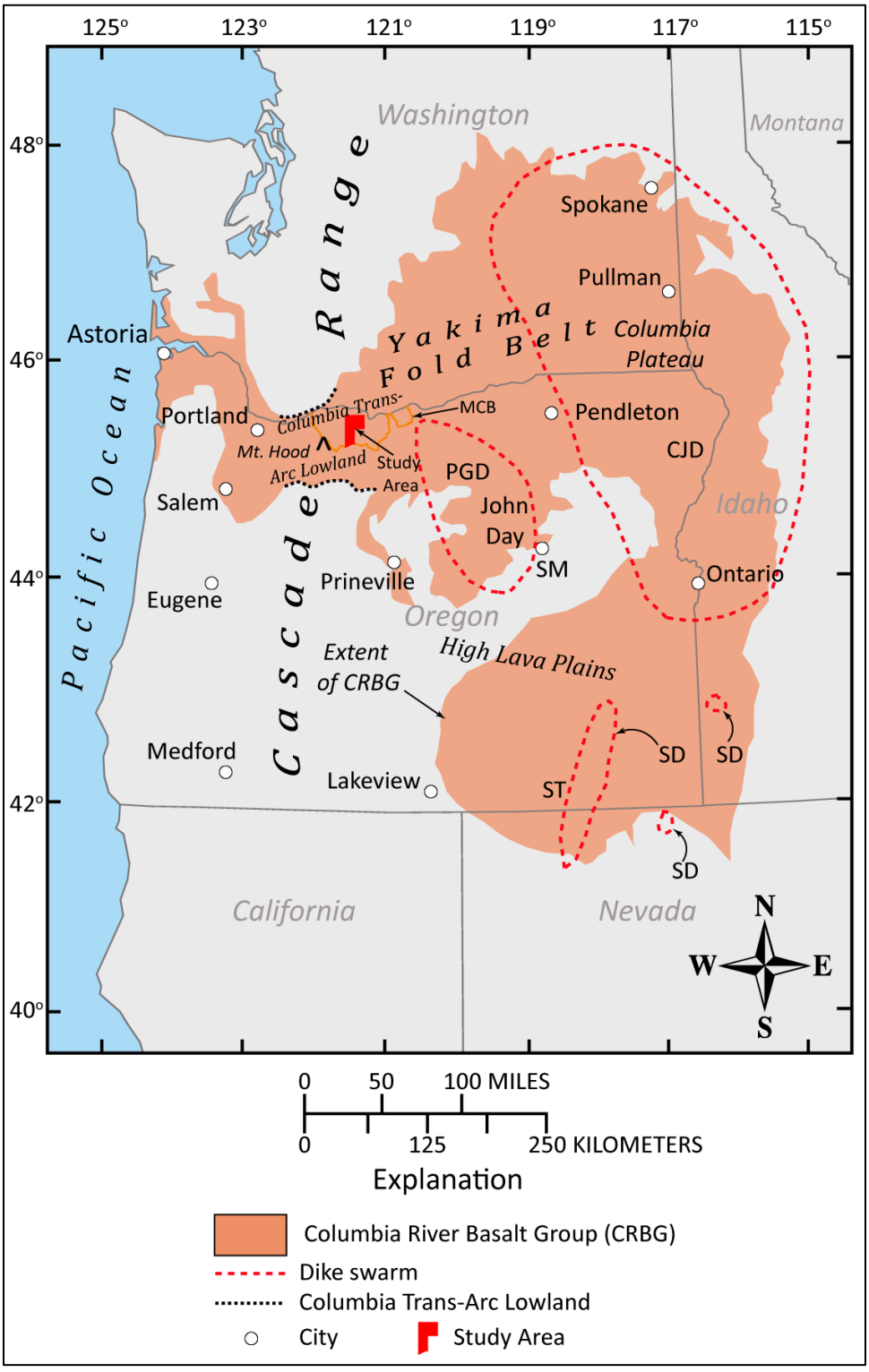

5.4.1.1.2 *Age*

Isotopic dating of CRBG lava flows has struggled with accuracy and precision issues, complicating the development of an unambiguous chronology for the timing and duration of CRBG volcanism (Baksi, 2013, 2022; Barry and others, 2013).

The Age of the Pomona Member (**Tsp**) of the Saddle Mountains Basalt is commonly cited as 12 Ma based on K-Ar dating reported by McKee and others (1977). Nash and Perkins (2012) correlated an ash that underlies the Pomona Member (**Tsp**) in the Yakima-Tri Cities area of southern Washington with the 11.81 ± 0.03 Ma Cougar Point Tuff VII, erupted from the Bruneau-Jarbidge volcanic center in southwestern Idaho (Perkins and others, 1998; redated to 11.855 ± 0.006 and 11.852 ± 0.006 Ma by Finn and others, 2016), This provided a maximum depositional age for the lava flow. Cogliatti and others (2021) used $^{40}Ar^{39}Ar$ techniques to date silicic glass in interbeds to bracket the age of the Pomona Basalt (**Tsp**) to between 11.34 ± 0.17 and 10.70 ± 0.18 Ma. These bracketing ages are consistent with the whole rock $^{40}Ar/^{39}Ar$ age of 11.21 ± 0.42 Ma reported for the Pomona Basalt by Barry and others (2013).

Work by Kasbohm and Schoene (2018), Baksi (2022), and Kasbohm and others (2023) have established a more accurate and precise eruption age model for the Wanapum and Grande Ronde Basalt (**Figure 5-6**). Whole rock $^{40}Ar/^{39}Ar$ dating experiments by Baksi (2022) determined ages for the Wanapum Basalt of 16.10 ± 0.03 Ma for the Basalt of Roza, 16.12 ± 0.05 for the Basalt of Ginkgo, and 16.12 ± 0.04 for the Basalt of Palouse Falls. The underlying Grande Rone Basalt returned whole rock $^{40}Ar/^{39}Ar$ ages of 16.15 ± 0.07 for the Sentinel Bluffs Member (Museum flow) at the top of the formation, 16.39 ± 0.08 at the N2/R2 boundary, and 16.43 ± 0.04 Ma for lava flows in the middle part of the R2 unit. The ages of Baksi (2022) are broadly aligned with the dating efforts of Kasbohm and Schoene (2018) and Kasbohm and others (2023) who examined interbeds between basalt lava flows on the Columbia Plateau and dated them by high precision U-Pb geochronology on single zircon crystals (**Figure 5-6**). The age of the Basalt of Rosalia (**Twpr**) in the Priest Rapids Member and the Frenchman Springs Member (**Twfs**, **Twfh**, **Twfg**) is bracketed by U-Pb dates of 15.923 ± 0.030 Ma for white ash between the Basalt of Rosalia (**Twpr**) and Basalt of Lolo (**Twpl**) and 16.111 ± 0.049 Ma on pumice clasts and 16.134 ± 0.03 Ma for white mud from the Vantage Member between the Basalt of Ginkgo (**Twfg**) and the Sentinel Bluffs Member(**Tgsb**) (**Figure 5-7**; Kasbohm and others, 2023). Upper Grande Ronde lava flow units, including the Sentinel Bluffs (**Tgsb**), Winter Water (**Tgww**), Ortley (**Tgo**), and Grouse Creek (**Tggc**) members are bracketed by U-Pb dates of 16.134 ± 0.03 Ma for white mud from the overlying Vantage Member and 16.260 ± 0.03 Ma for red clay (bole) between the Wapshilla Ridge and Meyers Ridge members of the underlying R2 magnetostratigraphic unit (**Figure 5-7**; Kasbohm and others, 2023). U-Pb ages place an end to Grande Ronde volcanism at ~16.1 Ma, while more than 77 percent of Wanapum Basalt completed eruption prior to ~15.9 Ma.

Figure 5-7. Chart showing stratigraphy and nomenclature for the CRBG (*following page*). Modified from Reidel and others (2002), with updated stratigraphy from Reidel and others (2013a) and Reidel and Tolan (2013). Reported ages are from the following sources: [1]Barry and others (2013); [2]Ferns and others (2010); [3]Kasbohm and Schoene (2018) and Kasbohm and others (2023) (U-Pb); [4]Kasbohm and others (2023) ($^{40}Ar/^{39}Ar$); [5]Baksi (2022); [6]Mahood and Benson (2017); [7]Moore and others (2018); [8]Cahoon and others (2020, 2023). Red lines show horizons of local erosional unconformities. CRBG units mapped in the Mill Creek area are shown in boldface.

Figure 5-7. (CRBG stratigraphy – *caption on previous page*)

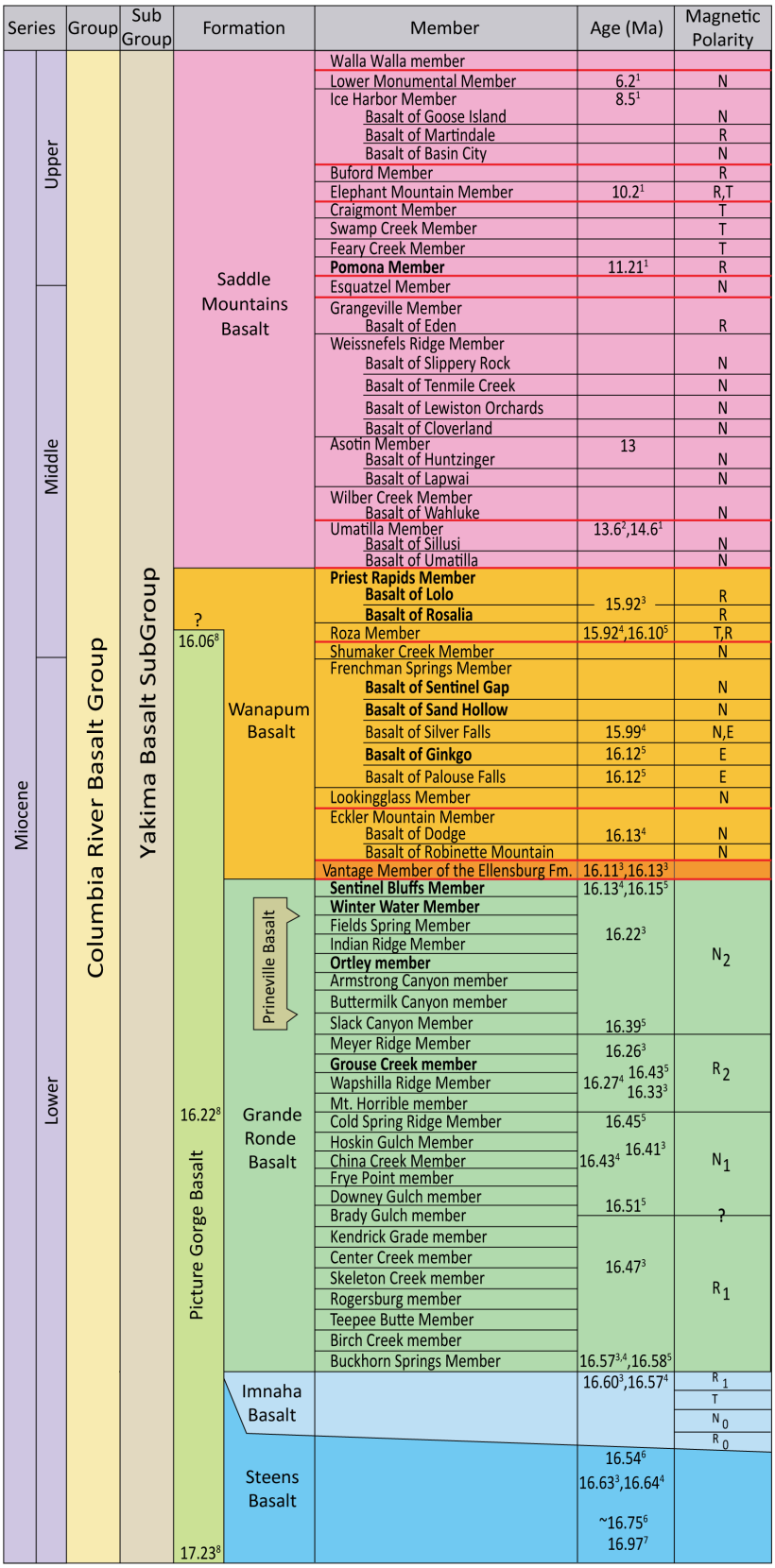

Figure 5-8. Total alkalis ($Na_2O + K_2O$) vs. silica (SiO_2)(TAS) classification of the CRBG from whole-rock XRF analyses (normalized to 100 percent anhydrous). Fields and rock names are from Le Bas and others (1986) and Le Maitre and others (1989). Red-dashed line is the dividing line between alkaline (above) and subalkaline/tholeiitic (below) fields after Cox and others (1979). Data shown include 588 CRBG analyses from the Middle Columbia Basin reported in this paper, in McClaughry and others (2012, 2020a, 2021), and Madin and McClaughry (2019).

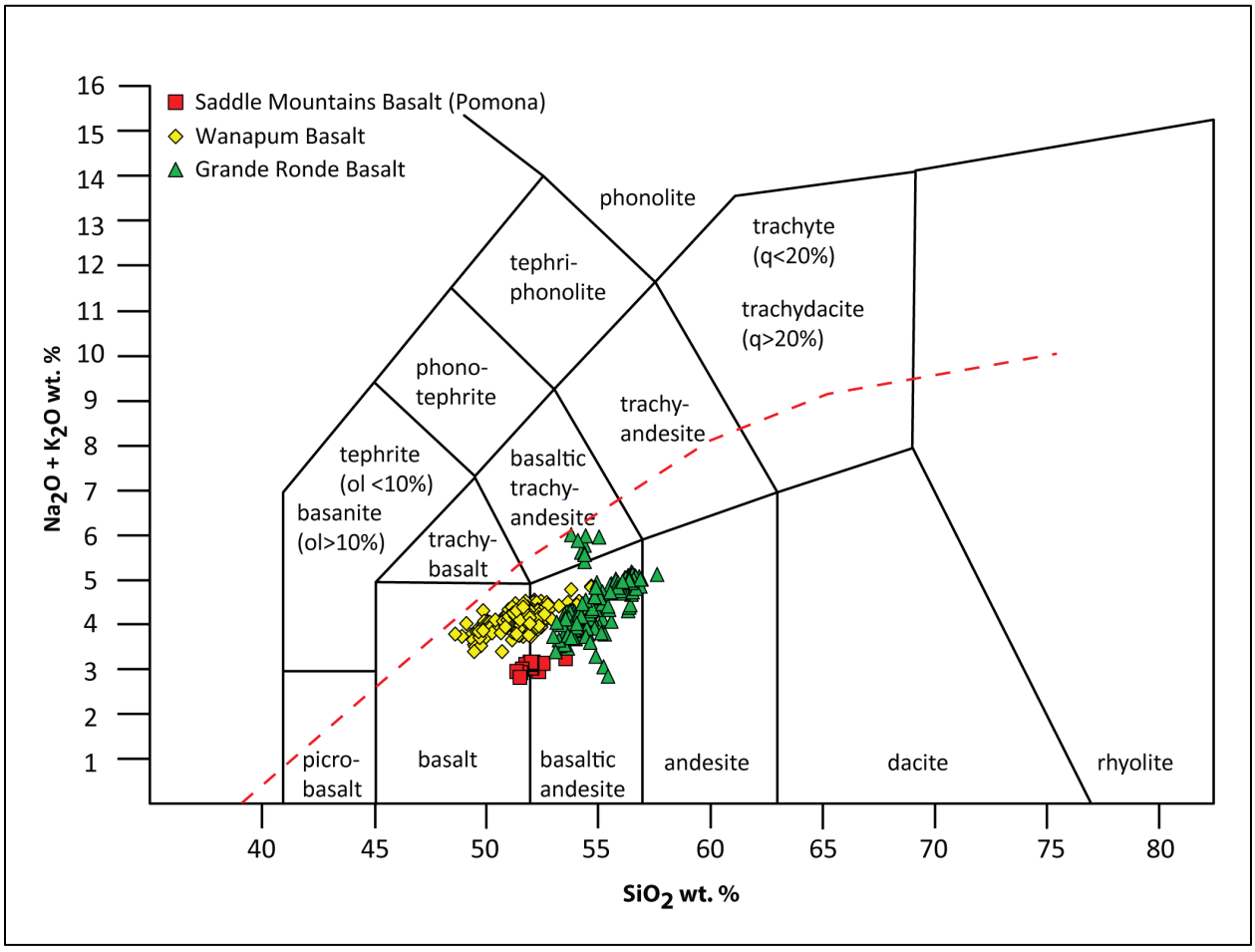

Figure 5-9. Total iron/magnesium (FeOTotal/MgO) versus silica (SiO_2) diagram for the CRBG wherein the FeOTotal/MgO ratio increases as SiO_2 increases. Tholeiitic and calc-alkaline dividing line is from Miyashiro (1974). Data shown include 588 CRBG analyses from the Middle Columbia Basin reported in this paper, McClaughry and others (2012, 2020a, 2021), and Madin and McClaughry (2019).

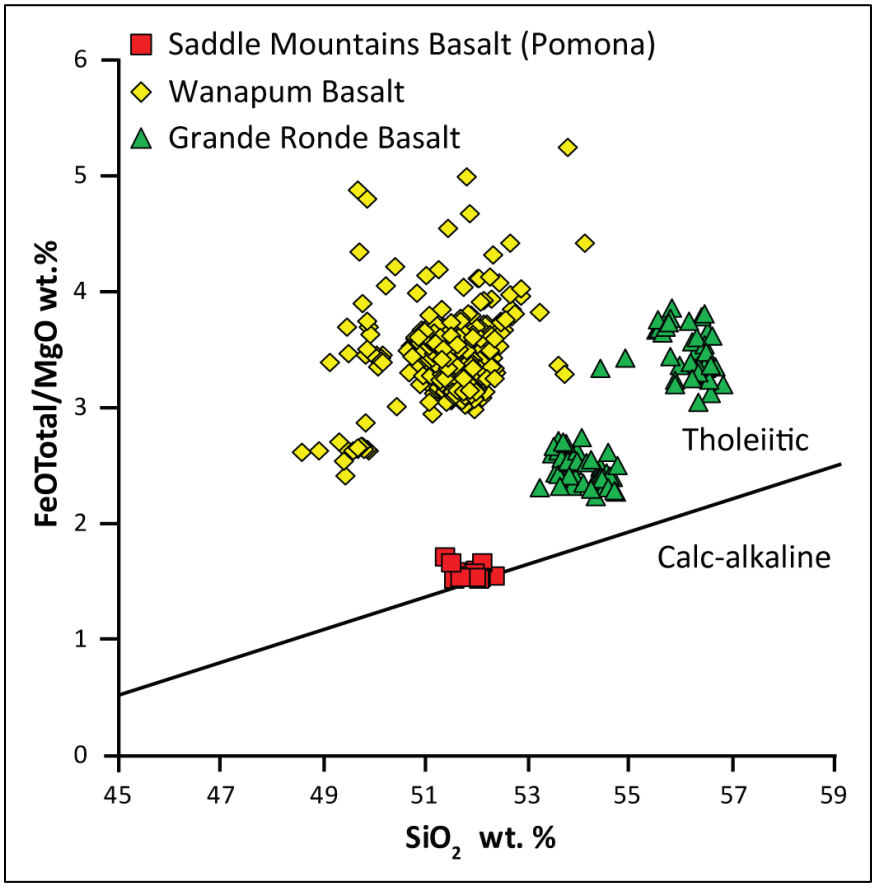

Figure 5-10. Chemical variation diagrams for the CRBG. (a) Phosphorus (P_2O_5) versus titanium (TiO_2). The "titanium gap" is after Seims and others (1974). (b) Titanium (TiO_2) versus chromium (Cr). (c) Chromium (Cr) versus titanium/zirconium (Ti/Zr) identifying Saddle Mountains and Wanapum Basalt units. (d) Phosphorus (P_2O_5) versus titanium/zirconium (Ti/Zr) identifying Saddle Mountains and Wanapum Basalt units. Data shown include 588 CRBG analyses from the Middle Columbia Basin reported in this paper, McClaughry and others (2012, 2020a, 2021), and Madin and McClaughry (2019).

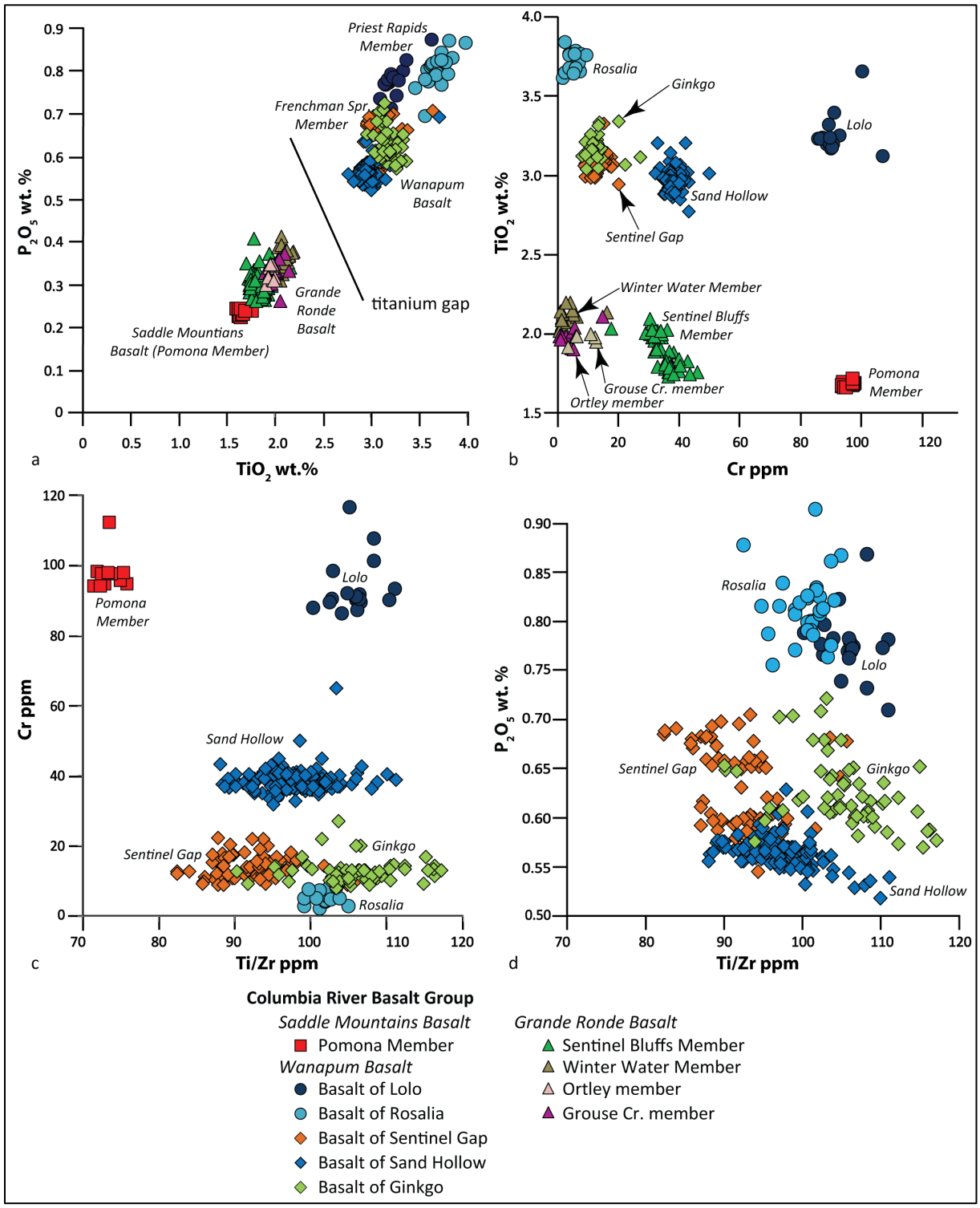

5.4.2 Lower Pliocene and Upper Miocene volcanic and sedimentary rocks of the early High Cascades

5.4.2.1 Dalles Formation

5.4.2.1.1 *Distribution, composition, and lithology*

Regional CRBG units in this part of north-central Oregon are unconformably overlain by volcanic and sedimentary rocks of the upper Miocene and lower Pliocene Dalles Formation (**Figure 5-5**; Plates 1, 2, and 3). The Dalles Formation was emplaced across a broad constructional volcanic highland along the East Fork Hood River and in areas underlying present-day Mount Hood (McClaughry and others, 2020a). Correlative strata form a broad NE-sloping arc-adjacent volcanic plain stretching ~40 km (25 mi) from the East Fork Hood River, NE to the Columbia River (**Figure 5-4**; McClaughry and others, 2020a, 2021). In the eastern escarpment of the Hood River graben, along the East Fork Hood River, the Dalles Formation is characterized by interlayered vent-proximal lava flows and domes (**Tmdh**, **Tmdb**), hypabyssal intrusions, block-and-ash flow deposits, and ash-flow tuff (Plate 3; McClaughry and others, 2020a). Deposits mapped eastward through the Mill Creek area to The Dalles and Dufur, become increasingly rich in thick sections of block-and-ash-flow deposits, volcanogenic debris flow (lahar) deposits, hyperconcentrated flood-flow deposits, and ash-flow tuff, interbedded with horizons of fluvial conglomerate, sandstone, and siltstone (**Tmdl**, **Tmdd**)(Plates 1, 2, and 3). Intracanyon lava flows (**Tmdj**, **Tmde**, **Tmdf**, **Tmdv**, **Tmds**, **Tmdw**) are nested into the volcaniclastic rocks along several northeast-directed drainages (Plate 3). These lithologic associations indicate a transition from proximal volcanic-dominated highlands along the East Fork Hood River on the west to a more distal broad volcaniclastic apron on the east, characterized by ENE-directed stream drainages (**Figure 5-4**, **Figure 5-5**). The Dalles Formation thins and pinches out to the south and thickens toward The Dalles where it reaches a maximum thickness of ~550 m (1,800 ft)(**Figure 5-5**; Plates 1, 2, and 3; Piper, 1932; Newcomb, 1969). The Dalles Formation is deeply incised in the eastern part of the Middle Columbia Basin, yielding a distinctive and rugged finger-mesa and canyon topography (**Figure 5-4**, **Figure 5-5**; Plates 1, 2, and 3).

Geochemical analyses of the Dalles Formation's volcanic units (primary deposits and clasts) in the Middle Columbia Basin (Wise, 1969; Gray and others, 1996; Westby, 2014; McClaughry and others, 2020a; Jason McClaughry unpublished geologic mapping) show the formation is dominated by medium- to low-potassium calc-alkaline andesite and dacite, with SiO_2 ranging between 57.47 and 67.35 weight percent and K_2O ranging between 0.42 and 2.22 weight percent (avg K_2O = 1.27 weight percent at SiO_2 = 63.83 weight percent [avg]; *n* = 199 analyses)(**Figure 5-11**; **Figure 5-12a**). Intermediate composition rocks also contain characteristically low concentrations of large-ion lithophile elements like barium (Ba<573 ppm; avg Ba = 308 ppm), high-field strength elements, such as niobium (Nb<19.1 ppm; avg Nb = 8.3 ppm) and zirconium (Zr<248 ppm; avg Zr = 148 ppm), light rare earth elements, such as lanthanum (La<39 ppm; avg La = 17 ppm) and cerium (Ce<61 ppm; avg Ce = 34 ppm), and heavy rare earth elements like yttrium (Y<32 ppm; avg Y = 15 ppm) (**Figure 5-12**). The 7.91 Ma dacite of Wolf Run (**Tmdw**) is enigmatic in the Dalles Formation, having markedly higher potassium (avg = 2.87 weight percent K_2O at 64.38 weight percent SiO_2 [avg]; *n* = 13 analyses), zirconium (avg Zr = 317 ppm), niobium (avg Nb = 15.9 ppm), lanthanum (avg La = 35 ppm), and cerium (avg Ce = 66 ppm). Mineralogy of rocks in the Dalles Formation includes plagioclase, pyroxene (orthopyroxene ≥ clinopyroxene), and at times hornblende.

Figure 5-11. Total alkalis ($Na_2O + K_2O$) vs. silica (SiO_2)(TAS) classification of late Miocene and early Pliocene Dalles Formation and early Pliocene intermediate composition volcanic rocks in the Mill Creek area from whole-rock XRF analyses (normalized to 100 percent anhydrous). Fields are from Le Bas and others (1986) and Le Maitre and others (1989). Red-dashed line is the dividing line between alkaline (above), subalkaline/tholeiitic (below) fields, after Cox and others (1979). Data shown include 229 analyses from the Middle Columbia Basin reported in this paper, Wise, (1969), Conrey and others (1996), Gray and others (1996), Westby (2014), and McClaughry and others (2020a, 2021).

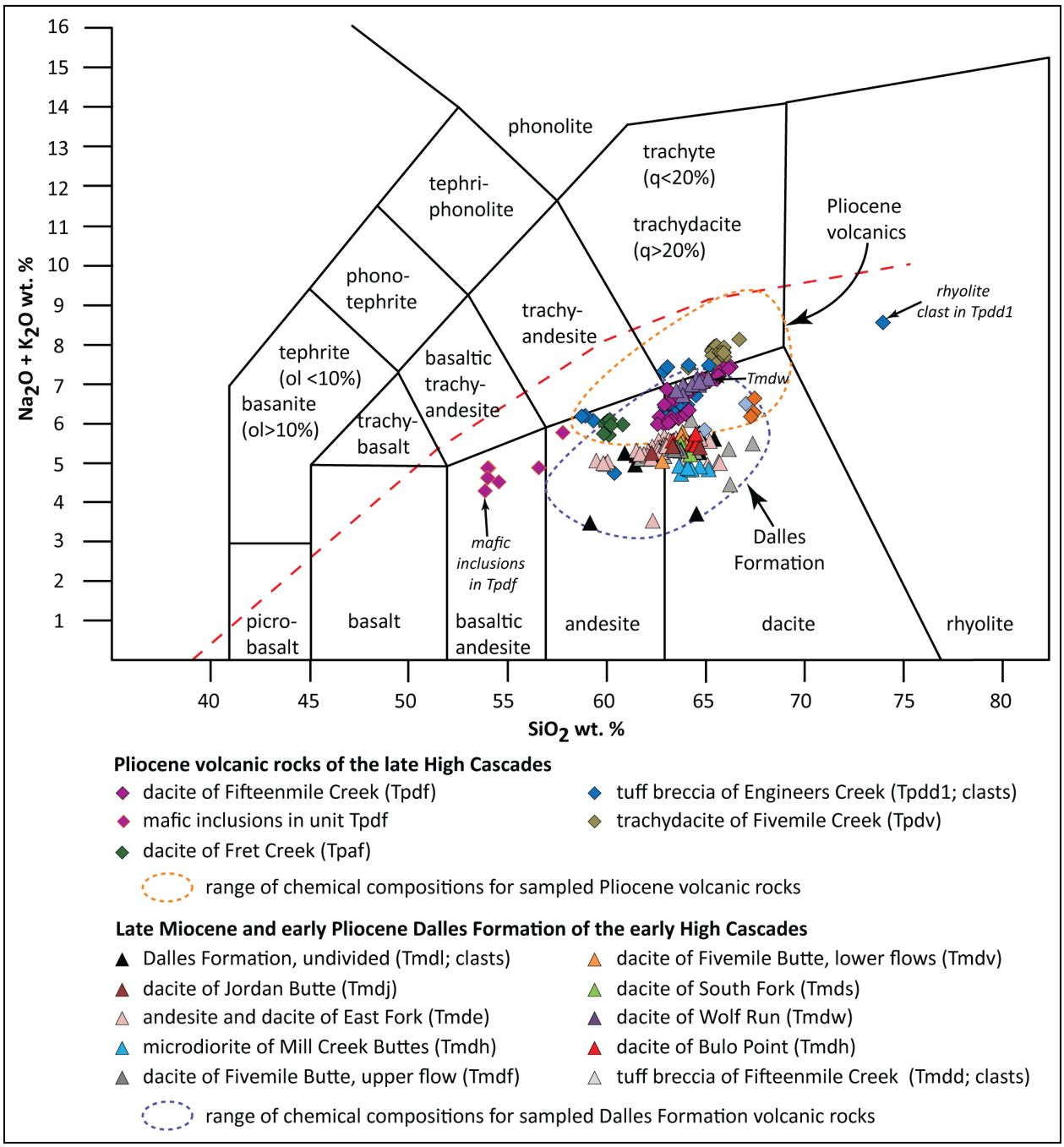

Figure 5-12. Chemical variation diagrams for late Miocene and early Pliocene Dalles Formation and early Pliocene intermediate composition volcanic rocks in the Mill Creek area. (a) Potassium (K_2O) versus silica (SiO_2). (b) Barium (Ba) versus silica (SiO_2). (c) Zirconium (Zr) versus Niobium (Nb). (d) Cerium (Ce) versus silica (SiO_2). Classification boundaries distinguishing low-, medium-, and high-potassium (K_2O) rocks in (a) are from Peccerillo and Taylor (1976). Data shown include 229 analyses from the Middle Columbia Basin reported in this paper, Wise, (1969), Conrey and others (1996), Gray and others (1996), Westby (2014), and McClaughry and others (2020a, 2021).

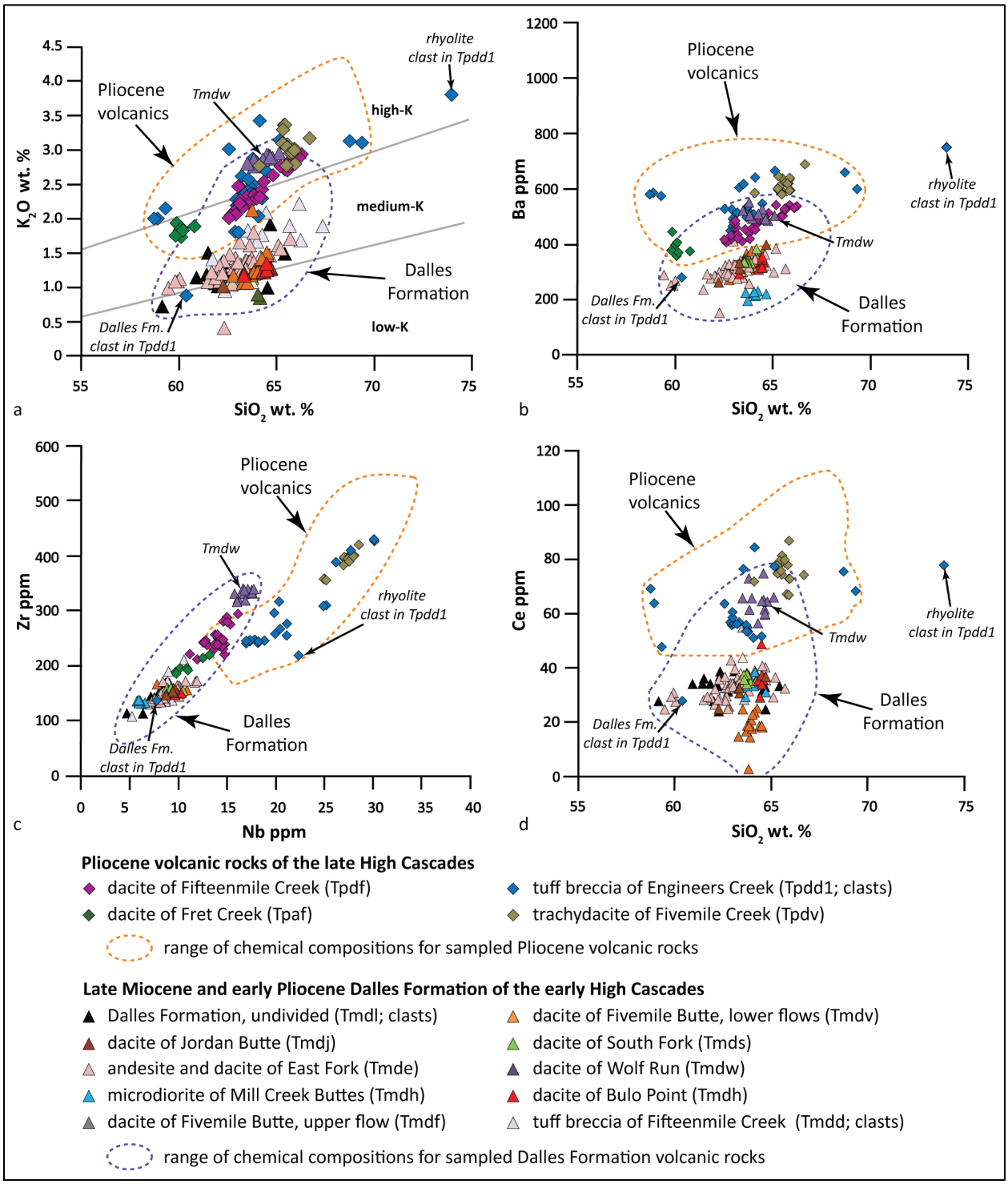

Upper Miocene and lower Pliocene rocks in the Mill Creek area are equivalent to the Dalles Formation as used and described by previous workers in the area (Buwalda and Moore, 1929, 1930; Piper, 1932; Newcomb, 1966, 1969; Gannett, 1982; Korosec, 1987; Luttrell and others, 1991; Gray and others, 1996). The term "Dalles Group" was originally used for these rocks by Condon (1874, 1902), Cope, 1880 (a,b), and McCornack (1928). Buwalda and Moore (1929, 1930) subsequently referred to these rocks as "Dalles formation" in their fossil-based chronology work. Piper (1932) was the first to map the "Dalles Group" of Condon (1874) as the Dalles formation. Newcomb (1966, 1969) formalized the Dalles Formation and extended it eastward from The Dalles to the Arlington area. Farooqui and others (1981a,b) suggested substituting the name Chenoweth in place of Dalles Formation in this area and the promotion of Dalles to group status. Their Dalles Group was considered to include all upper Miocene and lower Pliocene volcanogenic and epiclastic sedimentary rocks, pyroclastic rocks, and basaltic lava flows that unconformably overlie the lower to middle Miocene CRBG east of the Cascade Range in Oregon. Five mappable formations were assigned to the Dalles Group by Farooqui and others (1981a,b), including the Chenoweth (previously Dalles), Deschutes, Alkali Canyon, McKay, and Tygh Valley formations. Several workers in the northern Oregon Cascade Range have adopted usage of the Chenoweth Formation and Dalles Group (Farooqui and others, 1981a,b; Tolan and Beeson, 1984; Lite and Grondin, 1988; Burns and others, 2012). However, usage of the term Dalles Group is inappropriate as the terminology combines geographically separated, lithologically diverse, and genetically unrelated geologic formations (e.g., intra-Cascade arc and rift related Deschutes and Tygh Valley Formations versus the pre-rift Dalles Formation or epiclastic sedimentary rocks of the Alkali Canyon and McKay Creek Formations; Smith and Fritz, 1989; Conrey and others, 1996; McClaughry and others, 2012; McClaughry and others, 2020a, 2021). We therefore retain the conventional name Dalles Formation as established by earlier workers (Condon, 1874).

5.4.2.1.2 *Age*

Rocks of the upper Miocene and lower Pliocene Dalles Formation represent part of the early High Cascade episode in this part of the High Cascades of north-central Oregon (**Figure 5-4**). They were chiefly erupted between ~8.8 and 5 Ma as determined by a number of isotopic ages. Several $^{40}Ar/^{39}Ar$ ages have been obtained on Dalles Formation rocks, both from proximal volcanic units in the East Fork Hood River area (McClaughry and others, 2020a) and from distal volcaniclastic apron deposits in the Dufur area (McClaughry and others, 2021). $^{40}Ar/^{39}Ar$ ages determined on distal apron deposits in the Dufur area include 8.75 ± 0.05 Ma obtained from a lahar clast (**Tmdd**) near the base of the formation at the intersection of Fifteenmile Creek and Rail Hollow, 8.07 ± 0.10 Ma on the tuff of Rail Hollow in the upper reaches of Rail Hollow, and 7.91 ± 0.08 Ma on the dacite of Wolf Run (**Tmdw**) mapped along Eightmile Creek (McClaughry and others, 2021). Welded tuff cropping out near Friend has an $^{40}Ar/^{39}Ar$ age of ~5.3 Ma (McClaughry and others, 2021). Broadly similar $^{40}Ar/^{39}Ar$ ages in vent-proximal areas include 6.83 ± 0.01 Ma on a microdiorite dome forming part of Mill Creek Buttes and 5.37 ± 0.06 Ma on a hypabyssal intrusion mapped along the East Fork Hood River (McClaughry and others, 2020a). A basalt lava flow lying atop the Dalles Formation at Fulton Ridge, near the mouth of the Deschutes River, returned $^{40}Ar/^{39}Ar$ ages of 5.432 ± 0.086 and 5.451 ± 0.083 Ma (Cannon and O'Connor, 2019; O'Connor and others, 2021).

Previously published K-Ar ages on Dalles Formation rocks have returned similar, but typically less precise ages. Along the East Fork Hood River, lava flows comprising the andesite and dacite of East Fork (McClaughry and others, 2020a) have returned K-Ar ages of 7.15 ± 0.8 Ma (Wise, 1969) and 8.18 ± 0.06 Ma (Keith and others, 1985). Other K-Ar ages include 7.74 ± 0.16 Ma obtained from a lahar clast in Fifteenmile Creek (Gray and others, 1996), 7.71 ± 0.17 Ma from lava flows forming Fivemile Butte (**Tmdv**;

Plate 3; Gray and others, 1996), 7.5 ± 0.4 Ma from domes forming the Mill Creek Buttes (Hull and Riccio, 1979; McClaughry and others, 2020a), 5.87 ± 0.6 Ma and 5.7 ± 0.6 Ma obtained from lahar clasts on Chenoweth Creek (**Tmdl**; Plate 1; Farooqui and others, 1981a,b; Bunker and others, 1982), and 5.28 ± 0.5 Ma (Bunker and others, 1982) and 5.1 ± 0.5 Ma (Farooqui and others, 1981a,b) for lava flows at Jordan Butte (south of the Mill Creek area). Vertebrate and leaf fossil data reported by Buwalda and Moore (1929, 1930), Chaney (1944), and Newcomb (1966) are also consistent with a late Miocene and early Pliocene age for the Dalles Formation.

5.4.3 Pliocene volcanic and sedimentary rocks of the late High Cascades

5.4.3.1 Pliocene volcanic and sedimentary rocks

5.4.3.1.1 *Distribution, composition, and lithology*

A series of late High Cascades Pliocene volcanic rocks unconformably overlie and partially fill paleochannels incised into the Dalles Formation and CRBG in the Mill Creek area. Mapped Pliocene volcanic units include: 1) a flow-on-flow succession of upper Pliocene low-potassium tholeiitic (LKT) basaltic lava flows (**Tpbh**, **Tpbrc**, **Tpbs**) cropping out in the northwest part of the Ketchum Reservoir 7.5′ quadrangle (Plate 2); and 2) intracanyon andesite, dacite, and trachydacite lava flows (**Tpdf**, **Tpas**, **Tpdv**,) and breccia (**Tpdd1**) mapped along Fivemile and Fifteenmile creeks in the Flag Point, Fivemile Butte, and Brown Creek 7.5′ quadrangles (Plates 1 and 3). The trachydacite of Fivemile Creek (**Tpdv**) is overlain by sand and gravel of unit **QTpg** along Fivemile Creek that may be of latest Pliocene or earliest Pleistocene age (Plate 3). LKT basaltic lava flows erupted along the eastern structural margin of the Hood River graben and flowed northeast along narrow paleochannels that approximately parallel the axis of the Mosier syncline and the modern drainages of Rock Creek and the West Fork Mosier Creek (Plate 2). LKT basalt lava flows (SiO_2 = 47.67 to 50.35 weight percent) cropping out in the Ketchum Reservoir 7.5′ quadrangle are characterized by high amounts of iron (FeO_{Total} = 9.10 to 13.07 weight percent) and magnesium (MgO = 6.49 to 8.42 weight percent) and low amounts of potassium (K_2O = 0.16 to 0.39 weight percent)(*n* = 29 analyses [16 outside Mill Creek area]). Plagioclase, clinopyroxene, and olivine are the primary mineralogy of LKT basalt lava flows. Geochemical analyses of Pliocene lava flows in the Fivemile Butte and Flag Point 7.5′ quadrangles are medium-to high-potassium andesite, dacite, and trachydacite with SiO_2 ranging between 59.83 and 66.67 weight percent and K_2O ranging between 1.73 and 3.36 weight percent (*n* = 54 analyses [43 outside Mill Creek area]). Unit **Tpdd1** clasts are medium-to high-potassium andesite, trachyandesite, dacite, and trachydacite with SiO_2 between 58.91 and 68.72 weight percent and K_2O between 2.00 to 3.42 weight percent, similar to contemporaneous lava flows (*n* = 26 analyses outside the map area). Intermediate composition lava flows and breccia clasts are dominated by plagioclase and pyroxene (orthopyroxene ≥ clinopyroxene). Relative to the older Dalles Formation, Pliocene intermediate-to-silicic rocks across the wider Middle Columbia Basin contain higher amounts of large-ion lithophile elements such as potassium (avg K_2O = 2.49 weight percent at SiO_2 = 66.48 weight percent [avg]) and barium (Ba<748 ppm; avg Ba = 505 ppm), high-field strength elements such as niobium (Nb<33.7 ppm; avg Nb = 20.1 ppm) and zirconium (Zr<525 ppm; avg Zr = 296 ppm), and the light rare earth elements such as lanthanum (La<64 ppm; avg La = 30 ppm), cerium (Ce<108 ppm; avg Ce = 59 ppm), and yttrium (Y<62 ppm; avg Y = 35 ppm)(*n* = 70)(**Figure 5-12**). Thickness of Pliocene volcanic units in the map area ranges widely from thin gravel and tuff beds <2 m (6.6 ft) thick to intracanyon lava flows as thick as 70 m (230 ft).

The Pliocene and early Pleistocene interval between 4.2 and 2.5 Ma signaled a key period in the volcanic and structural evolution of the late High Cascades of north-central Oregon. Intra-arc faulting

initiated during the Pliocene and early Pleistocene along NNW-striking normal or normal oblique-slip faults and north-south-striking normal faults led to the formation of the north-striking Hood River graben along the axis of the High Cascades volcanic arc (**Figure 5-2**, **Figure 5-3**; McClaughry and others, 2012, 2013, 2020a, 2022). Development of the southern part of the Hood River graben was temporally and spatially associated with the eruption of a compositionally diverse suite of volcanic rocks (basalt to rhyolite) (McClaughry and others, 2020a). In contrast to the relatively wide regional distribution of early High Cascades rocks of the Dalles Formation (**Figure 5-6**), younger Pliocene and early Pleistocene volcanics were increasingly confined to the Hood River graben (McClaughry and others, 2020a). Distribution of Pliocene and early Pleistocene volcanics was controlled by a combination of constructional volcanic topography on remnant Dalles volcanoes, NE-striking stream channels incised into the Dalles Formation arc-adjacent volcaniclastic apron, and structural relief created along active faults. Pliocene and early Pleistocene volcanics, erupted along the structural margins of the Hood River graben, largely filled the accommodation spaces created by active extensional and transtensional structures. Few lava flows of this age, with the exception of a 3.69 Ma trachydacite of Fivemile Creek (**Tpdv**), andesite of Fret Creek (**Tpaf**), and the 3.02 Ma dacite of Fifteenmile Creek (**Tpdf**), escaped the developing graben (McClaughry and others, 2020a). Those lavas that did exit the graben to the east were confined within channels incised into the older Dalles arc-adjacent plain, approximately paralleling modern-day canyon patterns and gradient. The trachydacite of Fivemile Creek (**Tpdv**) entered the upper parts of Fivemile Creek south of Mill Creek Buttes, and descended that drainage for a distance of ~24 km (15 mi), nested as an intracanyon lava within older Dalles Formation strata (**Tmdl**)(Plate 3; McClaughry and others, 2021). Likewise, both the andesite of Fret Creek (**Tpaf**) and the dacite of Fifteenmile Creek (**Tpdf**) flowed east into the NE-striking Fifteenmile Creek drainage as intracanyon lava flows; the farther traveled dacite of Fifteenmile Creek (**Tpdf**) flowed ~13.6 km (8.5 mi) to the ENE of the map area inset into the volcaniclastic strata of the Dalles Formation (**Tmdl**)(Plate 3; McClaughry and others, 2021).

Compositionally diverse Pliocene volcanics in the Mill Creek area contrast with the dominantly low-K_2O andesite and dacites characterizing the older Dalles Formation and are unique for this part of the northern Oregon Cascades volcanic arc due to the conspicuous presence of rhyolite units (McClaughry and others, 2020a). Rhyolites are not present in either preceding or subsequent volcanic episodes marking the Mount Hood region. Rhyolites were erupted contemporaneously with 3.7 Ma trachyandesite and trachydacite lavas in the Dog River–Badger Lake area (McClaughry and others, 2020a) as well as 3.68 Ma trachydacitic tuff of Friend and ~3.71 Ma trachydacite-clast tuff breccia of Engineers Creek (**Tpdd1**) cropping out between the East Fork Hood River, Dufur, and Rice (McClaughry and others, 2021). These rocks are temporally equivalent to a similar suite of silicic volcanic rocks emplaced outside the map area at nearby Gordon Butte (8.6 km [5.4 mi] southeast of Lookout Mountain) and Graveyard Buttes (28 km [17.4 mi] southeast of Lookout Mountain) between 3.8 and 3.6 Ma (Westby, 2014). Early-phase silicic volcanism in the Gordon and Graveyard Buttes areas are considered by Westby (2014) to share geochemical and mineralogical traits consistent with petrogenesis in an intraplate or extensional setting, while late-phase silicic rocks appear to be more arc related. Intermediate to silicic volcanism between Gordon Butte and the East Fork Hood River was also contemporaneous with a more widespread pulse of high-MgO LKT mafic volcanism in the northern Oregon Cascade Range dated between 4.4 Ma and 2.1 Ma (Conrey and others, 1996; McClaughry and others, 2012, 2020a). Extrusion of LKT lavas during the late Pliocene was accompanied by Yakima Fold Belt deformation, inception of rifting along the axis of this part of the Cascade arc, and formation of the Hood River graben after 3.7 Ma (**Figure 5-2**; McClaughry and others, 2012, 2020, 2022). Foundering of the Cascade volcanic arc into a half graben during the early to

late Pliocene was accompanied by regional uplift or upwarp of the Cascade Range and formation of the modern Columbia River Gorge after 3 Ma (Tolan and Beeson, 1984; Beeson and Tolan, 1990).

5.4.3.1.2 *Age*

Pliocene volcanics in the Mill Creek area were chiefly emplaced between 4 and 3 Ma, representing part of the late High Cascade episode in this part of the High Cascades of north-central Oregon (**Figure 5-4, Figure 5-5;** Plates 1, 2, and 3). LKT basalt lava flows (**Tpbh**, **Tpbrc**, **Tpbs**) mapped along the eastern side of the Hood River graben in the Ketchum Reservoir 7.5′ quadrangle are undated, but may be as old as 4.2 Ma. The basalt of Snakehead Creek (**Tpbs**) is compositionally comparable to and shares the same stratigraphic position as the basalt and basaltic andesite of Rimrock, which directly overlies the Dalles Formation in the northeast corner of the Dog River 7.5′ quadrangle. McClaughry and others (2020a) report an $^{40}Ar/^{39}Ar$ groundmass age of 4.19 ± 0.01 Ma for the basalt and basaltic andesite of Rimrock. Within the Hood River graben, K-Ar ages range from 3.67 ± 0.17 and 3.53 ± 0.08 Ma for the basalt of Ruthton Point and the basalt of Post Canyon has an $^{40}Ar/^{39}Ar$ age of 3.05 ± 0.22 Ma (Conrey and others, 1996; McClaughry and other, 2012). Fleck and others (2014) reported an $^{40}Ar/^{39}Ar$ age of 3.548±0.03 Ma for an LKT basalt in the headwaters of Pertham Creek, west of Hood River.

Intracanyon lava flows (**Tpdf**, **Tpas**, **Tpdv**) and breccia (**Tpdd1**) mapped along Fivemile and Fifteenmile creeks also directly overly the upper Miocene and lower Pliocene Dalles Formation, with unit ages constrained by isotopic analyses reported in adjacent quadrangles. The trachydacite of Fivemile Creek (**Tpdv**) has an $^{40}Ar/^{39}Ar$ plateau age of 3.69 ± 0.02 Ma and an older K-Ar age of 3.7 ± 0.2 Ma obtained for outcrops in the Wolf Run 7.5′ quadrangle along Fivemile Creek (Anderson, 1987; McClaughry and others, 2021). The canyon-filling tuff breccia of Engineers Creek (**Tpdd1**) cropping out along Fifteenmile Creek is nearly identical in age to intracanyon trachydacite exposed along Fivemile Creek. Non-welded tuff exposed at the base of canyon-filling breccia (**Tpdd1**) in the Dufur West 7.5′ quadrangle has an $^{40}Ar/^{39}Ar$ age of 3.83 ± 0.01 Ma. A single clast obtained from the breccia (**Tpdd1**) directly overlying the tuff has an $^{40}Ar/^{39}Ar$ age of 3.71 ± 0.01 Ma (McClaughry and others, 2021). Near Friend, east of the map area, unit **Tpdd1** is interbedded with and overlain by two units, forming the tuff of Friend. The upper unit of the tuff of Friend has an $^{40}Ar/^{39}Ar$ plateau age of 3.68 ± 0.02 Ma (McClaughry and others, 2021). The youngest dated Pliocene unit in the Mill Creek area is the dacite of Fifteenmile Creek (**Tpdf**), which overlies the tuff breccia of Engineers Creek (**Tpdd1**) along Fifteenmile Creek. A sample of the dacite of Fifteenmile Creek (**Tpdf**), obtained from an outcrop in the southwest corner of the Wolf Run 7.5′ quadrangle, 3 km (1.9 mi) east of the map area, has an $^{40}Ar/^{39}Ar$ plateau age of 3.02 ± 0.02 Ma (McClaughry and others, 2021). The 3.02 Ma age is similar to a K-Ar age of 2.86 ± 0.06 Ma (sample RCS88-25) reported by Sherrod and Scott (1995) and Gray and others (1996) for a sample from the lava flow unit near Cold Point, ~0.5 km (0.3 mi) south of the map area (Flag Point 7.5′ quadrangle).

Isotopic ages on Pliocene volcanics in the Mill Creek area correspond closely to $^{40}Ar/^{39}Ar$ results for stratigraphically and age-equivalent sections mapped along the East Fork Hood River (McClaughry and others, 2020a) and those found south of the map area at Graveyard and Gordon Buttes (Westby, 2014).

5.4.4 Quaternary and Upper Pliocene volcanic and sedimentary rocks of the late High Cascades

5.4.4.1 Products of regional Quaternary volcanoes

5.4.4.1.1 *Distribution, composition, and lithology*

Pliocene and older rocks are locally disconformably overlain in the Mill Creek area by a series of upper Pliocene and Quaternary olivine-phyric basalt, basaltic andesite, and andesite lava flows (**Qran**, **Qrbr**, **Qrbs**, **Qr5dr**, **Qrbhp**, **Qrba**, **Qrbw**, **Qrbe**, **Qrbj**, **Qrbp**, **Qrbf**, **QTbk**) erupted from small volcanoes located along the eastern escarpment of the Hood River graben (**Figure 5-2**, **Figure 5-5;** Plates 1 and 2). Scott and Gardner (2017) and McClaughry and others (2020a) referred to these basaltic-to-andesitic lava flows and corresponding vents of Quaternary age surrounding Mount Hood as products of regional Quaternary volcanoes. In the Mount Hood region, Quaternary volcanic rocks crop out over a 160- km-wide (99 mi) area between the forearc Boring Volcanic Field in the Portland Basin, through the Cascade Range, and eastward to the backarc Simcoe volcanic field (Washington state)(**Figure 5-2**; Hildreth, 2007). More than 300 vents of Quaternary age lie within an ~50-km-wide (31 mi) east-west swath spanning the Columbia River, including the large composite volcanoes of Mount St. Helens, Mount Adams, and Mount Hood (**Figure 5-2**).

Mafic to intermediate volcanism was predominant along the axis of the High Cascades arc during the Quaternary, with lava flows erupting from a north-south-striking belt of volcanoes coincident with NW-striking fault strands high on the broad eastern escarpment of the Hood River graben (McClaughry and others, 2020a). Basalt and basaltic andesite (SiO_2 = 49.06 and 54.88 weight percent, avg = 52.04; K_2O = 0.24 to 1.43 weight percent, avg = 0.91; *n* = 64) compositions dominate in Quaternary lavas erupted prior to 1.87 Ma along the Dog River–Mill Creek divide (**Figure 5-13**, **Figure 5-14**). Post-1.87 Ma lavas have basaltic andesite to andesite compositions (SiO_2 = 55.34 to 59.50 weight percent, avg = 57.03; K_2O = 0.63 to 1.69, avg = 1.01; *n* = 45; (**Figure 5-13**, **Figure 5-14**). Mineralogy of regional Quaternary lavas includes plagioclase and olivine ± pyroxene.

Mafic to intermediate volcanism was predominant along the eastern escarpment of the Hood River graben at the Dog River-Mill Creek divide, just to the west of the Fivemile and Flag Point 7.5′ quadrangles during Quaternary time (**Figure 1-2;** Dog River and Badger Lake 7.5′ quadrangles; McClaughry and others, 2020a). Basalt, basaltic andesite, and andesite lavas erupted from a north-south trending belt of extant vents situated between Mill Creek Buttes and Lookout Mountain, along the broad eastern escarpment of the Hood River graben (**Qr5dr**, **Qrbhp**, **Qrba**, **Qrbw**, **Qrbe**, **Qrbj**, **Qrbp**, **Qrbf**, **QTbk**)(**Figure 5-4**, **Figure 5-5**). Vent alignments are spatially associated with NNW-trending fault strands (McClaughry and others, 2020a). Lavas flowed away from source vents down an east-sloping landscape, confined to NNE-directed drainages carved into older upper Miocene and Pliocene rocks (**Figure 5-5d;** Plate 3). These drainages were of similar location and orientation to those followed by older Pliocene intracanyon lavas (**Tpdv**, **Tpdd1**, **Tpaf, Tpdf**). Regional Quaternary lava flows also moved northwest, down into the low, fault-controlled topography of the Hood River graben along a wide drainage paralleling the modern Dog River and Puppy Creek (McClaughry and others, 2020a). The 1.87 Ma basaltic andesite of Dog River (**Qr5dr**), erupted from a fault-controlled cinder cone-capped fissure along the Dog River-Mill Creek Divide, west of the map area, at an altitude of 1,391 m (4,565 ft). It was the farthest traveled of the regional Quaternary lava flows in the Mill Creek area. Dog River lavas (**Qr5dr**) descended northeast into South Fork Mill Creek, flowing at least 26 km (16 mi) downstream to Oak Flat, near The Dalles (**Figure 5-4;** Plate 1). An

additional lobe of the basaltic andesite of Dog River (**Qr5dr**) was also directed west and northwest into the structural low of the Hood River graben (McClaughry and others, 2020a). This western lobe extended at least 6 km (3.7 mi) from the vent area to now down-faulted exposures, outcropping at an elevation of 716 m (2,350 ft) in the canyon of the modern East Fork Hood River.

At least three regional Quaternary eruptive centers and flow sequences are mapped; these forming the highlands of Fir Mountain in the Ketchum Reservoir 7.5′ quadrangle (Plate 2). These units include, from oldest to youngest, the basaltic andesite of Beaver Spring (**Qrbs**), basaltic andesite of Round Prairie (**Qrbr**), and andesite of Neal Creek (**Qran**). The older of the flow units, the basaltic andesite of Beaver Spring (**Qrbs**), erupted from a vent mapped across the northern part of Fir Mountain. The lava poured from the vent downstream to the northwest into the headwaters of Beaver Creek toward the Hood River graben (McClaughry and others, 2012); another lava flow lobe also flowed to the northeast, spreading out into the headwaters of both Indian and Mosier creeks (Plate 2). Downstream of McVey Spring, the lava flow descended into Mosier Creek as an intracanyon lava flow, extending for an additional distance of ~6 km (3.7 mi)(Plates 1 and 2). The total distance covered by the lava flow from vent to its end was ~12 km (4.6 mi). The basaltic andesite of Round Prairie (**Qrbr**) erupted from a vent forming high topography, ~2 km (1.3 mi) south of Fir Mountain. Separate lobes of the lava flow streamed away from the vent to the northwest into the headwaters of the mainstem of Neal Creek and to the northeast spreading out into the headwaters of Mosier and Spring creeks (Plate 2; McClaughry and others, 2012). The andesite of Neal Creek (**Qran**) was erupted from a vent, forming high ground east of the headwaters of the West Fork Neal Creek in the southwest corner of the Ketchum Reservoir 7.5′ quadrangle (Plate 2; McClaughry and others, 2012). The lava flowed northwest away from the vent toward the Hood River graben, where it was confined within the canyon of the West Fork of Neal Creek (McClaughry and others, 2012). Collectively, these lava flows and vents (**Qran**, **Qrbr**, **Qrbs**) form a ~4-km-long (1.5 mi) chain of aligned, southwest younging volcanoes mapped within 1 to 5 km (0.4 to 2 mi) east of the Hood River fault zone in the Upper Hood River Valley (Plate 2). These lavas have not been identified west of the Hood River fault zone but may lie buried in the subsurface beneath the Upper Hood River Valley (McClaughry and others, 2012).

Figure 5-13. Total alkalis ($Na_2O + K_2O$) vs. silica (SiO_2)(TAS) classification of upper Pliocene and lower Pleistocene mafic lava flows in the Mill Creek area from whole-rock XRF analyses (normalized to 100 percent anhydrous). Fields are from Le Bas and others (1986) and Le Maitre and others (1989). Red-dashed line is the dividing line between alkaline (above), subalkaline/tholeiitic (below) fields, after Cox and others (1979). Data shown include 121 analyses from the Middle Columbia Basin reported in this paper, Wise (1969), and McClaughry and others (2012, 2020a, 2021).

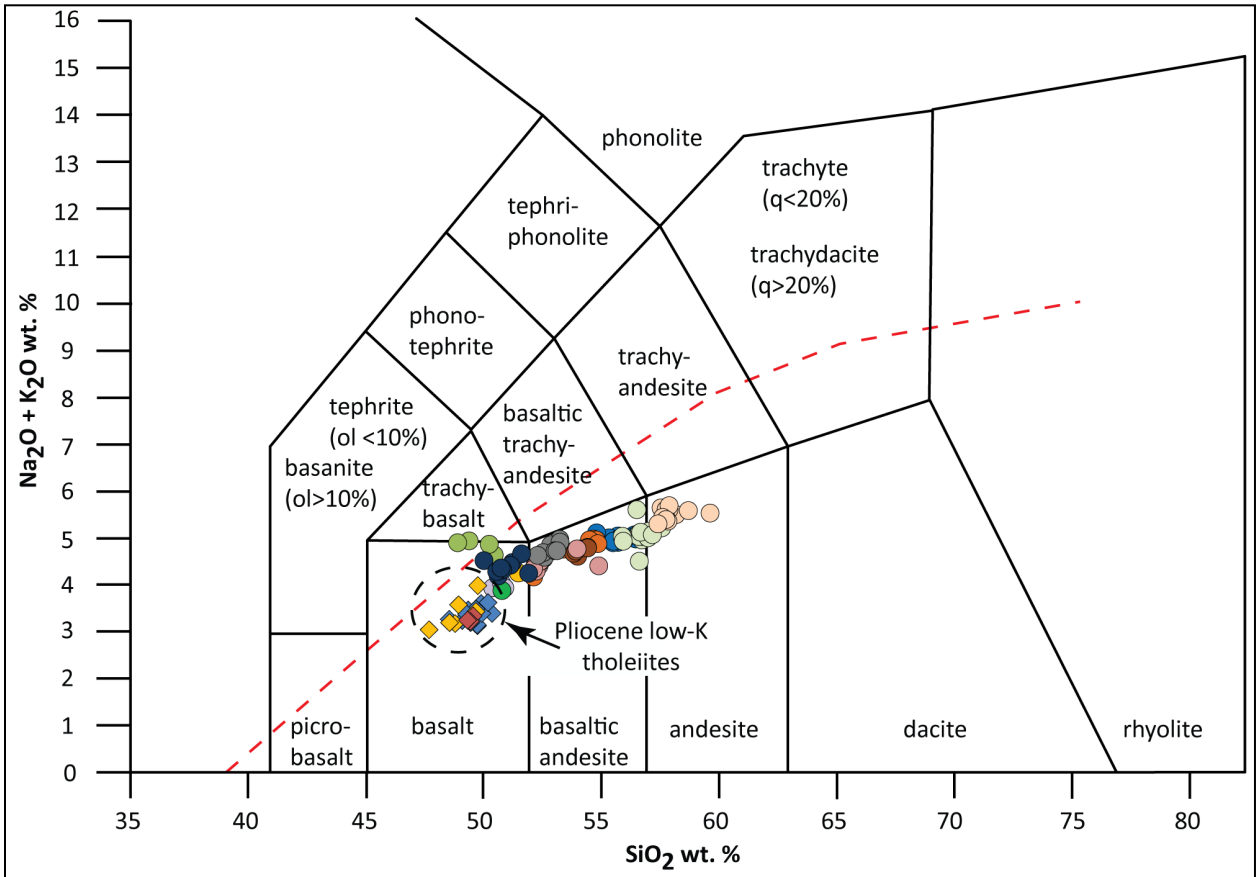

Upper Pliocene and Quaternary volcanic rocks of the Late High Cascades

- andesite of Neal Creek (Qran)
- glomeroporphyritic basaltic andesite of Round Prairie (Qrbr)
- basaltic andesite of Beaver Spring (Qrbs)
- basaltic andesite of Dog River (Qr5dr)
- basaltic andesite of High Prairie (Qrbhp)
- basalt of Agnes Spring (Qrba)
- basaltic andesite of Ward Creek (Qrbw)
- basalt of Hesslan Canyon (Qrbe)
- basalt of Jacket Springs (Qrbj)
- basalt of Bennett Pass Road (Qrbp)
- basaltic andesite of Flag Point (Qrbf)
- basalt of Knebal Spring (QTbk)

Pliocene low-potassium tholeiitic (LKT) basalt lava flows of the Late High Cascades

- basalt of Hood River (Tpbh)
- basalt of Rock Creek (Tpbrc)
- basalt of Snakehead Creek (Tpbs)

Figure 5-14. Chemical variation diagrams for upper Pliocene and lower Pleistocene mafic lava flows in the Mill Creek area. (a) Total iron/magnesium (FeOTotal/MgO) versus silica (SiO_2). Tholeiitic/calc-alkaline dividing line after Miyashiro (1974). (b) Titanium (TiO_2) versus silica (SiO_2). (c) Magnesium (MgO) versus silica (SiO_2). (d) Potassium (K_2O) versus silica (SiO_2). Classification boundaries distinguishing low-, medium-, and high-potassium (K_2O) rocks in (d) are from Peccerillo and Taylor (1976). Data shown include 121 analyses from the Middle Columbia Basin reported in this paper, Wise (1969), and McClaughry and others (2012, 2020a, 2021).

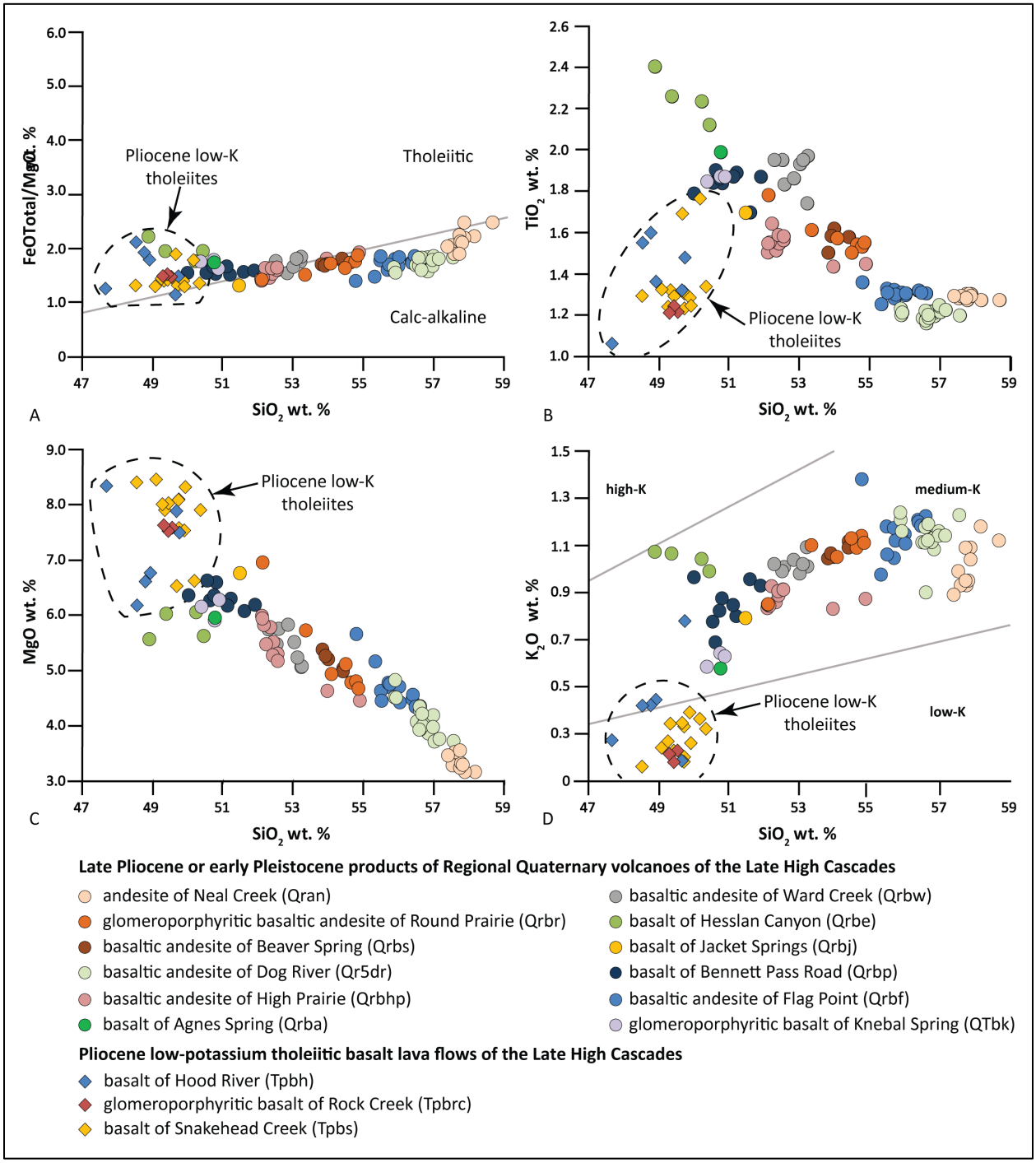

5.4.4.1.2 *Age*

Lava flows capping the eastern escarpment of the Hood River graben are assigned a latest-Pliocene or Quaternary age on the basis of intracanyon geomorphic setting, spatial and temporal association with still present cinder cones, and isotopic ages. Isotopic ages obtained outside the map area include an $^{40}Ar/^{39}Ar$ age of 2.57 ± 0.02 Ma for the basaltic andesite of Flag Point (**Qrbf**)(McClaughry and others, 2021) and a K-Ar age of 2.35 ± 0.03 Ma for the basalt of Bennett Pass Road (**Qrbp**)(McClaughry and others, 2020a). The basaltic andesite of Dog River (**Qr5dr**) has an $^{40}Ar/^{39}Ar$ plateau age of 1.87 ± 0.02 Ma along Dog River-Mill Creek divide, west of the map area (McClaughry and others, 2020a). Anderson (1987) reported a similar, but less precise K-Ar age of 1.7 ± 0.4 Ma (whole-rock, sample JA85023) for the basaltic andesite of Dog River (**Qr5dr**) along South Fork Mill Creek (Plate 1). Emplacement of Quaternary lava flows predates erosion that carved the modern canyons in the Mill Creek area.

5.4.5 Upper Cenozoic surficial deposits

5.4.5.1 Holocene and Upper Pleistocene surficial deposits

5.4.5.1.1 *Distribution, composition, and lithology*

Much of the Mill Creek area is covered by unconsolidated or only slightly indurated sedimentary units, including windblown loess (**Qlo**), glacial deposits (**Qgot**), Missoula flood deposits (**Qmfs**), alluvial deposits (**Qa, Qao**), and valley fringing landslides (**Qls**), colluvium (**Qc**), fan deposits (**Qaf**), and modern fill and construction material (**Qf**)(**Figure 5-5**; Plates 1, 2, and 3).

Plateaus in the southeast part of the Brown Creek 7.5′ quadrangle are capped by a variably thick and discontinuous blanket of Pleistocene loess (**Qlo**) that accumulated by episodic deposition of airborne silts by southwesterly winds during the Quaternary (Plate 1; McDonald and others, 2012). Over the last century, loess deposits (**Qlo**) have been extensively modified by dryland agriculture.

Glacial deposits are mapped chiefly in the southwest part of the Mill Creek area and consist of till and minor outwash forming ground or lateral moraines that obscure underlying lava flows (Plate 3). Undifferentiated till (**Qgot**) forms muted moraines, filling small valleys and cirques, and capping older bedrock (Plate 3). Older till deposits (**Qgot**) are typically poorly exposed and may include till of several glaciations.

The drainages of Mill Creek, Brown Creek, and Chenoweth Creek in the northeast part of the Brown Creek 7.5′ quadrangle contain unconsolidated gravel, sand, and silt (**Qmfs**), deposited by the Late Pleistocene Missoula Floods (Plate 1). These deposits are interpreted as those left behind by repeated Missoula Floods that flowed west down the Columbia River Gorge, when glacial dams in the upper Columbia River drainage failed catastrophically. As the floods passed the mouths of Mill and Chenoweth creeks at The Dalles, floodwaters backed up into these Columbia River tributaries (Plate 1). O'Connor and others (2020) reported that the maximum water stage in the Dalles basin, including the Mill Creek area, was 340 m (1,115 ft). Floodwaters stretched at least 11 km (6.8 mi) up Mill Creek from the Columbia River at The Dalles; the maximum extent of flood deposits mapped in the upper part of Mill Creek is 213 m (700 ft). Floodwaters reached at least 7 km (4.3 mi) up Chenoweth Creek from the Columbia River at The Dalles, and an additional 5.5 km (3.4 mi) up the tributary of Brown Creek; the maximum extent of flood deposits mapped in the upper part of Brown Creek is 260 m (850 ft). Missoula Flood sands and silts have a Columbia Basin provenance and are composed primarily of quartz, feldspar, ferromagnesian minerals, and mica, with varying amounts of clay. Deposits locally enclose isolated pebbles, cobbles, and boulders

of volcanic, granitic, and metamorphic lithologies exotic to The Dalles area that were dropped by melting icebergs as floodwaters receded (Allison, 1935; Newcomb, 1969; Benito and O'Connor, 2003).

Upper Pleistocene and Holocene surficial units have accumulated on steep slopes and in valley bottoms in the Mill Creek area, including stream alluvium (**Qa, Qao**), fan deposits (**Qaf**), landslide deposits (**Qls**), and colluvium (**Qc**)(Plates 1, 2, and 3). These units reflect Late Pleistocene and younger landscape adjustments as major drainages have continued to incise into bedrock units. In the Mill Creek area, streams and landforms are adjusting to late Quaternary variations in climate, young faulting (after 3 Ma), changes in base level at the Columbia River, and land-use changes. These geomorphic adjustments are further complicated by the presence of alternating hard and soft rock in the subsurface as well as nesting of Pliocene and Quaternary intracanyon lava flows within older bedrock units.

5.4.5.1.2 *Age*

Surficial deposits in the Mill Creek area largely range in age from the Middle-Late Pleistocene to upper Holocene, but age constraints are few. Most surficial deposits postdate the emplacement of widespread loess (**Qlo**). Loess deposits in the eastern Middle Columbia Basin are assigned a Middle to Late Pleistocene age on the basis of stratigraphic position and may be as old as ~600 ka. Medley (2012) interpreted loess deposits and Missoula flood deposits exposed along U.S. Highway 197 between Dufur and The Dalles to lie above a series of older paleosols that contain pumice correlated to the ~600 ka Dibekulewe tuff from Nevada (Cordero, 1997). Pluhar and others (2014) reported paleomagnetically reversed paleosols at the base of the U.S. Highway 197 section, so loess in this area may in some places be older than 780 ka.

Older glacial till (**Qgot**) may include deposits of several glaciations, with no age constraints in the Mill Creek area. On the basis of comparison to glacial sequences elsewhere in the Pacific Northwest, parts of the unit **Qgot** could be as young as marine oxygen isotope stage 6 (about 150 ka) (Scott and Gardner, 2017).

Geochronology for Missoula flood deposits, established through radiocarbon dating, tephrochronology, optically stimulated luminescence dating, and stratigraphic relationships, indicates passage of multiple cataclysmic floods through the Columbia River Gorge largely after 23 ka and prior to 14.5 Ma (age in calendar years; O'Connor and others, 2020, 2021). The largest floods through the Gorge post-date humates from a soil clast that gave a calibrated age of 23.4 to 22.5 ka; dates from detrital organic materials in gravel flood bars are as young as 16.9 to 16.2 ka (Benito and O'Connor, 2003; O'Connor and others, 2020). Missoula flood deposits both predated and postdated the ~16 ka Mount Saint Helens Set S tephra (Berger and Busacca, 1995; Benito and O'Connor, 2003; O'Connor and others, 2020). All Missoula floods preceded the eruption of the 13.7 to 13.5 ka Glacier Peak tephra (Kuehn and others, 2009; O'Connor and others, 2020).

Alluvial (**Qa, Qao**, **Qaf**), colluvial (**Qc**), and landslide deposits (**Qls**) are largely Holocene in age with older deposits extending back into the Late Pleistocene. Absolute age constraints are few.

6.0 EXPLANATION OF MAP UNITS

This chapter describes the basis for subdividing rocks into stratigraphic units on the geologic maps shown on Plates 1, 2, and 3. A time-rock chart graphically displaying age ranges and relations for the 52 upper Cenozoic bedrock and surficial map units is shown in **Figure 6-1** and on Plates 1, 2, and 3. Unit names follow formal stratigraphic names or local stratigraphic nomenclature when available; informal names are given on the basis of composition or sites of good exposure when formal rock names are lacking.

Formal stratigraphic names have been established only for the CRBG; those rocks are assigned to units following conventions established by Swanson and others (1979b), Tolan and others (1989, 2009a) and Reidel and others (2013a). The Dalles Formation is formally named, but separate strata within the formation are only informally named. Few Cascade Range units have been formally named, and none in the map area.

Late Miocene to Holocene Cascade volcanic rocks in the Mill Creek area are subdivided here on the basis of conventions established by Peck and others (1964), Priest and others (1983), Priest (1990), and Conrey and others (1997) for rocks of the Cascade Range. Priest and others (1983) divided rocks of the Western Cascades into four time-stratigraphic units on the basis of apparent time-breaks that generally correspond to regional compositional changes. These time-stratigraphic intervals include: 1) an early Western Cascade episode at ~40 to 18 Ma; 2) a late Western Cascade episode at ~18 to 9 Ma; 3) an early High Cascade episode at ~9 to 4 Ma; and 4) a late High Cascade episode at ~4 Ma to present. Rocks of the late Miocene to early Pliocene-aged Dalles Formation correspond to volcanism during the early High Cascades episode at ~9 to 4 Ma, while younger Pliocene to Holocene volcanic rocks are considered part of the ~4 Ma to present late High Cascades episode. CRBG lava flows are temporally correlative with the late Western Cascade episode but are not included within this time-stratigraphic unit, as they were erupted from distant vents located in northeast Oregon and southeast Washington (**Figure 5-6**).

6.1 Overview of map units

UPPER CENOZOIC SURFICIAL DEPOSITS

Qf modern fill and construction material (upper Holocene)
Qa alluvium (Holocene and Upper Pleistocene)
Qaf fan deposits (Holocene and Upper Pleistocene)
Qls landslide deposits (Holocene and Upper Pleistocene)
Qc colluvium (Holocene and Upper Pleistocene)
Qmfs Missoula flood deposits (Upper Pleistocene)
Qao older alluvium (Holocene and Upper Pleistocene)
Qlo loess (Holocene and Pleistocene)
Qgot older till (Middle Pleistocene[?])

Unconformity

UPPER CENOZOIC VOLCANIC AND SEDIMENTARY ROCKS

QUATERNARY AND UPPER PLIOCENE VOLCANIC AND SEDIMENTARY ROCKS OF THE LATE HIGH CASCADES

Products of regional Quaternary volcanoes

Volcanics of Fir Mountain

Qran andesite of Neal Creek (lower Pleistocene)
Qrbs basaltic andesite of Beaver Spring (lower Pleistocene)
Qrbr basaltic andesite of Round Prairie (lower Pleistocene)
Qgc gravel (lower Pleistocene)
Qr5dr basaltic andesite of Dog River (lower Pleistocene)

1.87 ± 0.01 Ma ($^{40}Ar/^{39}Ar$; outside Mill Creek area); 1.7 ± 0.4 Ma (K-Ar)

Qrbhp basaltic andesite of High Prairie (lower Pleistocene)

Qrba basalt of Agnes Spring (lower Pleistocene)

Qrbw basaltic andesite of Ward Creek (lower Pleistocene)

Qrbe basalt of Hesslan Canyon (lower Pleistocene)

Qrbj basalt of Jacket Springs (lower Pleistocene)

Qrbp basalt of Bennett Pass Road (lower Pleistocene)
2.35 ± 0.03 Ma (K-Ar; outside Mill Creek area)

Qrbf basaltic andesite of Flag Point (lower Pleistocene or upper Pliocene)
2.57 ± 0.02 Ma ($^{40}Ar/^{39}Ar$; outside Mill Creek area)

QTbk basalt of Knebal Spring (lower Pleistocene[?] or upper Pliocene[?])

Disconformity

PLIOCENE VOLCANIC AND SEDIMENTARY ROCKS OF THE LATE HIGH CASCADES

QTpg sedimentary deposits (lower Pleistocene and/or upper Pliocene)

Tpdf dacite of Fifteenmile Creek (upper Pliocene)
3.02 ± 0.02 Ma ($^{40}Ar/^{39}Ar$; outside Mill Creek area); 2.86 ± 0.06 Ma (K-Ar; outside Mill Creek area)

Tpaf andesite of Fret Creek (upper Pliocene)

Tpbh basalt of Hood River (upper Pliocene)

Tpdd1 tuff breccia of Engineers Creek, lower unit (lower Pliocene)
3.71 ± 0.02 Ma ($^{40}Ar/^{39}Ar$; clast; outside Mill Creek area); 3.83 ± 0.02 Ma ($^{40}Ar/^{39}Ar$; basal tuff; outside Mill Creek area)

Tpdv trachydacite of Fivemile Creek (lower Pliocene)
3.69 ± 0.01 ($^{40}Ar/^{39}Ar$); 3.7 ± 0.2 Ma (K-Ar; outside Mill Creek area)

Tpbrc basalt of Rock Creek (lower Pliocene)

Tpbs basalt of Snakehead Creek (lower Pliocene)

Disconformity

LOWER PLIOCENE AND UPPER MIOCENE VOLCANIC AND SEDIMENTARY ROCKS OF THE EARLY HIGH CASCADES

Dalles Formation

Tmdl Dalles Formation, undivided (lower Pliocene[?] and upper Miocene)

Tmdj dacite of Jordan Butte (lower Pliocene or upper Miocene)
5.28 ± 0.5 Ma (K-Ar; outside Mill Creek area)

Tmde andesite and dacite of East Fork (upper Miocene)
7.15 ± 0.8 Ma, 8.18 ± 0.06 Ma (K-Ar; outside Mill Creek area)

Mill Creek Buttes

Tmdh hornblende-porphyritic microdiorite of Mill Creek Buttes (upper Miocene)

Tmdf dacite of Fivemile Butte, upper flow (upper Miocene)

Tmdv dacite of Fivemile Butte, lower flows and domes (upper Miocene)
7.71 ± 0.17 Ma (K-Ar)

Tmds dacite of South Fork Fivemile Creek (upper Miocene)

Tmdw dacite of Wolf Run (upper Miocene)
7.91 ± 0.08 Ma ($^{40}Ar/^{39}Ar$; outside Mill Creek area); 8.2 ± 0.8 Ma (K/Ar)

Tmdb dacite of Bulo Point (upper Miocene)

Tmdd tuff breccia of Fifteenmile Creek (upper Miocene)
8.75 ± 0.05 Ma ($^{40}Ar/^{39}Ar$; clast; outside Mill Creek area)

Angular unconformity to disconformity

MIDDLE AND LOWER MIOCENE VOLCANIC AND SEDIMENTARY ROCKS

COLUMBIA RIVER BASALT GROUP

Saddle Mountains Basalt

Tsp Pomona Member (late Miocene) 11.21 ± 0.42 Ma ($^{40}Ar/^{39}Ar$; outside Mill Creek area)

Disconformity to angular unconformity(?)

Wanapum Basalt

Priest Rapids Member

Twpl Basalt of Lolo (middle Miocene)

Twpr Basalt of Rosalia (middle Miocene)

Frenchman Springs Member

Twfs Basalt of Sentinel Gap (lower Miocene)

Twfh Basalt of Sand Hollow (lower Miocene)

Twfg Basalt of Ginkgo (lower Miocene) 16.12 ± 0.05 Ma ($^{40}Ar/^{39}Ar$; outside Mill Creek area)

Disconformity

Grande Ronde Basalt

Normal-polarity (N2) magnetostratigraphic unit

Tgsb Sentinel Bluffs Member (lower Miocene) 16.135 ± 0.04 Ma; 16.15 ± 0.07 Ma ($^{40}Ar/^{39}Ar$; outside Mill Creek area)

Tgww Winter Water Member (lower Miocene)

Tgo Ortley member (lower Miocene)

Reversed-polarity (R2) magnetostratigraphic unit

Tggc Grouse Creek member (lower Miocene)

Undivided Grande Ronde Basalt

Tgu Grande Ronde Basalt, undivided (lower Miocene) (cross section only)

OTHER ROCKS

QTfb Fault breccia (upper Pleistocene[?] to lower Miocene)

Figure 6-1. Time-rock chart showing the 52 geologic units portrayed on the geologic maps and in geologic cross sections on Plates 1, 2, and 3. Note that the depth of exposure in the map area does not extend beneath the Grouse Creek Member (Tggc).

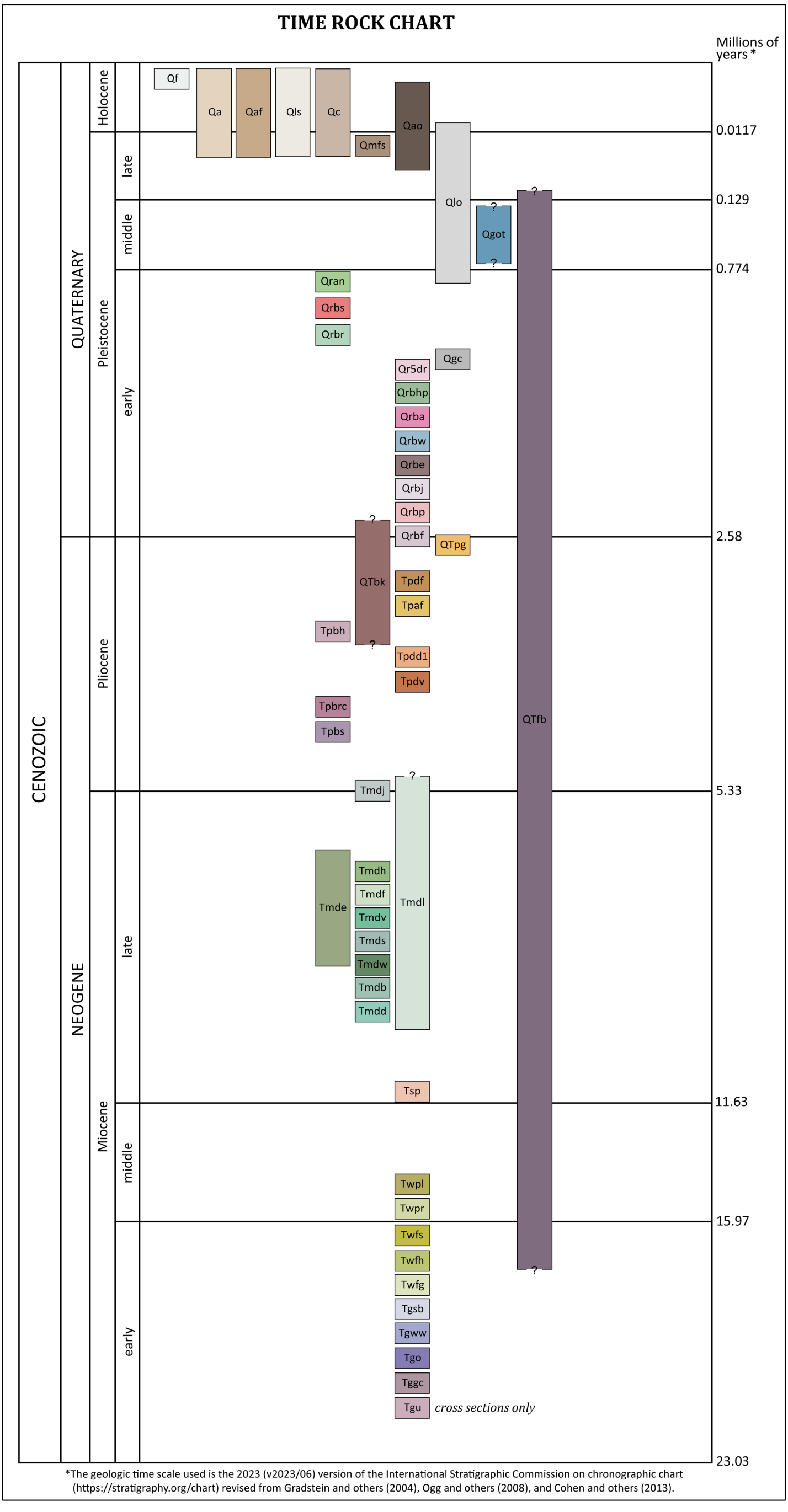

*The geologic time scale used is the 2023 (v2023/06) version of the International Stratigraphic Commission on chronographic chart (https://stratigraphy.org/chart) revised from Gradstein and others (2004), Ogg and others (2008), and Cohen and others (2013).

6.2 Upper Cenozoic surficial deposits

Qf **modern fill and construction material (upper Holocene)**—Artificial or constructed fill deposits of poorly sorted and crudely layered mixed gravel, sand, clay, and other engineered fill (Plates 1, 2, and 3). These deposits usually contain rounded to angular clasts ranging from small pebbles up to several meters across. The orientation of clasts is typically less uniform than is found in naturally occurring imbricated or bedding-parallel gravel. Older fills are likely uncompacted versus newer fills, which are likely engineered and reinforced using geotextiles or retaining structures. Deposits mapped as modern fill and construction material in the map area are generally associated with road embankments, causeways, culvert fills, and mined land (Plates 1, 2, and 3). The thickness of fill deposits may exceed 30 m (98 ft). **Qf** is assigned a late Holocene age (**Figure 6-1**).

Qa **alluvium (Holocene and Upper Pleistocene)**—Unconsolidated, poorly to moderately stratified gravel and sand along streams (Plates 1, 2, and 3). Thickness of **Qa** is generally ≤5 to 7 m (16 to 23 ft); bedrock units may be locally exposed in the base of stream channels within areas mapped as **Qa**. **Qa** is assigned a Late Pleistocene and Holocene age on the basis of stratigraphic position and a lack of more precise age indications (**Figure 6-1**). Areas mapped as **Qa** are known to have been inundated by record floods during 1861, 1964, 1974, 1996, and 2006 (Plates 1, 2, and 3). They may include deposits containing human-made debris or artifacts, or deposits filling areas known to have been modified by humans such as excavations, roadways, or gravel pits.

Qaf **fan deposits (Holocene and Upper Pleistocene)**—Unconsolidated, poorly sorted deposits of boulders, cobbles, pebbles, granules, sand, silt, and clay in upland drainages and as fan-shaped accumulations at the transition between low-gradient valley floodplains and steeper uplands (Plates 1, 2, and 3). **Qaf** may locally include debris flow deposits and talus from rockfall in steep drainages. Individual fans (generally cover ≤4 hectares (10 acres). The local thickness of alluvial fan deposits is variable but is probably ≤15 m (50 ft). **Qaf** includes fan deposits of Late Pleistocene and Holocene age (**Figure 6-1**).

Qls **landslide deposits (Holocene and Upper Pleistocene)**—Unconsolidated masses of rock and soil deposited by landslides (e.g., slumps, slides, debris flows, rock avalanches; Plates 1, 2, and 3). **Qls** in the map area typically consist of individual slide masses covering ≤45 hectares (111 acres) and more typically ≤6 hectares (≤15 acres). A majority of mapped **Qls** are simple slump or shallowly-seated earthflow-type features that occur along major drainages associated with Pliocene and younger intracanyon lava flows inset into sparsely vegetated, moderately to steep slopes underlain by weakly consolidated rocks of the Dalles Formation (Plates 1, 2, and 3). **Qls** locally includes rockfalls, large talus piles, shallow-seated landslides of colluvium, debris flow deposits, and more deeply-seated bedrock slides. Thickness of **Qls** is highly varied, but may be more than several tens of meters in larger deposits. **Qls** range in age from Late Pleistocene, relatively stable features, to those that have been recurrently active in relatively recent time (**Figure 6-1**). **Qls** are typically referred to as clay, boulders, rock, or rock and clay in water-well logs.

Qc **colluvium (Holocene and Upper Pleistocene)**—Unconsolidated poorly sorted deposits of rock and soil deposited along valley walls and as fans and aprons of debris at the foot of steep slopes (Plates

1, 2, and 3). **Qc** locally includes now completely vegetated talus deposits, debris flow deposits, and coarse-grained alluvium. Thickness of **Qc** is highly varied; maximum thickness is several meters. **Qc** is assigned a Late Pleistocene and Holocene age on the basis of stratigraphic position (**Figure 6-1**).

Qmfs **Missoula flood deposits (Upper Pleistocene)**—Medium gray (N5) to grayish yellow (5Y 8/4), horizontally bedded, massive to interstratified, fine-grained sand, silt, and clay mapped unconformably over the Dalles Formation (**Tmdl**) along the valleys of Brown Creek, Chenoweth Creek, and Mill Creek (**Figure 6-2**; Plate 3). **Qmfs** have a Columbia Basin provenance and are composed primarily of quartz, feldspar, ferromagnesian minerals, and mica, with varying amounts of clay. Deposits locally enclose isolated pebbles, cobbles, and boulders of volcanic, granitic, and metamorphic lithologies exotic to the Mill Creek area that were dropped by melting icebergs as floodwaters receded (Allison, 1935; Newcomb, 1969; Gannett and Caldwell, 1998; O'Connor and others, 2001; Benito and O'Connor, 2003). **Qmfs** are as thick as 55 m (180 ft) in the map area. The maximum elevation of **Qmfs** is ~260 m (850 ft) along Brown Creek, 213 m (700 ft) along Mill Creek, and 183 m (600 ft) along Chenoweth Creek. **Qmfs** has been extensively eroded by receding floodwaters and incision of modern streams (Plate 3). Land associated with **Qmfs** is used for agriculture in the form of dryland wheat, vineyards, and orchards (**Figure 6-2**).

Qmfs are assigned a Late Pleistocene age on the basis of stratigraphic position and isotopic ages. Geochronology for Missoula flood deposits established through radiocarbon dating, tephrochronology, and stratigraphic relations indicates passage of multiple cataclysmic floods through the Columbia River Gorge between ~20 ka and 14 ka (O'Connor and others, 2020).

Figure 6-2. Missoula flood deposits in the Brown Creek area. An unconsolidated, well-sorted, quartz-feldspar-mica sand and silt (Qmfs) mapped near the intersection of Brown Creek Road and Chenoweth Road (45.61202, -121.26386). View is looking northeast. Scale bar is 1 m (3.3 ft) high. Photo credit: Clark Niewendorp, 2016.

Qao **older alluvium (Holocene and Upper Pleistocene)**—Unconsolidated, well to poorly sorted, stratified gravel, sand, silt, and clay mapped along Fifteenmile Creek and smaller tributary streams. Thickness of **Qao** is ≤6 m (20 ft). **Qao** is assigned a Late Pleistocene and Holocene age on the basis of stratigraphic position (**Figure 6-1**).

Qlo **loess (Holocene and Pleistocene)**—Pale yellowish brown (10YR 6/2), micaceous, quartzo-feldspathic silt and minor amounts of very fine-grained sand and clay mantling uplands in the southeast part of the Brown Creek 7.5′ quadrangle (Plate 1). **Qlo** typically forms a massive, featureless deposit that has been extensively modified by dryland agriculture over the past century. Where the antecedent deposit was originally thin or has been further thinned by tilling, silt may be mixed with larger rock fragments from the underlying bedrock geology. Commonly, the edges of wheatfields constructed in **Qlo** are characterized by steep 1- to 2-m-high (3.3 to 6.5 ft) embankments created from circular, annual tilling of large fields. Long-term residents of the area report that annual tilling in the same circular direction has led to often thicker accumulations of **Qlo** along the outer edges of fields, in places removing the entire thickness of the unit near the center of fields. Thickness of **Qlo** ranges from thin veneers <1 m (3.3 ft) to as much as 6 m (20 ft), on the basis of information reported from well logs; roadcuts may locally show up to 5 m (16.4 ft) of loess in vertical section.

The distribution of **Qlo**, as mapped here, has been determined on the basis of a combination of field observations, soils mapping by Green (1982), geologic mapping by Waters (1968), 1-m lidar DEMs, and 2014 and 2018 National Agriculture Imagery Program orthophotos (Plate 1). The distribution portrayed generally follows divisions in the soils map of Green (1982). Areas that Green (1982) described as dominantly silt or silty loam and that are of significant thickness to conceal the underlying bedrock geology have been mapped as **Qlo**; areas identified as mixtures of silt and rock (e.g., cobbly loam) have been mapped as part of the underlying bedrock geology. Most of the contacts portrayed represent human-modified boundaries, such as field edges, where silt-dominated deposits lie adjacent to or surround rock areas of mixed grain size. Thin and small **Qlo** deposits have not been mapped where the underlying geology can be reasonably inferred or is known to be present at the surface.

The distribution of **Qlo** across this part of the Columbia Plateau indicates episodic deposition by southwesterly winds (McDonald and others, 2012). **Qlo** deposits in the eastern Middle Columbia Basin are assigned a Pleistocene and Holocene age on the basis of stratigraphic position and may be as old as ~600 ka (**Figure 6-1**). Medley (2012) interprets loess deposits and Missoula flood deposits exposed along U.S. Highway 197 between Dufur and The Dalles to lie above a series of older paleosols that contain pumice correlated to the ~600 ka Dibekulewe tuff from Nevada (Cordero, 1997). Pluhar and others (2014) reported paleomagnetically reversed paleosols at the base of U.S. Highway 197 section, so loess in that area may be older than 780 ka.

Qgot **older till (middle Pleistocene[?])**—Unconsolidated, very poorly sorted glacial till preserved above an elevation of 1402 m (4,600 ft) in the cirque basin drained by upper Fifteenmile and Fret Creeks in the northwest part of the Flag Point 7.5′ quadrangle (Plate 3). **Qgot** contains very poorly sorted, angular to subrounded pebbles, cobbles, and boulders in a fine-grained silty sand matrix. Many clasts are faceted into crude pentagonal shapes and some are striated. Till may locally be complexly interbedded with poorly sorted silt, sand, and gravel. **Qgot** lies above and can obscure older bedrock. Well-weathered till deposits may display argillic B horizons tens of centimeters thick with weathering rinds 1 mm (0.04 in) or thicker on fine-grained clasts.

Glacial deposits are typically poorly exposed and may include tills of several glaciations. Age constraints are few. Older till could be as young as marine oxygen isotope stage 6 (about 150 ka) (Scott and Gardner, 2017; **Figure 6-1**). **Qgot** till was chiefly deposited in ground or lateral moraines.

Unconformity

6.3 Upper Cenozoic volcanic and sedimentary rocks

6.3.1 Quaternary and upper Pliocene and volcanic and sedimentary rocks of the late High Cascades

6.3.1.1 Products of regional Quaternary volcanoes

6.3.1.1.1 *Volcanics of Fir Mountain*

Qran **andesite of Neal Creek (lower Pleistocene)**—Andesite lava flow (SiO_2 = 57.42 to 59.62 weight percent; K_2O = 0.89 to 1.18 weight percent; *n* = 12 analyses [6 outside Mill Creek area]) mapped in the headwaters of Mosier and West Fork Neal Creek (**Figure 6-3**; **Table 6-1**; Plate 2; **Appendix**). **Qran** outcrops are characterized by broad blocky columns ≤3 m (9.8 ft) across and zones of platy jointing (**Figure 6-3**). Thickness of **Qran** is as much as 60 m (200 ft) in the headwaters of West Fork Neal Creek (Parkdale 7.5′ quadrangle; McClaughry and others, 2012). Typical hand samples are medium-to-light gray (N6) and aphyric to sparsely porphyritic, containing ≤1 percent (vol.) colorless, euhedral, prismatic, seriate plagioclase phenocrysts ≤3.5 mm (0.1 in) contained within a fine-grained hypocrystalline groundmass (**Figure 6-4**). Groundmass olivine occasionally displays areas or rims of dark yellowish orange (10YR 6/6) iddingsite (**Figure 6-4b,c**). Glomerocrysts are present but are rare. Thin bands of submillimeter, irregular vesicles define diktytaxitic intervals throughout the unit.

Qran has reversed magnetic polarity and is assigned an early Pleistocene age (**Figure 6-1**; Plate 2; **Appendix**). Reversed polarity indicates an age older than 0.773 Ma. **Qran** was erupted from a vent that formed high topography between the headwaters of West Fork Neal Creek and Mosier Creek (Plate 2). The lava flow flowed northwest ~5 km (3.1 mi) from the vent, confined within the canyon of West Fork of Neal Creek (Plate 2; McClaughry and others, 2012).

Figure 6-3. Typical weathered blocky outcrop of the andesite of Neal Creek (Qran) just west of the map area in the Parkdale 7.5' quadrangle (45.54199, -121.52262). Automobile for scale. View is looking northwest. Photo credit: Jason McClaughry, 2011.

Table 6-1. Representative XRF analyses for regional Quaternary lava flows in the Mill Creek area.

Sample	RC 99-3	RC12 289 HRJ 11	KRL15-118	644 MCBJ 16	638 MCBJ 16[1]	JM DR 13-31[1]	RC98-186	179 DWFJ 15	RC98-192	403 MCBJ 16	695 MCBJ 16	456 MCBJ 16
Geographic Area	West Fork Neal Creek	Ketchum Reservoir	Ketchum Reservoir	South Fk. Mill Creek	Bottle Prairie	Agnes Spring	Knebal Spring	Bottle Prairie	Jacket Springs	Bottle Prairie	Frailey Point	Knebal Spring
Formation	Regional volcano	Regional volcano	Regional volcano	Regional volcano	Regional volcano	Regional volcano	Regional volcano	Regional volcano	Regional volcano	Regional volcano	Regional volcano	Regional volcano
Map Unit	Qran	Qrbs	Qrbr	Qr5dr	Qrbhp	Qrba	Qrbw	Qrbe	Qrbj	Qrbp	Qrbf	QTbk
Latitude	45.5110	45.5576	45.5230	45.4691	45.4059	45.3944	45.4364	45.3981	45.3878	45.3971	45.3565	45.4426
Longitude	-121.4973	-121.4285	-121.4756	-121.4615	-121.5167	-121.5008	-121.4665	-121.4916	-121.4780	-121.4971	-121.4300	-121.4686
Age (Ma)	nd	nd	nd	1.87 Ma	nd	nd	nd	nd	nd	2.35 Ma	2.57 Ma	nd
Plate	2	2	2	3	na	na	3	3	3	3	3	3
Map Label	G10	G57	G29	G69	na	na	G55	G30	G25	G29	G6	G58
Oxides, weight percent												
SiO_2	57.88	53.91	53.35	56.75	53.97	50.77	52.29	49.37	51.47	51.12	56.01	50.76
Al_2O_3	18.31	17.32	17.22	18.32	18.15	18.68	17.46	16.81	17.53	17.09	17.64	16.93
TiO_2	1.29	1.58	1.61	1.22	1.43	1.99	1.95	2.26	1.69	1.87	1.30	1.87
FeOTotal	7.19	8.85	8.68	6.98	8.39	10.39	9.39	11.74	8.94	10.32	7.90	10.56
MnO	0.12	0.15	0.14	0.12	0.14	0.16	0.15	0.18	0.15	0.17	0.14	0.17
CaO	6.28	7.81	8.16	7.22	8.26	7.81	8.04	8.20	8.95	8.50	7.14	9.57
MgO	2.89	5.23	5.69	4.09	4.60	5.92	5.71	5.99	6.73	6.14	4.67	5.87
K_2O	1.04	1.07	1.10	1.13	0.83	0.58	1.02	1.06	0.79	0.85	1.15	0.64
Na_2O	4.65	3.66	3.66	3.92	3.94	3.30	3.61	3.88	3.46	3.57	3.84	3.39
P_2O_5	0.36	0.42	0.39	0.26	0.30	0.41	0.38	0.49	0.28	0.38	0.22	0.24
LOI	nd	nd	nd	0.45	2.87	0.28	Nd	nd	nd	0.61	0.38	0.16
Total_I	nd	97.85	99.17	99.08	96.79	99.16	Nd	nd	nd	98.72	98.94	99.18
Trace Elements, parts per million												
Ni	20	82	94	51	48	48	80	79	110	97	71	70
Cr	28	138	141	60	66	59	110	105	129	147	103	149
Sc	17	22	22	19	20	18	16	24	27	23	18	26
V	117	171	180	163	160	163	165	185	206	200	152	223
Ba	295	411	389	321	274	348	212	221	188	249	300	190
Rb	12	11	15	17	11	17	7	10	8	10	16	9
Sr	605	642	737	767	680	786	485	516	457	513	502	516
Zr	195	203	166	159	146	158	192	218	133	154	154	112
Y	25	50	24	22	21	23	30	33	24	27	20	28
Nb	15.7	16.9	14.4	9.4	11.3	8.6	17.8	21.2	11.7	13.6	9.1	9.2
Ga	19	21	19	20	20	20	20	21	20	20	20	19
Cu	42	45	33	31	47	50	51	50	55	47	40	46
Zn	94	98	90	71	81	73	103	113	85	98	84	94
Pb	3	5	3	3	3	5	1	2	2	3	6	1
La	20	32	25	19	15	18	11	23	1	17	15	13
Ce	48	51	51	49	33	45	54	47	48	36	34	29
Th	1	3	2	3	2	4	1	2	1	2	4	0
Nd	0	33	27	27	20	26	0	29	0	23	17	18
U	0	0	0	2	3	1	0	0	0	3	1	1

Figure 6-4. Hand sample and thin section photographs of the andesite of Neal Creek (Qran). (a) Typical hand sample. Scale bar is 2.5 cm (1 in) . (b) Thin section under cross-polarized light. (c) Same view as in (b) under plane-polarized light. Scale bar in (b) and (c) is 7 mm (0.3 in). Photo credits: Jason McClaughry, 2016.

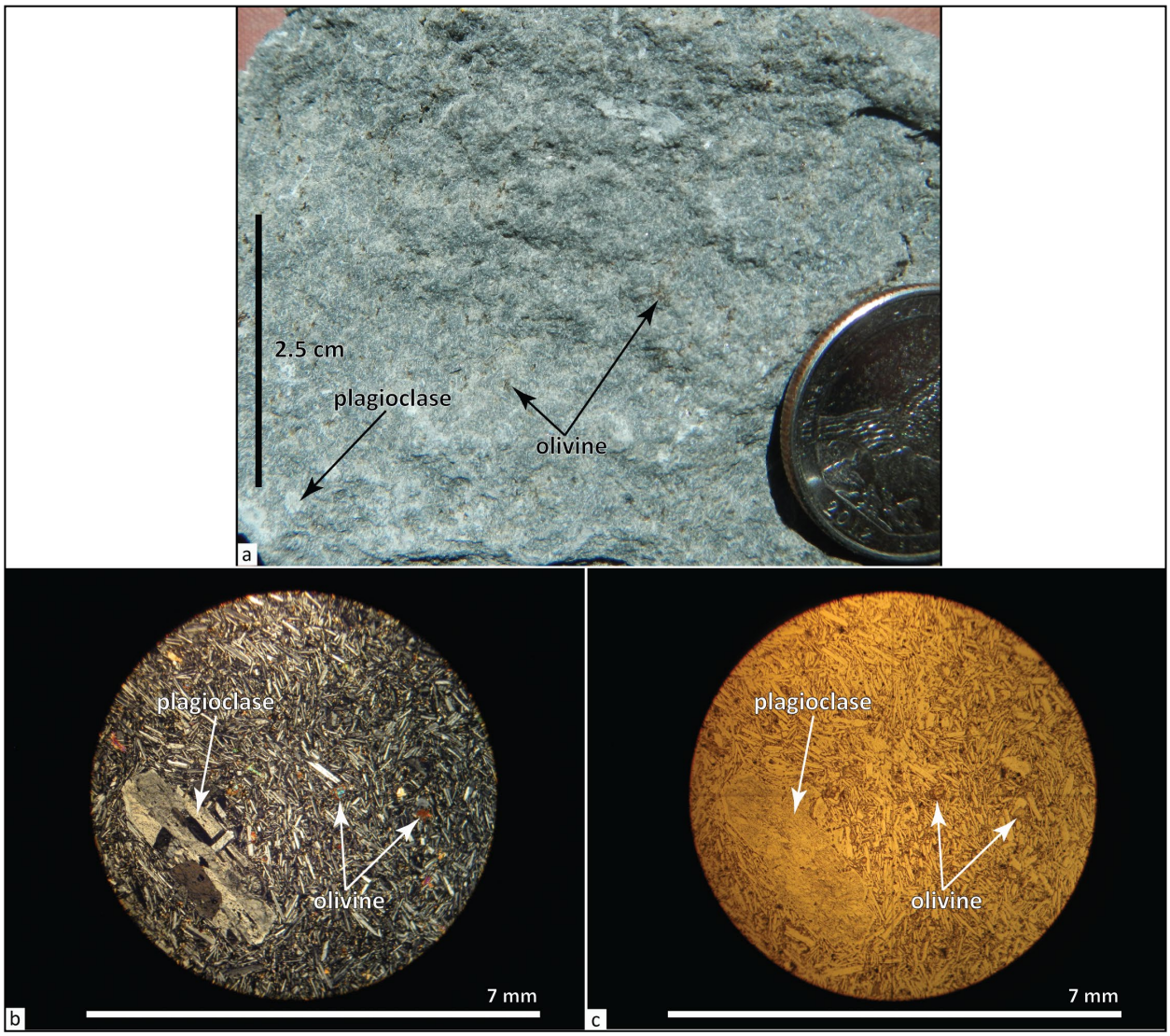

Qrbs **basaltic andesite of Beaver Spring (lower Pleistocene)**—Basaltic andesite lava flow (SiO_2 = 53.82 to 54.41 weight percent; K_2O = 1.04 to 1.12 weight percent; *n* = 5 analyses) mapped as a broad plateau across the summit of Fir Mountain in the headwaters of Mosier Creek (**Figure 6-5**; **Table 6-1**; Plate 2; **Appendix**; McClaughry and others, 2012). **Qrbs** is also mapped discontinuously as an intracanyon lava flow for 10 km (6.2 mi) from Beaver Spring east down Mosier Creek to the intersection of Honeysuckle Creek in the northeast part of the Ketchum Reservoir 7.5′ quadrangle (Plate 2). Additional distal remnants of the lava flow are also mapped east of Honeysuckle Creek and south of the Chenoweth fault in the northwest corner of the Brown Creek 7.5′ quadrangle (Plate 1). These mapped **Qrbs** areas east of Honeysuckle Creek (Plate 1) lie at higher elevations than comparable distal outcrops to the west (Plate 2) and span an elevation range of ~590 ft (180 m). Notable

differences in base elevation of the lava flow from west to east may be explained by complex faulting occurring near the junction of the Chenoweth and Maupin fault systems. The unit is very poorly exposed across Fir Mountain in a few roadbeds; more typically the unit is exposed as moderate orange-pink (5YR 8/4) to grayish orange (10YR 7/4) soils containing scattered loose blocks, 0.3 to >1 m (1 to 3.3 ft) in diameter (**Figure 6-5**). Thickness of the unit ranges from ~5 m (16.4 ft) to as much as 30 m (100 ft) across Fir Mountain; cliff-forming intracanyon parts of the unit mapped along Mosier Creek are as thick as 122 m (400 ft) (Plates 2 and 3). Typical hand samples are medium-light gray (N6) containing ≤1 percent (vol.) colorless, euhedral, prismatic, seriate plagioclase microphenocrysts and phenocrysts ≤2 mm (0.08 in) and 2 to 5 percent (vol.) fresh dusky green (5G 3/2) to dark greenish yellow (10Y 6/6), subhedral to anhedral, polygonal- to blocky-shaped, seriate olivine phenocrysts ≤2 mm (0.08 in), all contained within a fine-grained holocrystalline groundmass (**Figure 6-6**). Groundmass olivine occasionally displays areas or rims of dark yellowish orange (10YR 6/6) iddingsite (**Figure 6-6b,c**). Thin sections contain ~1 to 2 percent (vol.) opaque Fe-Ti oxides.

Magnetic polarity of **Qrbs** is unknown due to a lack of in place outcrops. **Qrbs** is assigned an early Pleistocene age on the basis of stratigraphic relationships with **Qran** and **Qrbr** (**Figure 6-1**). Two topographically high points forming the summit of Fir Mountain, ~1 km (0.6 mi) south of Beaver Springs, are the extant vent complexes from which these lava flows erupted (Plate 2; McClaughry and others, 2012). Lava flows flowed away from the source vents to the northwest into the headwaters of Beaver Creek and to the northeast spreading out into the headwaters area of Indian and Mosier creeks (Plate 2).

Figure 6-5. Basaltic andesite of Beaver Springs (Qrbs) cropping out across Fir Mountain. (a) Basaltic andesite boulders intermixed with moderate orange-pink (5YR 8/4) to grayish-orange (10YR 7/4) soils (45.56836, -121.48275). Hammer for scale is 38 cm (15 in) long. View is looking east. (b) Similar outcrop to (a) in the headwaters of Indian Creek (45.56395, -121.45811). Arrow points to iPad for scale, which is 25 cm (10 in) long. View is looking west. Photo credits: Jason McClaughry, 2015.

Figure 6-6. Hand sample and thin section photographs of the basaltic andesite of Beaver Springs (Qrbs). (a) Typical hand sample. Scale bar is 2.5 cm (1 in). (b) Thin section under cross-polarized light. (c) Same view as in (b) under plane-polarized light. Scale bar in (b) and (c) is 7 mm (0.3 in). Photo credits: Jason McClaughry, 2016.

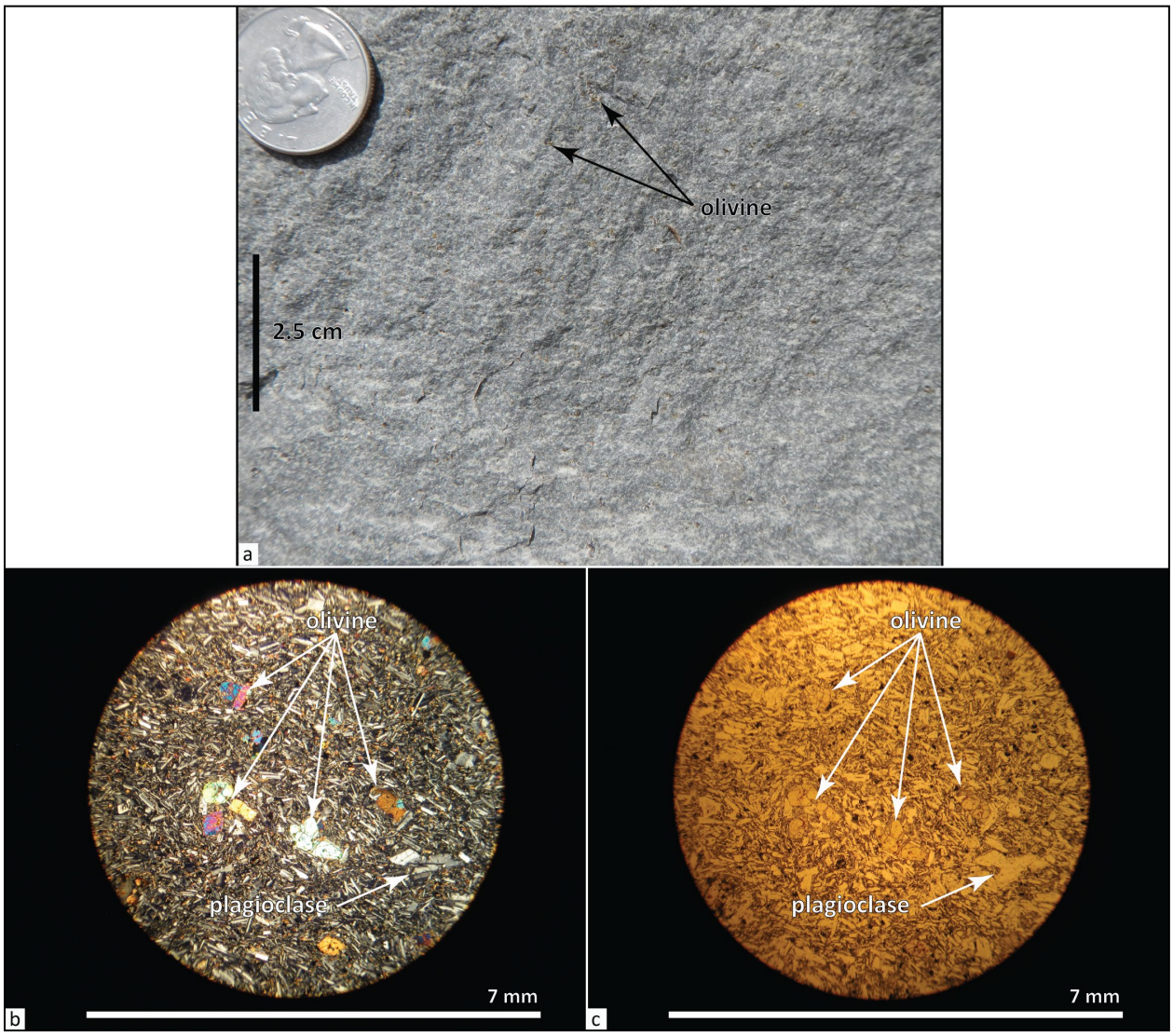

Qrbr **basaltic andesite of Round Prairie (lower Pleistocene)**—Basaltic andesite lava flow (SiO_2 = 53.35 to 54.85 weight percent; K_2O = 1.05 to 1.14 weight percent; *n* = 6 analyses [3 outside Mill Creek area]) mapped west of Round Prairie and Ketchum Reservoir in the headwaters of Mosier Creek (**Figure 6-7**; **Table 6-1**; Plate 2; **Appendix**; McClaughry and others, 2012). The reader should note that distribution of the unit is significantly modified from that originally shown by McClaughry and others (2012) on the basis of additional field mapping and sample analysis in 2015 and 2016. **Qrbr** is deeply weathered, typically recognized as piles of meter-scale boulders and slabs floating in a matrix of moderate orange-pink (5YR 8/4) to grayish orange (10YR 7/4) soils. Coherent outcrops are only found in a few rock pits and smaller excavations (**Figure 6-7**). Thickness of the unit is ≤60 m (200ft). Typical hand samples are mottled yellowish gray (5Y 8/1) to medium-light gray (N6) containing ~1 percent (vol.) colorless, euhedral, prismatic, seriate plagioclase microphenocrysts ≤2 mm (0.08 in) long; 2 to 5 percent (vol.) relatively fresh-

appearing dusky green (5G 3/2) to dark greenish yellow (10Y 6/6), subhedral to anhedral, polygonal- to blocky-shaped, seriate olivine ≤3 mm (0.08 in); ≥5 percent (vol.) glomerocrysts of plagioclase, olivine, ± pyroxene ≤5 mm (0.2 in); all contained within a fine-grained holocrystalline groundmass (**Figure 6-8**). Groundmass olivine occasionally displays areas or rims of dark yellowish orange (10YR 6/6) iddingsite (**Figure 6-8b,c**).

Qrbr has reversed magnetic polarity and is assigned an early Pleistocene (**Figure 6-1**; Plate 2; **Appendix**). Reversed polarity indicates an age older than 0.773 Ma. The lava flow was likely erupted from an extant vent or series of vents that formed high topography, ~2 km (1.3 mi) south of Round Prairie and ~3.2 km (2 mi) west of Ketchum Reservoir (Plate 2). **Qrbr** lava flowed away from source vents to the northwest into the headwaters of the mainstem Neal Creek; it also spread to the northeast into the headwaters area of Mosier and Spring Creeks (Plate 2; McClaughry and others, 2012). **Qrbr** is compositionally nearly identical to the basaltic andesite of Beaver Springs (**Qrbs**), but is distinguished on the basis of conspicuous glomerocrysts and geomorphic expression of the lava flow field.

Figure 6-7. Basaltic andesite of Round Prairie (Qrbr) cropping out across Fir Mountain. (a) South of Round Prairie, Qrbr is deeply weathered, typically forming piles of meter-scale boulders and slabs floating in a matrix of moderate orange-pink (5YR 8/4) to grayish-orange (10YR 7/4) soils (45.52113, -121.47381). Hammer for scale is 38 cm (15 in) long. View is looking north. (b) A rock pit developed in Qrbr, near the presumed vent area, south of Round Prairie (45.52301 -121.47538). The lava flow here has irregular, meter-scale columnar jointing. Photo credits: Jason McClaughry, 2015.

Figure 6-8. Hand sample and thin section photographs of the basaltic andesite of Round Prairie (Qrbr). (a) Typical hand sample with abundant glomerocrysts of plagioclase, olivine, ± pyroxene. Scale bar is 2.5 cm (1 in). (b) Thin section under cross-polarized light. (c) Same view as in (b) under plane-polarized light. Scale bar in (b) and (c) is 7 mm (0.3 in). Photo credits: Jason McClaughry, 2016.

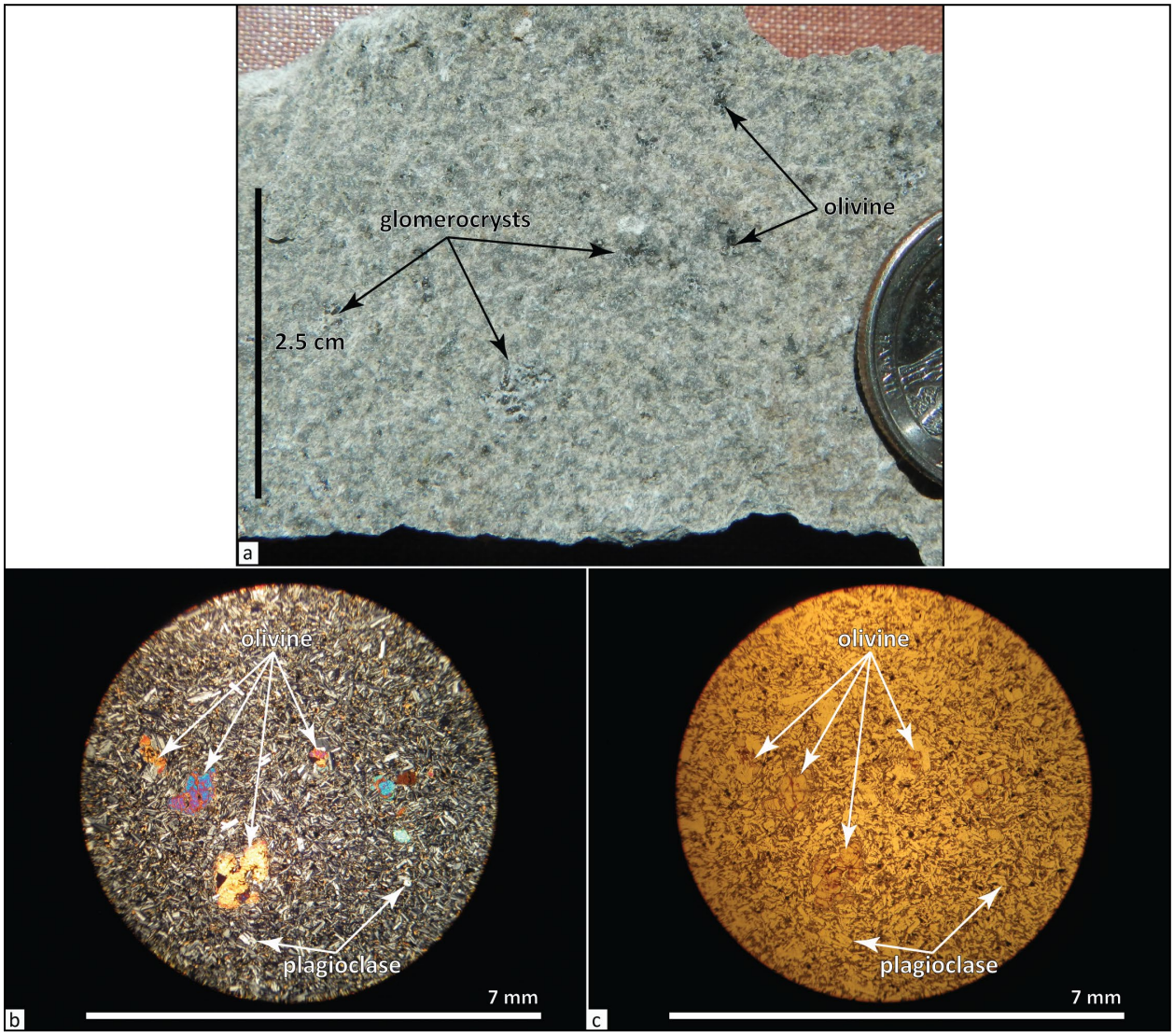

Qgc **gravel (lower Pleistocene)**—Unconsolidated heterolithogic gravel exposed in low-lying hills on the lower southeast flank of Mill Creek Ridge (Plate 3). Gravel is assigned an early Pleistocene age on the basis of stratigraphic position directly above the basaltic andesite of Dog River (**Qr5dr**) (**Figure 6-1**). The gravel is interpreted to have been deposited in the early Pleistocene as the South Fork Mill Creek drainage was disrupted and locally redirected as the 1.87 Ma basaltic andesite of Dog River (**Qr5dr**) entered the channel.

Qr5dr **basaltic andesite of Dog River (lower Pleistocene)**—Intracanyon basaltic andesite lava flow (SiO_2 = 55.88 to 57.56 weight percent; K_2O = 1.08 to 1.24 weight percent; *n* = 23 analyses [17 outside Mill Creek area]) mapped along the South Fork Mill Creek (**Figure 6-9** , **Figure 6-10**; **Table 6-1**; Plates 1 and 3; **Appendix**). Outcrops of **Qr5dr** are characterized by a massive, rounded form, by broad blocky meter-scale columns, or by intervals of thick platy or slabby jointing (**Figure 6-10**). **Qr5dr** typically weathers to subrounded boulders up to 0.5 m (1.6 ft) across or thick, angular slabs up to 2 m (6.6 ft) across. Maximum thickness of **Qr5dr** along South Fork Mill Creek is 40 m (131 ft)(Plates 1 and 3). Typical hand samples of the basaltic andesite are medium gray (N5), containing 15 to 25 percent (vol.) chalky light gray (N7), distinctly resorbed, euhedral to subhedral, blocky to prismatic, seriate plagioclase microphenocrysts and phenocrysts ≤5 mm (0.2 in); ≤1 percent (vol.) subhedral olivine microphenocrysts ≤1 mm (0.04 in); ≤1 percent (vol.) dusky blue-green (5BG 3/2), subhedral to anhedral, blocky- to lath-shaped clinopyroxene microphenocrysts <1 mm (0.04 in); all distributed within a fine-grained hypocrystalline groundmass (**Figure 6-11**). Rare subangular to subrounded andesite xenoliths ≤1 cm (0.4 in) have also been found. Sieve textures in plagioclase, displayed by corroded and partially resorbed crystals, are common (**Figure 6-11b,c**). Clinopyroxene is common as inclusions in some larger plagioclase phenocrysts. Thin sections contain ~1 to 2 percent (vol.) Fe-Ti oxides.

Qr5dr has normal magnetic polarity and is assigned an early Pleistocene age on the basis of stratigraphic position and an $^{40}Ar/^{39}Ar$ age of 1.87 ± 0.02 Ma (McClaughry and others, 2020a)(**Figure 6-1**; **Appendix**). A whole-rock K-Ar age of 1.7 ± 0.4 Ma (sample JA85023) was reported for this unit by Anderson (1987) for a sample collected along South Fork Mill Creek (Plate 1; **Appendix**). **Qr5dr** was erupted from an extant cinder cone-capped fissure located south of Mill Creek Buttes, along the Dog River-Mill Creek Divide at an altitude of 1,391 m (4,565 ft)(McClaughry and others, 2020a). South of Mill Creek Buttes, the lava flow descended into South Fork Mill Creek and flowed northeast as an intracanyon lava flow, ~25 km (15.5 mi) to Oak Flat, southwest of The Dalles (**Figure 6-9**; Plates 1 and 3). A **Qr5dr** lava flow lobe also flowed northwest into the Hood River graben and ancestral valley of the East Fork Hood River (McClaughry and others, 2020a).

Figure 6-9. Intracanyon basaltic andesite of Dog River (Qr5dr) cropping out above the Dalles Formation (Tmdl) on the northern side of Oak Flat (45.54130, -121.31913). View is looking northeast. Photo credit: Clark Niewendorp, 2016.

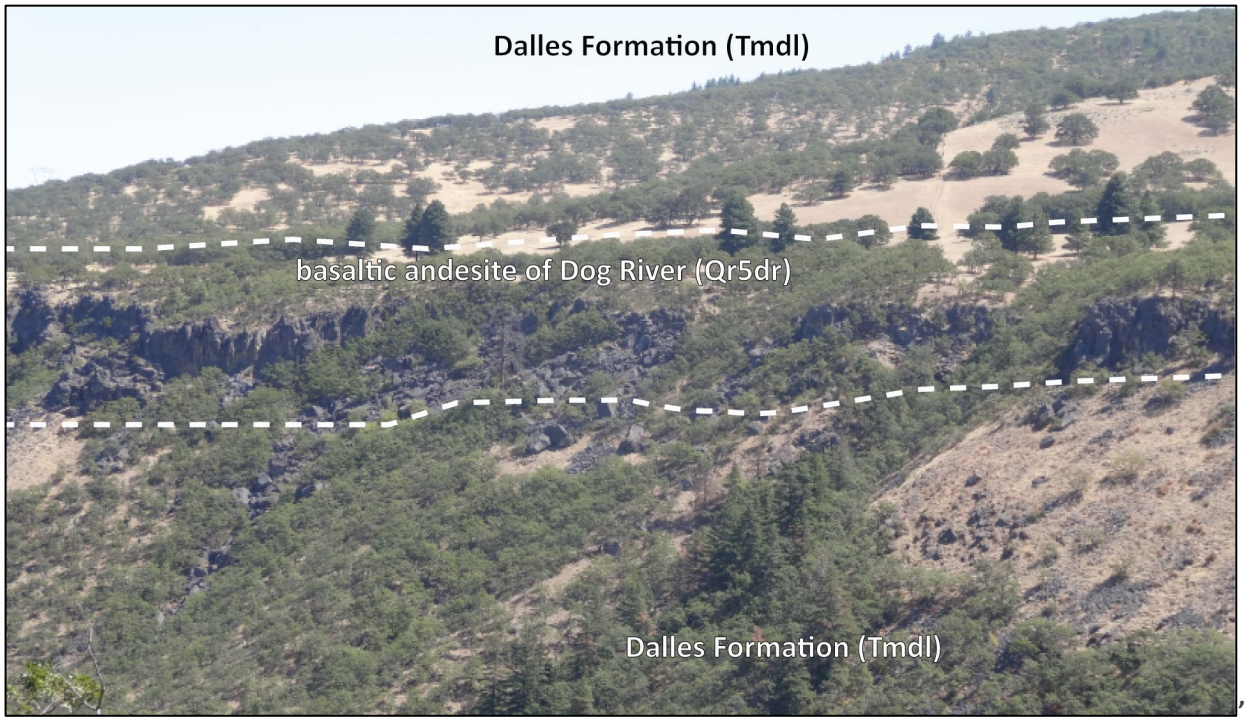

Figure 6-10. The basaltic andesite of Dog River (Qr5dr) cropping out on the southeast flank of Mill Creek Buttes (45.438261, -121.491110). Scale bar is 1 m (3.3 ft). View is looking west. Photo credit: Jason McClaughry, 2016.

Figure 6-11. Hand sample and thin section photographs of the basaltic andesite of Dog River (Qr5dr). (a) Typical abundantly plagioclase-phyric hand sample. Scale bar is 2.5 cm (1 in). (b) Thin section under cross-polarized light. (c) Same view as in (b) under plane-polarized light. Scale bar in (b) and (c) is 7 mm (0.3 in). Photo credits: Jason McClaughry, 2017.

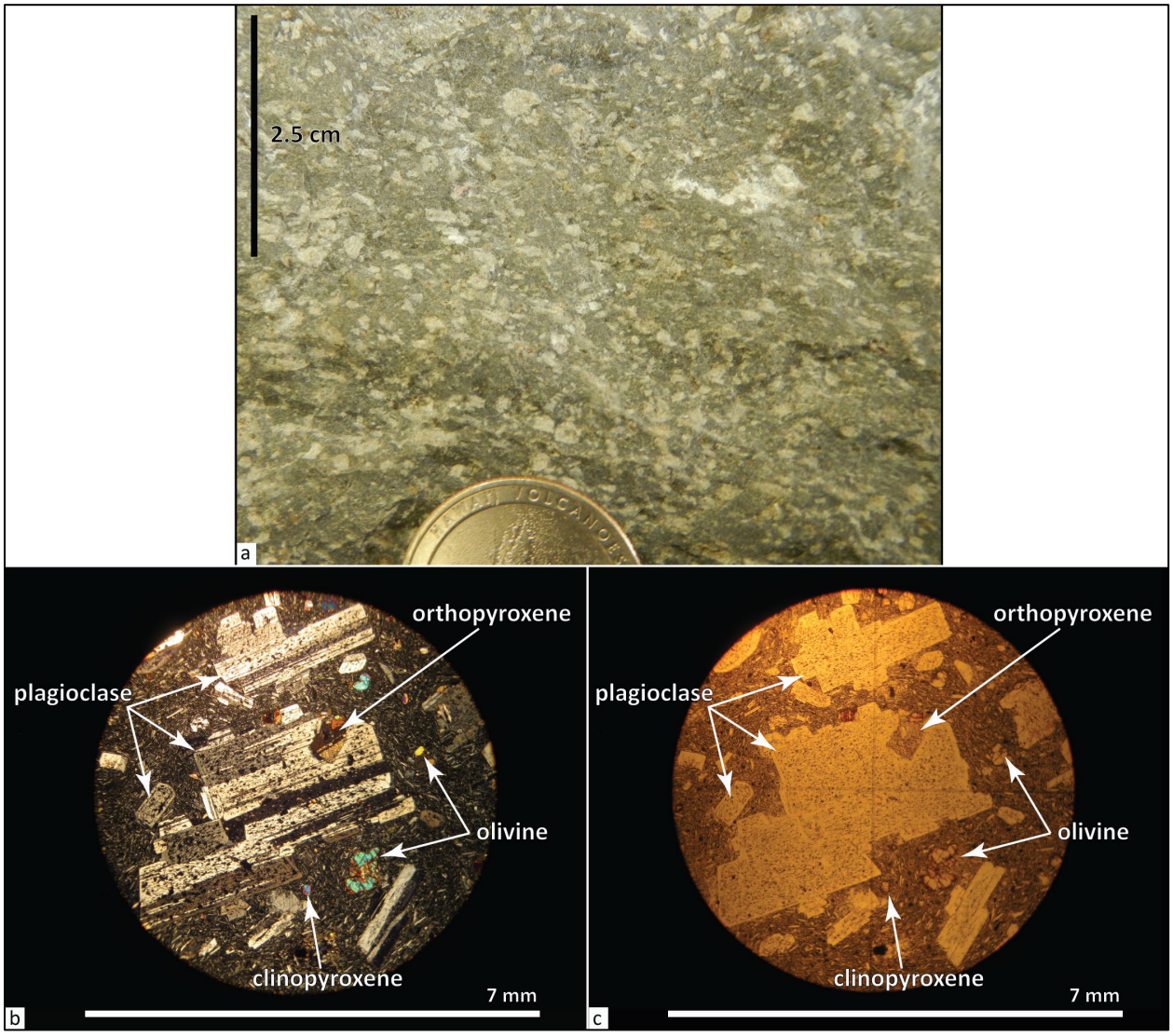

Qrbhp **basaltic andesite of High Prairie (lower Pleistocene)**—Basaltic andesite lava flows (SiO_2 = 52.10 to 52.65 weight percent; K_2O = 0.83 to 0.94 weight percent; Sr = 805 to 892 ppm; *n* = 9 analyses outside Mill Creek area) mapped between the summit of Lookout Mountain (Dog River 7.5′ quadrangle, McClaughry and others, 2020a), north into the uppermost reaches of Eightmile Creek and Dog River (**Figure 6-12**; **Table 6-1**; Plate 3; **Appendix**). The unit includes distal basaltic andesite lobes characterized by slightly higher silica (SiO_2 = 53.96 to 54.88) and lesser strontium (Sr = 631 to 679)(*n* = 2 analyses) mapped north to Bottle Prairie and the upper parts of Puppy Creek (Dog River 7.5′ quadrangle, McClaughry and others, 2020a). Outcrops consist of multiple flow lobes of massive to subhorizontal platy- to tabular- and blocky-jointed lava, separated by intervening horizons of sintered, moderate red brown-oxidized (5YR3/4) flow breccia (**Figure 6-12**). On Lookout Mountain, flow cores are characterized by ~5 percent (vol.) conspicuous

white-black speckled, subrounded plagioclase-pyroxene micro-gabbro inclusions (SiO_2 = 46.02 weight percent; K_2O = 0.17 weight percent; *n* = 1 analysis) ≤10 cm (4 in) across (**Figure 6-12b**; Plate 1). Maximum thickness of **Qrbhp** in the map area is ≤20 m (65 ft) (McClaughry and others, 2020a). Typical hand samples of the basaltic andesite are medium-light gray (N6) and medium gray (N5) to medium-bluish gray (5B 5/1), containing 3 to 8 percent (vol.) fresh clear to chalky white (N9), anhedral to subhedral, blocky, seriate plagioclase (commonly resorbed) microphenocrysts and phenocrysts ≤5 mm (0.2 in); 2 to 3 percent (vol.) waxy, iddingsitized dark yellowish brown (10YR 4/2) to fresh dusky green (5G 3/2), subhedral, blocky, seriate olivine microphenocrysts and phenocrysts 1 to 2 mm (0.04 to 0.08 in); 3 percent (vol.) grayish black (N2) subhedral blocky clinopyroxene phenocrysts 1 to 3 mm (0.04 to 0.1 in; locally megacrystic to 1 cm [2.5 in]); and 2 percent (vol.) plagioclase-pyroxene micro-gabbro inclusions; all contained within a mottled fine-grained holocrystalline groundmass (**Figure 6-12b**, **Figure 6-13**).

Qrbhp has reversed magnetic polarity and is assigned an early Pleistocene age on the basis of stratigraphic position above the 2.35 Ma basalt of Bennett Pass Road (**Qrbp**) (**Figure 6-1**; Plate 3; **Appendix**). Along Puppy Creek, **Qrbhp** is characterized by an intracanyon geomorphic setting lying above the 2.06 Ma basaltic andesite of Blue Bucket Springs and underlying the 1.87 Ma basaltic andesite of Dog River (**Qr5dr**)(Dog River 7.5′ quadrangle, McClaughry and others, 2020a). **Qrbhp** erupted from an extant cinder cone-capped vent on the west slope of Lookout Mountain (Dog River 7.5′ quadrangle, McClaughry and others, 2020a).

Figure 6-12. Basaltic andesite of High Prairie (Qrbhp) cropping out at High Prairie, west of the map area (45.34835, -121.53886). (a) Blocky-jointed outcrop of Qrbhp. Hammer for scale is 38 cm (15 in) long. View is looking east. (b) Micro-gabbro inclusion from the outcrop in (a). Quarter for scale is 2.5 cm (1 in) wide. Photo credits: Jason McClaughry, 2019.

Figure 6-13. Hand sample and thin section photographs of the basaltic andesite of High Prairie (Qrbhp). (a) Typical hand sample. Scale bar is 2.5 cm (1 in). (b) Thin section under cross-polarized light. (c) Same view as in (b) under plane-polarized light. Scale bar in (b) and (c) is 7 mm (0.3 in). Photo credits: Jason McClaughry, 2020.

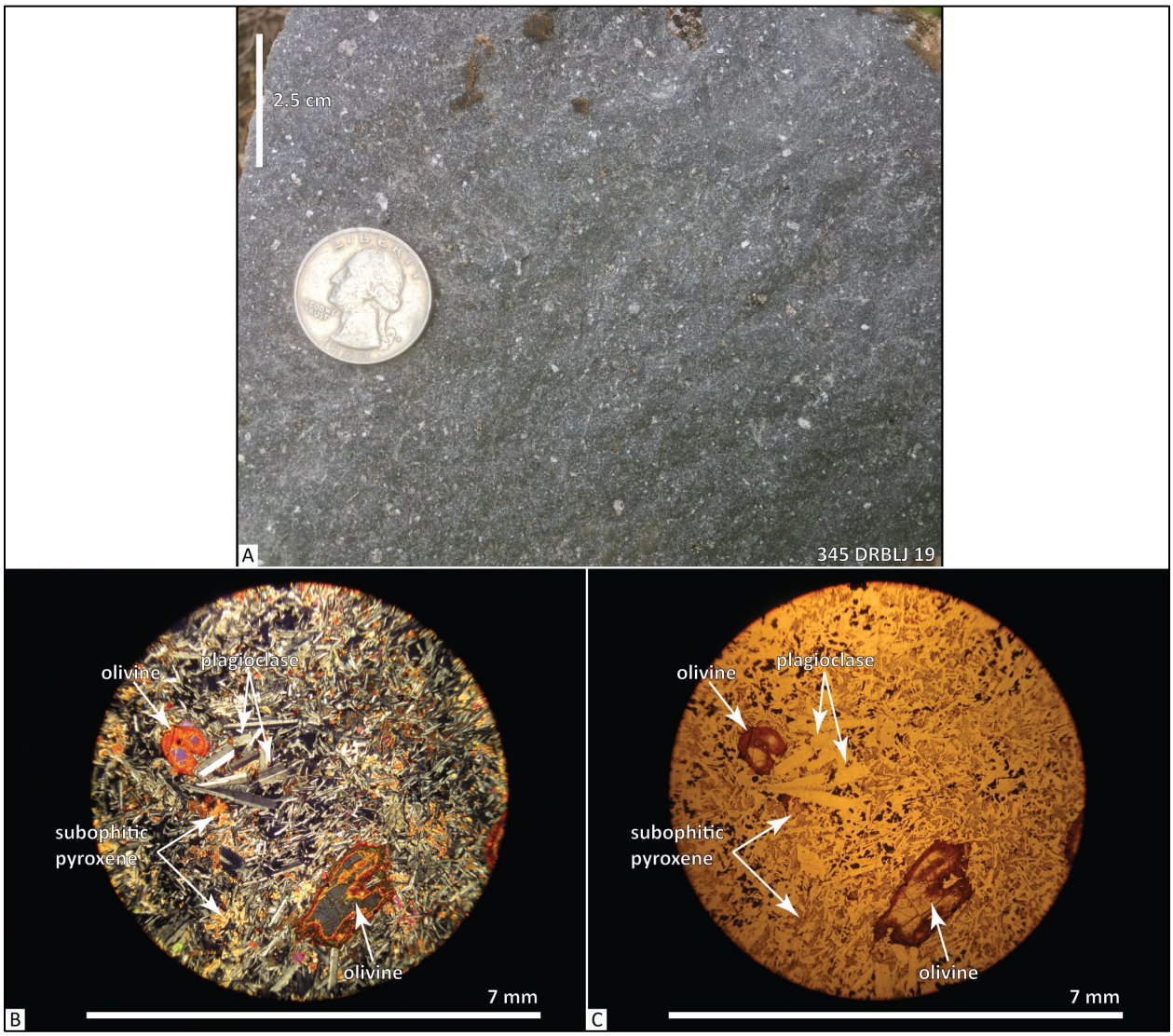

Qrba **basalt of Agnes Spring (lower Pleistocene)**—Basalt lava flow (SiO_2 = 50.76 weight percent; K_2O = 0.58 weight percent; *n* = 1 analysis) poorly exposed west of Perry Point (**Table 6-1**; Plate 3; **Appendix**). West of the map area, in the Dog River 7.5′ quadrangle, the basalt crops out in roadcuts between Brooks Meadow and Bottle Prairie (McClaughry and others, 2020a). Typical hand samples of **Qrba** are medium-light gray (N6) and aphyric to sparsely olivine phyric, containing 3 to 5 percent (vol.) fresh dusky green (5G 3/2) to dark greenish yellow (10Y 6/6), subhedral olivine microphenocrysts ≤1 mm (0.04 in), distributed within a mottled, locally diktytaxitic, fine-grained holocrystalline groundmass (**Figure 6-14**). Olivine are typically skeletal in form and partially resorbed, with rims altered to dark yellowish orange (10YR 6/6) iddingsite (**Figure 6-14b,c**).

Magnetic polarity **Qrba** is unknown due to a lack of in place outcrops. **Qrba** is assigned an early Pleistocene age on the basis of stratigraphic position above the 2.35 Ma basalt of Bennett Pass Road (**Qrbp**) (**Figure 6-1**; Plate 3; Dog River 7.5′ quadrangle, McClaughry and others, 2020a).

Figure 6-14. Outcrop, hand sample, and thin section photographs of the basalt of Agnes Spring (Qrba). (a) Basalt of Agnes Spring (Qrba) cropping out near Brooks Meadow, west of the map area (45.40605, -121.51680). Hammer for scale is 38 cm (15 in) long. View is looking east. (b) Typical hand sample. Scale bar is 2.5 cm (1 in). (c) Thin section under cross-polarized light. (d) Same view as in (c) under plane-polarized light. Scale bar in (c) and (d) is 7 mm (0.3 in). Photo credits: Jason McClaughry, 2024.

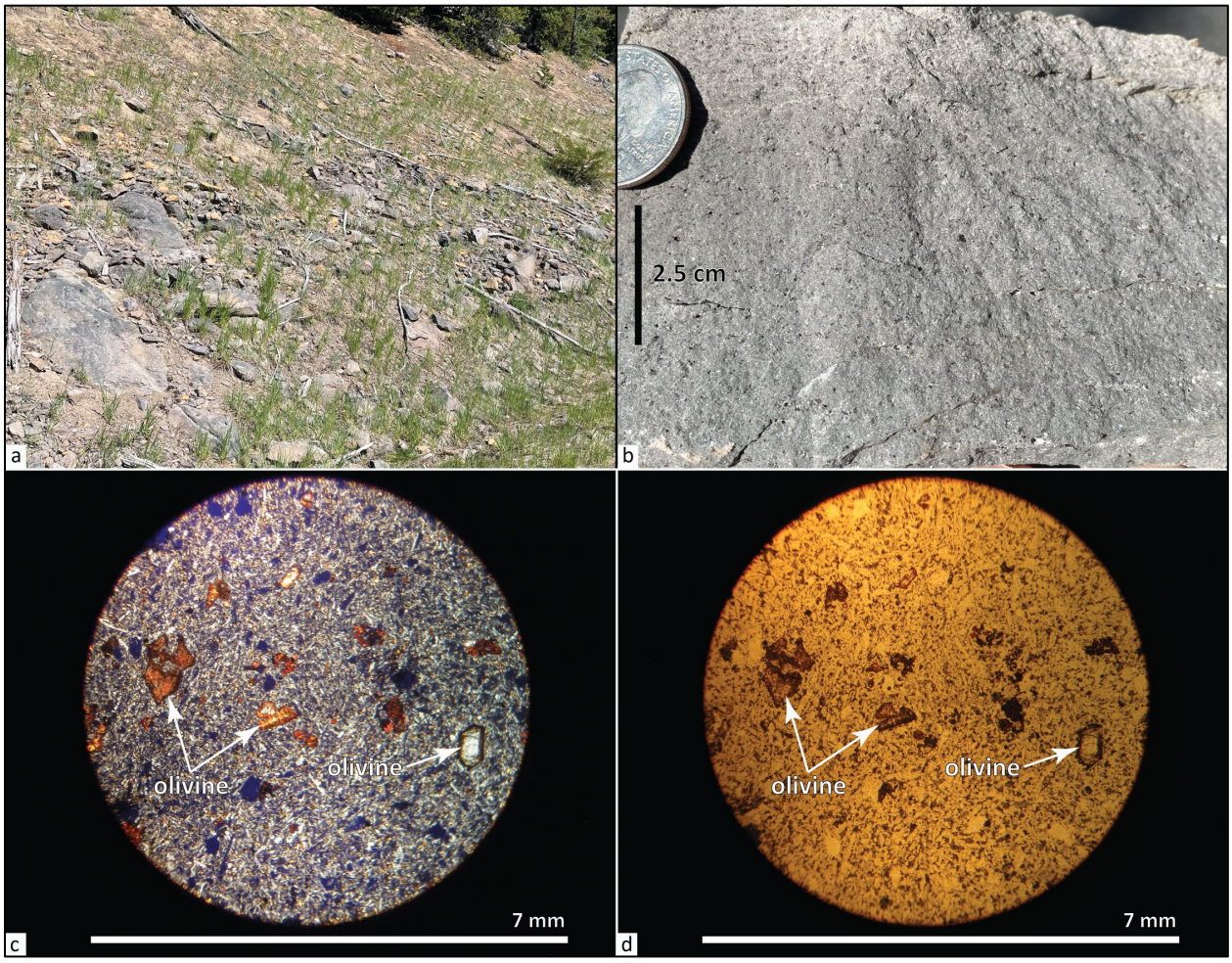

Qrbw **basaltic andesite of Ward Creek (lower Pleistocene)**—Basaltic andesite (SiO_2 = 52.29 to 53.24 weight percent; K_2O = 0.99 to 1.09 weight percent; *n* = 8 analyses [3 outside Mill Creek area]) cropping out in roadcuts between Brooks Meadow and Bottle Prairie (Dog River 7.5′ quadrangle, McClaughry and others, 2020a) and in the upper parts of Middle and South Forks Fivemile creeks (**Figure 6-15**; **Table 6-1**; Plate 3; **Appendix**). Limited roadcut exposures are characterized by intervals of poorly developed blocky columnar jointing and platy to tabular jointing (**Figure 6-15**). **Qrbw** weathers to a landscape mantled by subrounded boulders up to 1 m (3.3 ft) across. Thickness of **Qrbw** is ~20 to 30 m (66 to 98 ft). Typical hand samples of the basaltic andesite are light gray (N7) to medium-light gray (N6) and aphyric to microporphyritic or very sparsely porphyritic, containing <1 percent (vol.) clear, euhedral prismatic, seriate trachytic plagioclase microphenocrysts and phenocrysts ≤2 mm (0.08 in)(rarely with phenocrysts up to 5 mm [0.2 in]) and <1 percent (vol.) fresh dusky green (5G 3/2) to dark greenish yellow (10Y 6/6), subhedral, seriate olivine microphenocrysts ≤1 mm (0.04 in) across, distributed within a mottled, locally diktytaxitic, fine-grained holocrystalline groundmass (**Figure 6-16**).

Qrbw has normal magnetic polarity and is assigned an early Pleistocene age on the basis of stratigraphic position above the 2.35 Ma basalt of Bennett Pass Road (**Qrbp**) (**Figure 6-1**; Plate 3; **Appendix**). **Qrbw** lava flows vented from the upper part of Ward Creek (Dog River 7.5′ quadrangle, McClaughry and others, 2020a) and flowed at least 12 km (7.5 mi) downslope to the northeast, extending into upper reaches of both Middle and South Forks of Fivemile Creek (Plate 3).

Figure 6-15. Blocky-jointed basaltic andesite of Ward Creek (Qrbw) cropping out along USFS Road 4430 (45.43642, -121.46649). Hammer for scale is 38 cm (15 in) long. View is looking east. Photo credit: Jason McClaughry, 2016.

Figure 6-16. Hand sample and thin section photographs of the basaltic andesite of Ward Creek (Qrbw). (a) Typical hand sample with mottled-textured groundmass. (b) Typical hand sample with distinctly trachytic groundmass plagioclase. Scale bar in both (a) and (b) is 2.5 cm (1 in). (c) Thin section under cross-polarized light. (d) Same view as in (c) under plane-polarized light. Scale bar in (c) and (d) is 7 mm (0.3 in). Photo credits: Jason McClaughry, 2016 and 2017.

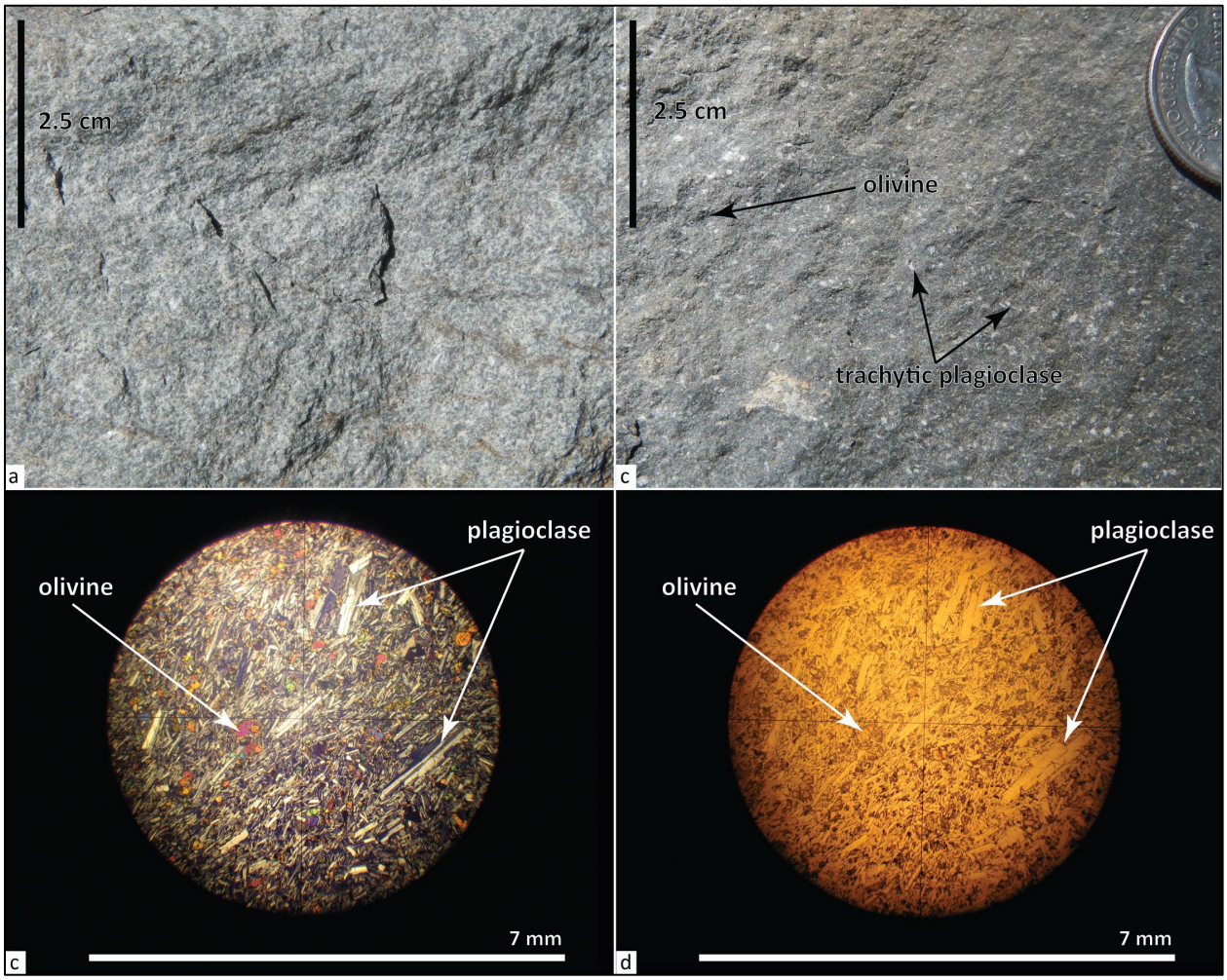

Qrbe **basalt of Hesslan Canyon (lower Pleistocene)**—Basalt lava flow (SiO_2 = 48.89 to 50.23 weight percent; K_2O = 0.99 to 1.07 weight percent; *n* = 4 analyses [1 outside Mill Creek area]) with high amounts of titanium (TiO_2 = 2.12 to 2.40 weight percent) mapped over an ~10.5 km (6.5 mi) long outcrop belt between Bottle Prairie on the west and Hesslan Canyon on the east (**Figure 6-17**; **Table 6-1**; Plate 3; **Appendix**; McClaughry and others, 2021). Limited outcrops of **Qrbe** are characterized by broad blocky meter-scale columns or intervals of platy jointing (**Figure 6-17**). **Qrbe** generally weathers to subangular plates 0.25 to 1 m (0.8 to 3.3 ft) across. Thickness of the lava flow exceeds 32 m (105 ft) in the western part of the map area (Plate 1). Typical hand samples of the basalt are medium-light gray (N6) to medium gray (N5), containing 1 to 2 percent (vol.) clear, euhedral, prismatic, seriate plagioclase microphenocrysts and phenocrysts ≤2 mm (0.04 to 0.1 in) and ~3 to 5 percent (vol.) dark greenish yellow (10Y 6/6), subhedral to anhedral, polygonal to blocky shaped, seriate olivine microphenocrysts ≤1 mm (0.04 in) across, all distributed within a fine-grained hypocrystalline groundmass (**Figure 6-18**). Olivine are typically skeletal in form and partially resorbed, with rims altered to dark yellowish orange (10YR 6/6) iddingsite (**Figure 6-18b,c**). Thin sections contain ≤1 percent (vol.) Fe-Ti oxides.

Qrbe has reversed magnetic polarity and is assigned an early Pleistocene age on the basis of stratigraphic position above the 2.35 Ma basalt of Bennett Pass Road (**Qrbp**)(**Figure 6-1**; Plate 3; **Appendix**). No outcrops or vent area for the lava flow have been found west of Bottle Prairie.

Figure 6-17. Tabular-jointed basalt of Hesslan Canyon (Qrbe) cropping out along USFS Road 44 (Dufur Mill Road)(45.399371, -121.484243). Hammer for scale is 38 cm (15 in) long. View is looking south. Photo credit: Jason McClaughry, 2016.

Figure 6-18. Hand sample and thin section photographs of the basalt of Hesslan Canyon (Qrbe). (a) Typical hand sample. Scale bar is 2.5 cm (1 in). (b) Thin section under cross-polarized light. (c) Same view as in (b) under plane-polarized light. Scale bar in (b) and (c) is 7 mm (0.3 in). Photo credits: Jason McClaughry, 2017.

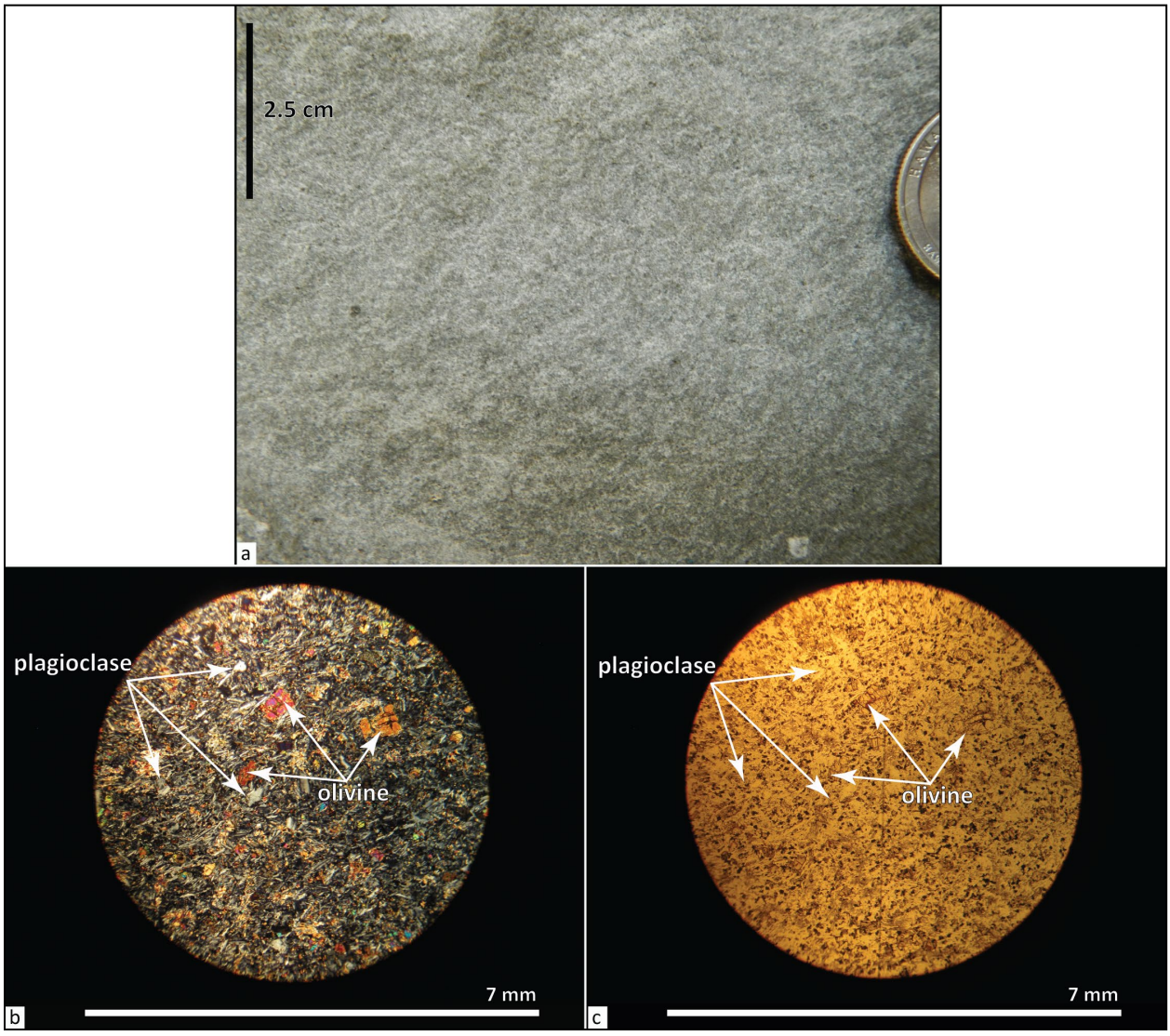

Qrbj **basalt of Jacket Springs (lower Pleistocene)**—Basalt lava flow (SiO_2 = 51.47 weight percent; K_2O = 0.79 weight percent; *n* = 1 analysis) mapped between Eightmile Meadow and Jacket Springs (**Figure 6-19**; **Table 6-1**; Plate 3; **Appendix**). **Qrbj** is typically poorly exposed, weathering to a landscape mantled by subrounded boulders up to 1 m (3.3 ft) across. Limited roadcut exposures are characterized by thick intervals of platy to tabular jointing (**Figure 6-19**). Thickness of **Qrbj** is <10 m (33 ft). Typical hand samples of **Qrbj** are light gray (N7) to medium-dark gray (N4), aphyric to sparsely microporphyritic, containing 2 to 3 percent (vol.) dark greenish yellow (10Y 6/6), subhedral to euhedral to skeletal, seriate olivine microphenocrysts ≤1 mm (0.04 in) across, and ≤1 percent (vol.) clear to chalky white (N9), euhedral, prismatic, seriate plagioclase microphenocrysts ≤2 mm (0.08 in) long, distributed within a diktytaxitic, fine-grained holocrystalline groundmass (**Figure 6-20**). Olivine phenocrysts and microphenocrysts are typically skeletal in form, commonly occurring as corroded and partially resorbed crystals; olivine rims are typically altered to dark yellowish orange (10YR 6/6) iddingsite (**Figure 6-20b,c**). Thin sections contain 1 to 3 percent (vol.) cubic- to needle-shaped Fe-Ti oxides.

Qrbj has normal magnetic polarity and is assigned an early Pleistocene age on the basis of stratigraphic association and chemical similarity with the basalt of Bennett Pass Road (**Qrbp**)(**Figure 6-1**; **Table 6-1**; Plate 3; **Appendix**). The map pattern, as shown on Plate 3, indicates that the **Qrbj** lava flow likely vented from upslope areas in the vicinity of High Prairie (3.3 km [2.0 mi] southwest of the map area, Dog River 7.5′ quadrangle), although no evidence of the vent remains (McClaughry and others, 2020a).

Figure 6-19. Tabular-jointed basalt of Jacket Springs (Qrbj) cropping out along USFS 4420 (Cold Springs Road)(45.38775, -121.47795). Hammer for scale is 38 cm (15 in) long. View is looking east. Photo credit: Jason McClaughry, 2016.

Figure 6-20. Hand sample and thin section photographs of the basalt of Jacket Springs (Qrbj). (a) Typical hand sample. Scale bar is 2.5 cm (1 in). (b) Thin section under cross-polarized light. (c) Same view as in (b) under plane polarized light. Scale bar in (b) and (c) is 7 mm (0.3 in). Photo credits: Jason McClaughry, 2017.

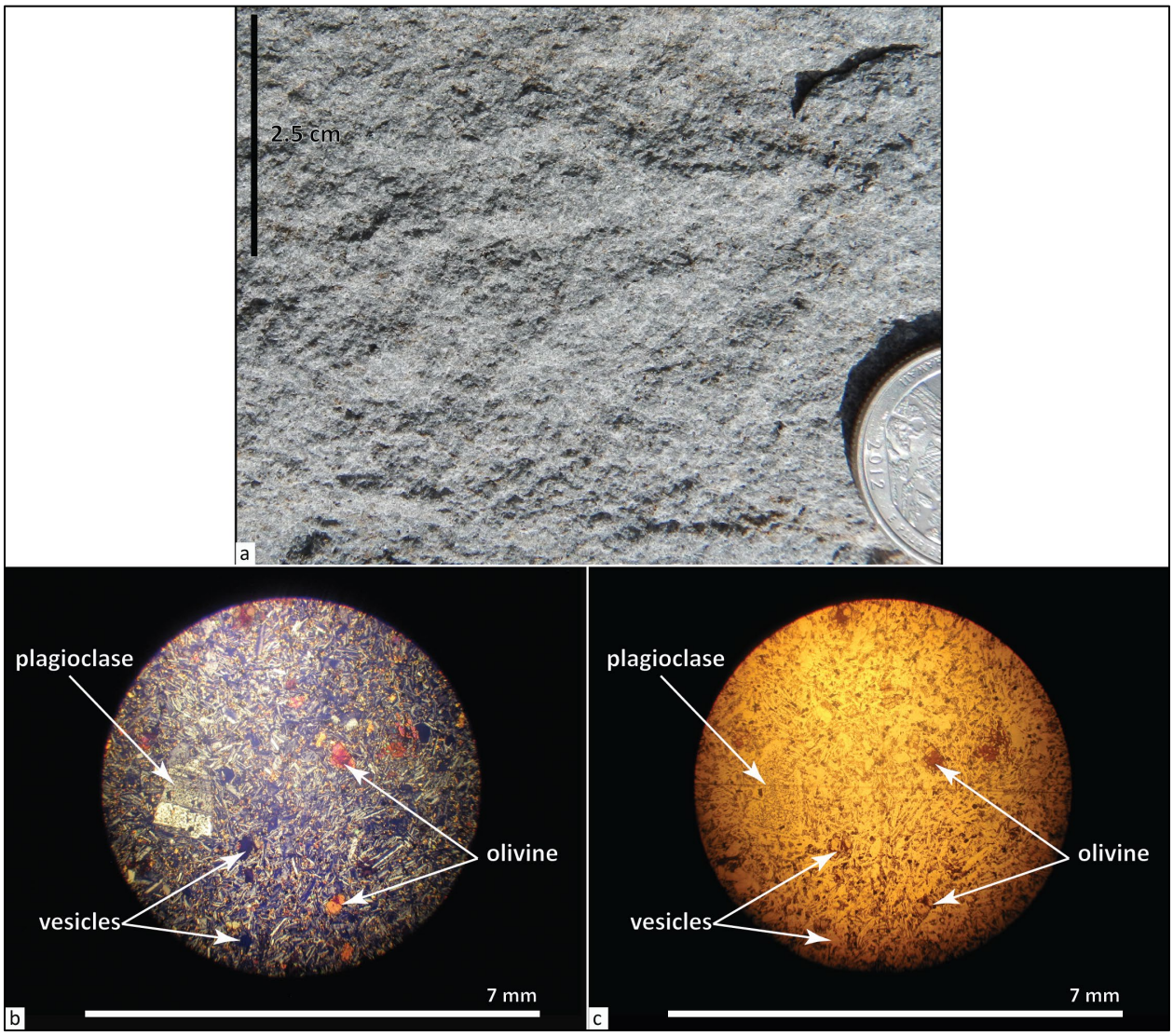

Qrbp **basalt of Bennett Pass Road (lower Pleistocene)**—Basalt lava flow (SiO_2 = 50.01 to 51.90 weight percent; K_2O = 0.78 to 0.96 weight percent; *n* = 9 analyses [7 outside Mill Creek area]) mapped between Bottle Prairie on the west ~10.5 km (6.5 mi) east to the mouth of Hesslan Canyon (**Figure 6-21**; **Table 6-1**; Plate 3; **Appendix**; McClaughry and others, 2020a, 2021). The lava flow is mapped an additional 6 km (3.7 mi) southwest to High Prairie (McClaughry and others, 2020a). Limited outcrops of **Qrbp** are characterized by broad blocky meter-scale columns or intervals of platy jointing (**Figure 6-21**); weathered parts of the flow are characterized by subangular plates 0.25 to 1 m (0.8 to 3.3 ft) across. Thickness of **Qrbp** is ≥32 m (105 ft) in Hesslan Canyon. Typical hand samples of the basalt are light gray (N7) to medium-dark gray (N4), aphyric to sparsely microporphyritic, containing ≤1 percent (vol.) clear, subhedral to anhedral, prismatic, seriate plagioclase microphenocrysts ≤1 mm (0.04 in) and 2 to 3 percent (vol.) fresh dark greenish yellow (10Y 6/6), subhedral olivine microphenocrysts ≤1 mm (0.04 in), contained within a fine-grained

holocrystalline groundmass (**Figure 6-22**). Very rare subhedral olivine phenocrysts occur up to 3 mm (0.1 in). Olivine microphenocrysts are typically skeletal in form and are partially to wholly altered to dark yellowish orange (10YR 6/6) iddingsite (**Figure 6-22b,c**). Sieve textures in plagioclase crystals are common. Thin sections contain 1 to 3 percent (vol.) cubic-shaped Fe-Ti oxides.

Qrbp has reversed magnetic polarity and is assigned an early Pleistocene age on the basis of stratigraphic position, intracanyon geomorphic setting, and a weighted mean whole-rock K-Ar age of 2.35 ± 0.03 Ma for an outcrop at Lookout Mountain (Conrey and others, 1996; McClaughry and others, 2020a)(**Figure 6-1**; Plate 1; **Appendix**). The map pattern, as shown on Plate 3, indicates that **Qrbp** lava flow likely vented from upslope areas in the vicinity of High Prairie (3.3 km [2.0 mi] southwest of the map area, Dog River 7.5′ quadrangle, McClaughry and others, 2020a). The lava flow descended into parts of Eightmile Creek and Hesslan Canyon, flowing east ~17 km (10.5 mi) downstream to the mouth of Hesslan Canyon (Plate 3; Wolf Run 7.5′ quadrangle; McClaughry and others, 2020a, 2021).

Figure 6-21. The basalt of Bennett Pass Road (Qrbp) cropping out at the mouth of Hesslan Canyon (45.417423, -121.368405). Hammer for scale is 38 cm (15 in) long. View is looking south. Photo credit: Jason McClaughry, 2017.

Figure 6-22. Hand sample and thin section photographs of the basalt of Bennett Pass Road (Qrbp). (a) Typical hand sample. Scale bar is 2.5 cm (1 in). (b) Thin section under cross-polarized light. (c) Same view as in (b) under plane-polarized light. Scale bar in (b) and (c) is 7 mm (0.3 in). Photo credits: Jason McClaughry, 2017.

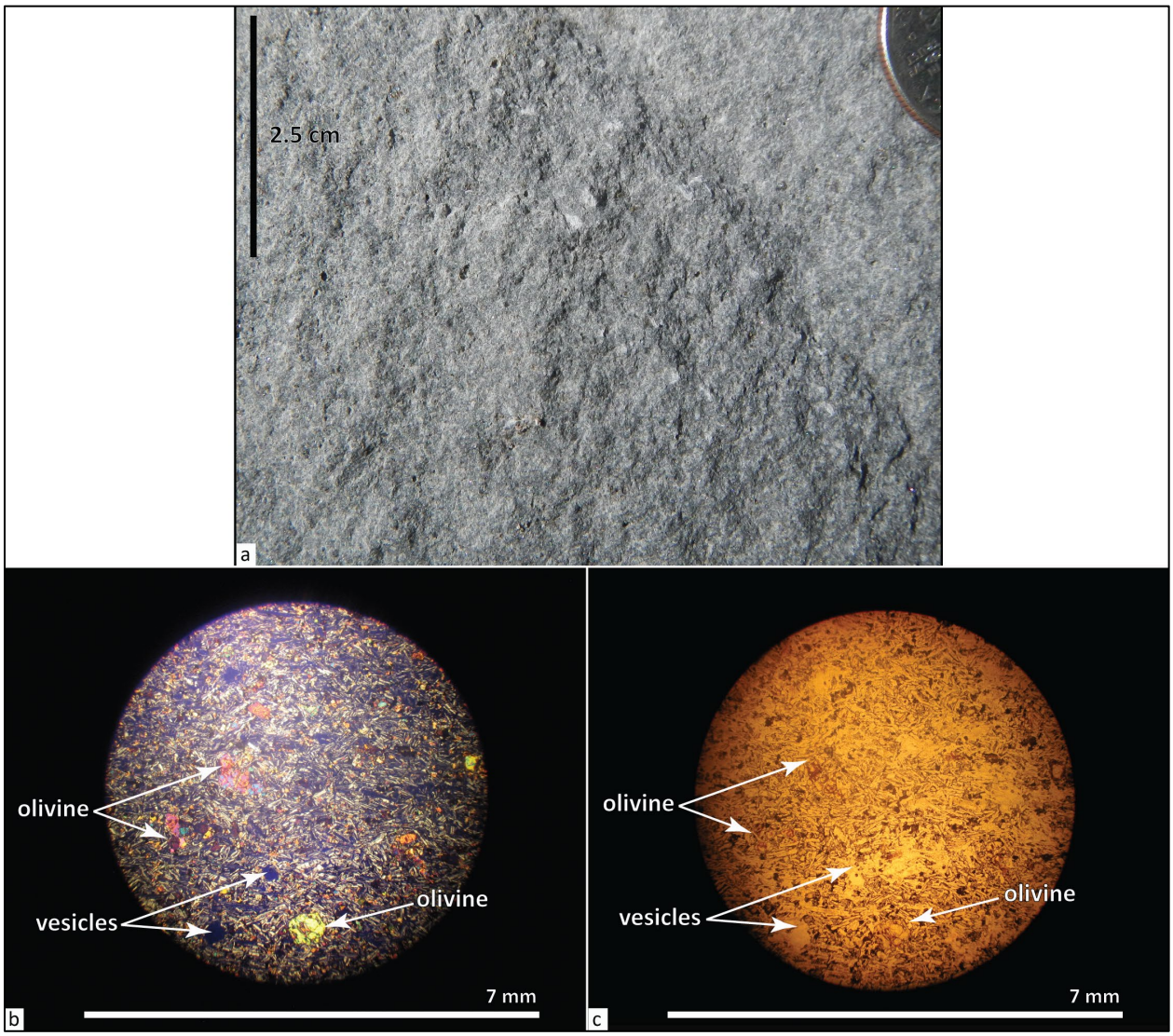

Qrbf **basaltic andesite of Flag Point (lower Pleistocene or upper Pliocene)**—Basaltic andesite lava flow (SiO_2 = 54.79 to 56.61 weight percent; K_2O = 0.98 to 1.38 weight percent; *n* = 14 analyses [9 outside Mill Creek area]) mapped along Cedar Creek and at Frailey Point in the northern part of the Flag Point 7.5′ quadrangle (**Figure 6-23**; **Table 6-1**; Plate 3; **Appendix**). Outcrops of **Qrbf** along Cedar Creek form the distal snout of an intracanyon lava flow discontinuously exposed ~5 km (3.1 mi) southwest to a vent area at Flag Point (Jason McClaughry unpublished geologic mapping, 2016). Roadcuts and outcrops of **Qrbf** are characterized by a massive, rounded form; by broad blocky meter-scale columns; or intervals of platy jointing (**Figure 6-23**). **Qrbf** generally weathers to rounded boulders up to 1 m (3.3 ft) across. Thickness of **Qrbf** is ~25 m (82 ft) in the southwest corner of the map area. Typical hand samples of the basaltic andesite are medium gray (N5) to medium-dark gray (N4) containing 3 to 5 percent (vol.) colorless, euhedral, prismatic, seriate plagioclase microphenocrysts and phenocrysts ≤2 mm (0.1 in) long (rarely with

phenocrysts up to 7 mm [0.3 in] long) and <1 percent (vol.) dark greenish yellow (10Y 6/6), subhedral to anhedral, polygonal- to blocky-shaped, seriate olivine microphenocrysts <1 mm (0.04 in) across, all distributed within a locally diktytaxitic, fine-grained holocrystalline groundmass (**Figure 6-24**). Sieve textures in plagioclase crystals are common (**Figure 6-24b,c**). Olivine microphenocrysts are typically skeletal in form and have rare areas or rims altered to dark yellowish orange (10YR 6/6) iddingsite. Thin sections contain 1 to 3 percent (vol.) Fe-Ti oxides and include rare anhedral, embayed clear quartz xenocrysts rimmed by glass and an aggregate of granular pyroxene crystals, which separate it from the groundmass.

Qrbf has reversed magnetic polarity and is assigned an late Pliocene or early Pleistocene age on the basis of stratigraphic position and an $^{40}Ar/^{39}Ar$ plateau age of 2.57 ± 0.02 Ma for outcrops located on the north edge of Owl Hollow in the Friend 7.5′ quadrangle (**Figure 6-1**; Plate 3; **Appendix**; McClaughry and others, 2021). Texture, chemical composition, and map pattern indicate that **Qrbf** was erupted from an extant cinder cone-capped vent underlying the lookout at Flag Point (south of the Mill Creek area; Sherrod and Scott, 1995). Conrey and others (1996) reported a whole-rock K-Ar age of 1.92 ± 0.2 Ma for similar composition basalt underlying the Flag Point lookout.

Figure 6-23. Platy-jointed basaltic andesite of Flag Point (Qrbf) cropping out along Fifteenmile Creek Trail #456 between Fifteenmile Creek and Cedar Creek (45.36923, -121.42008). Person for scale is 1.8 m (5.9 ft) tall. View is looking north. Photo credit: Jason McClaughry, 2016.

Figure 6-24. Hand sample and thin section photographs of the basaltic andesite of Flag Point (Qrbf). (a) Typical hand sample. Scale bar is 2.5 cm (1 in). (b) Thin section under cross-polarized light. (c) Same view as in (b) under plane-polarized light. Scale bar in (b) and (c) is 7 mm (0.3 in). Photo credits: Jason McClaughry, 2017.

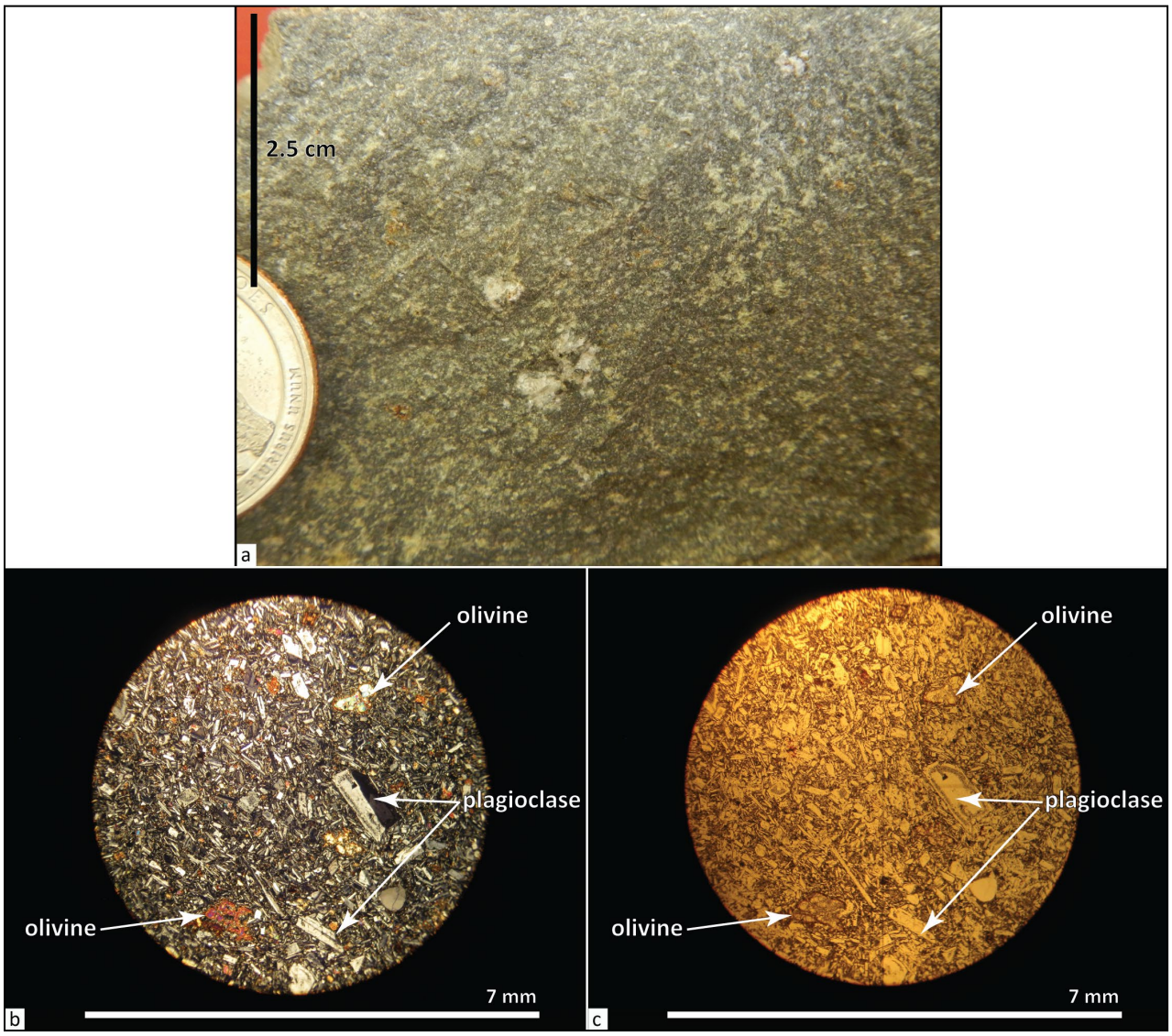

QTbk **basalt of Knebal Spring (lower Pleistocene[?] or upper Pliocene[?])**—Basalt lava flow (SiO_2 = 50.38 to 50.88 weight percent; K_2O = 0.58 to 0.64 weight percent; *n* = 5 analyses [2 outside Mill Creek area]) mapped above the trachydacite of Fivemile Creek (**Tpdv**) at Knebal Spring between South Fork Mill Creek and Middle Fork Fivemile Creek (**Figure 6-25**; **Table 6-1**; Plate 3; **Appendix**). **QTbk** is also mapped west, ~3.3 km (2.0 mi) to the vicinity of Brooks Meadow (Dog River 7.5′ quadrangle, McClaughry and others, 2020a). Good outcrops of **QTbk** are rare; lava flows are typically exposed as piles of meter-scale boulders and slabs across the forest floor. Limited exposures are characterized by intervals of platy to tabular jointing. The maximum thickness of **QTbk** in the map area is as much as 58 m (190 ft). Typical hand samples of the basalt are light gray (N7) to medium-light gray (N6) and abundantly plagioclase and olivine phyric, containing 5 to 10 percent (vol.) chalky white (N9) to clear, euhedral, prismatic, seriate plagioclase

microphenocrysts and phenocrysts ≤8 mm (0.3 in); 5 to 10 percent (vol.) variably altered, fresh dark greenish yellow (10Y 6/6) to dark yellowish orange (10YR 6/6) iddingsitized, subhedral, blocky, seriate olivine microphenocrysts and phenocrysts ≤5 mm (0.2 in); and ≤5 percent (vol.) plagioclase-olivine glomerocrysts ≤5 mm (0.2 in); all distributed within a diktytaxitic, fine-grained holocrystalline groundmass (**Figure 6-26**).

QTbk has reversed magnetic polarity and is assigned a late Pliocene(?) or early Pleistocene(?) age on the basis of stratigraphic position (**Figure 6-1**; Plate 3; **Appendix**). **QTbk** sits directly upon the 3.69 Ma trachydacite of Fivemile Creek (**Tpdv**) and predates the 1.87 Ma basaltic andesite of Dog River (**Qr5dr**)(Plate 3). Mapped distribution of **QTbk** suggests the vent area for the lava flow is likely to be the high ground immediately north of Brooks Meadow in the Dog River 7.5′ quadrangle (McClaughry and others, 2020a).

Figure 6-25. Tabular-jointed basalt of Knebal Spring (QTbk) cropping out near USFS Road 1720 (Brooks Meadow Road; 45.44260, -121.46858). Hammer for scale is 38 cm (15 in) long. View is looking south. Photo credit: Jason McClaughry, 2016.

Figure 6-26. Hand sample and thin section photographs of the basalt of Knebal Spring (QTbk). (a) Typical hand sample. Scale bar is 2.5 cm (1 in). (b) Thin section under cross-polarized light. (c) Same view as in (b) under plane-polarized light. Scale bar in (b) and (c) is 7 mm (0.3 in). Photo credits: Jason McClaughry, 2017.

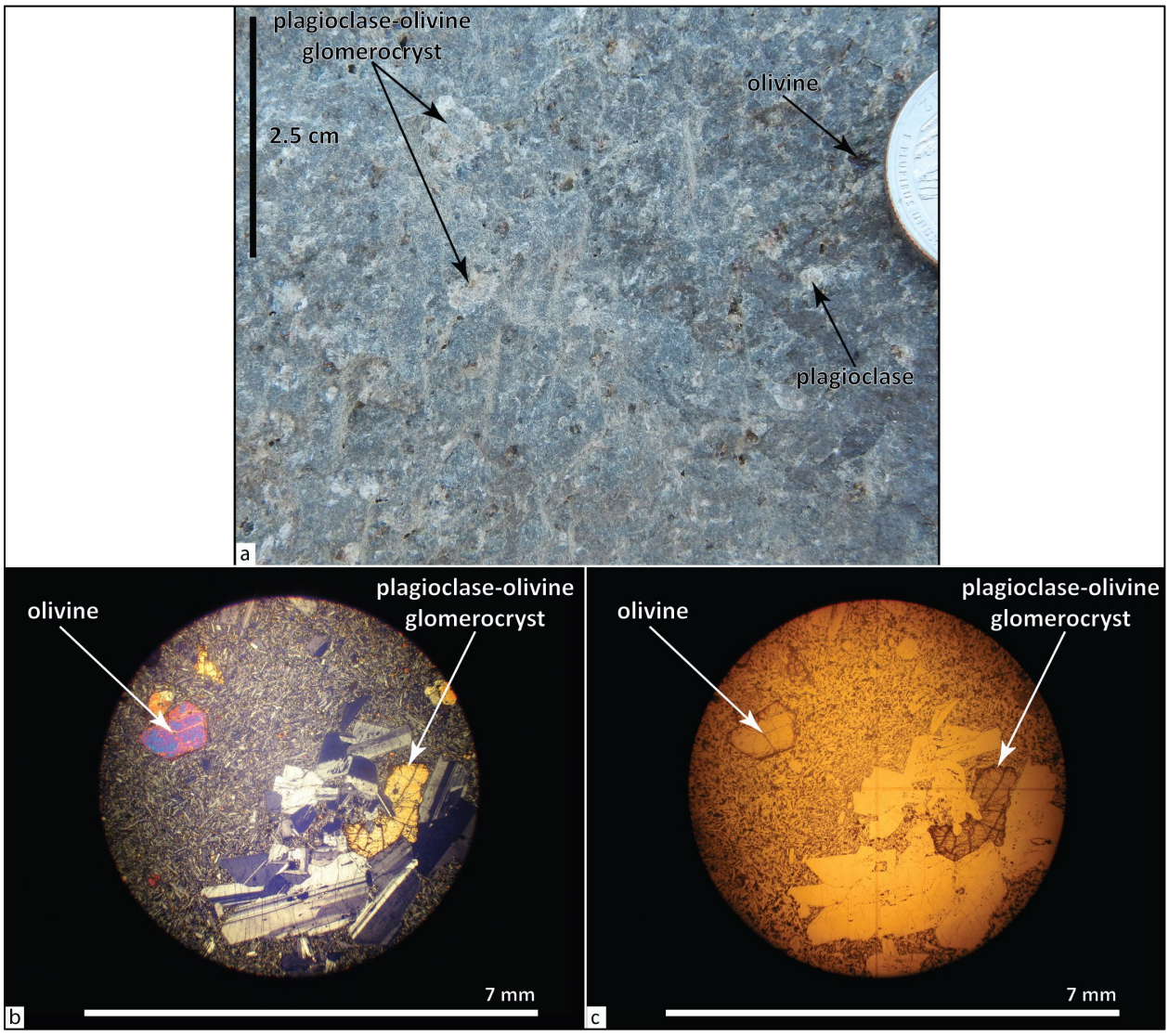

Disconformity

6.3.2 Pliocene volcanic and sedimentary rocks of the late High Cascades

QTpg **sedimentary deposits (lower Pleistocene and/or upper Pliocene)**—Unconsolidated to partially indurated cobble gravel and sand mapped as canyon-restricted lobes above the trachydacite of Fivemile Creek (**Tpdv**) in the northern part of the Fivemile Butte 7.5′ quadrangle. The unit is also mapped further east into the Wolf Run 7.5′ quadrangle in the Dufur area (McClaughry and others, 2021; **Figure 6-27**; Plate 1). Typical thickness of **QTpg** along Fivemile Creek is ≤25 m (80 ft). **QTpg** is assigned a late Pliocene and/or early Pleistocene age on the basis of stratigraphic position above the 3.69 Ma trachydacite of Fivemile Creek (**Tpdv**) (**Figure 6-1**).

Figure 6-27. Sedimentary deposits (QTpg) exposed along Dutch Flat Road in the Wolf Run 7.5′ (45.48948, -121.29928). Hammer for scale is 25 cm (10 in) long. View is looking northeast. Photo credit: Clark Niewendorp, 2015.

Tpdf **dacite of Fifteenmile Creek (upper Pliocene)**—Intracanyon dacite lava flow (SiO_2 = 62.55 to 66.26 weight percent; K_2O = 2.01 to 3.02 weight percent; *n* = 27 analyses [20 outside Mill Creek area]) capping a narrow ENE-trending, ~15 km (9.3 mi) long ridge along Fifteenmile Creek in the northern part of the Flag Point 7.5′ quadrangle and southern part of the Fivemile Butte 7.5′ quadrangle (**Figure 6-28**; **Table 6-2**; Plate 3; **Appendix**). Compositionally identical dacite lava flows and several prominent N15°E- to N25°E-striking dacite dikes (SiO_2 = 62.55 to 66.26 weight percent; K_2O = 2.01 to 3.01 weight percent; *n* = 19 analyses) mapped to the west in the upper parts of Culvert Creek in the Badger Lake 7.5′ quadrangle mark the vent area (McClaughry and others, 2020a). **Tpdf** crops out as precipitous cliff-forming exposures marked by meter-scale columnar jointing; columns are often characterized by internal, horizontal platy joint sets (**Figure 6-28a,b**; **Figure 6-29a,b**). Outcrops weather to meter-scale, subround boulders and angular slabs, forming extensive talus slopes beneath cliffs. Irregularly shaped gabbro-norite inclusions (SiO_2 = 53.85 to 57.77 weight percent; K_2O = 0.72 to 1.88 weight percent; *n* = 7 analyses outside Mill Creek area), ranging from centimeters up to several meters across, are a conspicuous and distinguishing feature of this unit throughout its outcrop distribution (**Figure 6-29c**; McClaughry and others, 2020a). Concentration of inclusions ranges from ~5 to ≤50 percent (vol.). The composite thickness of the unit in the map area is ~60 to 70 m (197 to 230 ft)(Plate 1). Typical hand samples of **Tpdf** are medium-light gray (N6), medium-dark gray (N4), light-bluish gray (5B 7/1), to medium-bluish gray (5B 5/1), containing 10 to 20 percent (vol.) clear to chalky white (N9), euhedral to subhedral, prismatic to blocky, seriate plagioclase microphenocrysts and phenocrysts ≤1 cm (0.4 in); 2 to 3 percent (vol.) grayish black (N2), euhedral to subhedral, blocky to prismatic, seriate pyroxene microphenocrysts and phenocrysts ≤3 mm (0.1 in)(amount of orthopyroxene > clinopyroxene); and ~2 percent (vol.) plagioclase-pyroxene glomerocrysts ≤6 mm (0.2 in); all distributed within a very fine-grained holocrystalline to hypocrystalline groundmass (**Figure 6-30**). Gabbro-norite inclusions are medium-light gray (N6) to pale yellowish brown (10YR 6/2) and equigranular, with a mottled medium-grained holocrystalline groundmass of plagioclase and pyroxene (clinopyroxene + orthopyroxene) (**Figure 6-29c**).

Tpdf has normal magnetic polarity and is assigned a late Pliocene age on the basis of stratigraphic position and a groundmass $^{40}Ar/^{39}Ar$ plateau age of 3.02 ± 0.02 Ma obtained from outcrops between Fifteenmile and Larch Creeks in the Wolf Run 7.5′ quadrangle (**Figure 6-1**; Plate 3; **Appendix**). The 3.02 Ma age is similar to a previously obtained K-Ar analysis of 2.86 ± 0.06 Ma (plagioclase) reported by Sherrod and Scott (1995) and Gray and others (1996) for a sample near Cold Point.

Figure 6-28. The dacite of Fifteenmile Creek (Tpdf) cropping out in the upper Fifteenmile Creek drainage (45.387246, -121.335311). (a) Tpdf fills a paleochannel incised into the underlying tuff breccia of Engineers Creek (Tpdd1). View is looking west up Fifteenmile Creek toward Mount Hood. (b) Close-up of cliff-forming outcrops in (a), showing characteristic massive columnar to platy jointing (45.383368, -121.337802). View is looking northwest. Photo credits: Clark Niewendorp, 2015.

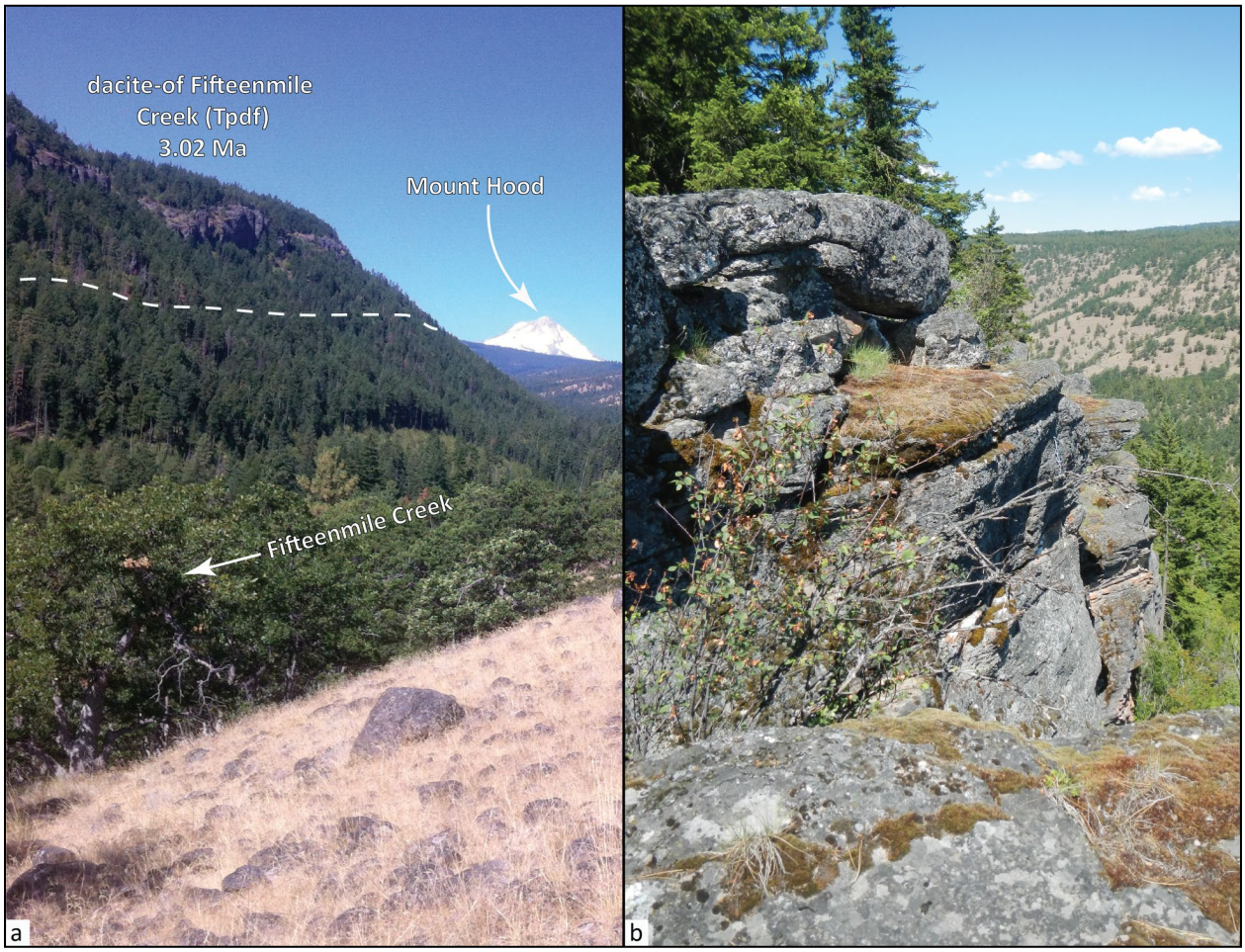

Figure 6-29. Outcrops of the dacite of Fifteenmile Creek (Tpdf). (a) Precipitous cliff-forming outcrops of Tpdf in the upper part of Fret Creek, west of Oval Lake (45.33149, -121.49687). View is looking southwest into the Badger Creek drainage. (b) Close-up view of cliff-forming outcrops of Tpdf (45.37959, -121.38030). Hammer for scale is 38 cm (15in) long. View is looking north. (c) Tpdf conspicuously includes irregularly shaped gabbro-norite inclusions throughout its outcrop distribution (outlined with black dashes) 45.35267, -121.42572). Pen magnet for scale is 12 cm (4.8 in) long. Photo credits: Jason McClaughry, 2016 and 2017.

Table 6-2. Representative XRF analyses for Pliocene volcanic rocks in the Mill Creek area.

Sample	692 MCBJ 16	RC98-193	57 HRJ 11[1]	121 WRCN 15[2]	498 MCBJ 16	106 MCBJ 16	105 MCBJ 16
Geographic Area	Fifteenmile Creek	Marion Point	Hood River	Larch Creek	Middle Fork Fivemile Creek	Snakehead Creek	Snakehead Creek
Formation	Pliocene volcanics	Pliocene volcanics	Pliocene volcanics	Pliocene volcanics	Pliocene volcanics	Pliocene volcanics	Pliocene volcanics
Map Unit	Tpdf	Tpaf	Tpbh	Tpdd1 (clast)	Tpdv	Tpbrc	Tpbs
Latitude	45.3769	45.3607	45.7127	45.3724	45.4646	45.5871	45.5890
Longitude	-121.3804	-121.4708	-121.5450	-121.3703	-121.3846	-121.4834	-121.4847
Age (Ma)	3.02	nd	nd	3.7	3.69	nd	nd
Plate	3	3	na	na	3	2	2
Map Label	G21	G9	na	na	G67	G92	G97
Oxides, weight percent							
SiO_2	63.24	60.20	47.67	62.96	65.78	49.54	49.67
Al_2O_3	16.51	17.15	18.34	16.62	14.96	17.23	16.97
TiO_2	0.91	0.99	1.06	0.91	0.92	1.21	1.69
FeOTotal	5.60	6.06	10.57	5.69	6.41	11.25	12.37
MnO	0.09	0.10	0.17	0.10	0.10	0.17	0.19
CaO	5.08	6.03	10.69	5.09	2.94	9.59	8.97
MgO	2.18	3.33	8.31	2.18	0.81	7.55	6.49
K_2O	2.19	1.83	0.27	2.19	2.96	0.23	0.35
Na_2O	3.96	4.13	2.78	4.02	4.84	3.12	3.14
P_2O_5	0.23	0.18	0.15	0.24	0.28	0.11	0.16
LOI	0.58	nd	1.17	0.77	0.49	0.00	0.46
Total_I	98.82	nd	101.18	98.41	99.19	99.76	99.48
Trace Elements, parts per million							
Ni	24	32	92	26	1	119	100
Cr	37	42	263	31	1	212	194
Sc	12	10	30	13	12	29	32
V	91	116	195	93	21	184	206
Ba	435	370	178	465	617	87	140
Rb	50	35	2.3	49	71	2	5
Sr	473	519	594	473	254	258	302
Zr	239	192	87	240	391	73	96
Y	24	22	21	25	62	22	33
Nb	13.6	10.9	2.0	14.2	27.4	3.5	6.4
Ga	21	19	17	18	23	18	20
Cu	30	38	50	23	21	47	49
Zn	75	68	76	75	109	89	104
Pb	8	2	nd	6	9	1	2
La	29	23	16	37	64	5	10
Ce	54	51	29	59	67	14	18
Th	6	6	0	6	9	0	1
Nd	24	0	nd	30	70	10	16
U	4	0	1	2	4	1	0

Major element determinations have been normalized to a 100-percent total on a volatile-free basis and recalculated with total iron expressed as FeOTotal; nd = no data or element not analyzed; na = not applicable or no information. LOI = Loss on Ignition; Total_I = original analytical total. Data from: [1]McClaughry and others (2012); McClaughry and others (2021).

Figure 6-30. Hand sample and thin section photographs of the dacite of Fifteenmile Creek (Tpdf). (a) Typical abundantly plagioclase-phyric hand sample. Scale bar is 2.5 cm (1 in). (b) Thin section under cross-polarized light. (c) Same view as in (b) under plane-polarized light. Scale bar in (b) and (c) is 7 mm (0.3 in). Photo credits: Jason McClaughry, 2015.

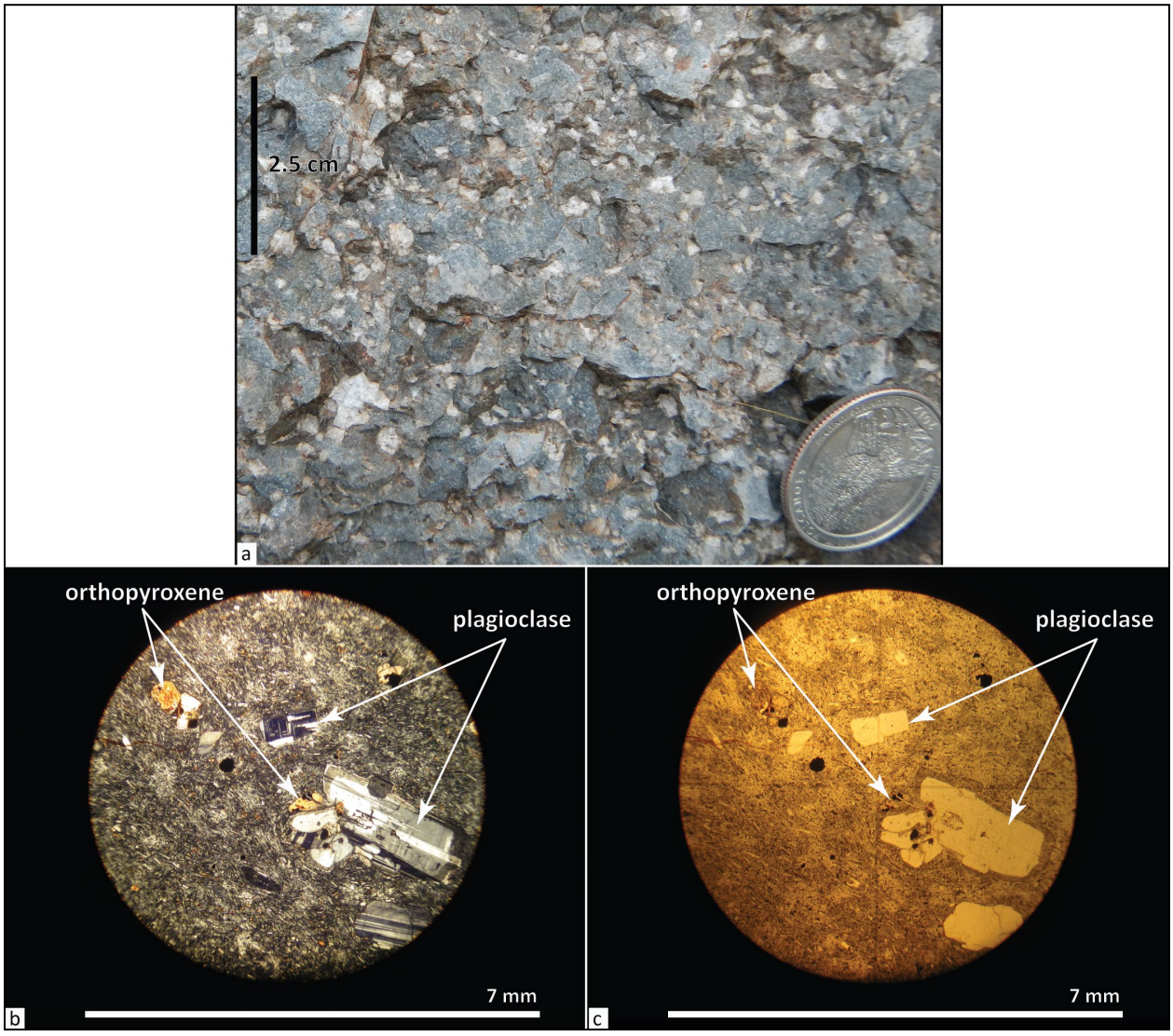

Tpaf **andesite of Fret Creek (upper Pliocene)**—Andesite lava flow (SiO_2 = 59.83 to 60.79 weight percent; K_2O = 1.73 to 1.94 weight percent; *n* = 7 analyses [5 outside Mill Creek area]) mapped between Oval Lake and Eightmile Meadow in the broad glacial cirque forming upper Fifteenmile and Fret Creeks in the northern part of the Flag Point 7.5′ quadrangle (**Figure 6-31**; **Table 6-2**; Plate 3; **Appendix**; McClaughry and others, 2020a). **Tpaf** lava flows are mapped eastward into the vicinity of Fifteenmile Campground and Cold Springs (Plate 1). Outcrops of **Tpaf** are characterized by thick intervals of platy to tabular jointing; more typically the unit is exposed as piles of meter-scale boulders and slabs scattered across the forest floor (**Figure 6-31**). The unit has an apparent thickness exceeding 300 m (984 ft) in upper Fifteenmile Creek (Plate 1). Typical hand samples of the andesite are medium-dark gray (N4) to medium-bluish gray (5B 5/1) and pale blue (5B 6/2), containing 5 to 10 percent (vol.) clear to chalky white (N9), euhedral to subhedral, prismatic to blocky, seriate plagioclase microphenocrysts and phenocrysts ≤4 mm (0.1 in); ~2 percent (vol.) grayish black (N2), subhedral to euhedral, blocky to prismatic, seriate pyroxene microphenocrysts and phenocrysts ≤2 mm (0.08 in)(orthopyroxene > clinopyroxene); and ≤1 percent (vol.) plagioclase-pyroxene glomerocrysts ≤1 cm (0.4 in), all contained within a fine-grained holocrystalline groundmass (**Figure 6-32**).

Tpaf has normal magnetic polarity and is assigned a late Pliocene age on the basis of stratigraphic position below the ~3.02 Ma dacite of Fifteenmile Creek (**Tpdf**) and the 3.14 Ma andesite and dacite of Senecal Spring (**Figure 6-1**; Plate 3; **Appendix**; McClaughry and others, 2020a). **Tpaf** overlies the 3.77 Ma porphyritic trachydacite of Culvert Creek between the East Fork Hood River and Brooks Meadow Road in the Dog River 7.5′ quadrangle (and others, 2020a).

Figure 6-31. The andesite of Fret Creek (Tpaf) cropping out near Fifteenmile Campground (45.34949, -121.47108). Hammer for scale is 38 cm (15 in) long. View is looking south. Photo credit: Jason McClaughry, 2016.

Figure 6-32. Hand sample and thin section photographs of the andesite of Fret Creek (Tpaf). (a) Typical hand sample. Scale bar is 2.5 cm (1 in). (b) Thin section under cross-polarized light. (c) Same view as in (b) under plane-polarized light. Scale bar in (b) and (c) is 7 mm (0.3 in). Photo credits: Jason McClaughry, 2017.

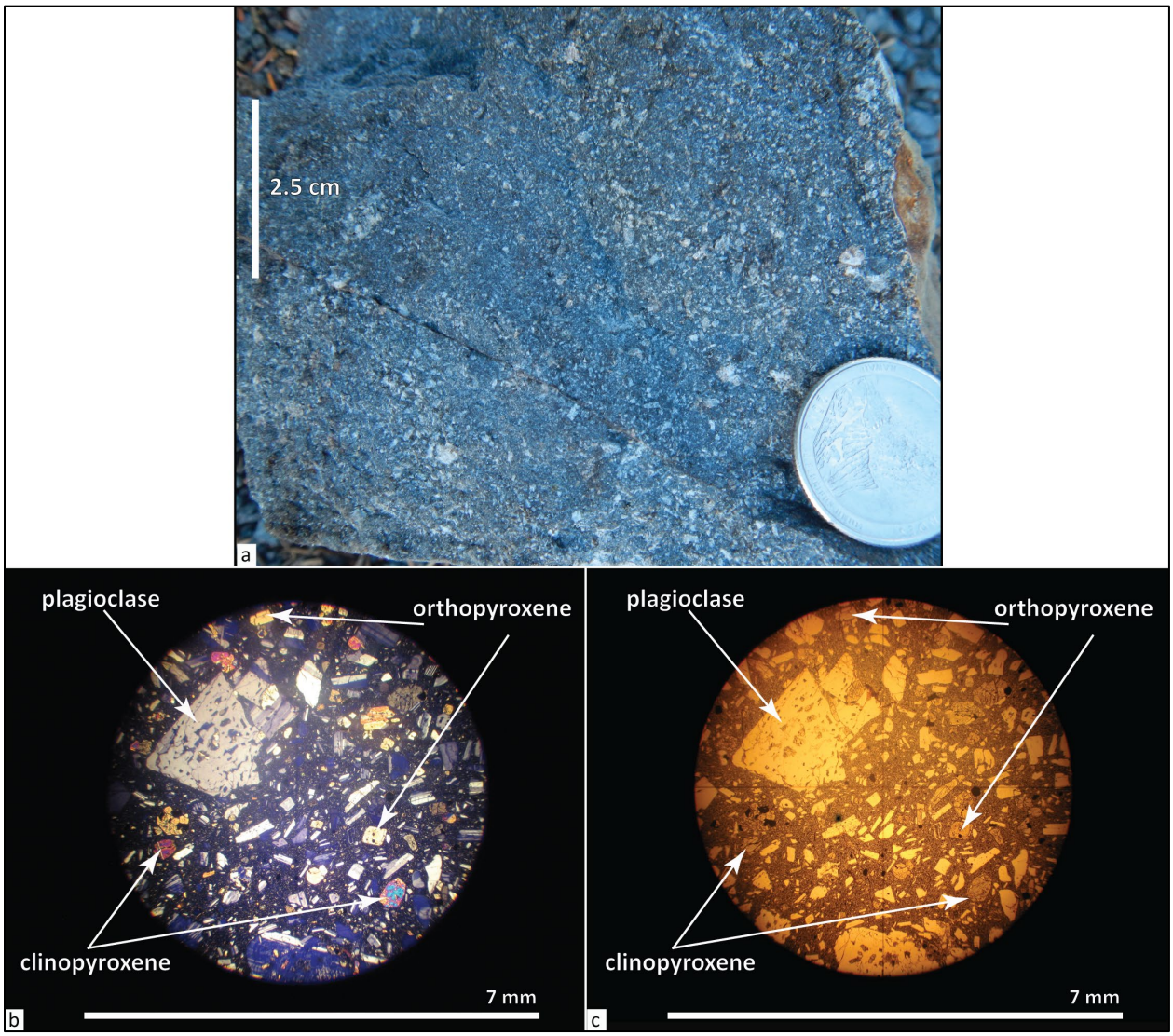

Tpbh **basalt of Hood River (upper Pliocene)**—Basalt lava flows (SiO_2 = 47.67 to 49.75 weight percent; FeOTotal = 9.10 to 13.07 weight percent; 6.14 to 8.31 weight percent MgO; K_2O = 0.19 to 0.78 weight percent; *n* = 7 analyses outside Mill Creek area) mapped above the Dalles Formation (**Tmdl**) in the northwest part of the Ketchum Reservoir 7.5′ quadrangle (**Table 6-2**; Plate 2). **Tpbh** in the map area is equivalent to abundantly plagioclase-porphyritic basalt that underlies the city of Hood River, ~10 km (6.2 mi) to the northwest (McClaughry and others, 2012). At Hood River, the basalt typically outcrops as interstratified, blocky-jointed, vesicular pahoehoe lobes and tumuli ranging from 2 m to 8 m (6.6 ft to 26 ft) thick. The composite thickness of the lava flow succession in the Hood River area is ~30 m (98 ft) (McClaughry and others, 2012). Typical hand samples of the basalt are medium light gray (N6) to medium-bluish gray (5B 5/1) and distinctly plagioclase-porphyritic, containing ≤50 percent (vol.), colorless, euhedral, prismatic, seriate plagioclase (labradorite) microphenocrysts and phenocrysts ≤8 mm (0.3 in); 2 to 3 percent (vol.)

greenish black (5GY2/1), subhedral, blocky clinopyroxene ≤3 mm (0.1 in); and ~5 to 10 percent (vol.) greenish black (5GY2/1) to dusky red (5R 3/4), subhedral to anhedral, polygonal to blocky shaped, seriate iddingsitized olivine microphenocrysts and phenocrysts ≤4 mm (0.2 in); all contained within a diktytaxitic, trachytic, intersertal to ophimottled, coarse-grained hypocrystalline groundmass (**Figure 6-33**). Thin sections show subophitic clinopyroxene with numerous embedded plagioclase laths and contain 1 to 3 percent (vol.) Fe-Ti oxides (**Figure 6-33b,c**).

Tpbh has normal magnetic polarity and is assigned a late Pliocene age on the basis of stratigraphic position between the 3.05 Ma basalt of Post Canyon and the 3.67 Ma basalt of Ruthton Point near Hood River (McClaughry and others, 2012; **Figure 6-1**).

Figure 6-33. Hand sample and thin section photographs of the basalt of Hood River (Tpbh). (a) Typical abundantly plagioclase-porphyritic hand sample. Scale bar is 2.5 cm (1 in). (b) Thin section under cross-polarized light. (c) Same view as in (b) under plane-polarized light. Scale bar in (b) and (c) is 7 mm (0.3 in). Photo credits: Jason McClaughry, 2012.

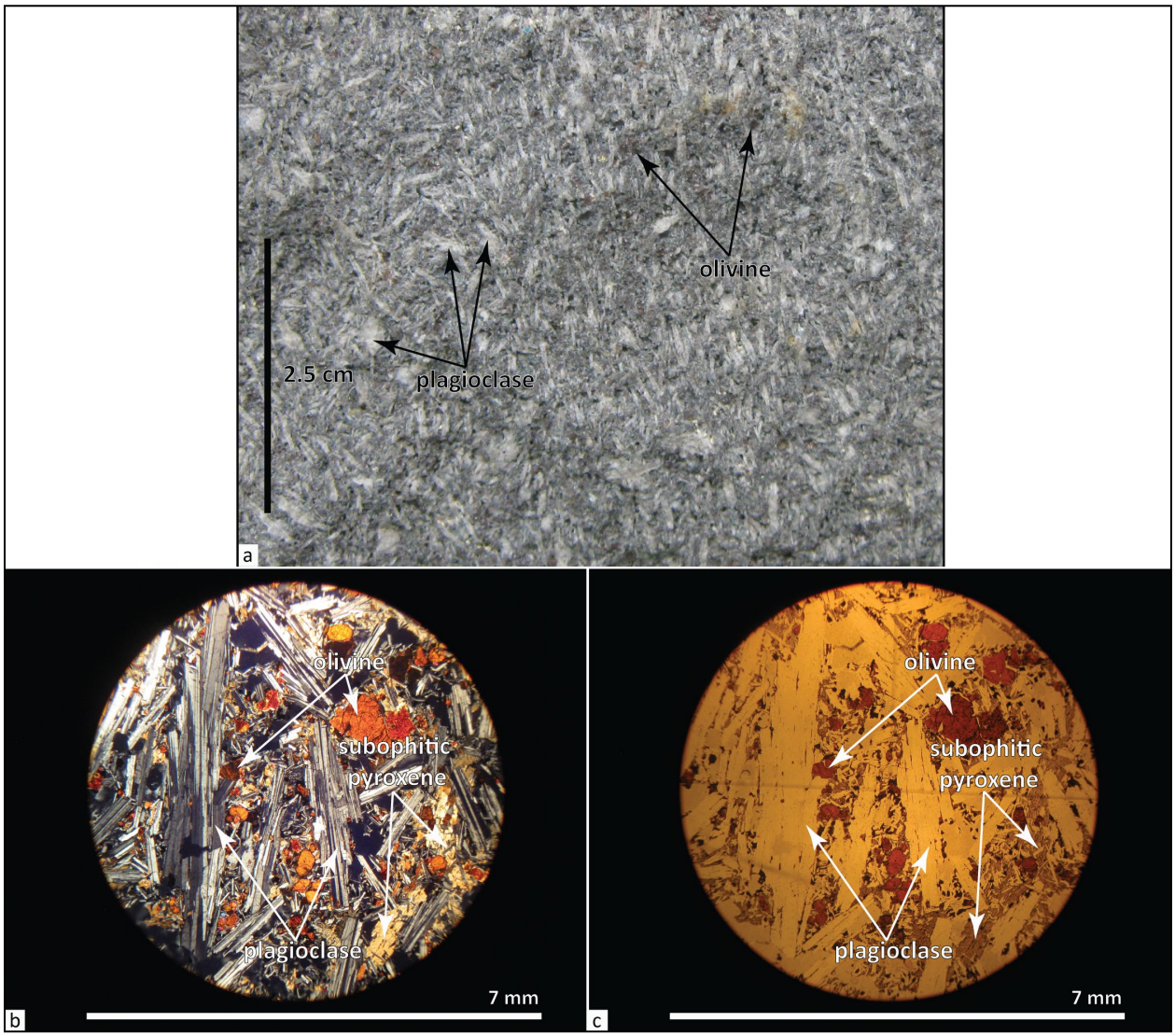

Tpdd1 **tuff breccia of Engineers Creek, lower unit (lower Pliocene)**—Tuff breccia and pumice tuff mapped below the dacite of Fifteenmile Creek (**Tpdf**) in a NE-oriented outcrop belt along Fifteenmile, Cedar, and Larch creeks in the Fivemile Butte and Flag Point 7.5′ quadrangles (Plate 1). **Tpdd1** is mapped ~5 km (3 mi) west of Fifteenmile Campground into the headwaters of Engineers Creek, along the eastern escarpment of the Hood River graben (McClaughry and others, 2020a), and is also mapped northeast of the headwaters of Larch Creek for ~40 km (25 mi) through Dufur to Rice (**Figure 6-34**; McClaughry and others, 2021). In the Dufur area to the east, **Tpdd1** is interbedded with a compositionally similar sequence of ash-flow tuff and additional tuff breccia units (units Tpdd2, Tptf1, and Tptf2 of McClaughry and others, 2021). **Tpdd1** is massively bedded to faintly stratified, matrix- to clast-supported, and very poorly sorted. **Tpdd1** characteristically contains highly angular, texturally similar-appearing clasts of dense to highly vesiculated, grayish black (N2) plagioclase-phyric glassy andesite to rhyolite. Most clasts are ≤10 cm (4 in) across, but deposits occasionally contain outsized blocks ranging from 10 cm (4 in) to several meters across. **Tpdd1** has a dusky red (5R 3/4) oxidized to grayish yellow (5Y 8/4), yellowish gray (5Y 7/2), and grayish orange pink (5YR 7/2), poorly sorted matrix tuffaceous sandstone matrix. **Tpdd1** contains a texturally similar, but chemically diverse assemblage of dense to vesiculated and fractured, angular to subangular clasts of medium-dark gray (N4) to black (N1) porphyritic andesite, trachyandesite, dacite, and trachydacite (SiO_2 = 58.91 to 68.72 weight percent; K_2O = 2.00 to 3.42 weight percent; Nb = 14.2 to 29.9 ppm; Zr = 194 to 428 ppm; *n* = 26 analyses outside the map area)(**Table 6-2**; McClaughry and others, 2020a, 2021). The breccia also includes very sparse angular clasts of light brownish gray (5YR 6/1) to very pale orange (10YR 8/2), flow-banded rhyolite (SiO_2 = 69.34 to 75.31 weight percent; K_2O = 3.09 to 4.38 weight percent; Nb = 22.2 to 29.9 ppm; Zr = 150 to 430 ppm; *n* = 3 analyses outside the map area), and black (N1) perlitic obsidian nodules (McClaughry and others, 2020a, 2021).

Tpdd1 is assigned an early Pliocene age on the basis of stratigraphic position beneath the 3.02 Ma dacite of Fifteenmile Creek (**Tpdf**) and 3.68 Ma tuff of Friend (**Figure 6-1**; Plate 3; McClaughry and others, 2021). A sample of the non-welded pumice tuff, defining the base of **Tpdd1** near Dufur, has an $^{40}Ar/^{39}Ar$ plateau age from plagioclase of 3.83 ± 0.01 Ma (McClaughry and others, 2021). A single clast also obtained from **Tpdd1** near Dufur has an $^{40}Ar/^{39}Ar$ plateau age on plagioclase of 3.71 ± 0.02 Ma (McClaughry and others, 2021). Collectively, **Tpdd1** mapped between Engineers Creek and Rice, define a ~50-km-long (31-mi-long) early Pliocene paleochannel (**Figure 6-34**; McClaughry and others, 2020a, 2021). The source area for **Tpdd1** is presumed to lie within the Hood River graben.

Figure 6-34. Distribution of the lower unit of the tuff breccia of Engineers Creek (Tpdd1) and related units of McClaughry and others (2021) mapped between the headwaters of Fifteenmile Creek, Friend, Dufur, and Rice. The inferred source area is located an additional 15 km (9.3 mi) west of site 244b DFWJ 15 along the East Fork Hood River (out of figure view). Red arrows represent sample sites for size measurements of clasts reported in McClaughry and others (2021). Base map is a Google Earth™ image, with an oblique view looking north toward The Dalles and the Columbia River.

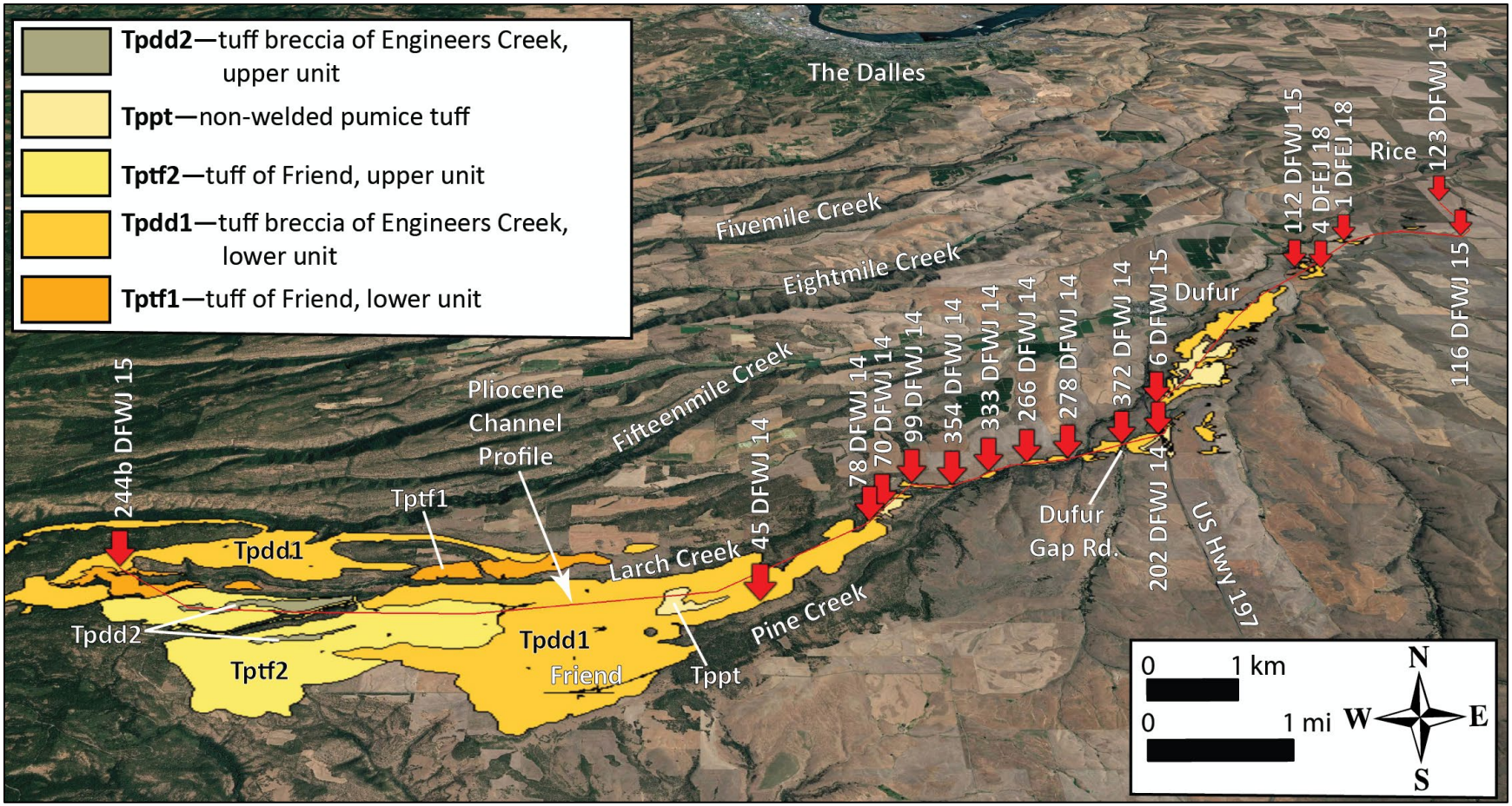

Tpdv **trachydacite of Fivemile Creek (lower Pliocene)—**Trachydacite lava flow (SiO_2 = 64.09 to 66.67 weight percent; K_2O = 2.76 to 3.36 weight percent; Nb = 24.8 to 31 ppm; Zr = 356 to 421 ppm; *n* = 20 analyses [18 outside Mill Creek area]) mapped as an intracanyon lava flow along Fivemile Creek (**Figure 6-35**; **Table 6-2**; Plates 1 and 3; **Appendix**). Mapping over the larger Middle Columbia Basin indicates that **Tpdv** is present from western exposures on the East Fork Hood River and south of Mill Creek Buttes (McClaughry and others, 2020a), heading northeast ~30 km (18.6 mi) downstream to outcrops along Fivemile Creek at Pleasant Ridge Road in The Dalles South 7.5′ quadrangle (**Figure 1-2**). **Tpdv** crops out as prominent cliffs and benches marked by massive to meter-scale columnar-joints and irregular zones of horizontal platy jointing (**Figure 6-35**). The common bench and rise topography associated with outcrops along Fivemile Creek and intervening vesicular horizons may indicate that two chemically identical and age-equivalent intracanyon lava flows are present within the unit (**Figure 6-35**). Outcrops weather to meter-scale, angular subrounded boulders and angular plates forming extensive talus slopes beneath cliffs. Composite thickness of unit **Tpdv** is ≥90 m (296 ft) in the canyon of Fivemile Creek (Plates 1 and 3). **Tpdv** is locally capped by sedimentary deposits of **QTpg** (**Figure 6-27**). Typical hand samples of the **Tpdv** are dark gray (N3) containing 1 to 2 percent (vol.) clear, subhedral to anhedral, prismatic to blocky, seriate plagioclase microphenocrysts and phenocrysts ≤3 mm (0.1 in); ~1 percent (vol.) grayish black (N2), euhedral to subhedral, prismatic- to lath-shaped pyroxene microphenocrysts ≤1 mm (0.04 in)(orthopyroxene ≥ clinopyroxene); and ≤1 percent (vol.) plagioclase-pyroxene microglomerocrysts ≤1 mm (0.1 in); all distributed within a very fine-grained holocrystalline to hypocrystalline groundmass (**Figure 6-36**).

Tpdv has reversed magnetic polarity and is assigned an early Pliocene age on the basis of stratigraphic position and an $^{40}Ar/^{39}Ar$ groundmass plateau age of 3.69 ± 0.02 Ma obtained from the outcrops in Fivemile Canyon (**Figure 6-1**; **Appendix**; McClaughry and others, 2021).

Figure 6-35. Cliff- and bench-forming trachydacite of Fivemile Creek (Tpdv) cropping out along Upper Fivemile Road (45.46541, -121.37739). View is looking north. Photo credit: Jason McClaughry, 2016.

Figure 6-36. Hand sample and thin section photographs of the trachydacite of Fivemile Creek (Tpdv). (a) Typical hand sample. Scale bar is 2.5 cm (1 in) tall. (b) Thin section under cross-polarized light. (c) Same view as in (b) under plane-polarized light. Scale bar in (b) and (c) is 7 mm (0.3 in). Photo credits: Jason McClaughry, 2016.

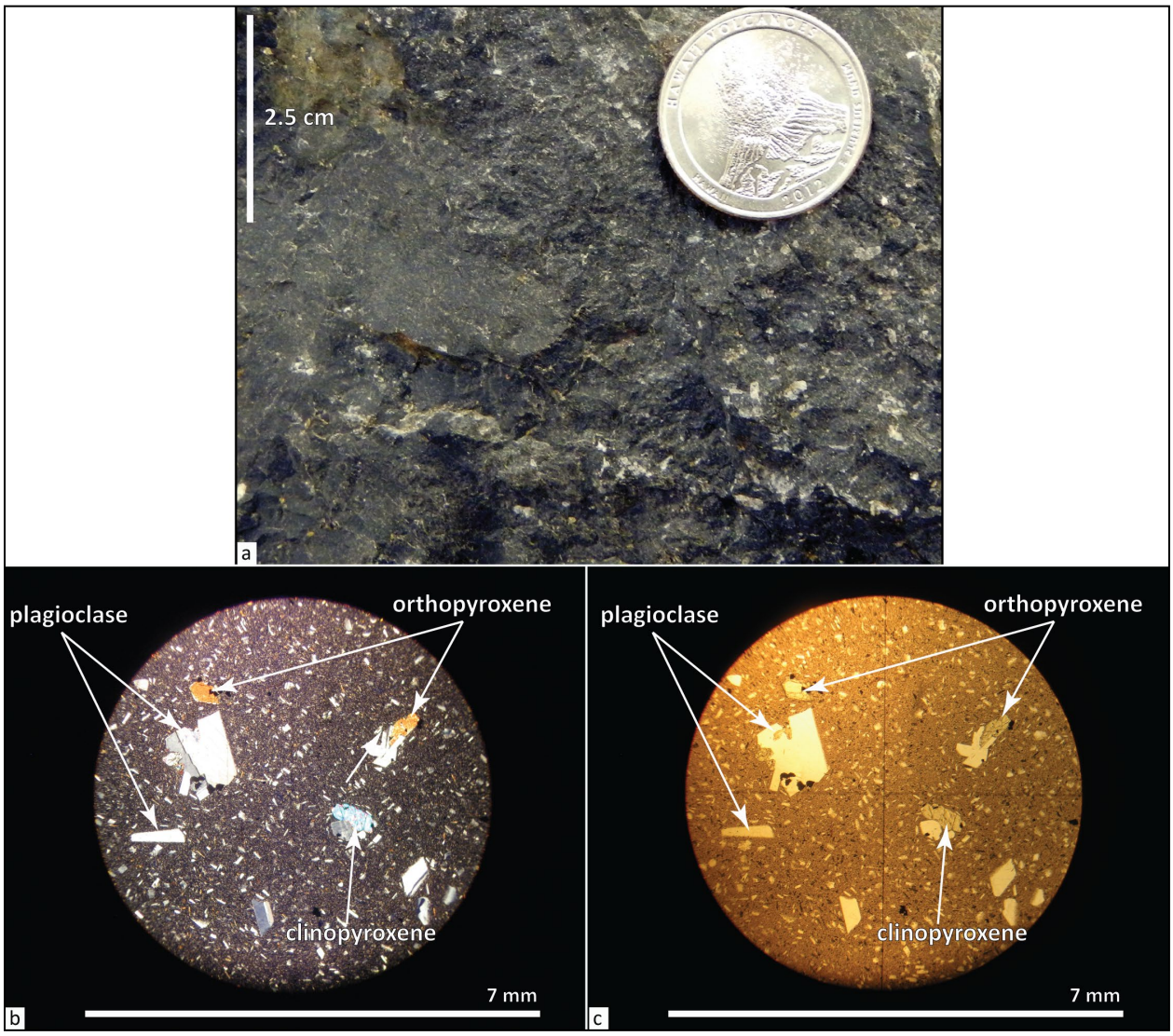

Tpbrc **basalt of Rock Creek (lower Pliocene)**—Low-potassium tholeiitic basalt lava flow (SiO_2 = 49.3 to 49.54 weight percent; FeOTotal = 11.25 to 11.54 weight percent; 7.49 to 7.59 weight percent MgO; K_2O = 0.18 to 0.23 weight percent; *n* = 3 analyses) mapped in a NNE-trending outcrop belt between Rock Creek and Snyder Canyon in the northwest part of the Ketchum Reservoir 7.5′ quadrangle (**Figure 6-37**; **Table 6-2**; Plate 2; **Appendix**). **Tpbrc** is deeply weathered, typically recognized as piles of meter-scale boulders and slabs floating in a matrix of moderate orange-pink (5YR 8/4) to grayish orange (10YR 7/4) soils (**Figure 6-37**). Coherent outcrops are only found in a few rock pits and smaller excavations. Thickness of the unit is as much as 20 m (66 ft). Typical hand samples are medium-light gray (N6), containing 2 to 5 percent (vol.) clear to white (N9), euhedral, prismatic, seriate plagioclase microphenocrysts and phenocrysts ≤7 mm (0.3 in); ≤1 percent (vol.) grayish black (N2) to dusky green (5G 3/2), subhedral, blocky, clinopyroxene ≤3 mm (0.1 in); and 2 to 5 percent (vol.), dark greenish yellow (10Y 6/6), euhedral to anhedral,

polygonal to blocky, seriate olivine microphenocrysts and phenocrysts ≤3 mm (0.1 in) across, and 5 to 10 percent (vol.) glomerocrysts of plagioclase, olivine, ±pyroxene ≤1 cm (0.4 in); all contained within an intersertal to ophimottled, fine-grained holocrystalline groundmass (**Figure 6-38**). Thin sections show subophitic clinopyroxene with numerous embedded plagioclase laths (**Figure 6-38b,c**). Olivine are typically skeletal in form, corroded and partially resorbed, with rims altered to dark yellowish orange (10YR 6/6) iddingsite (**Figure 6-38b,c**). Thin sections contain 1 to 3 percent (vol.) Fe-Ti oxides.

Tpbrc has reversed magnetic polarity and is assigned an early Pliocene age on the basis of stratigraphic position and geochemical composition (**Figure 6-1**; Plate 2; **Appendix**). **Tpbrc** is geochemically similar to the underlying basalt of Snakehead Creek (**Tpbs**); it is distinguished on the basis of conspicuous glomerocrysts and geomorphic expression (**Figure 6-38a,b**). **Tpbrc** was erupted from an extant vent that forms high topography between the headwaters of Rock Creek and Snakehead Creek in the west-central part of the Ketchum Reservoir 7.5′ quadrangle (Plate 2). The lava flow flowed north away from source vents into the headwaters of Rock Creek and south toward Beaver Creek.

Figure 6-37. Basalt of Rock Creek (Tpbrc) cropping out north of Snakehead Creek and west of the Hood River fault zone (45.58708, -121.48347). Hammer for scale is 38 cm (15 in) long. View is looking northeast. Photo credit: Jason McClaughry, 2015.

Figure 6-38. Hand sample and thin section photographs of the basalt of Rock Creek (Tpbrc). (a) Typical hand sample. Scale bar is 2.5 cm (1 in). (b) Thin section under cross-polarized light. (c) Same view as in (b) under plane-polarized light. Scale bar in (b) and (c) is 7 mm (0.3 in). Photo credits: Jason McClaughry, 2016.

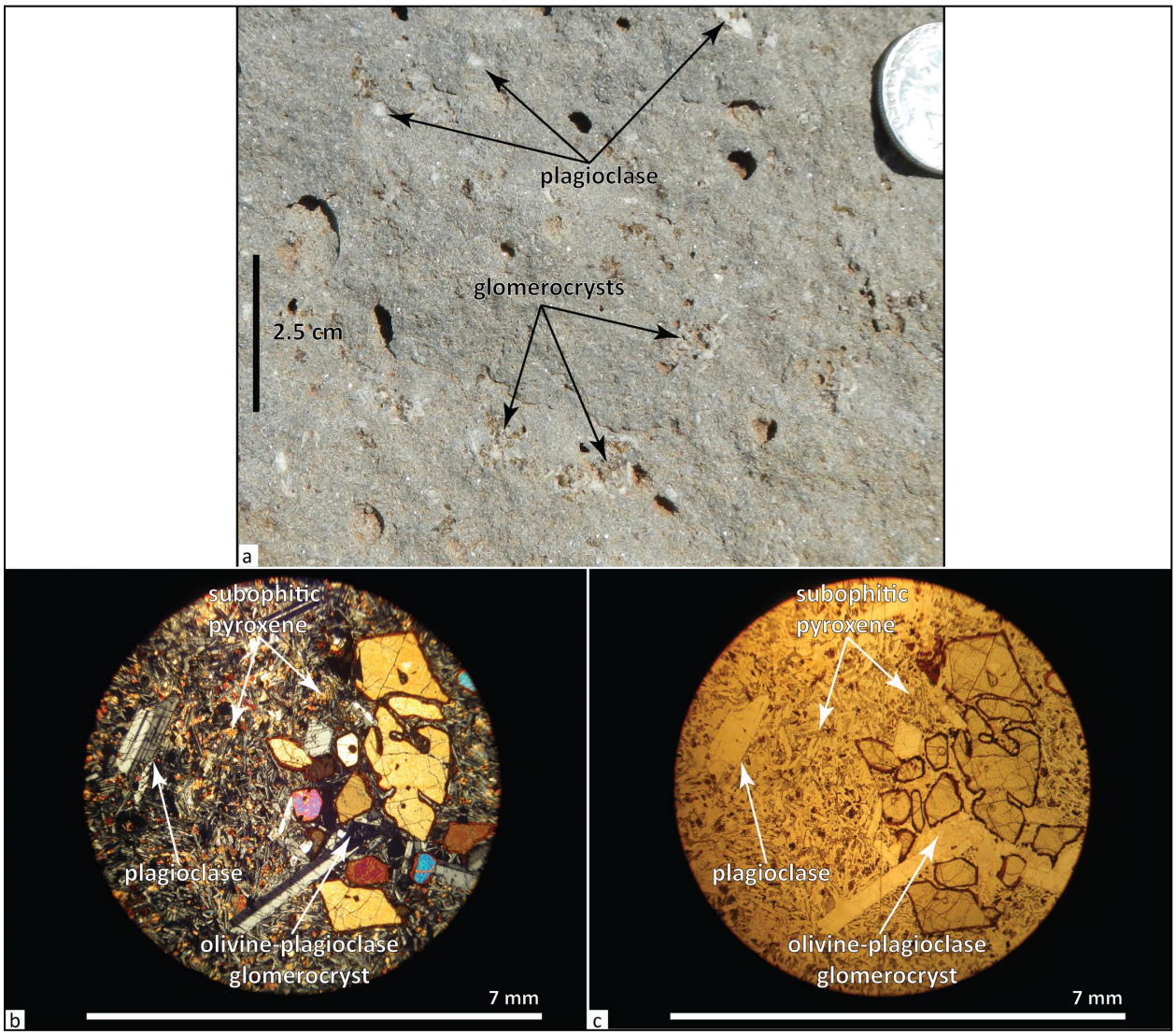

Tpbs **basalt of Snakehead Creek (lower Pliocene)**—Low-potassium tholeiitic basalt lava flows (SiO_2 = 48.53 to 50.35 weight percent; FeOTotal = 10.62 to 12.37 weight percent; 6.49 to 8.42 weight percent MgO; K_2O = 0.16 to 0.39 weight percent; *n* = 19 analyses [6 outside Mill Creek area]) mapped in a NNE-trending outcrop belt between Neal Creek and Snyder Canyon in the northwest part of the Ketchum Reservoir 7.5′ quadrangle (**Figure 6-39**; **Table 6-2**; Plate 2; **Appendix**). Precipitous cliffs between Neal Creek and Snakehead Creek are composed of a stacked flow-on-flow succession of thin (1 to 5 m [3.3 to 16.4 ft]) blocky- to columnar-jointed pahoehoe lava flows (**Figure 6-39a**). Individual pahoehoe flow lobes are separated by intervening layers of 'A'ā flow breccia. Singular vesicles or vesicle cylinders are common within individual lava flow layers (**Figure 6-39b**). Composite thickness of **Tpbs** is as much as 110 m (360 ft). Typical hand samples are medium-light gray (N6), containing ≤1 percent (vol.) clear to white (N9), euhedral, prismatic, seriate plagioclase microphenocrysts ≤1 mm (0.04 in); ≤1 percent (vol.) fresh grayish black (N2)

to dusky green (5G 3/2), subhedral, blocky, clinopyroxene ≤3 mm (0.1 in); 2 to 3 percent (vol.) fresh dark greenish yellow (10Y 6/6), euhedral to anhedral, polygonal- to blocky-shaped, seriate olivine microphenocrysts and phenocrysts ≤3 mm (0.1 in) across; and ≤1 percent (vol.) glomerocrysts of plagioclase, olivine, ±pyroxene ≤5 mm (0.2 in); all contained within an intersertal to ophimottled, fine-grained hypocrystalline groundmass (**Figure 6-40**). Thin sections show subophitic clinopyroxene with numerous embedded plagioclase laths. Olivine are typically skeletal in form, corroded and partially resorbed, with rims altered to dark yellowish orange (10YR 6/6) iddingsite (**Figure 6-40b,c**). Thin sections contain 1 to 3 percent (vol.) Fe-Ti oxides. The relatively equal distribution of groundmass plagioclase and intergranular olivine results in a typical speckled appearance for the rock.

The lowest lava flow in **Tpbs** has normal magnetic polarity, while upper lava flows have reversed magnetic polarity (**Appendix**). **Tpbs** is assigned a lower Pliocene age as the unit shares a similar stratigraphic position and geochemical composition with the 4.19 Ma basalt and basaltic andesite of Rimrock Creek (McClaughry and others, 2020a) on Surveyors Ridge (**Figure 6-1**; Plate 2; **Appendix**). Magnetic transition from normal polarity lower lava flows to upper reversed polarity lava flows is also consistent with eruption of **Tpbs** during the normal to reversed polarity transition at 4.2 Ma in the upper part of the Gilbert reversed polarity chron.

Figure 6-39. The basalt of Snakehead Creek (Tpbs) cropping out between Neal Creek and Snakehead Creek in the Ketchum Reservoir 7.5′ quadrangle. (a) A stacked flow-on-flow succession of Tpbs, characterized by meter-scale columnar jointing (45.58035, -121.48116). View is looking northwest. (b) Arrow points to a vesicle cylinder in Tpbs (45.56848 -121.48845). Hammer for scale is 38 cm (15 in) long. Photo credits: Jason McClaughry, 2015.

Figure 6-40. Hand sample and thin section photographs of the basalt of Snakehead Creek (Tpbs). (a) Typical hand sample. Scale bar is 2.5 cm (1 in). (b) Thin section under cross-polarized light. (c) Same view as in (b) under plane-polarized light. Scale bar in (b) and (c) is 7 mm (0.3 in). Photo credits: Jason McClaughry, 2016.

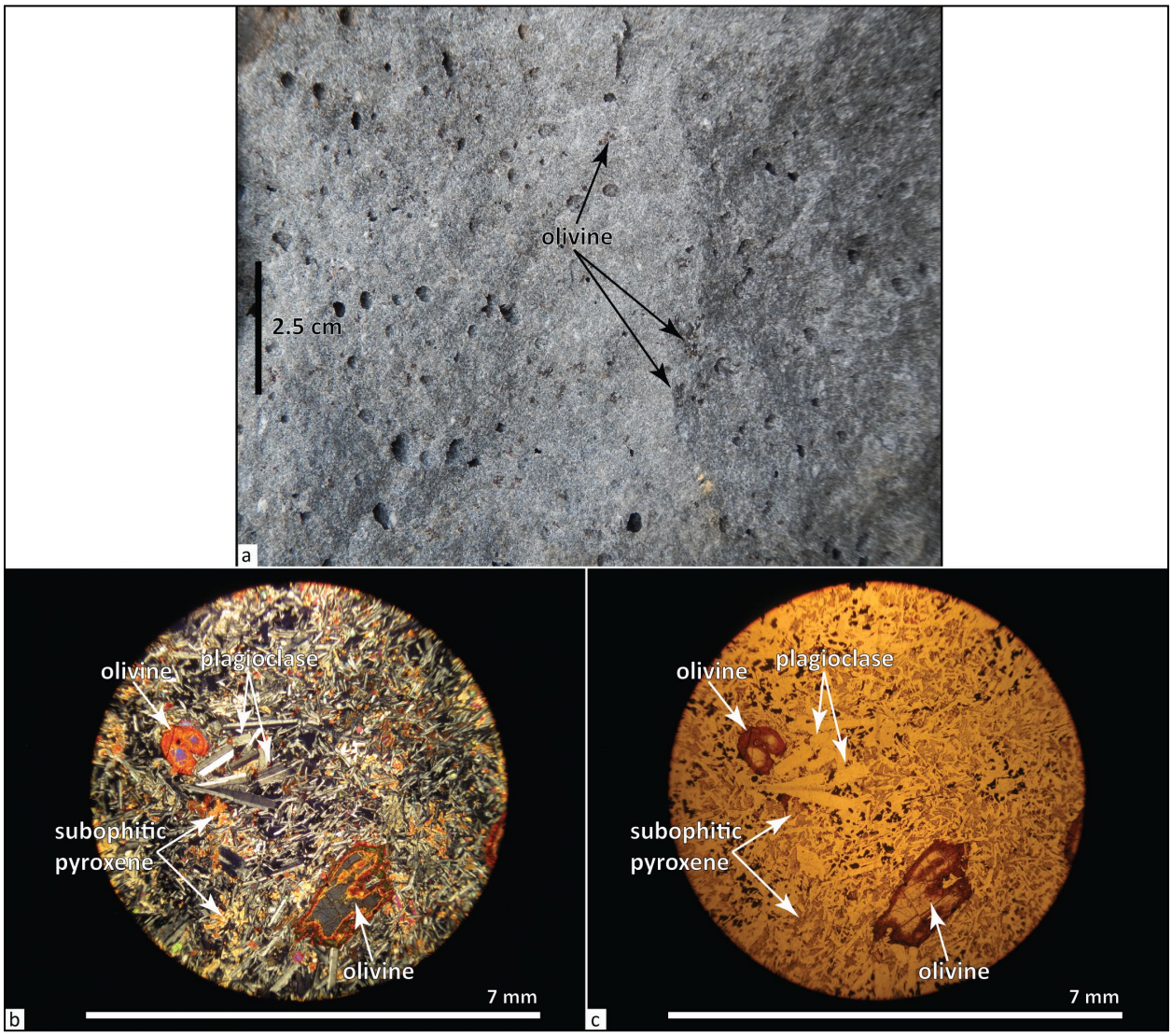

Disconformity

6.3.3 Lower Pliocene and upper Miocene volcanic and sedimentary rocks of the early High Cascades

6.3.3.1 Dalles Formation

Tmdl **Dalles Formation, undivided (lower Pliocene[?] and upper Miocene)**—Moderately to well indurated, pale yellowish brown (10YR 6/2), medium gray (N5) to very light gray (N8) boulder breccia, fluvial conglomerate and sandstone, tuffaceous siltstone, and pumice-, ash-, and lithic-tuff, broadly exposed above the CRBG in the Mill Creek area (**Figure 6-41**, **Figure 6-42**, **Figure 6-43;** Plates 1, 2, and 3). A majority of **Tmdl** beds are often thin, discontinuous, texturally indistinct, and occur at a scale too small to map separately and are therefore grouped here. Thickness of undivided **Tmdl** is ≤487 m (1,600 ft) in the Brown Creek 7.5′ quadrangle (Plate 1), ≤460 m (1510 ft) in the Ketchum Reservoir 7.5′ quadrangle (Plate 2), and ≤495 m (1,625 ft) in the Fivemile Butte 7.5′ quadrangle (Plate 3).

Breccia beds are typically well exposed, forming erosionally resistant ledges along canyon walls (**Figure 6-41e**). Where breccia beds are deeply weathered, surfaces are mantled by meter-scale boulders, intermixed with coarse-grained sandy soils (**Figure 6-41f**, **Figure 6-42a**). Breccia is typically matrix supported with localized clast-supported areas (**Figure 6-41a**, **Figure 6-42b**, **Figure 6-43b,c**). The deposits range from monolithologic to heterolithologic, dominated by a variety of medium-light gray (N6) to pale blue (5B 6/2) and pale purple (5P 6/2), subrounded to subangular clasts of plagioclase and two-pyroxene (± hornblende) andesite and dacite (SiO_2 = 59.14 to 65.14 weight percent; K_2O = 0.73 to 1.92 weight percent; Nb = 4.6 to 9.2 ppm; Zr = 113 to 169 ppm; *n* = 17 analyses [13 outside Mill Creek area]) (**Table 6-3**; **Appendix**: McClaughry and others, 2020a, 2021). Clasts are typically enclosed in a matrix composed of volcanic lithics, pumice, partly altered volcanic glass, and plagioclase and pyroxene crystals. Locally, breccia is interbedded with massive to planar stratified sandstone and pebble conglomerate deposited by hyperconcentrated flood-flows, tuff deposited by pyroclastic flows and falls, and lenticular bedded, massive to trough- and planar-cross bedded, pebble- to cobble-rich conglomerate, pebbly sandstone, and sandstone and massive to laminated tuffaceous siltstone deposited in fluvial environments (**Figure 6-41b-d**). Fluvial conglomerate in the map area is locally exposed consisting of 3- to 15-m-thick (9.9- to 49-ft) typically lenticular beds, containing moderately to well-sorted, well-rounded cobbles and pebbles derived from Cascadian volcanic sources and the underlying CRBG. Exotic metamorphic clasts or non-Cascadian clasts were not found in fluvial deposits in the map area. Northeast of the map area, roughly along Dalles-Umatilla syncline of Newcomb (1967, 1969). **Tmdl** as presently mapped, includes fluvial facies with an inferred Deschutes River provenance. These strata contain clasts thought to be derived from older Tertiary volcanic sources unique to parts of Central Oregon (e.g., John Day and Clarno Formations; Cannon and O'Connor, 2019; O'Connor and others, 2021).

Tmdl is assigned a late Miocene and early Pliocene(?) age, ranging between ~8.8 and 5 Ma, on the basis of stratigraphic position, numerous isotopic ages in the Middle Columbia Basin, and vertebrate and leaf fossils (**Figure 6-1**; Plates 1,2, and 3; **Appendix**; Buwalda and Moore, 1929; Chaney, 1944; McClaughry and others, 2020a, 2021).

Figure 6-41. Examples of the Dalles Formation (Tmdl) cropping out in the Brown Creek 7.5' quadrangle. (a) Boulder-rich, clast-supported breccia on Mill Creek Road (45.53469, -121.37327). Scale bar is 1 m (3.3 ft). View is looking north. (b) Interbedded fluvial conglomerate and sandstone (45.53697, -121.31820). View is looking west. (c) Bed of tuffaceous siltstone (45.54325, -121.31898). View is looking east. (d) Bed of pumice, ash, and lithic tuff (45.54291, -121.32316). View is looking south. Hammer for scale in b, c, and d is 30 cm (12 in) long. (e) Breccia beds forming distinct, erosionally resistant ledges along canyon walls (45.54327, -121.31136). View is looking north. (f) A deeply weathered Dalles bed (45.58052, -121.34002). Photo credits: Clark Niewendorp, 2016.

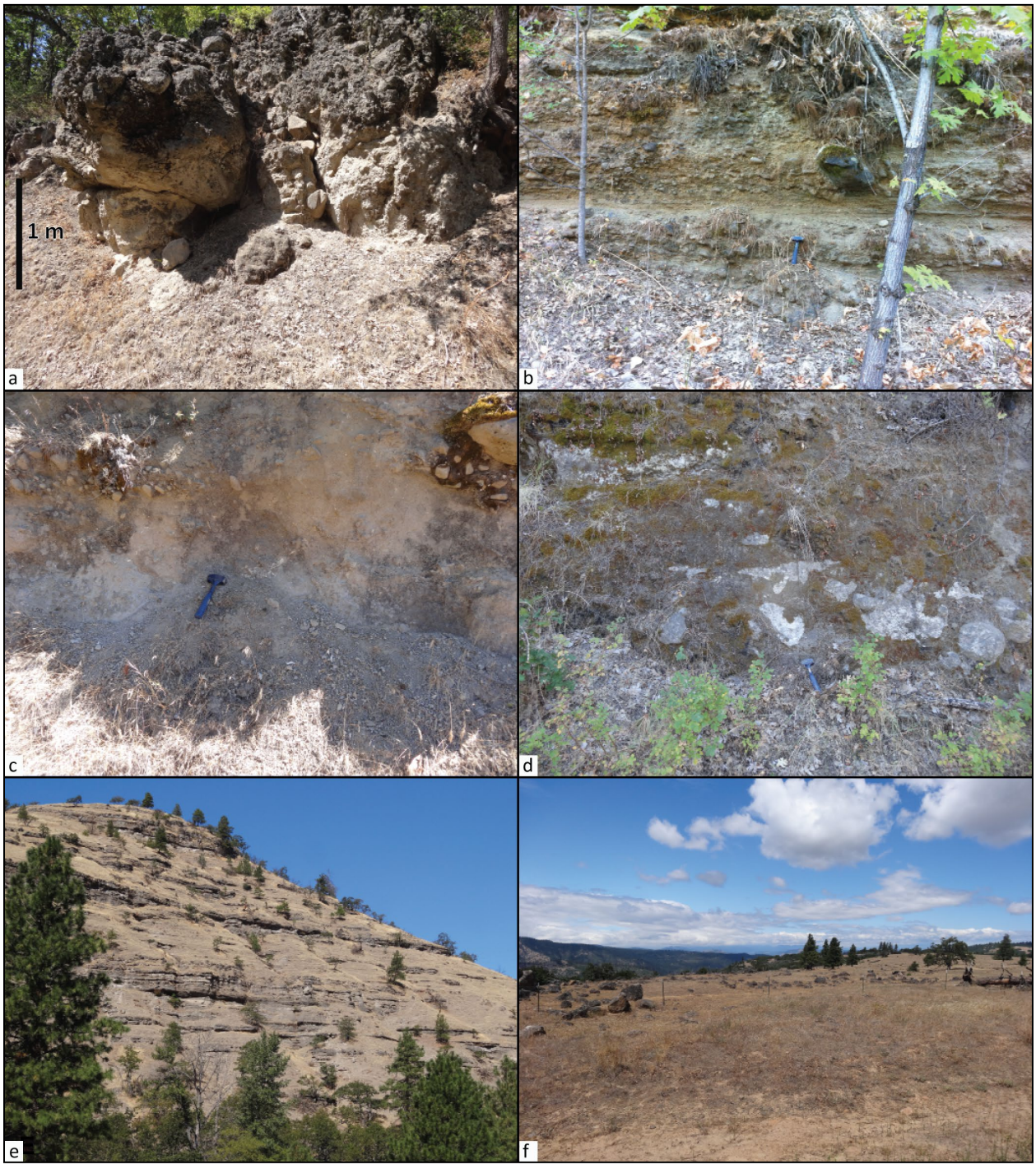

Figure 6-42. Examples of the Dalles Formation (Tmdl) cropping out in the Ketchum Reservoir 7.5' quadrangle. (a) A weathered Tmdl breccia bed eroding into surfaces mantled by meter-scale boulders intermixed with coarse-grained sandy soils (45.59772, -121.49244). View is looking east. (b) Boulder-rich, clast-supported Tmdl breccia cropping out between Old Schoolhouse Spring and Neal Creek (45.59890, -121.49362). Hammer for scale is 38 cm (15 in) long. View is looking southeast. Photo credits: Jason McClaughry, 2015.

Figure 6-43. Examples of the Dalles Formation (Tmdl) cropping out in the Fivemile Butte 7.5' quadrangle. (a) Tmdl cobble-boulder breccia exposed along USFS Road 4430 (45.42811, -121.47247). Automobile for scale. View is looking southwest. (b) The breccia in (a) is lithified and very poorly sorted, containing angular cobble- and boulder-sized clasts of plagioclase-hornblende-phyric andesite and dacite in a poorly sorted, coarse-grained sandstone matrix. Hammer for scale is 25 cm (10 in) long. (c) Tmdl cobble-boulder breccia exposed along Upper Fivemile Road (45.46189, -121.39457). Hammer for scale is 38 cm (15 in) long. View is looking north. Photo credits: Jason McClaughry, 2016.

Table 6-3. Representative XRF geochemical analyses for the Dalles Formation in the Mill Creek area.

Sample	KRL15-107	157 DFWJ 15	428 MCBJ 16	668 MCBJ 16	401 MCBJ 16	519 MCBJ 16	464 MCBJ 16	586 MCBJ 16	RC98-194	141 WRCN 15[1]
Geographic Area	Ketchum Reservoir	Owl Quarry	Mill Creek Buttes	Mill Creek Buttes	Fivemile Butte	Camp Baldwin	Pollywog Spring	Eightmile Meadow	Bulo Point	Larch Creek
Formation	Dalles Formation	Dalles Formation	Dalles Formation	Dalles Formation	Dalles Formation	Dalles Formation	Dalles Formation	Dalles Formation	Dalles Formation	Dalles Formation
Map Unit	Tmdl (clast)	Tmdj	Tmde	Tmdh	Tmdf	Tmdv	Tmds	Tmdw	Tmdb	Tmdd (clast)
Latitude	45.5403	45.3593	45.4678	45.4447	45.4109	45.4067	45.4551	45.3646	45.3728	45.3749
Longitude	-121.4438	-121.3805	-121.4904	-121.4980	-121.4689	-121.4374	-121.4406	-121.4955	-121.4731	-121.3584
Age (Ma)	nd	~5.3	~7-8	nd	nd	7.7	nd	7.91	nd	~7.7 to 8.7
Plate	2	3	3	3	3	3	3	3	3	na
Map Label	G48	G7	G68	G61	G42	G39	G62	G14	G18	na
Oxides, weight percent										
SiO_2	64.68	62.26	62.67	64.03	63.72	63.69	63.57	64.59	64.48	62.34
Al_2O_3	17.69	18.14	17.76	16.79	17.48	17.37	17.46	15.86	17.36	17.80
TiO_2	0.72	0.78	0.75	0.73	0.70	0.73	0.73	0.98	0.69	0.77
FeOTotal	4.94	5.63	5.30	4.21	4.99	4.95	5.05	5.46	4.61	5.39
MnO	0.07	0.08	0.09	0.07	0.08	0.12	0.08	0.08	0.07	0.08
CaO	4.55	5.63	5.78	6.37	5.54	5.48	5.48	3.97	5.16	5.91
MgO	1.93	2.06	2.19	2.71	2.02	2.06	2.05	1.79	1.74	2.52
K_2O	1.28	1.02	1.05	0.90	1.09	1.18	1.16	2.91	1.35	0.96
Na_2O	3.99	4.24	4.23	3.99	4.22	4.25	4.23	4.16	4.39	4.09
P_2O_5	0.15	0.17	0.18	0.19	0.16	0.17	0.19	0.19	0.17	0.13
LOI	nd	nd	0.36	0.53	0.61	0.50	0.89	0.77	nd	0.96
Total_I	97.44	98.67	99.23	99.08	98.72	99.16	98.85	98.72	nd	98.41
Trace Elements, parts per million										
Ni	24	18	17	39	19	21	26	17	17	21
Cr	31	29	31	58	37	29	46	19	31	36
Sc	11	12	11	10	10	10	10	12	10	12
V	83	85	84	81	78	78	83	86	76	95
Ba	447	262	299	224	305	366	340	498	316	230
Rb	28	16	19	16	19	20	19	71	25	15
Sr	429	510	501	1045	483	500	501	326	444	595
Zr	153	147	139	135	154	153	160	339	151	108
Y	12	15	15	12	16	19	23	37	13	11
Nb	9.2	8.7	8.4	5.7	9.2	10.3	9.2	17.4	10.2	5.2
Ga	20	21	21	20	20	21	21	20	19	19
Cu	24	39	30	45	32	35	24	23	27	34
Zn	71	76	70	52	74	79	86	70	70	60
Pb	5	6	4	4	5	5	7	9	1	4
La	15	16	12	18	20	17	32	36	28	13
Ce	25	25	30	35	37	35	38	65	49	27
Th	4	1	3	3	2	2	3	10	2	1
Nd	15	17	17	22	19	21	36	33	0	13
U	1	1	2	1	1	1	2	3	0	1

Major element determinations have been normalized to a 100-percent total on a volatile-free basis and recalculated with total iron expressed as FeOTotal; nd = no data or element not analyzed; na = not applicable or no information. LOI = Loss on Ignition; Total_I = original analytical total. Data from: [1]McClaughry and others (2021).

Tmdj **dacite of Jordan Butte (lower Pliocene or upper Miocene)**—Andesite and dacite lava flows (SiO_2 = 62.26 to 64.69 weight percent; K_2O = 1.02 to 1.28 weight percent; *n* = 4 analyses [3 outside Mill Creek area]) mapped on the north side of Owl Hollow along USFS Road 2730 in the northeast part of the Flag Point 7.5′ quadrangle (**Figure 6-44**; **Table 6-3**; Plate 3; **Appendix**). Outcrops here are correlative with chemically and lithologically similar lava flows that underlie Jordan Butte, ~4 km (2.5 mi) south of the map area (Sherrod and Scott, 1995). Roadcuts and outcrops of **Tmdj** are characterized by blocky meter-scale columns or intervals of platy jointing (**Figure 6-44**); **Tmdj** generally weathers to rounded boulders up to 1 m (3.3 ft) across. Thickness of **Tmdj** in the map area is ≥25 m (82 ft). Typical hand samples of the andesite and dacite are light gray (N7) to medium-light gray (N4), containing ~3 to 5 percent (vol.) clear to chalky light gray (N7), prismatic to blocky, seriate plagioclase microphenocrysts and phenocrysts up to 1 cm (0.4 in) long; ~1 percent (vol.) fresh black (N1), subhedral to anhedral, prismatic- to lath-shaped, seriate orthopyroxene and clinopyroxene microphenocrysts and phenocrysts ≤2 mm (0.08 in)(orthopyroxene > clinopyroxene), and sparse microglomerocrysts of plagioclase, pyroxene, glass, and Fe-Ti oxides ≤1 mm (0.1 in); all contained within a hypohyaline groundmass (**Figure 6-45**).

Tmdj has normal magnetic polarity and is assigned a late Miocene age on the basis of stratigraphic position (**Figure 6-1**; Plate 3; **Appendix**). Bunker and others (1982) reported a whole rock K-Ar age of 5.28 ± 0.5 Ma for andesite lava flows cropping out along USFS Road 27 and Jordan Creek (south of the map area, 5.3 km [3.3 mi] east of Jordan Butte). Sherrod and Scott (1995) interpreted this outcrop to be correlative with lava flows at nearby Jordan Butte. However, the isotopically dated andesite lava flows along Jordan Creek are chemically dissimilar from the lava flows that form the main mass of Jordan Butte and those cropping out north of Owl Hollow (**Appendix**). Geochemical sampling and mapping along USFS Road 27 north of Jordan Creek indicates that **Tmdj** overlies the 5.28 Ma andesite. Therefore, **Tmdj**, as defined here, is younger than 5.28 Ma.

Figure 6-44. Dacite of Jordan Butte (Tmdj) in Owl Quarry along USFS Road 2730 (45.35929, -121.38047). Hammer for scale is 38 cm (15 in) long. View is looking north. Photo credit: Jason McClaughry, 2015.

Figure 6-45. Hand sample and thin section photographs of the dacite of Jordan Butte (Tmdj). (a) Typical hand sample. Scale bar is 2.5 cm (1 in). (b) Thin section under cross-polarized light. (c) Same view as in (b) under plane-polarized light. Scale bar in (b) and (c) is 7 mm (0.3 in). Photo credits: Jason McClaughry, 2016.

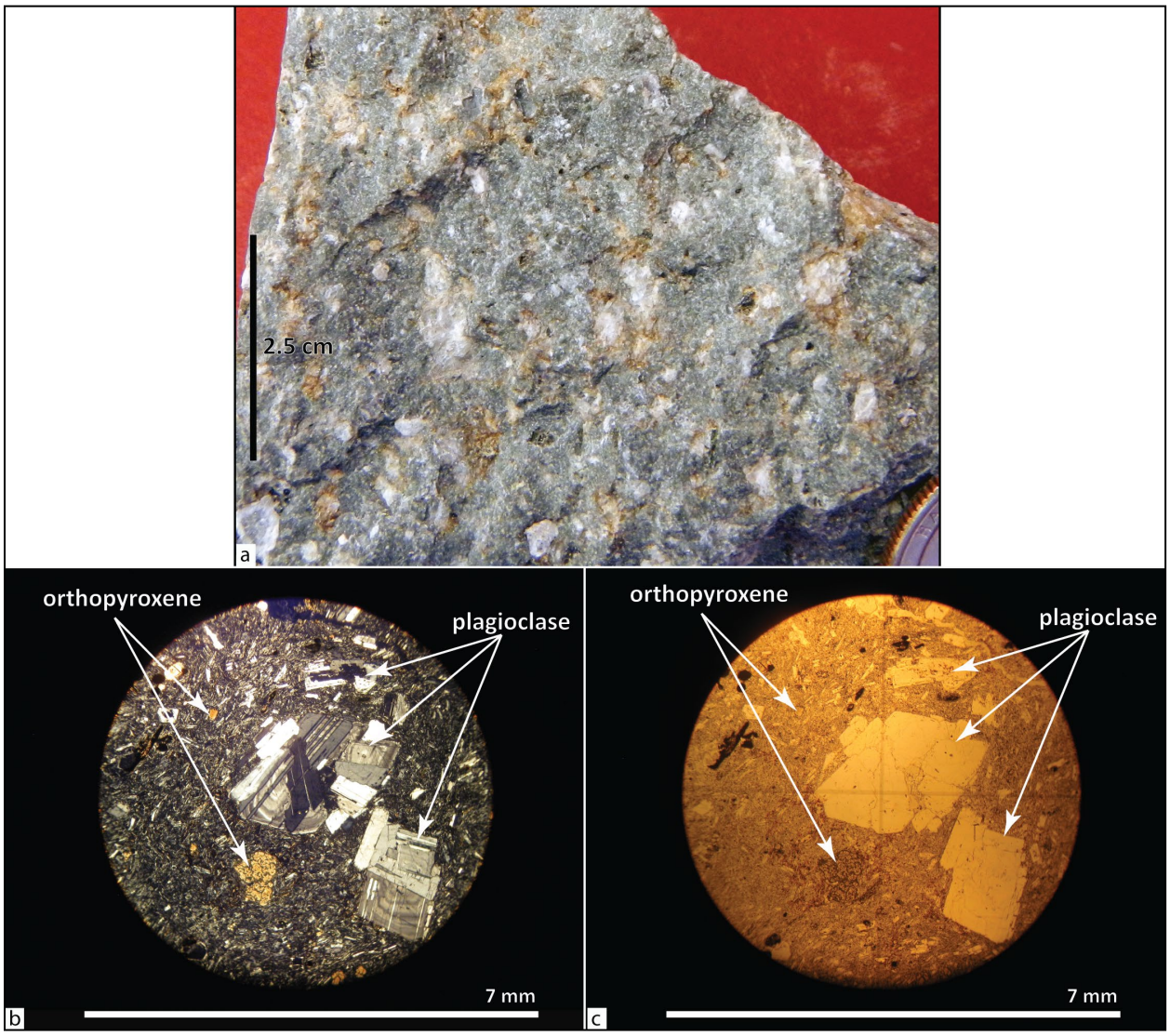

Tmde **andesite and dacite of East Fork (upper Miocene)**—Andesite and dacite lava flows (SiO_2 = 59.45 to 65.68 weight percent, avg = 62.86 weight percent; K_2O = 0.99 to 1.65, avg = 1.27 weight percent; *n* = 53 analyses [50 outside Mill Creek area]) cropping out in an east-west trending ridge on the north flank of Mill Creek Buttes in the Fivemile Butte 7.5′ quadrangle and in a NNE-trending ridge in the southwest corner of the Ketchum Reservoir 7.5′ quadrangle (**Figure 6-46**; **Table 6-3**; Plates 2 and3; **Appendix**; McClaughry and others, 2020a). **Tmde** is also mapped extensively west of the map area in the Dog River 7.5′ quadrangle between Mill Creek Buttes and Gibson Prairie and along the East Fork Hood River (McClaughry and others, 2020a). In the Dog River 7.5′ quadrangle **Tmde** includes multiple porphyritic lava flow sequences, interfingering with Dalles Formation volcaniclastic rocks (**Tmdl**) at variable stratigraphic intervals. Outcrops of **Tmde** in the map area are commonly characterized by meter-scale, poorly developed columnar joint sets or intervals of platy jointing (**Figure 6-46**). Weathered outcrops break down to meter scale, subrounded boulders, forming extensive talus slopes beneath ridge-capping outcrops. In some locations, **Tmde** lava flows have elongated, irregular diktytaxitic vesicles. Dissolution of plagioclase on weathered surfaces leaves vesicle-like pits. Thickness of **Tmde** in the map area is ≤70 m (230 ft). Typical hand samples of **Tmde** are grayish blue (5PB 5/2) to medium-bluish gray (5B 5/1), containing 10 to 20 percent (vol.) clear to chalky white (N9), subhedral to anhedral, prismatic to blocky, seriate plagioclase microphenocrysts and phenocrysts ≤6 mm (0.2 in); and 1 to 2 percent (vol.) grayish black (N2) euhedral to subhedral, prismatic to blocky seriate pyroxene microphenocrysts and phenocrysts ≤4 mm (0.1 in; orthopyroxene ≥ clinopyroxene); all contained within in a very fine-grained holocrystalline to hypocrystalline groundmass (**Figure 6-47**). Rare andesitic or dacitic rock fragments <2 mm (0.08 in) across are also present. The abundant conspicuous plagioclase phenocrysts distinguish **Tmde** from adjacent units (**Figure 6-47**).

Tmde has both normal and reversed magnetic polarity flows. It is assigned a late Miocene age on the basis of stratigraphic position and whole rock K-Ar ages of 7.15 ± 0.8 Ma and 8.18 ± 0.06 Ma in the Dog River 7.5′ quadrangle, west of the map area (**Figure 6-1**; Plates 1 and 2; **Appendix**; Wise, 1969; Keith and others, 1985; McClaughry and others, 2020a).

Figure 6-46. The andesite and dacite of East Fork (Tmde) cropping out north of Mill Creek Buttes in the western part of the Fivemile Butte and Ketchum Reservoir 7.5' quadrangles. (a) Cliff-forming Tmde outcrops in The Dalles Municipal Watershed Unit, north of Mill Creek Buttes (45.46780, -121.49041). Automobile for scale in upper left part of photograph. View is looking west. (b) Tmde outcrops are characterized by massive to meter-scale, crude columnar jointing (45.50616, -121.49887). Hammer for scale is 38 cm (15 in) long. View is looking southwest. Photo credits: Jason McClaughry, 2016.

Figure 6-47. Hand sample and thin section photographs of the andesite and dacite of East Fork (Tmde). (a) Typical plagioclase-porphyritic hand sample. Scale bar is 2.5 cm (1 in) tall. (b) Thin section under cross-polarized light. (c) Same view as in (b) under plane-polarized light. Scale bar in (b) and (c) is 7 mm (0.3 in). Photo credits: Jason McClaughry, 2016.

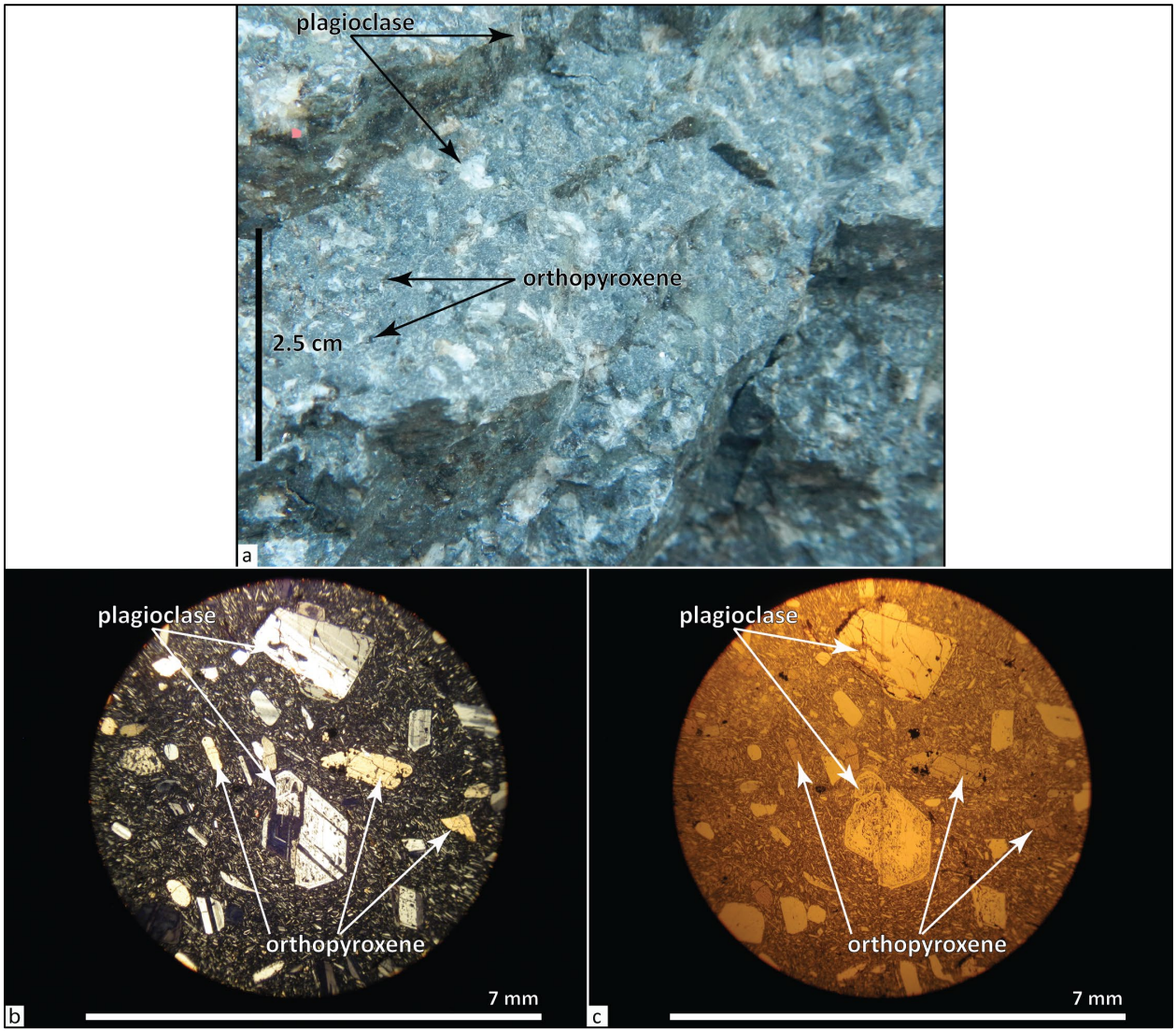

Mill Creek Buttes

Hornblende-phyric dacite and microdiorite exposed across Mill Creek Buttes in the headwaters of the South Fork of Mill Creek (Plate 3; Dog River 7.5′ quadrangle, McClaughry and others, 2020a). Relative to other units in the Dalles Formation, rocks at Mill Creek Buttes have lower potassium (K_2O = 0.75 to 1.08 weight percent) and higher strontium (Sr = 748 to 1047 ppm) (**Appendix**; McClaughry and others, 2020a). Isotopic ages obtained on Mill Creek Buttes indicate that rocks range in age from ~7.5 to 6 Ma (McClaughry and others, 2020a). The absence of vesicular zones between units, great apparent thickness, and high-standing topography of Mill Creek Buttes likely indicates emplacement as a late Miocene dome complex.

Tmdh **hornblende-porphyritic microdiorite of Mill Creek Buttes (upper Miocene)—** Microdiorite (SiO_2 = 63.64 to 65.13 weight percent; K_2O = 0.75 to 0.95, Sr = 778 to 1047 ppm; *n* = 9 analyses [7 outside Mill Creek area]) forming most of the eastern and southern flanks of Mill Creek Buttes (**Figure 6-48**; **Table 6-3**; **Appendix**). Outcrops of **Tmdh** are characterized by intervals of tabular to vertical platy jointing; the weathered unit forms land surfaces covered with angular plates or subangular blocks <0.5 m (1.6 ft) across (**Figure 6-48**). Thickness of **Tmdh** is ≤130 m (600 ft). Typical hand samples of the microdiorite are medium-light gray (N6), containing 3 to 10 percent (vol.) black (N1) to brownish black (5YR 2/1) iridescent, fresh to corroded, subhedral to anhedral, prismatic- to lath-shaped, seriate hornblende phenocrysts ≤5 mm up to 1.5 cm (0.2 to 0.6 in); <1 percent (vol.) clear, prismatic to blocky, seriate plagioclase microphenocrysts ≤1 mm (0.04 in), and <1 percent (vol.) plagioclase-hornblende glomerocrysts ≤1 mm (0.04 in); all distributed within a fine- to medium-grained holocrystalline groundmass (**Figure 6-49**).

Tmdh has reversed magnetic polarity and is assigned a late Miocene age on the basis of stratigraphic position below the 6.83 Ma microdiorite of Mill Creek Buttes in the Dog River 7.5′ quadrangle, west of the map area (**Figure 6-1**; Plate 3; **Appendix**; McClaughry and others, 2020a)

Figure 6-48. Hornblende-porphyritic microdiorite of Mill Creek Buttes (Tmdh) cropping out along the eastern summit of Mill Creek Buttes (45.44489, -121.49798). Hammer for scale is 38 cm (15 in) long. View is looking southwest. Photo credit: Jason McClaughry, 2016.

Figure 6-49. Hand sample and thin section photographs of the hornblende-porphyritic microdiorite of Mill Creek Buttes (Tmdh). (a) Typical plagioclase- and hornblende-porphyritic hand sample. Scale bar is 2.5 cm (1 in). (b) Thin section under cross-polarized light. (c) Same view as in (b) under plane-polarized light. Scale bar in (b) and (c) is 7 mm (0.3 in). Photo credits: Jason McClaughry, 2017.

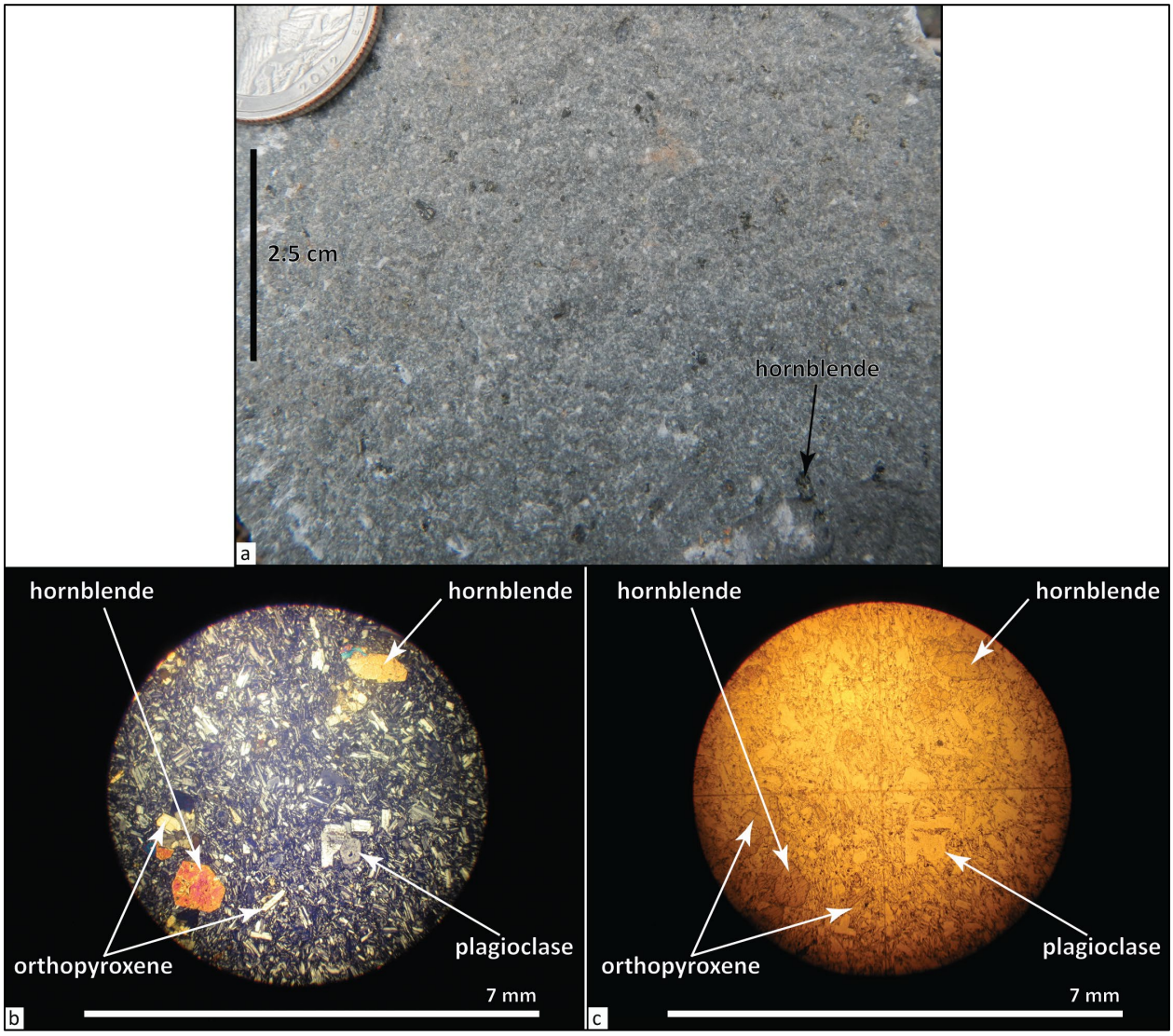

Tmdf **dacite of Fivemile Butte, upper flow (upper Miocene)**—Dacite lava flow (SiO_2 = 63.28 to 63.72 weight percent; K_2O = 1.07 to 1.09, *n* = 5 analyses, [2 outside Mill Creek area]) mapped forming a narrow ridge capping Fivemile Butte and continuing east for ~8.4 km (5.2 mi) to Joes Point (**Figure 6-50**; **Table 6-3**; Plate 3; **Appendix**). Roadcuts, quarry exposures, and outcrops of **Tmdf** are characterized by intervals of vertical to subvertical tabular to platy jointing. **Tmdf** weathers to subangular fragments ≤0.5 m (1.6 ft) across. Thickness of **Tmdf** in the map area is ≤40 m (130 ft). Typical hand samples of the dacite are light gray (N7) to medium-bluish gray (5B 5/1), containing 2 to 3 percent (vol.) clear to chalky white (N9), euhedral, prismatic, seriate plagioclase microphenocrysts and phenocrysts 1 to 4 mm (0.04 to 0.2 in) across and up to 1 cm (0.4 in) long; ≤1 percent (vol.) dark gray (N2), rod-like orthopyroxene phenocrysts ≤4 mm (0.2 in); and ~1 percent (vol.) plagioclase-pyroxene glomerocrysts ≤1 cm (0.4 in); all distributed within a fine-grained holocrystalline groundmass (**Figure 6-51**).

Tmdf has both normal and reversed magnetic polarity outcrops. **Tmdf** is assigned a late Miocene age on the basis of stratigraphic position directly above the 7.71 Ma lower flows and domes of the dacite of Fivemile Butte (**Tmdv**)(**Figure 6-1**; Plate 3; **Appendix**).

Figure 6-50. Upper flows of the dacite of Fivemile Butte (Tmdf) cropping out between Fivemile Butte and Joes Point. (a) Blocky-jointed Tmdf exposed on the summit of Fivemile Butte, 100 m (328 ft) north of the fire lookout (45.41094, -121.46887). Hammer for scale is 38 cm (15 in) long. View is looking south. (b) Blocky- to platy-jointed Tmdf exposed in the Joes Point quarry off of USFS Road 4440 (45.42245, -121.43337). Scale bar is 1 m (3.3 ft). View is looking south. Photo credits: Jason McClaughry, 2016.

Figure 6-51. Hand sample and thin section photographs of the dacite of Fivemile Butte, upper flows (Tmdf). (a) Typical hand sample. Scale bar is 2.5 cm (1 in). (b) Thin section under cross-polarized light. (c) Same view as in (b) under plane-polarized light. Scale bar in (b) and (c) is 7 mm (0.3 in). Photo credits: Jason McClaughry, 2017.

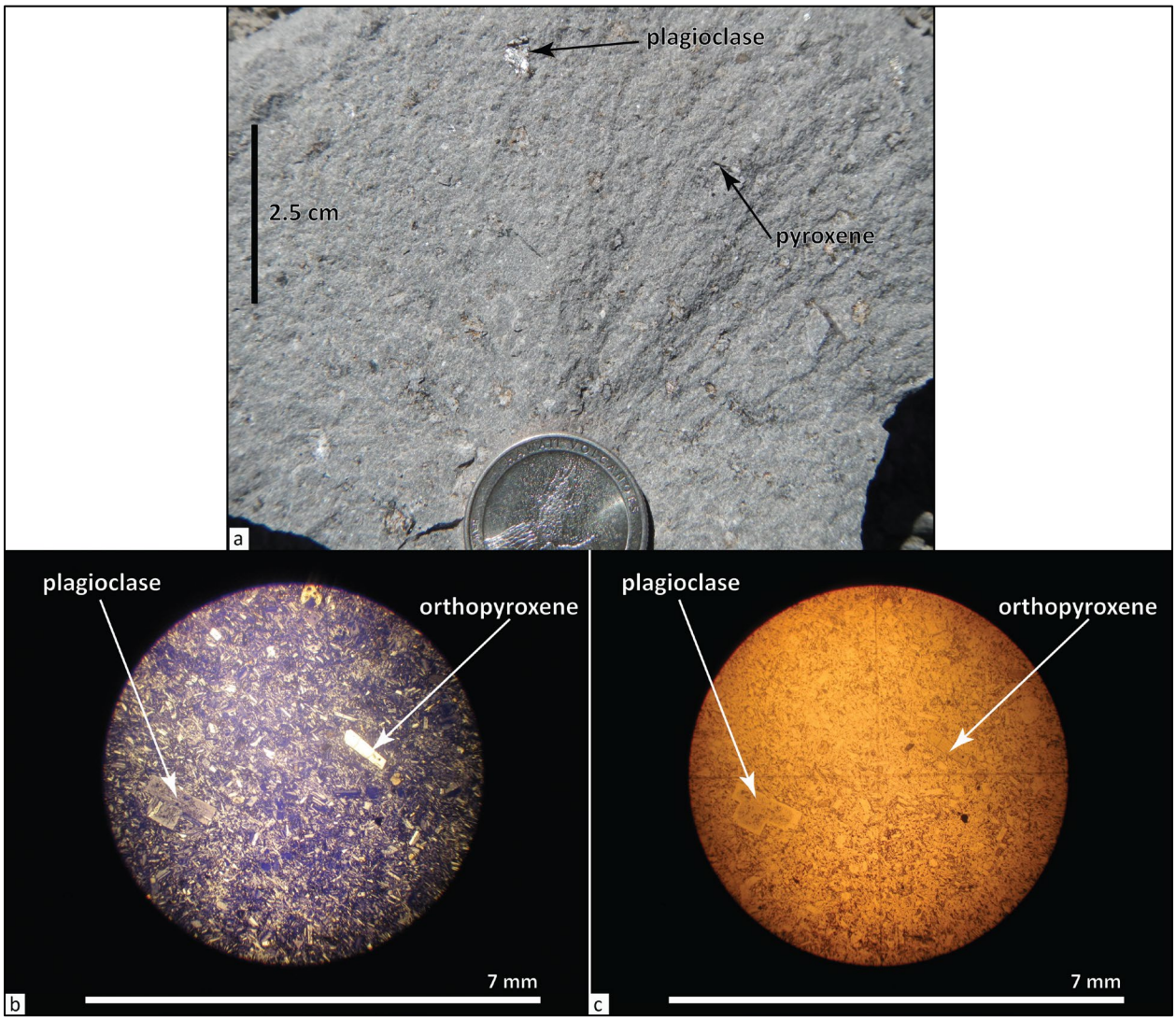

Tmdv **dacite of Fivemile Butte, lower flows and domes (upper Miocene)**—Dacite lava flows and/or domes (SiO_2 = 62.79 to 64.51 weight percent; 1.17 to 2.12 weight percent K_2O, *n* = 18 analyses, [9 outside Mill Creek area]) underlying the headwaters of Dog River, Fivemile Butte and Perry Point (**Figure 6-52**; **Table 6-3**; Plate 3; **Appendix**; McClaughry and others, 2020a). East of Perry Point **Tmdv** is mapped for ~8 km (5 mi) as an intracanyon lava flow across the top of the east-west-trending ridge between Eightmile Creek and Hesslan Canyon. Roadcuts and outcrops are either massive or characterized by broad blocky meter-scale columns or intervals of vertical platy jointing (**Figure 6-52**). **Tmdv** weathers to meter-scale, subrounded boulders and angular plates, forming extensive talus slopes beneath cliffs. Thickness of **Tmdv** in the map area is ~40 m (131 ft)(Plate 1). Typical hand samples of the dacite are medium gray (N5) to medium-dark gray (N4), containing ~3 to 5 percent (vol.), clear to chalky light gray (N7), euhedral, prismatic to blocky, seriate plagioclase microphenocrysts and phenocrysts ≤1 cm (0.4 in) long and ≤1 percent (vol.) fresh grayish black (N2) pyroxene microphenocrysts and phenocrysts ≤2 mm (0.08 in)(orthopyroxene ≥ clinopyroxene), all distributed within a very fine-grained holocrystalline to hypocrystalline groundmass (**Figure 6-53**).

Tmdv has both normal and reversed magnetic polarity outcrops. **Tmdv** is assigned a late Miocene age on the basis of stratigraphic position and a plagioclase K-Ar age of 7.71 ± 0.17 Ma obtained by Gray and others (1996) for an outcrop in the saddle between Perry Point and Fivemile Butte (**Figure 6-1**; Plate 3; **Appendix**). **Tmdv** is interpreted to be younger than the dacite of Wolf Run (**Tmdw**) on the basis of isotopic ages; no outcrops exposing the contact between the two units are known in the map area or adjacent Dog River 7.5′ quadrangle (McClaughry and others, 2020a).

Figure 6-52. Lower flows of the dacite of Fivemile Butte (Tmdv) cropping out between Fivemile Butte and Hesslan Canyon. (a) Blocky-jointed Tmdv cropping out in the saddle between Perry Point and Fivemile Butte (45.40612, -121.48184). Hammer for scale is 38 cm (15 in) long. View is looking north. Gray and others (1996) obtained a K-Ar age of 7.71 ± 0.17 Ma for Tmdv from this outcrop. (b) Intracanyon Tmdv lava flow capping the east-west-trending ridge between Eightmile Creek and Hesslan Canyon in the eastern part of the Fivemile Butte 7.5′ quadrangle (45.42043, -121.41410). View is looking southeast. Photo credits: Jason McClaughry, 2016.

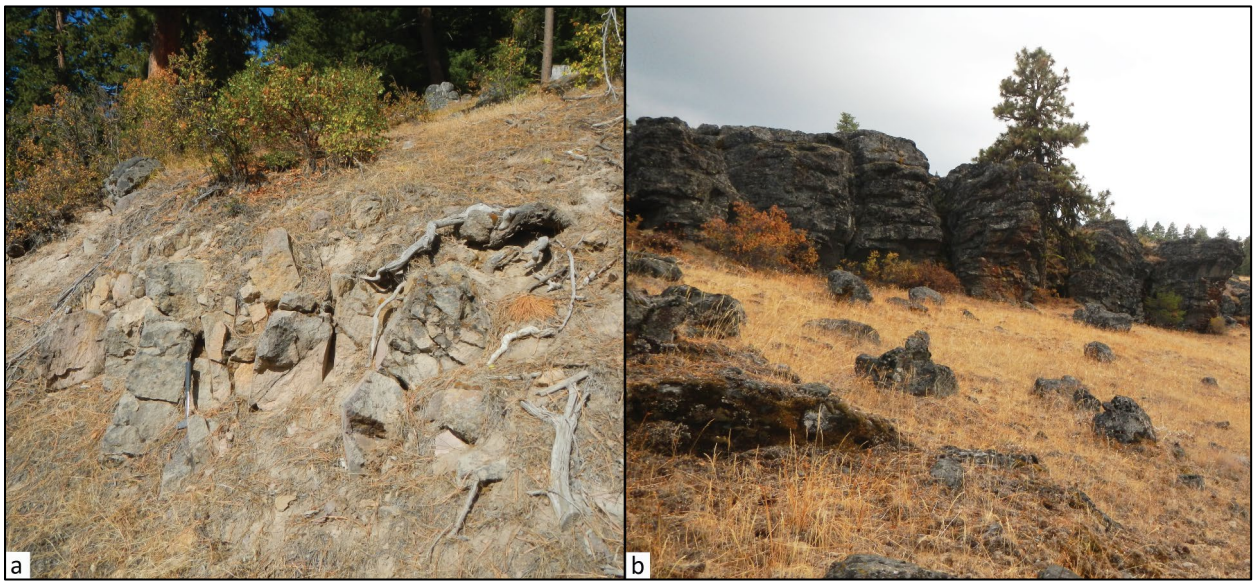

Figure 6-53. Hand sample and thin section photographs of the dacite of Fivemile Butte, lower flows (Tmdv). (a) Typical abundantly plagioclase porphyritic hand sample. Scale bar is 2.5 cm (1 in). (b) Thin section under cross-polarized light. (c) Same view as in (b) under plane-polarized light. Scale bar in (b) and (c) is 7 mm (0.3 in). Photo credits: Jason McClaughry, 2017.

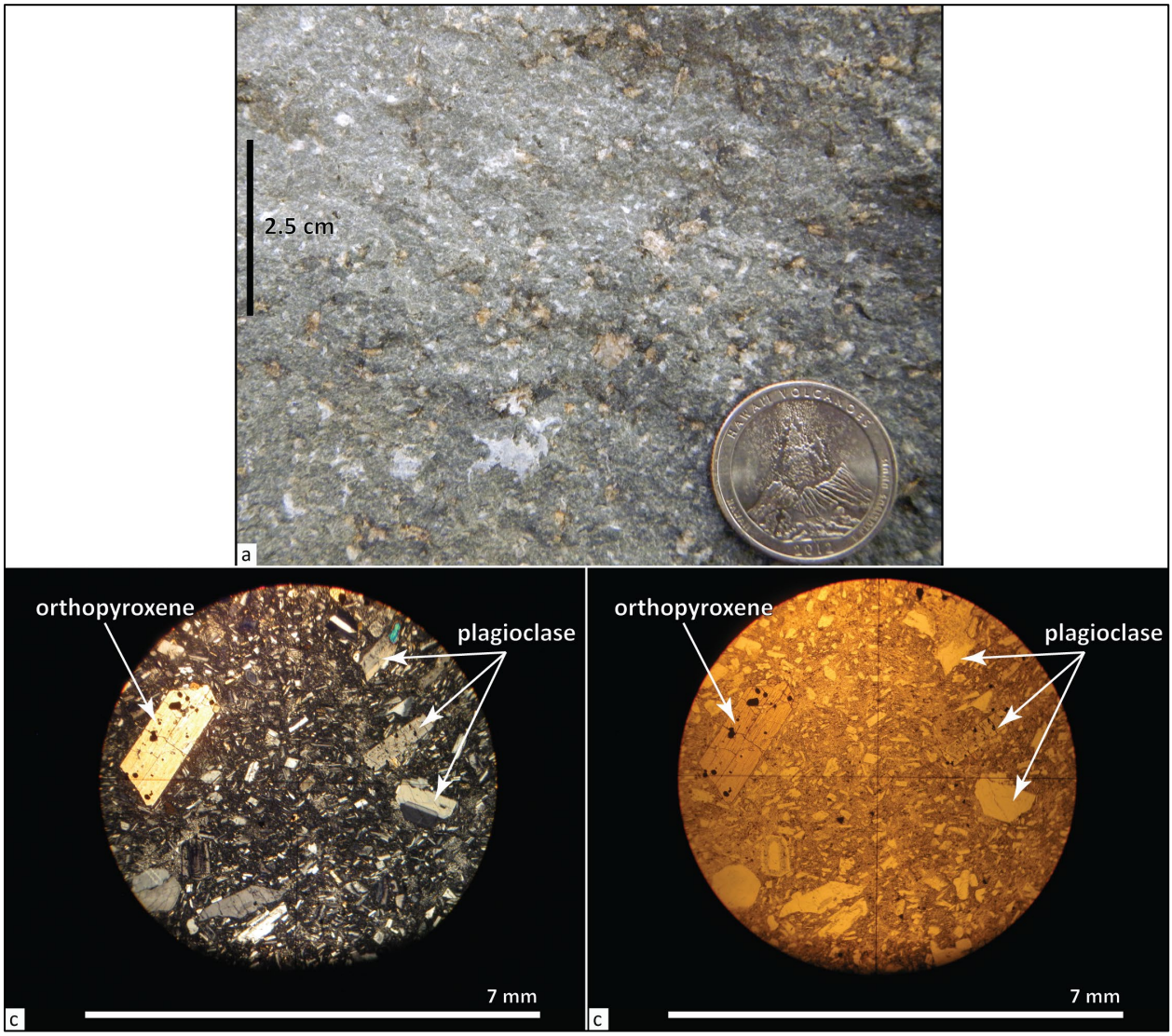

Tmds **dacite of South Fork Fivemile Creek (upper Miocene)**— Dacite lava flow (SiO_2 = 63.57 to 64.2 weight percent; 1.14 to 1.22 weight percent K_2O, *n* = 7 analyses) mapped in a narrow outcrop belt between Fivemile Butte on the west and Pollywog Butte on the east (**Figure 6-54**; **Table 6-3**; Plate 3; **Appendix**). **Tmds** is characterized by intervals of vertical platy jointing intermixed with zones of blocky meter-scale columns (**Figure 6-54**). When weathered, **Tmds** leaves a landscape covered in angular plates or subangular blocks ≤0.5 m (1.6 ft). Thickness of **Tmds** is ≤55 m (182 ft; Plate 1). Typical hand samples of the dacite are light bluish gray (5B 7/1) to medium-bluish gray (5B 5/1), containing ~3 to 5 percent (vol.) clear to chalky light gray (N7), subhedral to anhedral, prismatic to blocky, seriate plagioclase microphenocrysts and phenocrysts ≤4 mm (0.2 in); ≤3 percent (vol.) fresh black (N1) pyroxene microphenocrysts and phenocrysts ≤2 mm (0.08 in; orthopyroxene ≥ clinopyroxene); and ~1 percent (vol.) glomerocrysts of plagioclase-pyroxene ≤5 mm (0.2 in); all distributed within a fine-grained hypocrystalline groundmass (**Figure 6-55**). Thin sections contain 1 to 2 percent (vol.) opaque Fe-Ti oxides.

Tmds has normal magnetic polarity and is assigned a late Miocene age on the basis of stratigraphic position (**Figure 6-1**; Plate 3; **Appendix**). **Tmds** directly underlies the 3.69 Ma dacite of Fivemile Creek (**Tpdv**) between Skyline Quarry and Pollywog Spring (Plate 3); the lava flow also appears to underlie 7.71 Ma **Tmdv**, so is therefore also older than that unit.

Figure 6-54. Blocky- to platy-jointed dacite of South Fork Fivemile Creek (Tmds) in Skyline Quarry off of USFS Road 1720 (Brooks Meadow Road) (45.44104, -121.46215). Scale bar is 1 m (3.3 ft). View is looking northwest. Photo credit: Jason McClaughry, 2016.

Figure 6-55. Hand sample and thin section photographs of the dacite of South Fork (Tmds). (a) Typical hand sample. Scale bar is 2.5 cm (1 in). (b) Thin section under cross-polarized light. (c) Same view as in (b) under plane-polarized light. Scale bar in (b) and (c) is 7 mm (0.3 in). Photo credits: Jason McClaughry, 2017.

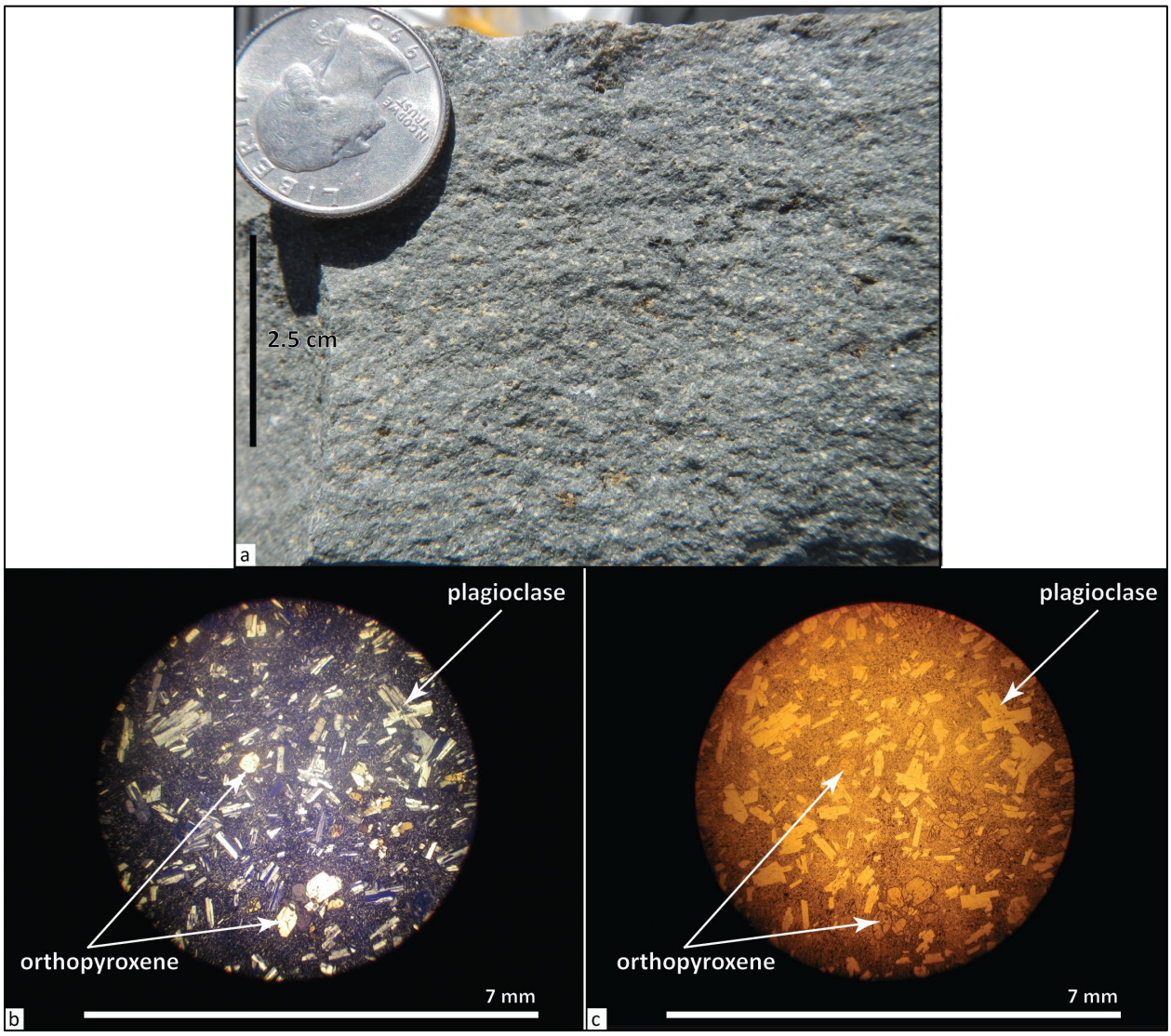

Tmdw **dacite of Wolf Run (upper Miocene)**—Dacite lava flow (SiO_2 = 63.49 to 65.11 weight percent; K_2O = 2.76 to 2.96, *n* = 13 analyses [7 outside Mill Creek area]) mapped capping a NE-trending ridge between Eightmile Meadow and Hesslan Canyon in the Fivemile Butte 7.5′ quadrangle (**Figure 6-56**; **Table 6-3**; Plate 3; **Appendix**; McClaughry and others, 2020a, 2021). **Tmdw** has a unique chemical composition for a lava flow of Dalles Formation age with relatively higher potassium (K_2O >2.5 weight percent) and higher amounts of niobium (Nb = 15.7 to 17.6 ppm) and zirconium (Zr = 319 to 341 ppm) (**Table 6-3**; **Appendix**). The chemically distinct **Tmdw** forms an important stratigraphic marker in the Middle Columbia Basin, reaching ~24 km (15 mi) eastward from the headwaters of Eightmile Creek in the eastern escarpment of the Hood River graben to the intersection of Eightmile Creek and Wolf Run as a topographically inverted intracanyon lava flow overlying volcaniclastic rocks in the Dalles Formation (**Tmdl**) (Plate 1; McClaughry and others, 2020a, 2021). A vent area for the lava flow has not been determined and no outcrops of the unit

are known west of the single mapped exposure in the East Fork Hood River area (McClaughry and others, 2020a). **Tmdw** forms prominent cliff-forming exposures marked by meter-scale columnar jointing (**Figure 6-56**); outcrops weather to subrounded boulders, forming extensive talus slopes beneath cliff-forming outcrops. Vesicles are commonly lined by masses of white to pink zeolite. **Tmdw** is as thick as 105 m (345 ft) in the upper reach of Deadman Gulch (Plate 3). Typical hand samples of the dacite are medium gray (N5) to medium-dark gray (N4), containing 20 to 30 percent (vol.) clear to chalky white (N9), subhedral to anhedral, prismatic to blocky, seriate plagioclase microphenocrysts and phenocrysts ≤5 mm (0.2 in); ≤1 percent (vol.) grayish black (N2), euhedral to subhedral, prismatic pyroxene microphenocrysts and phenocrysts ≤2 mm (0.08 in; orthopyroxene ≥ clinopyroxene); and ≤1 percent (vol.) plagioclase-pyroxene glomerocrysts ≤3 mm (0.1 in); all contained within a very fine-grained holocrystalline to hypocrystalline groundmass (**Figure 6-57**).

Tmdw has normal magnetic polarity and is assigned a late Miocene age on the basis of stratigraphic position and an $^{40}Ar/^{39}Ar$ plateau age for plagioclase of 7.91 ± 0.08 Ma for a sample collected from outcrops at the intersection of Wolf Run and Eightmile Creek in the Dufur West 7.5′ quadrangle, east of the map area (**Figure 6-1**; Plate 3; **Appendix**; McClaughry and others, 2021). Farooqui and others (1981), Bunker and others (1982), and Bela (1982) reported a comparable, but less precise whole rock K-Ar age of 8.2 ± 0.8 Ma collected from this unit a short distance southwest of Camp Baldwin (Plate 3; **Appendix**).

Figure 6-56. Blocky- to platy-jointed dacite of Wolf Run (Tmdw) cropping out near USFS Road 4421-150 in the Fivemile Butte 7.5′ quadrangle (45.39656, -121.44020). Hammer for scale is 38 cm (15 in) long. View is looking northeast. Photo credit: Jason McClaughry, 2016.

Figure 6-57. Hand sample and thin section photographs of the dacite of Wolf Run (Tmdw). (a) Typical abundantly plagioclase-porphyritic hand sample. Scale bar is 2.5 cm (1 in). (b) Thin section under cross-polarized light. (c) Same view as in (b) under plane-polarized light. Scale bar in (b) and (c) is 7 mm (0.3 in). Photo credits: Jason McClaughry, 2015.

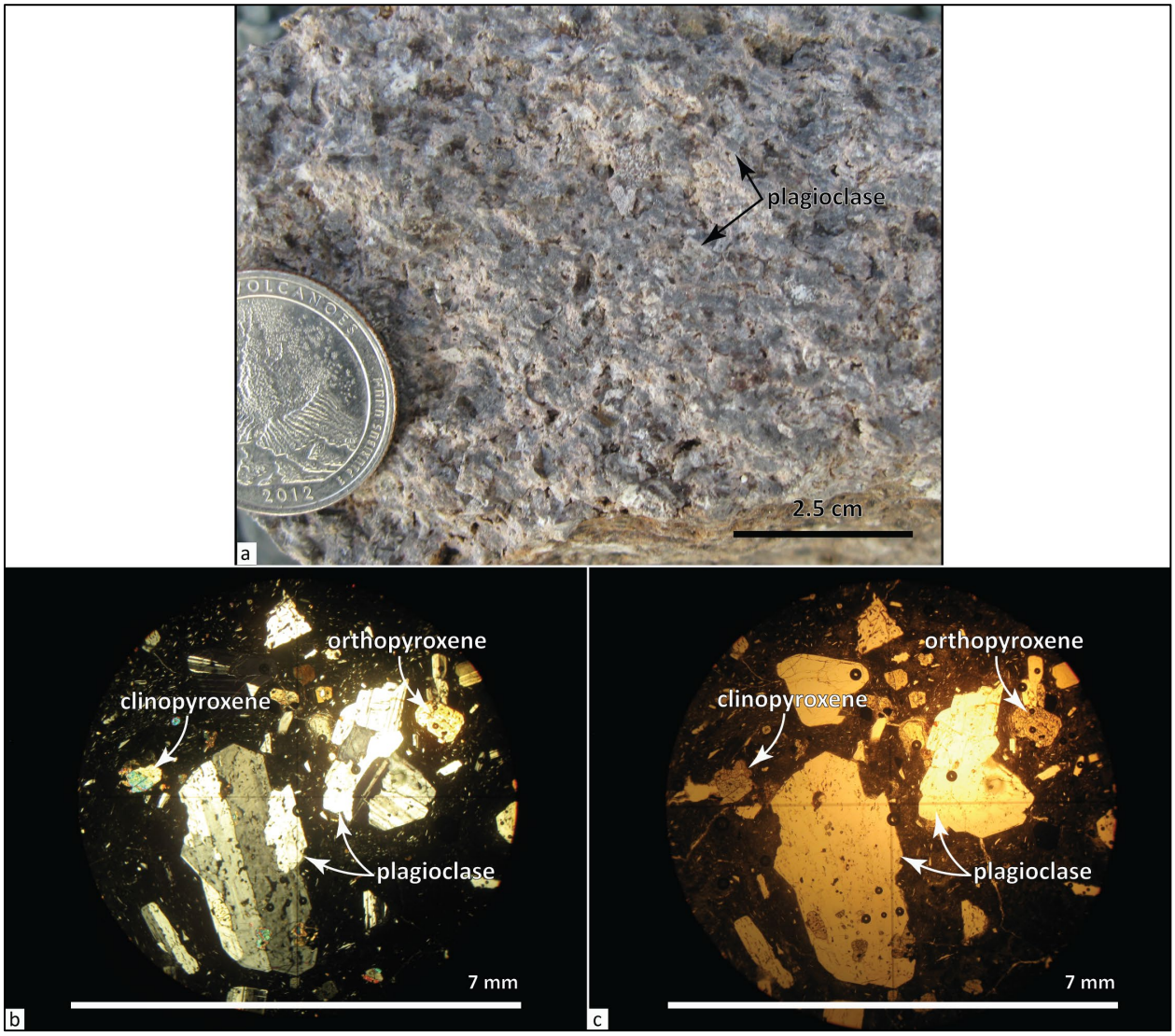

Tmdb **dacite of Bulo Point (upper Miocene)**—Dacite lava flows (SiO_2 = 63.31 to 64.6 weight percent; K_2O = 1.18 to 1.35, *n* = 8 analyses) mapped between Bulo Point and Cedar Creek in the northern part of the Flag Point 7.5′ quadrangle (**Figure 6-58**; **Table 6-3**; Plate 3; **Appendix**). **Tmdb** forms precipitous cliff-forming exposures, typically marked by horizontal to subvertical platy jointing (**Figure 6-58**). Weathered parts of **Tmdb** form landscapes mantled by meter-scale, subrounded boulders. Extensive talus slopes are common beneath cliff-forming outcrops. Maximum thickness of **Tmdb** is ≤70 m (230 ft) (Plate 3). Typical hand samples of **Tmdb** are light bluish gray (5B 7/1) to medium-bluish gray (5B 5/1), containing 3 to 5 percent (vol.) clear to chalky white (N9), subhedral to anhedral, prismatic to blocky, seriate plagioclase microphenocrysts and phenocrysts ≤1 cm (0.4 in); 1 to 2 percent (vol.) grayish black (N2), euhedral to subhedral, prismatic to lath-shaped pyroxene phenocrysts and microphenocrysts ≤2 mm (0.08 in); and ≤1 percent (vol.) light greenish gray (5GY 8/1), euhedral to subhedral, prismatic to lath-shaped hornblende microphenocrysts ≤1 mm (0.04 mm); all distributed within a fine-grained strongly trachytic holocrystalline groundmass (**Figure 6-59**). Thin sections contain 1 to 2 percent (vol.) cubic-shaped opaque Fe-Ti oxides.

Tmdb has normal magnetic polarity and is assigned a late Miocene age on the basis of stratigraphic position beneath the 7.91 Ma dacite of Wolf Run (**Tmdw**)(**Figure 6-1**; Plate 3; **Appendix**).

Figure 6-58. Platy- to tabular-jointed dacite of Bulo Point (Tmdb) cropping out at Bulo Point in the Flag Point 7.5′ quadrangle (45.37276, -121.47317). Hammer for scale is 38 cm (15 in) long. View is looking east. Photo credit: Jason McClaughry, 2016.

Figure 6-59. Hand sample and thin section photographs of the dacite of Bulo Point (Tmdb). (a) Typical abundantly plagioclase- and pyroxene-porphyritic hand sample. Scale bar is 2.5 cm (1 in). (b) Thin section under cross-polarized light. (c) Same view as in (b) under plane-polarized light. Scale bar in (b) and (c) is 7 mm (0.3 in). Photo credits: Jason McClaughry, 2017.

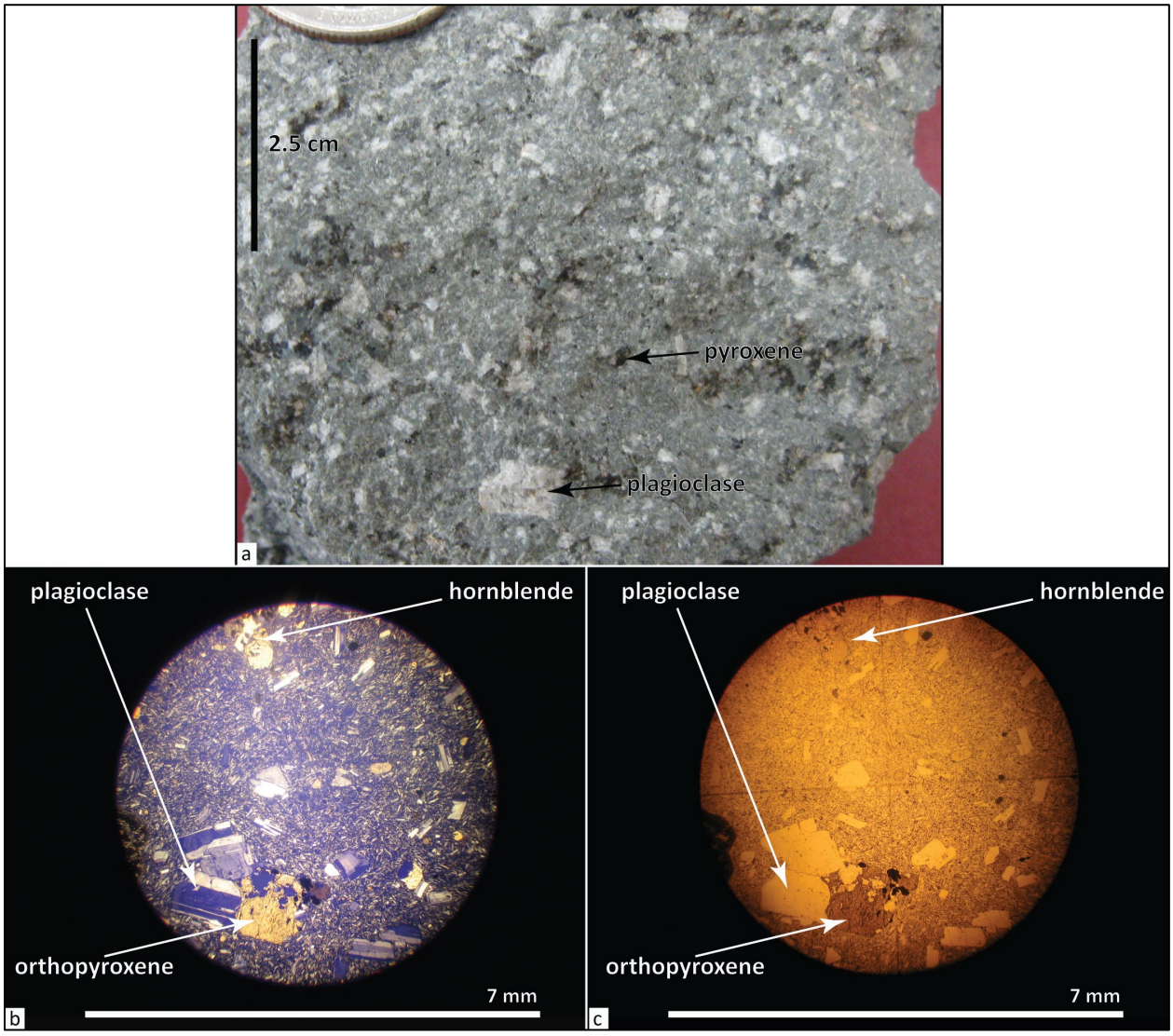

Tmdd **tuff breccia of Fifteenmile Creek (upper Miocene)**—Matrix- to clast-supported, cliff-forming boulder breccia mapped along Fifteenmile Creek (**Figure 6-60**; Plate 3). **Tmdd** is mapped eastward into the Dufur area (McClaughry and others, 2021). Breccia beds are typically massively bedded, very poorly sorted, and matrix supported, with localized clast-supported areas (**Figure 6-60**). Clasts are typically angular to subrounded, dense to pumiceous, accounting for 50 to 60 percent (vol.) of the deposit. Maximum observed clast size is ~2.0 m (6.6 ft); average size of the largest observed clasts at all outcrops is ~1.2 m (3.9 ft). **Tmdd** typically contains a texturally similar, but chemically diverse assemblage of unaltered, very light gray (N8) to medium-dark gray (N4) and grayish orange-pink (5YR 7/2) hornblende-porphyritic andesite and dacite (SiO_2 = 61.72 to 67.35 weight percent; K_2O = 1.39 to 2.22 weight percent; Nb = 8.3 to 10.5 ppm; Zr = 137 to 211 ppm; *n* = 12 analyses outside Mill Creek area)(**Table 6-3**; McClaughry and others, 2021). Typical hand samples of **Tmdd** clasts contain ~10 to 25 percent (vol.) clear euhedral to anhedral, prismatic to blocky, seriate plagioclase microphenocrysts and phenocrysts up to 6 mm (0.2 in) in length; ~5 to 10 percent (vol.) dark reddish brown (10R 3/4) euhedral to anhedral, prismatic- to lath-shaped, seriate hornblende microphenocrysts and phenocrysts up to 7 mm (0.3 in); and 1 to 3 percent (vol.) dark gray (N2) pyroxene microphenocrysts and phenocrysts up to 2 mm (0.08 in)(orthopyroxene > clinopyroxene); all distributed within a fine- to medium-grained hypocrystalline groundmass (McClaughry and others, 2021). Clasts are typically enclosed by a very light gray (N8) to grayish orange-pink (5YR 7/2), poorly sorted, coarse-grained tuffaceous sandstone matrix composed of angular to subrounded, very light gray (N8) to medium-dark gray (N4), and grayish orange-pink (5YR 7/2) porphyritic dacite lithics and plagioclase grains. The matrix component typically accounts for 40 to 50 percent (vol) of the deposit.

Tmdd is assigned a late Miocene age on the basis of stratigraphic position and an $^{40}Ar/^{39}Ar$ hornblende plateau age of 8.75 ± 0.05 Ma determined for a sample from a single boulder clast collected from outcrops east of the map area at the Henderson Pioneer Cemetery in the Dufur West 7.5′ quadrangle (**Figure 6-1**; McClaughry and others, 2021). Along Fifteenmile Creek, in the Wolf Run 7.5′ quadrangle, **Tmdd** contains a clast with a reported K-Ar age for plagioclase of 7.73 ± 0.16 Ma (Gray and others, 1996; McClaughry and others, 2021).

Figure 6-60. Tuff breccia of Fifteenmile Creek (Tmdd) exposed on the north side of Fifteenmile Creek Canyon, in the Wolf Run 7.5′ quadrangle (45.387535, -121.336587). View is looking north. Photo credit: Jason McClaughry, 2015.

Angular unconformity to disconformity

6.3.4 Middle and lower Miocene volcanic and sedimentary rocks

6.3.4.1 Columbia River Basalt Group

6.3.4.1.1 *Saddle Mountains Basalt*

The Saddle Mountains Basalt is represented by only the Pomona Member in the Mill Creek area (Plates 1 and 2). Effusion of 33 lava flows composing the Saddle Mountains Basalt produced ~2424 km^3 (581 mi^3) of lava that covered an area of ~34,800 km^2 (13,436 mi^2) in the Pacific Northwest (Reidel and others, 2013a). Saddle Mountains Basalt accounts for ~1.1 percent of the total volume erupted in the CRBG flood basalt province. Thickness of the Saddle Mountains Basalt in the map area is ≤37 m (120 ft)(Plates 1 and 2).

Tsp **Pomona Member (upper Miocene)**—High-magnesium basalt lava flow (SiO_2 = 51.42 to 53.61 weight percent; TiO_2 = 1.61 to 1.71 weight percent; FeOTotal = 9.97 to 11.05; MgO = 5.42 to 7.09 weight percent; *n* = 17 analyses [16 outside Mill Creek area]) mapped along Mosier Creek in the northeast corner of the Ketchum Reservoir 7.5′ quadrangle and northwest corner of the Brown Creek 7.5′ quadrangle (**Figure 6-61**; **Table 6-4**; Plates 1 and 2; **Appendix**). **Tsp** is characterized by entablature-style jointing with elongate, irregular, 5- to 20-cm-wide (2- to 8-in-wide) columns

(**Figure 6-61**). Locally exposed upper and lower colonnades consist of variably vesicular, massive meter-scale blocky columns. Deeply weathered outcrops are flanked by talus slopes consisting predominantly of angular fragments ≤20 (8 in). Thickness of **Tsp** in the map area is ≤37 m (120 ft), thinning to the south (Plates 1 and 2). Typical hand samples of **Tsp** are medium-dark gray (N4), containing 2 to 5 percent colorless to white (N9), euhedral to subhedral, prismatic to blocky plagioclase phenocrysts and glomerocrysts ranging from 5 mm (0.04 in) to ≤1 cm (0.4 in); and ≤1 percent (vol.), dusky green (5G 3/2) to dark greenish yellow (10Y 6/6), euhedral to anhedral, polygonal to blocky shaped, seriate olivine microphenocrysts and phenocrysts ≤3 mm (0.1 in); all distributed within a fine-grained, equigranular, hypocrystalline groundmass of plagioclase, intergranular clinopyroxene and olivine, minor Fe-Ti oxides, and intersertal glass (**Figure 6-62**). Olivine are typically skeletal in form, corroded and partially resorbed, with rims altered to dark yellowish orange (10YR 6/6) iddingsite (**Figure 6-62b,c**).

Tsp has reversed magnetic polarity (Choiniere and Swanson, 1979) and is assigned a late Miocene age (**Figure 5-7**, **Figure 6-1**; Plates 1 and 2; **Appendix**). McKee and others, (1977) reported a K-Ar age of 12 Ma for the Pomona Basalt (**Tsp**), while Barry and others (2013) provided a whole rock $^{40}Ar/^{39}Ar$ age of 11.21 ± 0.42 Ma. Cogliatti and others (2021) used $^{40}Ar^{39}Ar$ experiments to date silicic glass interbeds above and below the Pomona Basalt, constraining the age of the lava flow between 11.34 ± 0.17 and 10.70 ± 0.18 Ma. **Tsp** is equivalent to the Pomona chemical type of Wright and others (1973) and Swanson and others (1979b). Effusion of **Tsp** produced over 600 km^3 (143 mi^3) of lava covering an area >20,550 km^2 (7,934 mi^2) (Tolan and others, 1989). **Tsp** was erupted from vents and fissures in the Clearwater Embayment of western Idaho and flowed westward to the Pasco Basin along an ancestral tributary to the Columbia River (Camp, 1981; Anderson and Vogt, 1987). This lava flow covered large parts of the central Columbia Plateau as a conformable unit; west of Pasco, Washington, **Tsp** was largely confined as an intracanyon lava flow along an ancestral Columbia River channel (Anderson and Vogt, 1987). The longitudinal distance from the vent area to distal part of **Tsp** at the Pacific Coast is ~600 km (373 mi).

Figure 6-61. Entablature-style jointing typical in the Pomona Member (Tsp); 45.62207, -121.37751. Scale bar is 1 m (3.3 ft). View is looking west. Photo credit: Jason McClaughry, 2016.

Table 6-4. Representative XRF geochemical analyses for the Columbia River Basalt Group in the Mill Creek area.

Sample	280 MCBJ 16	277 MCBJ 16	KRL15-102	KRL15-38	KRL15-39	KRL15-19	KRL15-41	KRL15-42	8 MCBJ 16	9 MCBJ 16
Geographic Area	Mosier Creek	Mosier Creek	North Fork Mill Creek	Mill Creek Ridge	Mill Creek Ridge	Mosier Creek	Mill Creek Ridge	Mill Creek Ridge	Mill Creek Ridge	Mill Creek Ridge
Formation	Saddle Mountains Basalt	Wanapum Basalt	Wanapum Basalt	Wanapum Basalt	Wanapum Basalt	Wanapum Basalt	Grande Ronde Basalt	Grande Ronde Basalt	Grande Ronde Basalt	Grande Ronde Basalt
Map Unit	Tsp	Twpr	Twpl	Twfs	Twfh	Twfg	Tgsb	Tgww	Tgo	Tggc
Latitude	45.6226	45.5348	45.6222	45.5345	45.5348	45.6134	45.5366	45.5366	45.5187	45.5199
Longitude	-121.3774	-121.3726	-121.3752	-121.3843	-121.3858	-121.3767	-121.3900	-121.3950	-121.4201	-121.4207
Age (Ma)	11.2	15.9	15.9	16.1	16.1	16.1	16.2	16.2	16.2	16.2
Plate	2	2	1	2	2	2	2	2	2	2
Map Label	G123	G122	G2	G36	G37	G118	G41	G40	G23	G24
Oxides, weight percent										
SiO_2	52.39	50.16	49.79	51.82	51.97	51.21	53.99	56.32	56.67	56.23
Al_2O_3	14.89	12.87	13.73	13.14	13.65	13.14	13.92	13.55	14.05	13.93
TiO_2	1.69	3.66	3.22	3.09	2.96	3.12	2.06	2.14	1.95	1.91
FeOTotal	10.23	15.12	14.07	14.67	13.69	15.02	12.09	12.02	10.97	11.68
MnO	0.18	0.25	0.24	0.23	0.20	0.24	0.21	0.21	0.19	0.19
CaO	10.87	8.65	9.02	8.11	8.74	8.13	8.60	7.11	7.19	7.14
MgO	6.62	4.44	5.26	4.22	4.44	4.22	4.60	3.33	3.59	3.58
K_2O	0.57	1.35	1.11	1.24	1.07	1.33	1.15	1.88	1.98	1.75
Na_2O	2.34	2.69	2.79	2.90	2.70	2.92	3.03	3.08	3.07	3.29
P_2O_5	0.23	0.81	0.78	0.59	0.57	0.67	0.35	0.37	0.33	0.30
LOI	1.17	0.72	0.17	nd	2.65	nd	nd	nd	0.88	0.33
Total_I	98.18	98.56	98.81	98.73	96.90	98.03	98.67	98.50	98.71	99.12
Trace Elements, parts per million										
Ni	53	18	47	17	20	15	16	6	10	12
Cr	94	5	86	14	38	8	31	1	8	3
Sc	35	39	39	37	38	37	37	32	33	32
V	278	420	367	434	412	393	325	350	323	331
Ba	232	576	529	590	473	574	507	644	699	702
Rb	12	31	26	25	27	32	27	52	53	45
Sr	247	291	292	305	329	320	317	320	320	315
Zr	133	214	186	198	179	181	165	186	182	183
Y	31	50	45	43	40	41	36	38	36	35
Nb	12.1	17.9	15.0	15.4	13.6	13.2	10.9	12.5	11.2	11.7
Ga	19	22	21	21	20	21	21	21	21	20
Cu	54	24	46	27	27	26	29	10	21	19
Zn	98	161	144	148	140	143	124	134	129	120
Pb	7	5	6	7	7	6	7	9	9	9
La	22	32	26	25	23	22	20	26	26	24
Ce	38	66	66	62	55	54	45	54	55	54
Th	2	5	4	5	5	5	4	7	6	6
Nd	21	39	35	33	32	33	24	28	29	26
U	1	2	3	3	2	3	3	3	2	3

Major element determinations have been normalized to a 100-percent total on a volatile-free basis and recalculated with total iron expressed as FeOTotal; nd = no data or element not analyzed; na = not applicable or no information. LOI = Loss on Ignition; Total_I = original analytical total.

Figure 6-62. Hand sample and thin section photographs of the Pomona Member (Tsp). (a) Typical hand sample. Scale bar is 2.5 cm (1 in). (b) Thin section under cross-polarized light. (c) Same view as in (b) under plane-polarized light. Scale bar in (b) and (c) is 7 mm (0.3 in). Photo credits: Jason McClaughry, 2012.

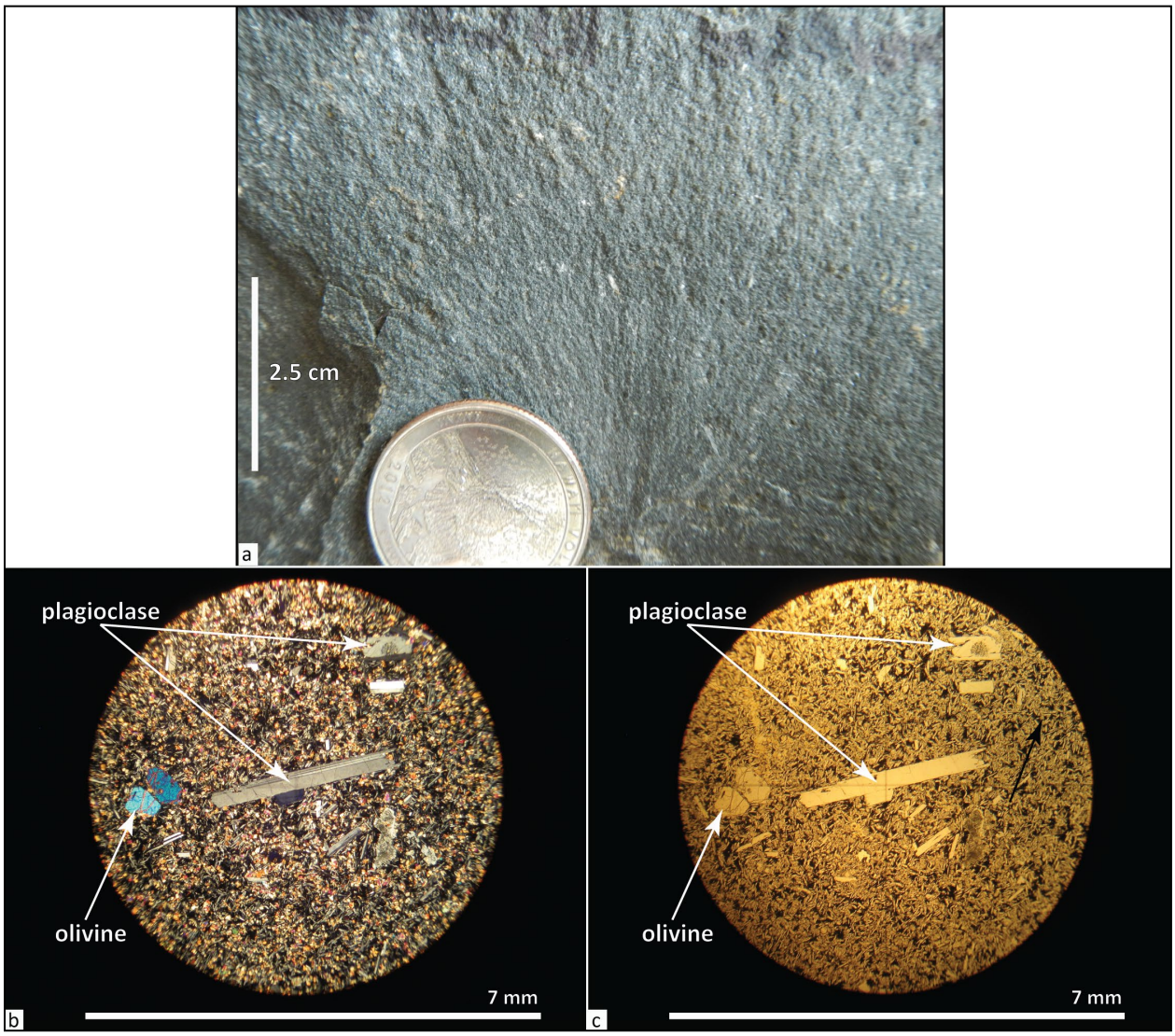

Disconformity to angular unconformity(?)

6.3.4.1.2 *Wanapum Basalt*

The Wanapum Basalt in the Mill Creek area consists of lava flows assigned to the Priest Rapids and Frenchman Springs members. Effusion of ~68 lava flows composing the Wanapum Basalt produced more than 12,175 km^3 (2,920 mi^3) of lava that covered an area exceeding 87,400 km^2 (33,745 mi^2) in the Pacific Northwest (Reidel and others, 2013a). Composite thickness of the Wanapum Basalt in the Mill Creek area is ≤220 m (720 ft) (Plates 1, 2, and 3).

Priest Rapids Member

The Priest Rapids Member forms the upper part of the Wanapum Basalt in the Mill Creek area, unconformably overlying the Frenchman Springs Member (Plates 1 and 2). The Priest Rapids Member consists of two lava flows, including the Basalt of Lolo (**Twpl**) and the Basalt of Rosalia (**Twpr**)(Wright and others, 1973; Camp, 1981; Anderson, 1987; Anderson and Vogt, 1987). Priest Rapids lava flows are distinguished from other CRBG units by their relatively high concentrations of magnesium, titanium (TiO_2 >3.0 weight percent), iron, and phosphorus (**Appendix**). Lava flows in the Priest Rapids Member also have reversed magnetic polarity, which serves to distinguish them from adjacent units (Swanson and others, 1979b). Lava flows of the Priest Rapids Member were erupted at 15.9 Ma (Kasbohm and Schoene, 2018; Kasbohm and others, 2023) from linear dike systems in the Clearwater Embayment of western Idaho and flowed west (Camp, 1981), covering most of the north and central parts of the Columbia Plateau. **Twpl** are mapped into the Mosier and Mill Creek areas east of the Cascade crest, while more extensive **Twpr** intracanyon lava flows traversed the area of the present-day Cascade Range (Anderson and Vogt, 1987; McClaughry and others, 2012) (**Figure 5-6**). Effusion of the Priest Rapids Member produced more than 2,800 km^3 (672 mi^3) of lava that covered an area exceeding 57,300 km^2 (22,123 mi^2) (Tolan and others, 1989; Reidel and others, 2013a). The composite thickness of the Priest Rapids Member in the Mill Creek area is >30 m (100 ft) and may exceed 150 m (492 ft) where lava flows filled paleocanyons (Plates 1 and 2). The Priest Rapids Member is divided in the Mill Creek area into:

Twpl **Basalt of Lolo (middle Miocene)**—High-titanium-phosphorus basalt lava flow (SiO_2 = 48.6 to 51.97 weight percent; TiO_2 = 3.11 to 3.65 weight percent; P_2O_5 = 0.73 to 0.78 weight percent; *n* = 19 analyses [10 outside Mill Creek area]) mapped beneath the Pomona Member (**Tsp**) in the northern part of the Brown Creek 7.5′ quadrangle (**Figure 6-63**; **Table 6-4**; Plate 1; **Appendix**). **Twpl** is also mapped along North Fork Mill Creek between Thompson Point and Willow Spring on the south limb of the Mill Creek Ridge anticline (Plates 1 and 2). Higher chromium concentrations (Cr = 87 to 122 ppm) differentiate **Twpl** from the underlying Basalt of Rosalia (**Twpr**; Hooper, 2000). Outcrops of **Twpl** are characterized by a well-developed colonnade, with sections of vertical platy jointing. A ≤5-m-thick (16 ft) interval of pillow palagonite locally occurs near the base of **Twpl** (**Figure 6-63**). In the Mosier area, **Twpl** is irregularly separated from the overlying Pomona Member by the Selah Member of the Ellensburg Formation; **Twpl** is locally underlain by a thin (<2 m [7 ft]) clay layer that is correlative to the Byron Member of the Ellensburg Formation (McClaughry and others, 2012; Lite, 2013). Thickness of **Twpl** in the map area is ~10 to 17 m (33 to 56 ft; Plate 1). Typical hand samples are medium-dark gray (N4), containing ≤5 percent colorless to white (N9), euhedral to subhedral, prismatic to blocky plagioclase phenocrysts and glomerocrysts <7 mm (0.3 in) to ≤1 cm (0.4 in) and ≤1 percent (vol.), dusky green (5G 3/2) to dark greenish yellow (10Y 6/6), euhedral to anhedral, blocky shaped, seriate olivine microphenocrysts and phenocrysts ≤3 mm (0.1 in), all distributed within a fine-grained, hypocrystalline groundmass of plagioclase, intergranular clinopyroxene and olivine, minor Fe-Ti oxides, and intersertal glass (**Figure 6-64**).

Twpl has reversed magnetic polarity and is assigned a middle Miocene age. The lava flow overlies a sedimentary interbed outside the Mill Creek area with a U/Pb age of 15.923 ± 0.030 Ma (Kasbohm and Schoene, 2018; Kasbohm and others, 2023). Watkins and Baksi (1974) reported a K-Ar age of 14.5 Ma for **Twpl** outside the Mill Creek area (**Figure 5-7**, **Figure 6-1**; Plates 1 and 2; **Appendix**). **Twpl** is equivalent to the Lolo chemical type of Bond (1963) and Wright and others (1979).

Figure 6-63. The Basalt of Lolo (Twpl) cropping out in the Brown Creek 7.5′ quadrangle. (a) Blocky columnar jointing in Twpl (45.62391, -121.28519). Hammer for scale is 38 cm (15 in) long. View is looking northwest. (b) Interval of pillow palagonite at the base of Twpl in the wall of a quarry (45.62411, -121.27613). Person for scale is 1.8 m (5.9 ft) tall. View is looking southeast. Photo credits: Jason McClaughry, 2016.

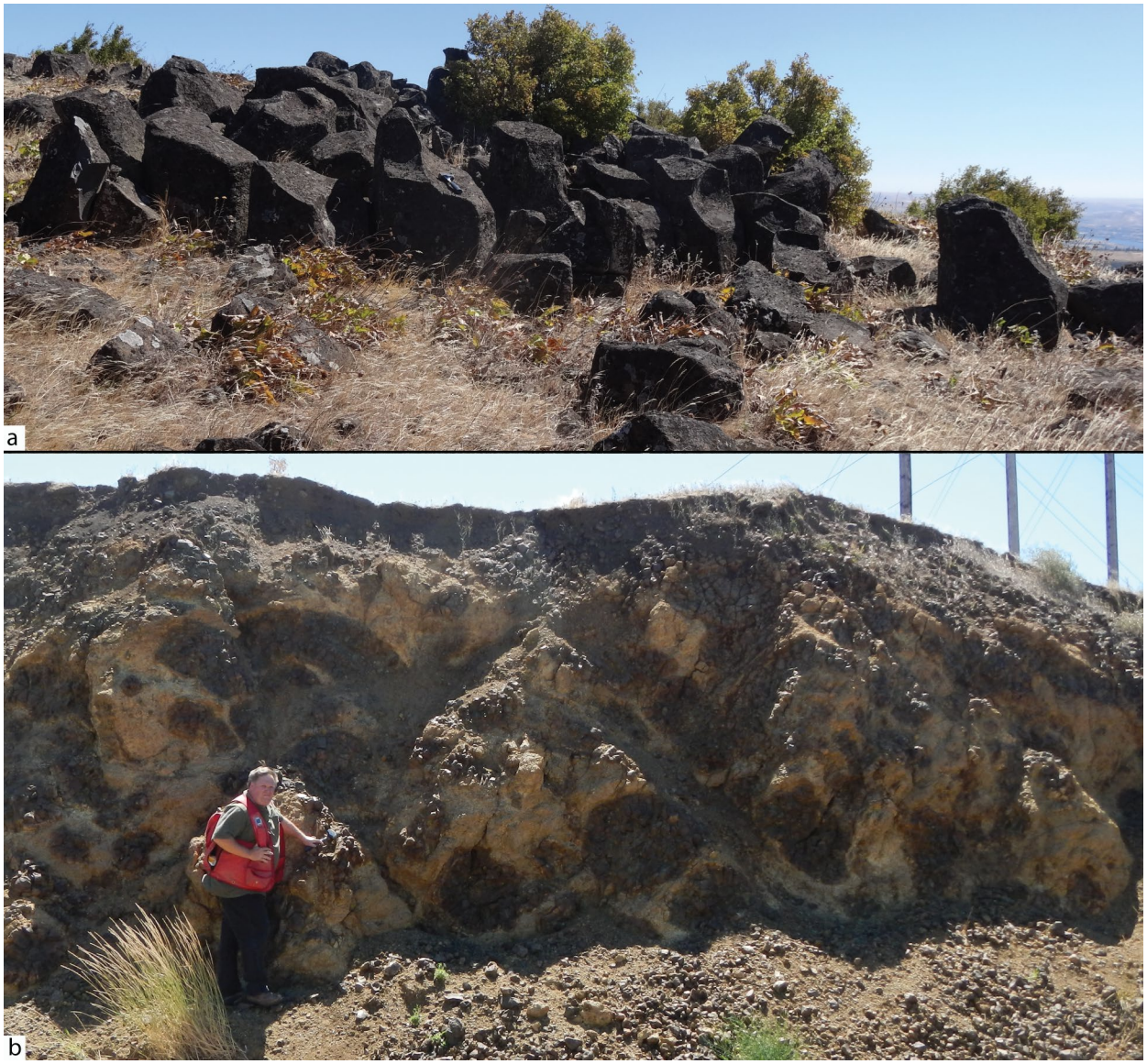

Figure 6-64. Hand sample and thin section photographs of the Basalt of Lolo (Twpl). (a) Typical hand sample. Scale bar is 2.5 cm (1 in). (b) Thin section under cross-polarized light. (c) Same view as in (b) under plane-polarized light. Scale bar in (b) and (c) is 7 mm (0.3 in). Photo credits: Jason McClaughry, 2017.

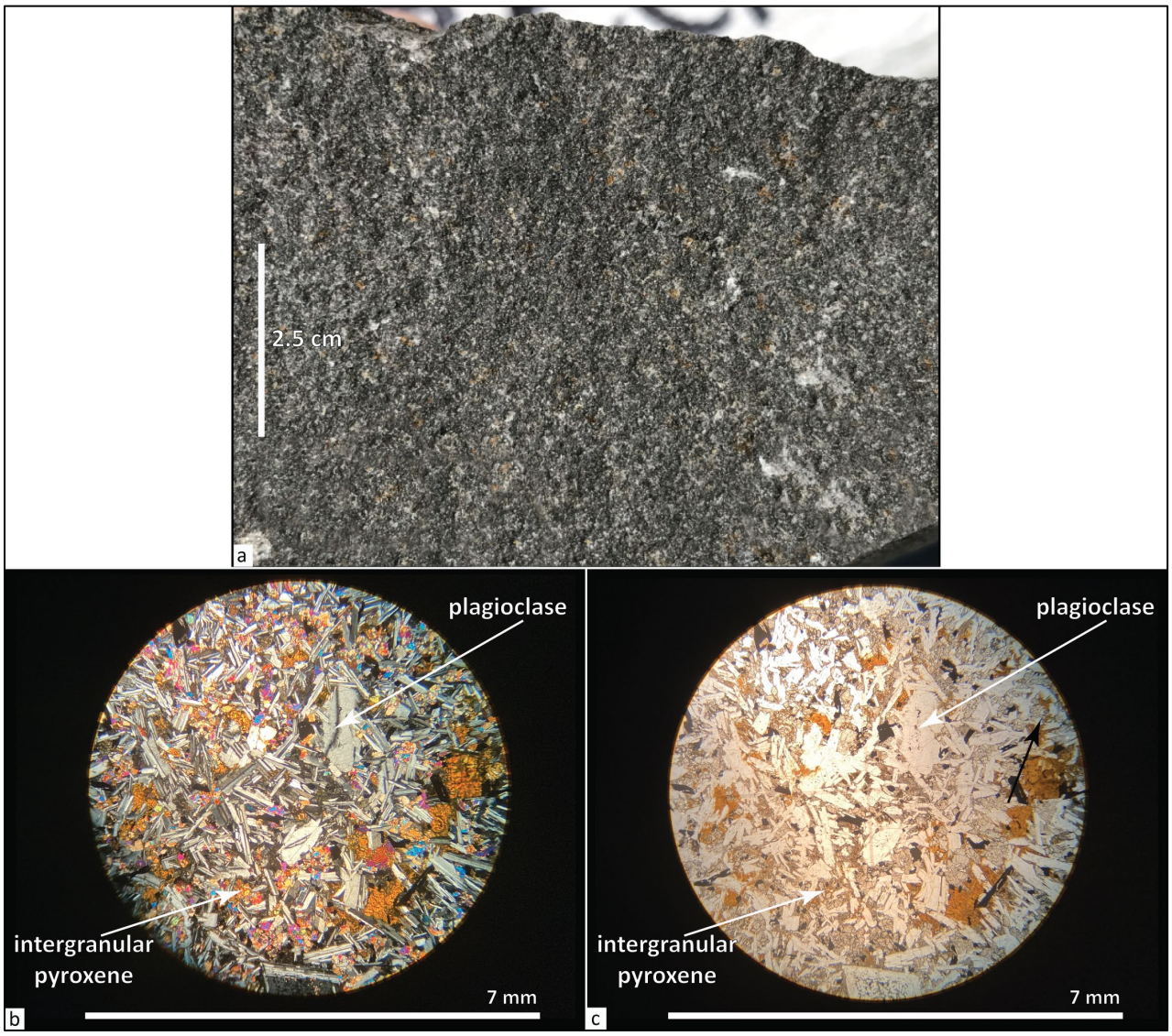

Twpr **Basalt of Rosalia (middle Miocene)**—High-titanium-phosphorus basalt lava flow (SiO_2 = 49.49 to 51.89 weight percent; TiO_2 = 3.47 to 4.13 weight percent; P_2O_5 = 0.69 to 0.91 weight percent; *n* = 33 analyses [20 outside Mill Creek area]) mapped beneath the Basalt of Lolo (**Twpl**) in the northern part of the Ketchum Reservoir and Brown Creek 7.5′ quadrangles (**Figure 6-65**, **Figure 6-66**; **Table 6-4**; Plates 1 and 2; **Appendix**). **Twpr** is also mapped along North Fork Mill Creek between Thompson Point and Willow Spring on the south limb of the Mill Creek Ridge anticline (Plates 1 and 2). Lower chromium concentrations (Cr = 2 to 10 ppm) differentiate **Twpr** from the overlying Basalt of Lolo (**Twpl**) (Hooper, 2000). **Twpr** is distinguished from older lava flows in the Frenchman Springs Member on the basis of reversed magnetic polarity and relatively higher amounts of titanium (avg TiO_2 = 3.74 weight percent) and phosphorus (avg P_2O_5 = 0.81 weight percent) and lesser amounts of chromium (avg Cr = 5 ppm)(*n* = 33 analyses in Middle Columbia

Basin; **Figure 5-10**; Madin and McClaughry, 2019; McClaughry and others, 2012, 2021). **Twpr** crops out as indistinct ledges characterized by a hackly-jointed entablature or basal colonnade with blocky columns ≤2 m (6.5 ft) across and vertical platy joint sets (**Figure 6-65**, **Figure 6-66**). Pillow lava and palagonite are notably absent over much of the Ketchum Reservoir and Brown Creek 7.5′ quadrangles, except in local rock-pit exposures in the north. This observation contrasts with intracanyon exposures that are prevalent to the north in the Hood River area (Anderson and Vogt, 1987; McClaughry and others, 2012). Where pillow lavas are present in the Mill Creek areas, pillows are often surrounded by sediment and display little or no vesiculation (Plates 1 and 2). Thickness of **Twpr** over much of the Ketchum Reservoir and Brown Creek 7.5′ quadrangles is ~40 m (130 ft) (Plates 1 and 2). The unit thins to the south toward the Mill Creek Ridge anticline and thickens to the north toward Hood River Mountain, where composite lava flow thickness locally ranges between ~150 and 200 m (492 and 656 ft)(McClaughry and others, 2012). Typical hand samples of the **Twpr** are dark gray (N3) and aphyric to sparsely porphyritic to abundantly microporphyritic, with 3 to 5 percent (vol.) dark yellowish orange (10YR 6/6), euhedral to subhedral, prismatic to blocky, seriate plagioclase microphenocrysts, phenocrysts, and glomerocrysts ranging from 1 mm to 1 cm (0.04 to 0.4 in); 1 to 2 percent (vol.) pale greenish yellow (10Y 8/2), euhedral to subhedral, prismatic to blocky clinopyroxene microphenocrysts ≤2 mm (0.08 in); and ≤1 percent (vol.) moderate olive-brown (5Y 4/4), euhedral to anhedral, polygonal to blocky olivine microphenocrysts ≤1 mm (0.04 in); all contained within a hypohyalline groundmass of plagioclase, intergranular clinopyroxene ± olivine, minor Fe-Ti oxides, and intersertal glass (**Figure 6-67**). Olivine are typically skeletal in form, corroded and partially resorbed, with rims altered to dark yellowish orange (10YR 6/6) iddingsite (**Figure 6-67b,c**).

Twpr has reversed magnetic polarity and is assigned a middle Miocene age (**Figure 5-7**, **Figure 6-1**; Plates 1 and 2; **Appendix**). U/Pb dating of an ash between the Basalt of Rosalia and the overlying Basalt of Lolo outside the Mill Creek area provided an age of 15.923 ± 0.030 Ma (Kasbohm and Schoene, 2018; Kasbohm and others, 2023). The Basalt of Rosalia overlies the ~16.1 Ma Frenchman Springs Member. **Twpr** is equivalent to the Rosalia chemical type of Swanson and Wright (1978) and Swanson and others (1979b).

Figure 6-65. Basalt of Rosalia (Twpr) cropping out in the Brown Creek 7.5′ quadrangle. (b) Blocky- to hackly-jointed Basalt of Rosalia (Twpr) (45.62219, -121.26761). Hammer for scale is 30 cm (12 in) long. View is looking north. Photo credit: Clark Niewendorp, 2016.

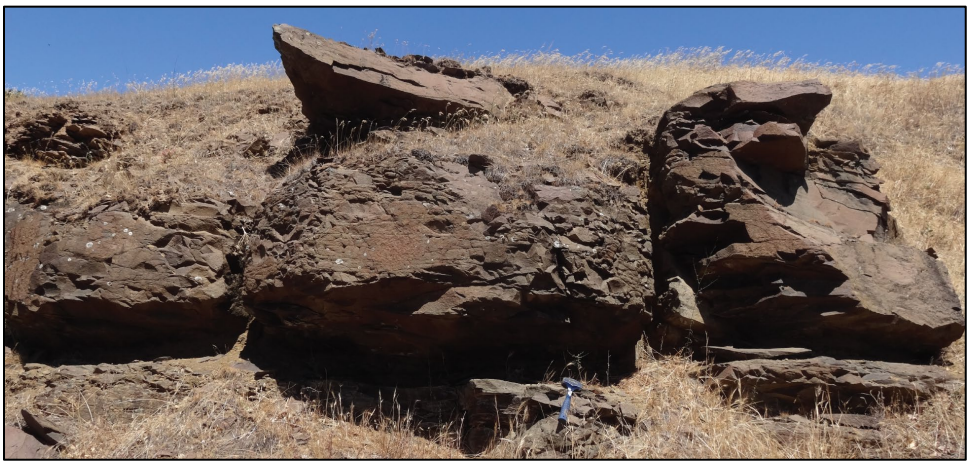

Figure 6-66. Basalt of Rosalia (Twpr) cropping out in the Ketchum Reservoir 7.5' quadrangle. (a) Massive to blocky-jointed Twpr cropping out between Neal Creek and Old Schoolhouse Spring (45.59744, -121.49659). The outcrop forms part of a down-faulted structural block within the Hood River fault zone. The iPad™ for scale is 25 cm (10 in) tall. View is looking northwest. (b) Blocky- to hackly-jointed Twpr exposed in a rock pit along West Fork Mosier Creek (45.60672, -121.42666). Hammer for scale is 38 cm (15 in) long. View is looking southeast. Photo credits: Jason McClaughry, 2015.

Figure 6-67. Hand sample and thin section photographs of the Basalt of Rosalia (Twpr). (a) Typical hand sample. Scale bar is 2.5 cm (1 in). (b) Thin section under cross-polarized light. (c) Same view as in (b) under plane polarized light. Scale bar in (b) and (c) is 7 mm (0.3 in). Photo credits: Jason McClaughry, 2016.

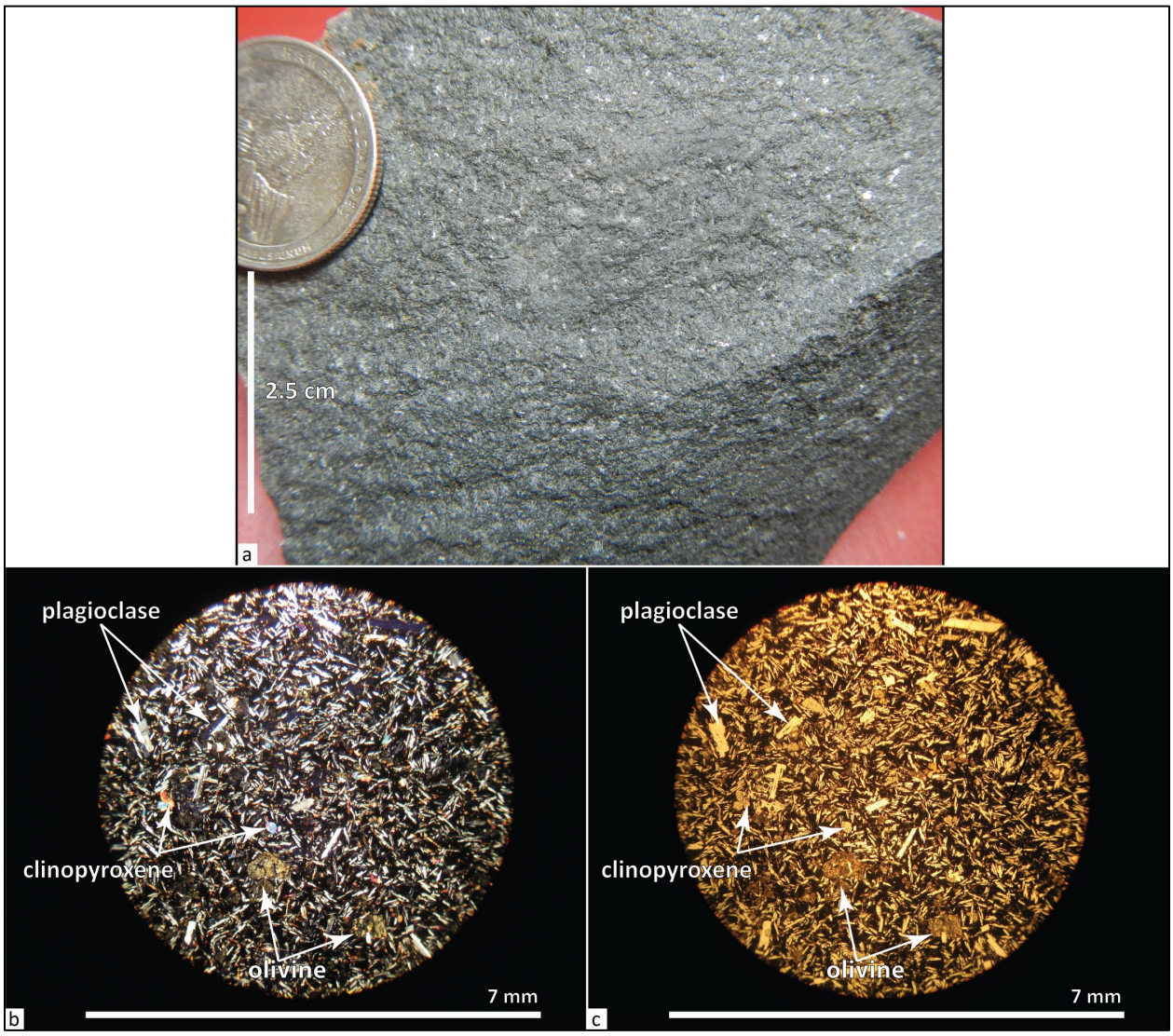

Frenchman Springs Member

The Frenchman Springs Member forms the lower part of the Wanapum Basalt in the Mill Creek area, consisting of 3 to 5 individual lava flows. On the basis of texture, phenocryst distribution, and geochemistry, these lava flows are divided from oldest to youngest into the Ginkgo (**Twfg**), Sand Hollow (**Twfh**), and Sentinel Gap (**Twfs**) basalt (**Figure 6-1**; **Table 6-4**; Plates 1, 2, and 3; Beeson and others, 1985; Martin and others, 2013). Frenchman Springs lava flows are distinguished other CRBG units by large, widely scattered to locally abundant plagioclase phenocrysts and high titanium contents (TiO_2 = ~2.9 to 3.06 weight percent) (**Figure 5-10**; Beeson and others, 1985, 1989; **Appendix**). Upper lava flows (**Twfs**, **Twfh**) in the Frenchman Springs Member have normal magnetic polarity, while those in the lower part of the member (**Twfg**) have excursional polarity. U/Pb ages obtained by Kasbohm and Schoene (2018) and Kasbohm and others (2023) from silicic tuff interbeds between lava flows on the Columbia Plateau constrain eruption of the Frenchman Springs Member between 15.9 and 16.1 Ma. $^{40}Ar/^{39}Ar$ dating

experiments by Baksi (2022) further refine eruption ages of the entirety of the Frenchman Springs Member to ~16.1 Ma. In the Mill Creek area, Frenchman Springs lava flows overlie the Sentinel Bluffs Member (**Tgsb**) at the top of the Grande Ronde Basalt; they are overlain by reversed-polarity lava flows of the 15.9 Ma Priest Rapids Member, forming the upper part of the Wanapum Basalt (**Twpr**)(**Figure 5-7**; Plates 1, 2, and 3). Frenchman Springs Member lava flows were erupted from a northerly-striking vent system in eastern Washington and northern Oregon (Kuehn, 1995) and flowed west down an ancestral paleoslope (**Figure 5-6**). Effusion of the Frenchman Springs Member produced more than 7628 km^3 (1830 mi^3) of lava that covered an area exceeding 72,595 km^2 (28,029 mi^2)(Martin and others, 2013). Composite thickness of the Frenchman Springs Member in the Mill Creek area is ~200 m (660 ft) (Plates 1, 2, and 3). The Frenchman Springs Member is subdivided in the Mill Creek area into:

Twfs **Basalt of Sentinel Gap (lower Miocene)**—High-titanium basalt and basaltic andesite lava flows (SiO_2 = 49.69 to 52.88 weight percent; TiO_2 =2.92 to 3.24 weight percent; *n* = 71 analyses [46 outside Mill Creek area]) mapped beneath the Dalles Formation (**Tmdl**) and above the Basalt of Sand Hollow (**Twfh**) along the Mill Creek Ridge anticline in the central part of the map area and along the northern parts of the Ketchum Reservoir and Brown Creek 7.5′ quadrangles (**Figure 5-7**, **Figure 6-68**; **Table 6-4**; Plates 1, 2, and 3; **Appendix**). **Twfs** is distinguished from the underlying Basalt of Sand Hollow (**Twfh**) on the basis of relatively higher amounts of titanium (avg TiO_2 = 3.09 weight percent) and phosphorus (avg P_2O_5 = 0.63 weight percent) and lesser amounts of chromium (avg Cr = 14 ppm)(*n* = 71 analyses in Middle Columbia Basin; **Figure 5-10; Table 6-4**; **Appendix**; Madin and McClaughry, 2019; McClaughry and others, 2012, 2020a, 2021). **Twfs** is differentiated from the overlying Priest Rapids Member on the basis of geochemistry and normal magnetic polarity (**Appendix**). **Twfs** outcrops are typically characterized by well-defined colonnade jointing and/or platy jointing (**Figure 6-68**). Where exposed, the upper part of **Twfs** is characterized by 0.2- to 2-m-thick (0.7- to 6.6-ft-thick) vesicular flow lobes. Thickness of **Twfs** in the map area is ~ 40 m (130 ft)(Plates 1, 2, and 3). Typical hand samples of the basalt are medium-dark gray (N4) to dark gray (N2) and aphyric to very sparsely porphyritic with ≤1 percent (vol.) clear to pale yellowish orange (10YR 8/6), euhedral to subhedral, prismatic to blocky, seriate plagioclase microphenocrysts and phenocrysts ≤7 mm (0.3 in) with ~1 phenocryst/m^2; ≤2 percent (vol.) grayish black (N2) clinopyroxene microphenocrysts ≤1 mm (0.04 in); and rare olivine microphenocrysts ≤1 mm (0.04 in); all enclosed within a fine-grained holocrystalline to hypocrystalline groundmass of plagioclase, intergranular clinopyroxene, Fe-Ti oxides, and intersertal glass (**Figure 6-69**).

Twfs has normal magnetic polarity and an early Miocene age (**Figure 5-7**, **Figure 6-1**; Plates 1, 2 and 3; **Appendix**). U/Pb dates obtained by Kasbohm and Schoene (2018) and Kasbohm and others (2023) on ash interbedded between lava flows outside the Mill Creek area bracket the eruption of the Basalt of Sentinel Gap between 16.1 and 15.9 Ma. Baksi (2022) reported $^{40}Ar^{39}Ar$ ages that constrain eruption of the Basalt of Sentinel Gap to 16.1 Ma. **Twfs** is equivalent to the Sentinel Gap flows of Mackin (1961), basalt of Sentinel Gap of Beeson and others (1985), and the flows of Union Gap of Powell (1982).

Figure 6-68. The Basalt of Sentinel Gap (Twfs) in the Ketchum Reservoir 7.5' quadrangle. (a) Twfs with meter-scale colonnade jointing on the south side of Mill Creek Ridge (45.52321, -121.40096). Scale bar is 1 m (3.3 ft). View is looking west. (b) Platy-jointed Twfs cropping out on the east end of Mill Creek Ridge. (45.53444, -121.38420). Hammer for scale in (b) is 25 cm (10 in) long. View is looking west. Photo credits: Jason McClaughry, 2015.

Figure 6-69. Hand sample and thin section photographs of the Basalt of Sentinel Gap (Twfs). (a) Typical hand sample. Scale bar is 2.5 cm (1 in). (b) Thin section under cross-polarized light. (c) Same view as in (b) under plane-polarized light. Scale bar in (b) and (c) is 7 mm (0.3 in). Photo credits: Jason McClaughry, 2015.

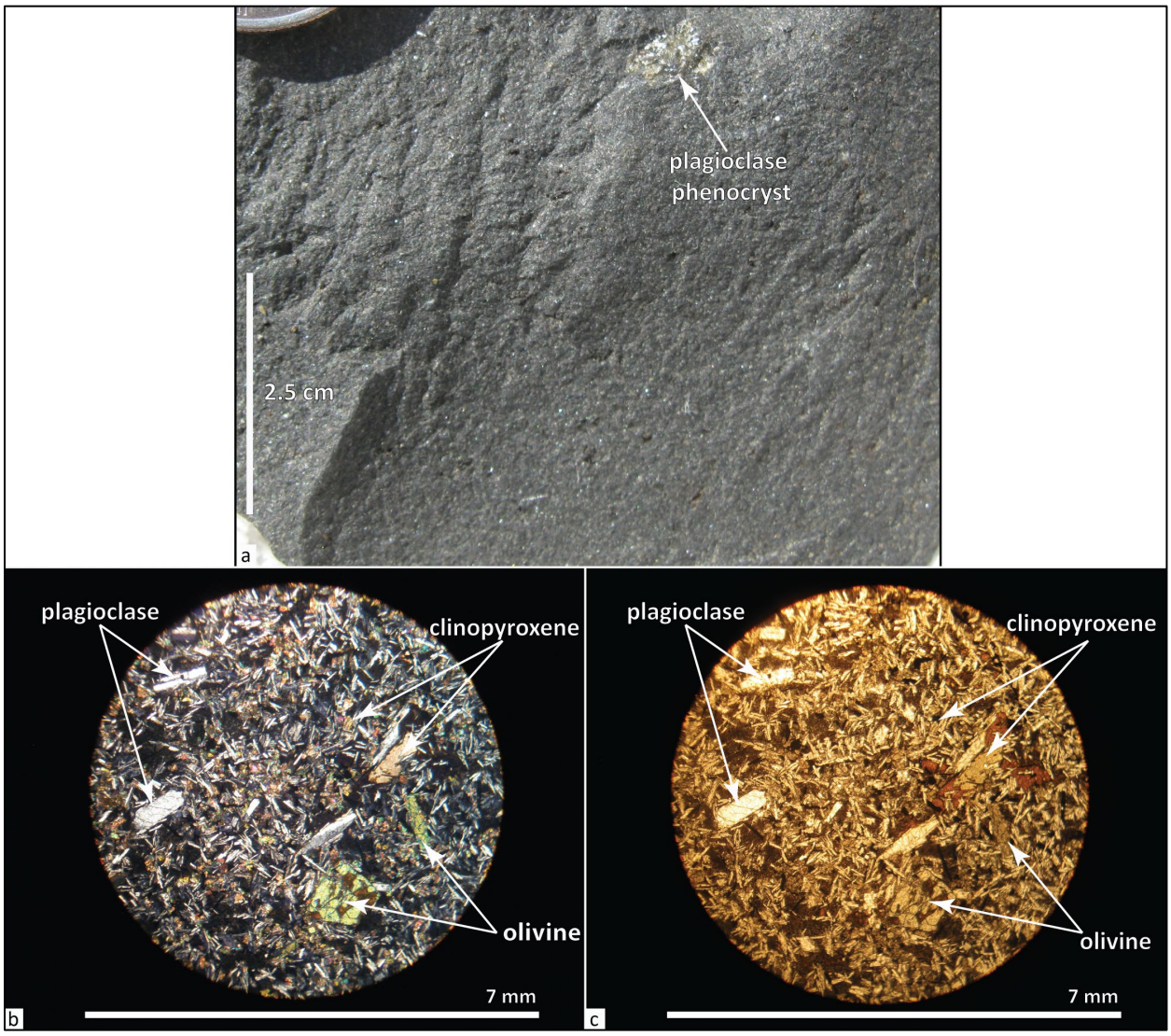

Twfh **Basalt of Sand Hollow (lower Miocene)**—High-titanium basalt and basaltic andesite lava flows (SiO_2 = 49.14 to 53.72 weight percent; TiO_2 = 2.85 to 3.27 weight percent; *n* = 156 analyses [129 outside Mill Creek area]) mapped beneath the Basalt of Sentinel Gap (**Twfs**) and above the Basalt of Ginkgo (**Twfg**) and Sentinel Bluffs Member (**Tgsb**) along the Mill Creek Ridge anticline in the central part of the map area and along the northern parts of the Ketchum Reservoir and Brown Creek 7.5′ quadrangles (**Figure 5-7**, **Figure 6-70**; **Table 6-4**; Plates 1, 2, and 3; **Appendix**). **Twfh** is distinguished from other Frenchman Springs units (**Twfs**, **Twfg**) on the basis of sparsely distributed plagioclase phenocrysts and relatively lower amounts of titanium (avg TiO_2 = 2.97 weight percent) and phosphorus (avg P_2O_5 = 0.56 weight percent) and higher amounts of chromium (avg Cr = 38 ppm)(*n* = 156 analyses in Middle Columbia Basin; **Table 6-4**; **Appendix**; Madin and McClaughry, 2019; McClaughry and others, 2012, 2020a, 2021). **Twfh** consists of two flow units in the Mill Creek area characterized by well-developed platy to blocky colonnade jointing (**Figure 6-70**). Where **Twfh** is deeply weathered, adjacent slopes are mantled by subrounded boulders, generally <1.5 m (4.9 ft) in diameter (**Figure 6-70a**). Thickness of **Twfh** in the map area ranges between ~90 and 120 m (300 and 400 ft) (Plates 1, 2, and 3).

The lower part of **Twfh** in the Middle Columbia Basin is aphyric to very sparsely porphyritic. Typical hand samples from the lower part of **Twfh** are pale blue (5B 6/2) to medium-dark gray (N4) and aphyric to microporphyritic and very sparsely porphyritic (~1 phenocryst/m^2)(**Figure 6-71a**). The basalt contains 1 to 2 percent (vol.) yellow brown (5YR 5/6) to very pale orange (10YR 8/2), euhedral to subhedral, prismatic- to lath-shaped and blocky, plagioclase phenocrysts up to 7 mm (0.3 in) in length; 1 to 2 percent (vol.) conspicuous blocky to lath-shaped plagioclase microphenocrysts ≤1 mm (0.04 in); and ≤1 percent (vol.) clinopyroxene microphenocrysts ≤1 mm (0.04 in); all enclosed within a fine-grained equigranular hypocrystalline groundmass of plagioclase, intergranular clinopyroxene, minor opaques, and intersertal to hyalophitic glass (**Figure 6-71a**,**c**,**d**). Very rare olivine microphenocrysts ≤0.5 mm (0.02 in) are also present.

The upper part of **Twfh** in the Middle Columbia Basin is distinctly plagioclase porphyritic, and a distinct flow-top zone, ≤25 m (82 ft) thick is commonly present. Typical hand samples from the upper part of **Twfh** are medium-dark gray (N4) to dark gray (N2) and abundantly porphyritic and microporphyritic (**Figure 6-71b**). The basalt contains 3 to 5 percent (vol.) yellow brown (5YR 5/6) to very pale orange (10YR 8/2), euhedral to subhedral, prismatic to lath-shaped, seriate plagioclase phenocrysts and glomerocrysts ≤2 cm (0.8 in); 2 to 3 percent (vol.) conspicuous blocky to lath-shaped plagioclase microphenocrysts ≤1 mm (0.04 in); and ≤1 percent (vol.) clinopyroxene microphenocrysts ≤1 mm (0.04 in); all enclosed within a diktytaxitic, fine-grained holocrystalline groundmass of plagioclase, intergranular clinopyroxene, and minor Fe-Ti oxides (**Figure 6-71b**,**e**,**f**).

Twfh has normal magnetic polarity and an early Miocene age (**Figure 5-7**, **Figure 6-1**; Plates 1, 2 and 3; **Appendix**). U/Pb dates obtained by Kasbohm and Schoene (2018) and Kasbohm and others (2023) on ash interbedded between lava flows outside the Mill Creek area bracket the eruption of the Basalt of Sand Hollow between 16.1 and 15.9 Ma. Baksi (2022) reported $^{40}Ar^{39}Ar$ ages that constrain eruption of the Basalt of Sand Hollow to 16.1 Ma. **Twfh** is equivalent to the Sand Hollow flows of Mackin (1961), basalt of Sand Hollow of Beeson and others (1985), and the Kelly Hollow flow of Powell (1982).

Figure 6-70. The Basalt of Sand Hollow (Twfh) in the Fivemile Butte 7.5′ and Ketchum Reservoir 7.5′ quadrangles. (a) Blocky- to platy-jointed Twfh cropping out along the north slope of Mill Creek Ridge (45.49753, -121.45118). Backpack for scale. View is looking north. (b) Platy- to blocky-jointed Twfh cropping out along Neal Creek (45.59603, -121.49902). Scale bar is 1 m (3.3 ft). View is looking east. Photo credits: Jason McClaughry, 2015 and 2016.

Figure 6-71. Hand sample and thin section photographs of the Basalt of Sand Hollow (Twfh). (a) Typical hand sample of the lower Twfh flow. (b) Typical hand sample of the upper unit Twfh flow. Scale bars for (a) and (b) are 2.5 cm (1 in). (c) Thin section of hand sample in (a) under cross-polarized light. (d) Same view as in (c) under plane-polarized light. (e) Thin section of hand sample in (b) under cross-polarized light. (f) Same view as in (e) under plane-polarized light. Scale bar in (c-f) is 7 mm (0.3 in). Photo credits: Jason McClaughry, 2015.

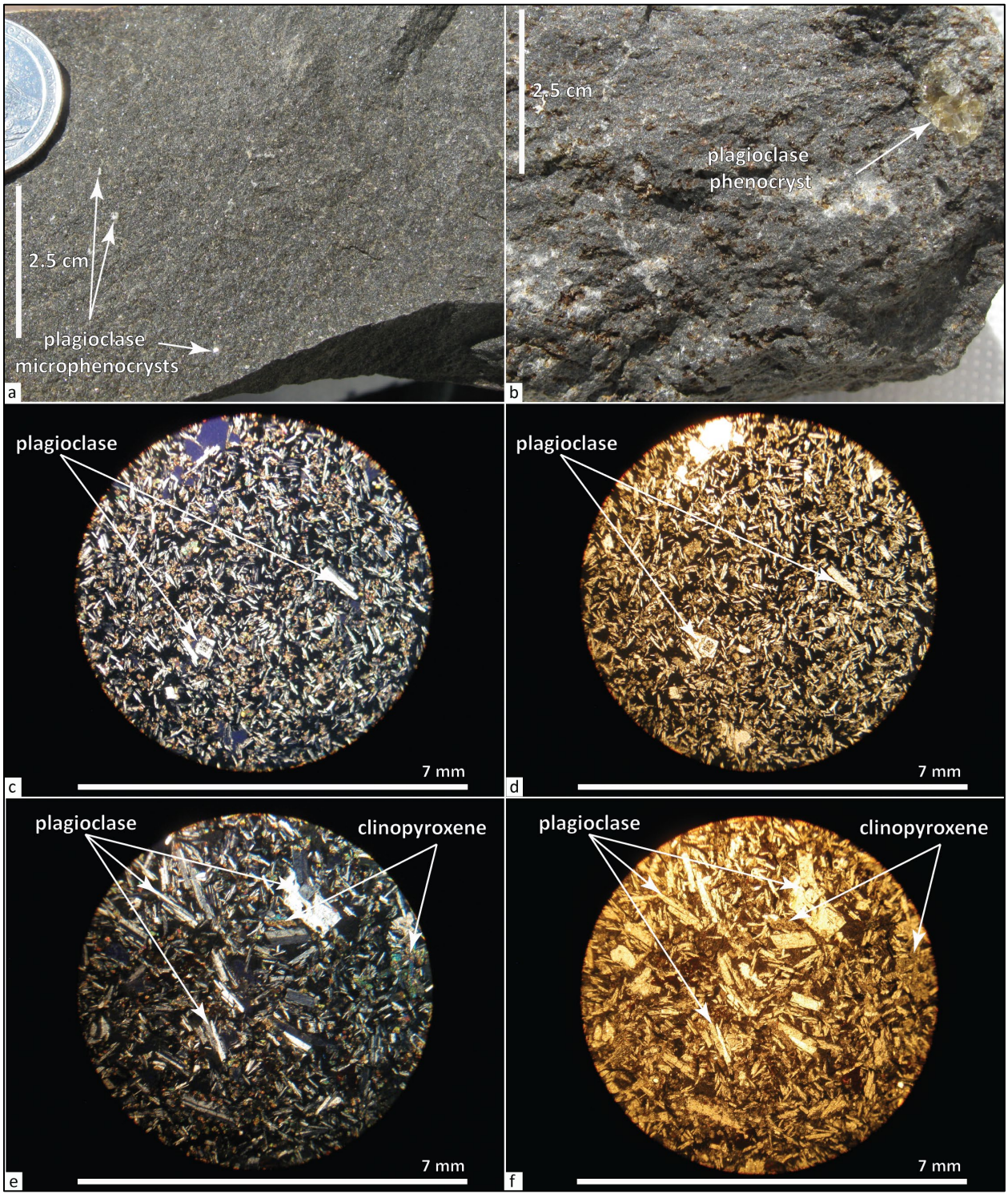

Twfg **Basalt of Ginkgo (lower Miocene)**—High-titanium basalt lava flows (SiO_2 = 50.67 to 52.76 weight percent; TiO_2 = 3.04 to 3.36 weight percent; *n* = 62 analyses [49 outside Mill Creek area]) mapped beneath the Basalt of Sand Hollow (**Twfh**) and above the Sentinel Bluffs Member (**Tgsb**) north of the Chenoweth fault in the Ketchum Reservoir and Brown Creek 7.5′ quadrangles (**Figure 5-7**, **Figure 6-72**; **Table 6-4**; Plates 1 and 2; **Appendix**). **Twfg** is distinguished from other Frenchman Springs units (**Twfs**, **Twfh**) on the basis of abundant (>5 percent [vol.]) plagioclase phenocrysts and glomerocrysts and relatively high amounts of titanium (avg TiO_2 = 3.18 weight percent) and phosphorus (avg P_2O_5 = 0.62 weight percent) and lower amounts of chromium (avg Cr = 14 ppm)(*n* = 62 samples in Middle Columbia Basin; **Table 6-4**; **Appendix**; Madin and McClaughry, 2019; McClaughry and others, 2012, 2020a, 2021). **Twfg** is typically not well exposed in the map area, tending to form talus-covered or boulder-armored slopes with rounded boulders 0.5- to 1-m (1.6 to 3.3 ft) across. Outcrops of **Twfg** are characterized by meter-scale blocky columnar jointing (**Figure 6-72**). Thickness of **Twfg** in the map area is typically ≤40 m (130 ft) (Plate 1 and 2). Typical hand samples of **Twfg** are medium-dark gray (N4) to dark gray (N2) and abundantly porphyritic and microporphyritic containing ~3 to 5 percent (vol.) yellow brown (5YR 5/6) to very pale orange (10YR 8/2), euhedral to subhedral, prismatic to lath-shaped, plagioclase phenocrysts and glomerocrysts ≤3 cm (1.2 in); and conspicuous blocky plagioclase microphenocrysts (**Figure 6-73**). Phenocrysts and microphenocrysts are distributed within an inequigranular holocrystalline groundmass of plagioclase, intergranular clinopyroxene, and minor Fe-Ti oxides (**Figure 6-73b,c**).

Twfg has excursional magnetic polarity and an early Miocene age (**Figure 5-7**, **Figure 6-1**; Plates 1 and 2; **Appendix**). U/Pb dates obtained by Kasbohm and Schoene (2018) and Kasbohm and others (2023) on ash interbedded between lava flows outside the Mill Creek area bracket the eruption of the Basalt of Ginkgo between 16.1 and 15.9 Ma. Baksi (2022) reported and $^{40}Ar/^{39}Ar$ plateau age of 16.12 ± 0.05 Ma for the Basalt of Ginkgo (**Twfg**). **Twfg** is equivalent to the Ginkgo flows of Mackin (1961) and basalt of Ginkgo of Beeson and others (1985).

Figure 6-72. The Basalt of Ginkgo (Twfg) cropping out in the Ketchum Reservoir 7.5′ quadrangle. (a) Blocky-jointed Twfg west of Neal Creek (45.57624, -121.50285). Hammer for scale is 38 cm (15 in) long. View is looking north. (b) Twfg is characterized by abundant, large plagioclase phenocrysts (45.57624, -121.50285). Scale bar is 2 cm (0.8 in). Photo credits: Jason McClaughry, 2015.

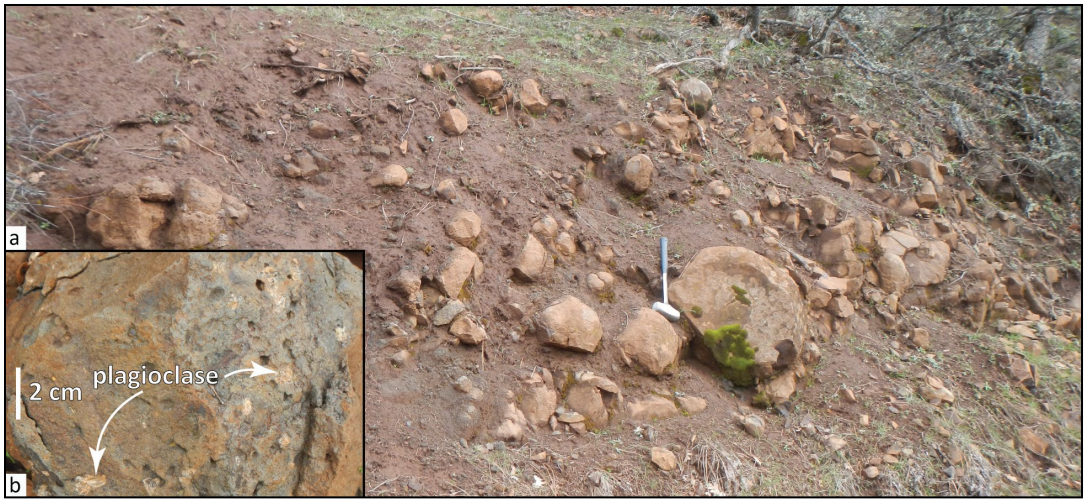

Figure 6-73. Hand sample and thin section photographs of the Basalt of Ginkgo (Twfg). (a) Typical hand sample. Scale bar is 2.5 cm (1 in). (b) Thin section under cross-polarized light. (c) Same view as in (b) under plane-polarized light. Scale bar in (b) and (c) is 7 mm (0.3 in). Photo credits: Jason McClaughry, 2015.

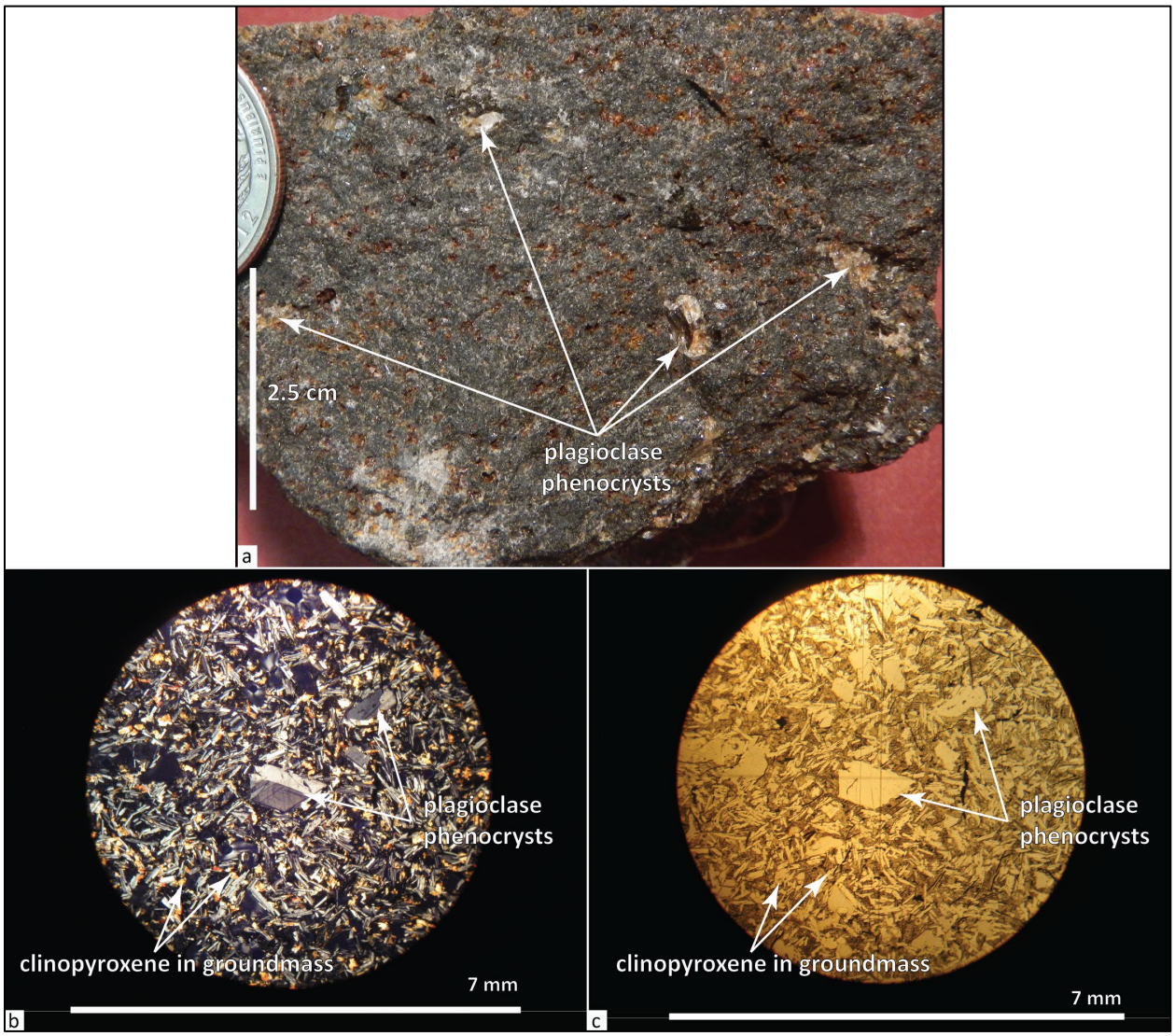

Disconformity

6.3.4.1.3 *Grande Ronde Basalt*

The Grande Ronde Basalt is the thickest, most voluminous formation of the CRBG representing 72 percent of total volume erupted (**Figure 5-7**; Reidel and Tolan, 2013). Effusion of the Grand Ronde Basalt from vents and fissures in the eastern and southeastern parts of the Columbia Plateau produced more than 150,400 km^3 (36,082 mi^3) of lava flows that covered an area exceeding 169,600 km^2 (65,482 mi^2) (**Figure 5-6**; Tolan and others, 1989; Reidel and others, 1989; Barry and others, 2010; Reidel and Tolan, 2013). The Grande Ronde Basalt spans at least four paleomagnetic zones and has been stratigraphically subdivided into the R1, N1, R2, N2 magnetostratigraphic units by Swanson and others (1979b) (**Figure 5-7**). The Grande Ronde Basalt mapped in the Mill Creek area consists of lava flows assigned to the Sentinel Bluffs (**Tgsb**), Winter Water (**Tgww**) and Ortley (**Tgo**) members of the N2 magnetostratigraphic unit (**Figure 5-7**). These lava flows directly overlie the Grouse Creek member (**Tggc**) of the R2 magnetostratigraphic unit, the stratigraphically lowest mapped geologic unit in the Mill Creek area. Composite thickness of the Grande Ronde Basalt in the Mill Creek area is ≥400 m (1,312 ft) (Plates 1, 2, and 3). Grande Ronde Basalt is generally monotonously fine-grained, aphyric, and petrographically non-distinctive, but can be distinguished on the basis of chemical composition combined with careful geologic mapping (**Table 6-4**). Grande Ronde lava flows are distinguished from the overlying Wanapum Basalt by the conspicuous absence of large plagioclase phenocrysts and glomerocrysts, and significantly lesser titanium contents (**Figure 5-10a-b**; **Table 6-4**; **Appendix**; Hooper, 2000; Tolan and others, 2009b).

Normal-polarity (N2) magnetostratigraphic unit

The N2 magnetostratigraphic unit is the youngest Grande Ronde Basalt magnetostratigraphic unit, made up of chemically distinctive lava flow packages that cover an area of ~114,500 km^2 (44,208 mi^2) (**Figure 5-7**). The estimated volume of the N2 magnetostratigraphic unit is ~35,300 km^3 (8,469 mi^3) (Reidel and Tolan, 2013). Ages of N2 Grande Ronde units are bracketed by U/Pb dates outside the Mill Creek area of 16.134 ± 0.03 Ma obtained on ash in the lower part of the overlying Vantage Member and 16.260 ± 0.03 Ma for ash between the Wapshilla Ridge and Meyer Ridge members of the underlying R2 magnetostratigraphic unit (Kasbohm and Schoene, 2018; Kasbohm and others, 2023; **Figure 5-7**, **Figure 6-1**; Plates 1, 2, and 3; **Appendix**)**.** The N2 magnetostratigraphic unit is subdivided into the following units:

Tgsb **Sentinel Bluffs Member (lower Miocene)**—Basaltic andesite to basaltic trachyandesite lava flows (SiO_2 = 53.30 to 55.19 weight percent; TiO_2 =1.74 to 2.06 weight percent; *n* = 139 analyses [111 outside Mill Creek area]) mapped beneath the Frenchman Springs Member (**Twfg**, **Twfh**) and above the Winter Water Member (**Tgww**). **Tgsb** forms the core of the Mill Creek Ridge anticline in the Fivemile Butte and Ketchum Reservoir 7.5′ quadrangles, crops out in fault blocks in the Hood River fault zone in the northwest part of the Ketchum Reservoir 7.5′ quadrangle, and is exposed in fault-bounded blocks north of the Chenoweth fault in the Brown Creek 7.5′ quadrangle (**Figure 5-7**, **Figure 6-74**; **Table 6-4**; Plates 1, 2, and 3; **Appendix**). **Tgsb** is distinguished from other members of the Grande Ronde Basalt on the basis of common diktytaxitic texture and higher contents of magnesium (avg MgO = 4.99 weight percent; 139 analyses in Middle Columbia Basin; **Figure 5-10a-b**; **Table 6-4**; Madin and McClaughry, 2019; McClaughry and others, 2012, 2020a, 2021). **Tgsb** is composed of thin lava flow lobes, generally <5 to 20m-thick (17 to 66 ft), that are characterized by well-developed vesicular flow tops and basal flow breccia. Flow interiors are

typically characterized by massive meter-scale colonnade jointing with lesser hackly entablatures (**Figure 6-74**). **Tgsb** is generally more resistant to erosion than the overlying Basalt of Ginkgo (**Twfg**), tending to form cliffs and steep slopes (**Figure 6-74**). Composite thickness of **Tgsb** in the Mill Creek area is as much as 170 m (560 ft) (Plates 1, 2, and 3). Typical hand samples of **Tgsb** are medium-light gray (N6) to medium gray (N5) and aphyric to very sparsely microporphyritic, containing ≤2 percent (vol.) clear, euhedral to subhedral, prismatic to blocky, plagioclase microphenocrysts distributed within an equigranular, fine-grained, diktytaxitic hypocrystalline groundmass of plagioclase, intergranular clinopyroxene, minor Fe-Ti oxides, and intersertal glass (**Figure 6-75**). Minor amounts of olivine microphenocrysts are also present in some lava flows.

Tgsb has normal magnetic polarity and an early Miocene age (**Figure 5-7**, **Figure 6-1**; Plates 1 and 2; **Appendix**). U/Pb dates obtained by Kasbohm and Schoene (2018) and Kasbohm and others (2023) on ash interbedded between lava flows outside the Mill Creek area bracket the eruption of the Sentinel Bluffs Member between 16.3 and 16.1 Ma. Kasbohm and others (2023) reported an $^{40}Ar/^{39}Ar$ groundmass age of 16.135 ± 0.04 Ma for the Basalt of Museum within the Sentinel Bluffs Member. Baksi (2022) reported a similar $^{40}Ar/^{39}Ar$ plateau age of 16.15 ± 0.07 Ma for the Basalt of Museum. **Tgsb** was erupted from a northerly trending vent system in eastern Washington and northern Oregon and flowed west down an ancestral paleoslope (**Figure 5-6**; Tolan and others, 2009b; Reidel and Tolan, 2013). Effusion of **Tgsb** produced ~10,150 km^3 (2,435 mi^3) of lava flows that covered an area exceeding 167,700 km^2 (64,749 mi^2)(Reidel and Tolan, 2013). **Tgsb** is equivalent to the high-MgO Yakima flows of Wright and others (1973), the Sentinel Bluffs unit of Reidel and others (1989), and the Sentinel Bluffs Member of Reidel (2005) and Reidel and Tolan (2013).

Figure 6-74. Cliff-forming, blocky- to columnar-jointed Sentinel Bluffs Member (Tgsb) cropping out near the intersection of Neal and Snakehead creeks (45.58547, -121.48965). Arrow points to the iPad for scale, which is 25 cm (10 in) long. View is looking east. Photo credit: Jason McClaughry, 2015.

Figure 6-75. Hand sample and thin section photographs of the Sentinel Bluffs Member (Tgsb). (a) Typical aphyric to very sparsely microporphyritic hand sample of Tgsb. (b) Thin section of the sample in (a) under cross-polarized light. (c) Hand sample of basalt from the middle part of Tgsb. (d) Thin section of the sample in (c) under cross-polarized light. (e) Hand sample of the lowermost part of Tgsb. (f) Thin section of the sample in (e) under cross-polarized light. Scale bar for (a), (c), and (e) is 2.5 cm (1 in). Scale bar in (b), (d), and (f) is 7 mm (0.3 in). Photo credits: Jason McClaughry, 2015.

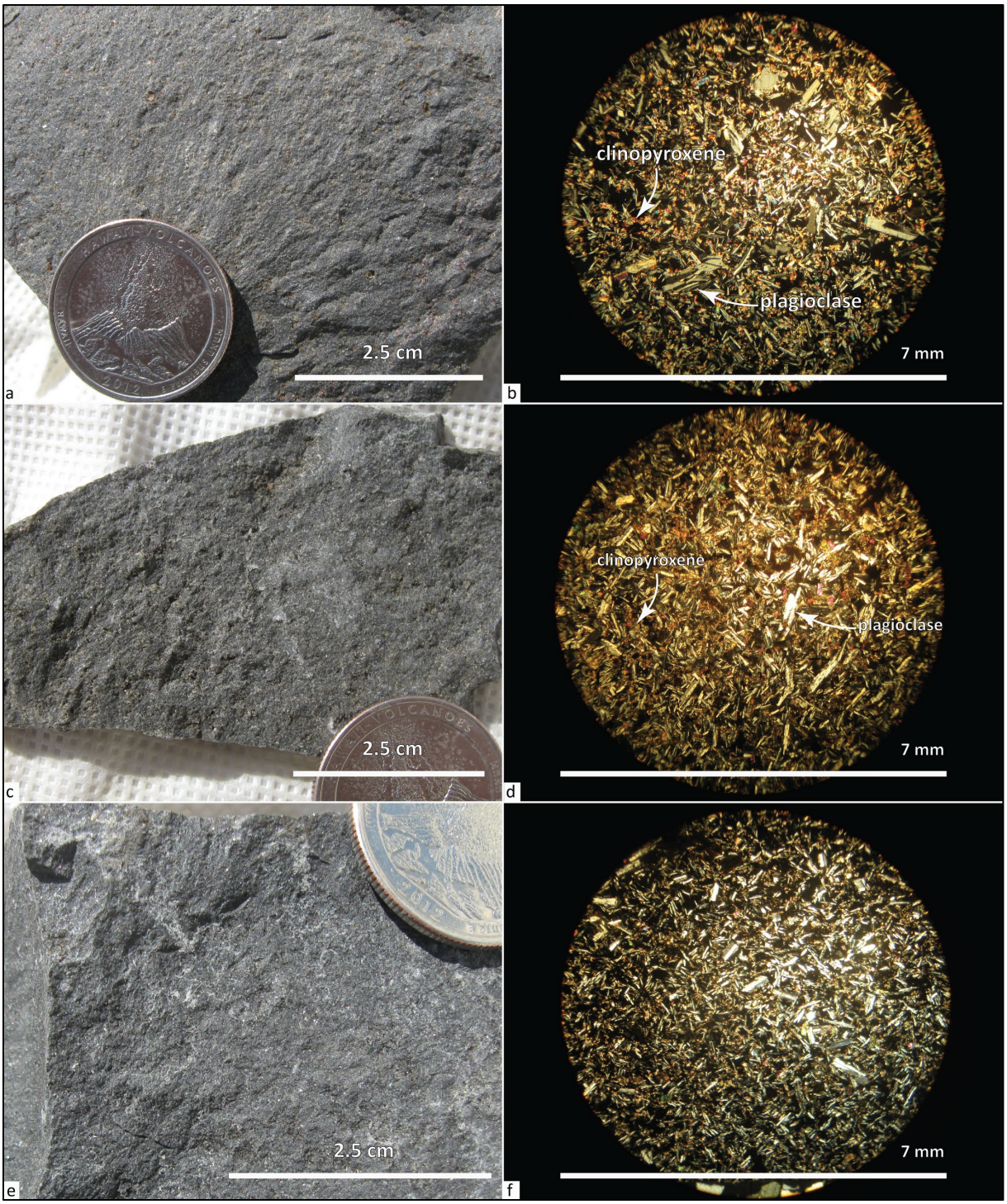

Tgww **Winter Water Member (lower Miocene)**—Basaltic andesite lava flows (SiO_2 = 54.44 to 57.56 weight percent; TiO_2 =2.01 to 2.25 weight percent; *n* = 41 analyses [24 outside Mill Creek area]) mapped below the Sentinel Bluffs Member (**Tgsb**) and above the Ortley Member (**Tgo**). **Tgww** is mapped in core of the Mill Creek Ridge anticline in the Fivemile Butte and Ketchum Reservoir 7.5′ quadrangles and crops out in fault blocks in the Hood River fault zone in the northwest part of the Ketchum Reservoir 7.5′ quadrangle (**Figure 5-7**, **Figure 6-76**; **Table 6-4**; Plates 2 and 3; **Appendix**). **Tgww** is chemically distinguished from the underlying Ortley Member (**Tgo**) by higher amounts of titanium (avg TiO_2 = 2.10 weight percent) and from the overlying Sentinel Bluffs Member (**Tgsb**) by lesser amounts of magnesium (avg MgO = 3.43 weight percent)(*n* = 41 analyses in the Middle Columbia Basin; **Table 6-4**; **Appendix**; Madin and McClaughry, 2019; McClaughry and others, 2012, 2020a, 2021). Outcrops of **Tgww** in the Mill Creek area are typically hackly jointed and are composed of irregular, narrow (5 to 15 cm [2 to 5.9 in] wide) columns that extend across horizontal, vesicle-rich bands (**Figure 6-76**). Talus slopes beneath outcrops are typically composed of angular, equidimensional fragments up to 10 cm (3.9 in) in diameter. Thickness of the **Tgww** in the Mill Creek area ranges between 46 to 61 m (150 to 200 ft) (Plates 2 and 3). Typical hand samples of the Winter Water Member (**Tgww**) are medium-dark gray (N4) to dark gray (N2), aphyric to very sparsely microporphyritic and glomeroporphyritic, containing 1 to 2 percent (vol.) clear, euhedral, prismatic plagioclase microphenocrysts and v-shaped or radial, spoked glomerocrysts ≤2 mm (0.08 in), all contained within an inequigranular hypocrystalline groundmass of plagioclase, intergranular clinopyroxene, intersertal glass, and Fe-Ti oxides (**Figure 6-77**). Conspicuous plagioclase phenocrysts and glomerocrysts are diagnostic field characteristics which distinguishes this unit from other lava flows in the N2 magnetostratigraphic unit (Reidel and others, 1989; Wells, personal commun., 2011). Glomerocrysts and phenocrysts can be less abundant in the basal colonnade relative to the entablature portion of the flow (Tolan, 1982; Reidel and Tolan, 2013a).

Tgww has normal magnetic polarity and is assigned an early Miocene age bracketed by isotopic ages from outside the Mill Creek area. The upper possible age for the Winter Water Member is constrained by $^{40}Ar/^{39}Ar$ ages of 16.13 and 16.15 Ma obtained for the overlying Sentinel Bluffs Member; the lower age of the unit is constrained by a U/Pb date of 16.260 ± 0.03 Ma obtained from ash between the Wapshilla Ridge and Meyer Ridge members of the underlying R2 magnetostratigraphic unit (Kasbohm and Schoene, 2018; Baksi, 2022; Kasbohm and others, 2023; **Figure 5-7**, **Figure 6-1**; Plates 2 and 3; **Appendix**). **Tgww** is equivalent to the Winter Water flow of Powell (1978), the Winter Water unit of Reidel and others (1989), and the Winter Water Member of Reidel and Tolan (2013).

Figure 6-76. Outcrops of the Winter Water Member (Tgww) in the Fivemile Butte and Ketchum Reservoir 7.5′ quadrangles. (a) Hackly-jointed Tgww basalt cropping out on the north slope of Mill Creek Ridge (45.51713, -121.41868), with people for scale in the upper right part of the photograph. View is looking southeast. (b) Hackly-jointed Tgww basalt cropping out along Neal Creek (45.58281, -121.48861). Hammer for scale is 38 cm (15 in) long. Photo credits: Jason McClaughry, 2015 and 2016.

Figure 6-77. Hand sample and thin section photographs of the Winter Water Member (Tgww). (a) Typical aphyric hand sample. Scale bar is 2.5 cm (1 in). (b) Thin section under cross-polarized light. (c) Same view as in (b) under plane-polarized light. Scale bar in (b) and (c) is 7 mm (0.3 in). Photo credits: Jason McClaughry, 2018.

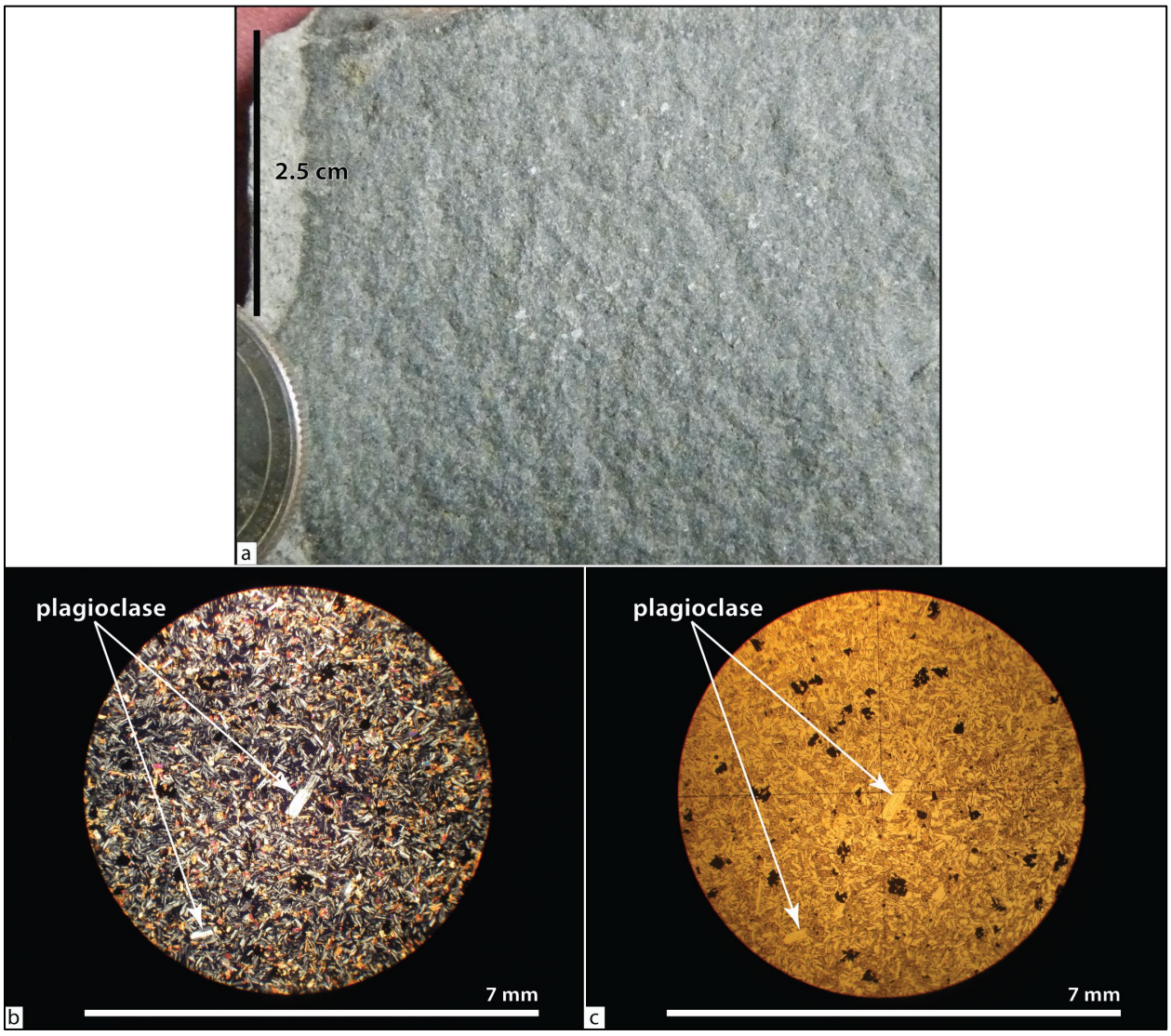

Tgo **Ortley member (lower Miocene)**—Basaltic andesite lava flows (SiO_2 = 54.65 to 57.6 weight percent; TiO_2 =1.90 to 2.15 weight percent; *n* = 30 analyses [19 outside Mill Creek area]) mapped below the Winter Water Member (**Tgww)** and above the Grouse Creek member (**Tggc**). **Tgo** is mapped to form the core of the Mill Creek Ridge anticline in the Fivemile Butte and Ketchum Reservoir 7.5′ quadrangles and crops out in fault blocks in the Hood River fault zone in the in the northwest part of the Ketchum Reservoir 7.5′ quadrangle (**Figure 5-7**, **Figure 6-78**; **Table 6-4**; Plates2 and 3; **Appendix**; McClaughry and others, 2012). **Tgo** is chemically and texturally similar to lava flows in the underlying reversed-polarity Grouse Creek member (**Tggc**), but is distinguished on the basis of normal magnetic polarity. **Tgo** lava flows are differentiated from the overlying Winter Water Member (**Tgww**) on the basis of overall absence of plagioclase phenocrysts and lesser amounts of titanium (avg TiO_2 = 1.98 weight percent)(*n* = 30 analyses in the Middle Columbia Basin; **Appendix**; McClaughry and others, 2012). **Tgo** outcrops are characterized by hackly-jointed entablatures alternating with more well-defined columnar-jointed intervals (**Figure 6-78**). The composite thickness of **Tgo** in the Mill Creek area is ~130 m (430 ft) (Plate 1). Typical hand samples of the Ortley Member (**Tgo**) are medium-dark gray (N4) to medium-bluish gray (5B 5/1) and aphyric to very sparsely microporphyritic, containing 1 to 2 percent (vol.) clear, euhedral to subhedral, prismatic to blocky, plagioclase micophenocrysts ≤1 mm (0.04 in) contained within a fine-grained, equigranular, hypocrystalline groundmass of plagioclase, intergranular clinopyroxene, Fe-Ti oxides, and intersertal glass (**Figure 6-79**).

Tgo has normal magnetic polarity and is assigned an early Miocene age bracketed by isotopic ages from outside the Mill Creek area. The upper possible age for the Ortley member is constrained by $^{40}Ar/^{39}Ar$ ages of 16.13 and 16.15 Ma obtained for the overlying Sentinel Bluffs Member; the lower age of the unit is constrained by a U/Pb date of 16.260 ± 0.03 Ma obtained from ash between the Wapshilla Ridge and Meyer Ridge members of the underlying R2 magnetostratigraphic unit (Kasbohm and Schoene, 2018; Baksi, 2022; Kasbohm and others, 2023; **Figure 5-7**, **Figure 6-1**; Plates 2 and 3; **Appendix**). **Tgo** is equivalent to the low-MgO Yakima flows of Wright and others (1973), the Ortley unit of Reidel and others (1989), and the Ortley member of Reidel and Tolan (2013).

Figure 6-78. Outcrops of the Ortley Member (Tgo) in the Ketchum Reservoir 7.5' quadrangle. (a) Blocky-jointed Tgo cropping out along Beaver Creek (45.57006, -121.49572). Hammer for scale is 38 cm (15 in) long. View is looking west. (b) Blocky-jointed Tgo on Mill Creek Ridge (45.53496, -121.39795). Hammer for scale is 38 cm (15 in) long. View is looking southeast. Photo credits: Jason McClaughry, 2015.

Figure 6-79. Hand sample and thin section photographs of the Ortley Member (Tgo). (a) Typically aphyric hand sample. Scale bar is 2.5 cm (1 in). (b) Thin section under cross-polarized light. (c) Same view as in (b) under plane-polarized light. Scale bar in (b) and (c) is 7 mm (0.3 in). Photo credits: Jason McClaughry, 2018.

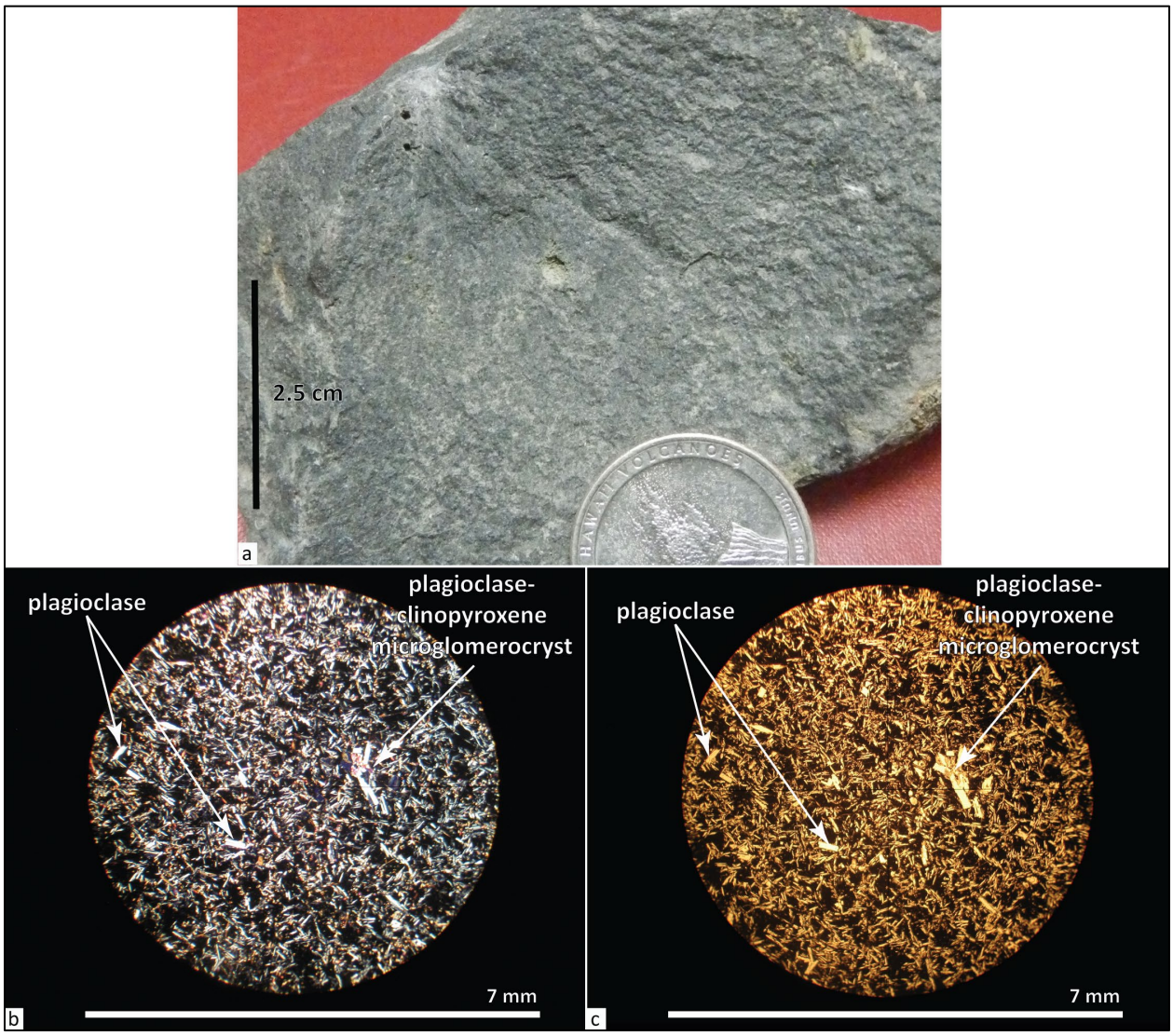

Reversed-polarity (R2) magnetostratigraphic unit

The R2 magnetostratigraphic unit is the most areally extensive Grande Ronde Basalt magnetostratigraphic unit, made up of chemically distinctive lava flow packages that cover an area of ~117,730 km^2 (45,456 mi^2). The estimated volume of the R2 magnetostratigraphic unit is ~56,000 km^3 (13,435 mi^3) (Reidel and Tolan, 2013). Kasbohm and others (2023) indicated that a majority of the R2 unit ranges in age between 16.260 ± 0.036 Ma and 16.327 ± 0.040 Ma (**Figure 5-7**). The R2 magnetostratigraphic unit in the map area includes the following map unit:

Tggc **Grouse Creek member (lower Miocene)**— Basaltic andesite lava flows (SiO_2 = 54.30 to 56.90 weight percent; TiO_2 =1.91 to 2.0 weight percent; *n* = 11 analyses [10 outside Mill Creek area]) mapped below the Ortley member (**Tgo**), forming the core of the Mill Creek Ridge anticline in the Ketchum Reservoir 7.5′ quadrangle (**Figure 5-7**, **Figure 6-80**; **Table 6-4**; Plate 2; **Appendix**;

McClaughry and others, 2012). **Tggc** is the oldest stratigraphic unit exposed in the Mill Creek area. **Tggc** is chemically and texturally similar to the overlying normal-polarity **Tgo** but is distinguished on the basis of reversed magnetic polarity (**Table 6-4**). Outcrops of **Tggc** are characterized by hackly-jointed entablatures alternating with more well-defined columnar-jointed intervals. Locally, lava flows have pillowed bases. The composite thickness of **Tggc** in the map area may exceed 60 m (200 ft); the base of the unit not exposed in the map area, so is therefore queried on geologic cross sections (Plates 1, 2, and 3, cross sections). Typical hand samples of **Tggc** are medium-dark gray (N4) to medium-bluish gray (5B 5/1) and aphyric to very sparsely microporphyritic, containing 2 percent (vol.) clear, euhedral to subhedral, prismatic to blocky, plagioclase micophenocrysts ≤2 mm (0.08 in); ~2 percent (vol.) greenish black (5G 2/1), euhedral, prismatic- to blocky clinopyroxene microphenocrysts ≤2 mm (0.08 in); and ~1 to 2 percent (vol.) glomerocrysts of plagioclase and clinopyroxene ≤2 mm (0.08 in); all contained within an equigranular, hypocrystalline groundmass of plagioclase, intergranular clinopyroxene, rhombohedral Fe-Ti oxides, and intersertal glass (**Figure 6-81**).

Tggc has transitional reversed magnetic polarity (Wells and others, 2009; **Appendix**). **Tggc** is assigned an early Miocene age bracketed by isotopic ages from outside the Mill Creek area. The age for the Grouse Creek member is constrained by U/Pb dates of 16.260 ± 0.036 Ma from red clay (bole) beneath the overlying Meyers Ridge Member and 16.327 ± 0.040 Ma obtained from red clay (bole) at the base of the older Wapshilla Ridge Member (Kasbohm and Schoene, 2018; Baksi, 2022; Kasbohm and others, 2023; **Figure 5-7**, **Figure 6-1**; Plate 2; **Appendix**). **Tggc** is equivalent to the Grouse Creek flows of Ross (1978), the Grouse Creek unit of Reidel and others (1989), and the Grouse Creek Member of Reidel and Tolan (2013).

Figure 6-80. Outcrop of the Grouse Creek Member (Tggc) in the Ketchum Reservoir 7.5' quadrangle. Tggc lava flows cropping out along North Fork Mill Creek include horizons of flow-top breccia (45.51922, -121.42173). Hammer for scale is 38 cm (15 in). View is looking west. Photo credits: Jason McClaughry, 2015.

Figure 6-81. Hand sample and thin section photographs of the Grouse Creek Member (Tggc). (a) Typical hand sample. Scale bar is 2.5 cm (1 in). (b) Thin section under cross-polarized light. (c) Same view as in (b) under plane-polarized light. Scale bar in (b) and (c) is 7 mm (0.3 in). Photo credits: Jason McClaughry, 2018.

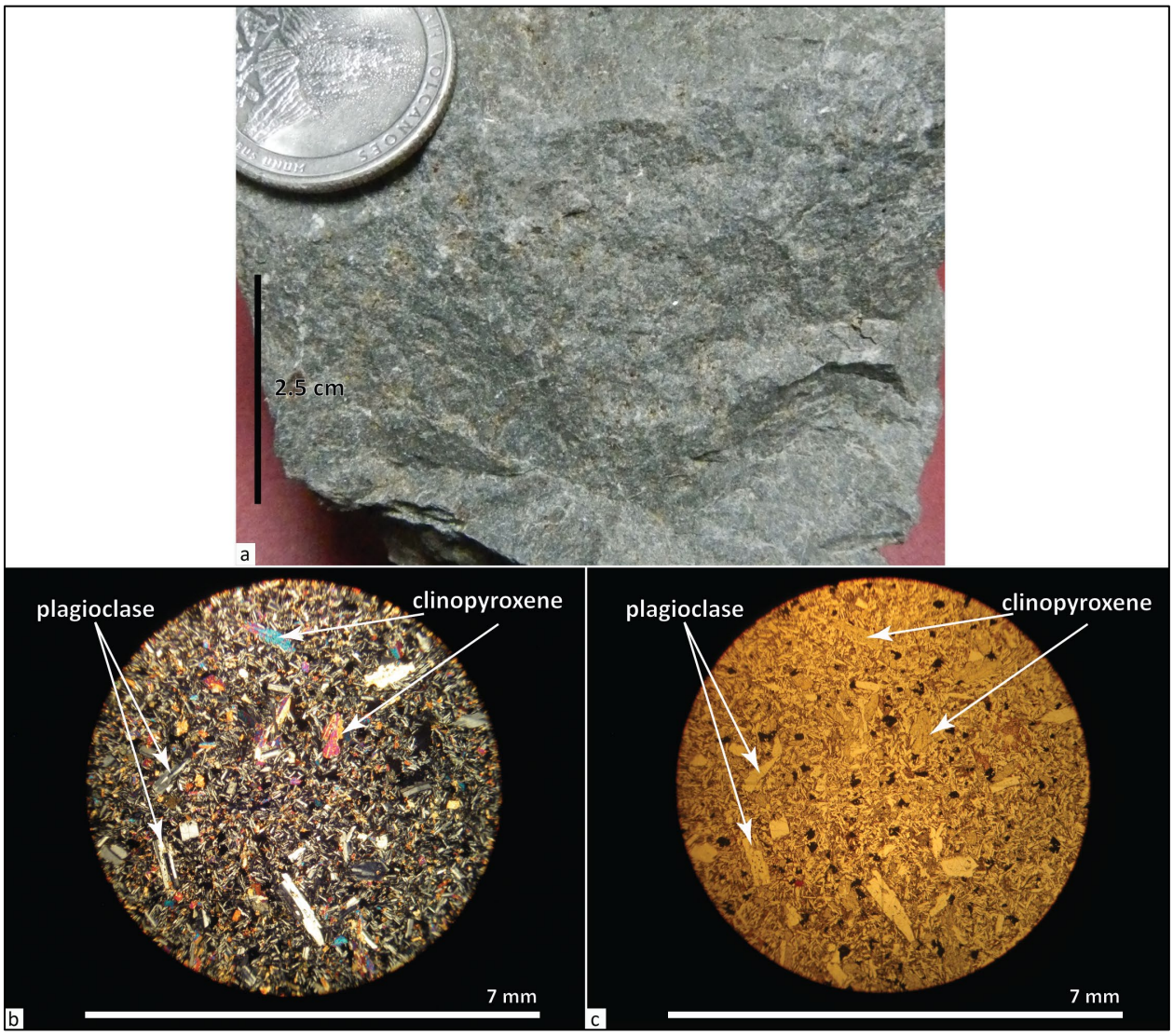

Undivided Grande Ronde Basalt

Tgu **Grande Ronde Basalt, undivided (lower Miocene) (cross sections only)**—Older lava flows of the Grande Ronde Basalt that lie stratigraphically below the Grouse Creek Member (**Tggc**) but do not crop out in the map area. The base of **Tgu** is therefore queried on geologic cross sections (**Figure 6-1**; Plates 1, 2, and 3, cross sections).

6.4 Other rocks

QTfb **Fault breccia (Upper Pleistocene[?] to lower Miocene)**—Brecciated rock mapped along and between fault strands in the North Fork Mill Creek fault zone, Hood River fault zone, and Chenoweth Creek fault zone (**Figure 6-82**, **Figure 6-83**; Plates 1 and 2). Other smaller areas of fault breccia locally crop out along many mapped fault strands in the area, but are of too small an extent to show separately. **QTfb** in the map area typically crops out in roadcuts and quarries or in high-standing erosionally resistant hoodoos (**Figure 6-82**, **Figure 6-83, Figure 6-84**). **QTfb** outcrops are flanked by loosely consolidated talus composed of mixed angular rock fragments (approximately ¾″ minus gravel fraction) and soils. Typical hand samples obtained from **QTfb** are intensely brecciated, being cross cut by a number of irregularly oriented fractures leading to a poorly defined, but pervasive fissility (**Figure 6-82b**, **Figure 6-83b**, **Figure 6-85**, **Figure 6-86**) The intersection of numerous foliation planes forms a pencil-like cleavage, where the rock easily breaks into irregularly faceted and smoothly curved interfering surfaces (**Figure 6-85**, **Figure 6-86**). Thin section analysis of **QTfb** shows rock pervasively cross cut by numerous anastomosing and intersecting microfractures, forming branch-like networks (**Figure 6-85c,d**, **Figure 6-86b,c**). Curvilinear to stair-stepped microfractures generally range from ≤0.1 to 0.5 mm (0.004 to 0.02 in) across. Microfractures either bound and crosscut ~2- to 3-mm-wide (0.08- to 0.1-in-wide) zones of intensely brecciated and disconnected rock fragments and crystals floating in a pulverized matrix of yellowish gray (5Y 7/2) to dark-yellowish orange (10YR 6/6) isotropic clay and zeolite or cross cut areas of apparently more coherent rock. At fracture intersections, rock fragments or larger microphenocrysts (~1 mm [0.04 in]) display incipient (crackle) to complete (jigsaw) brecciation, where once-fitted angular crystal or rock fragments are now separated by thin zones of finer matrix material. Fractures are filled by a fracture-parallel, foliated, dark yellowish brown (10YR 4/2) matrix of isotropic clay and zeolite. In places, this intrafracture foliation is well defined by blebs or feathered streaks of isotropic, moderate brown (5YR 3/4) to black (n1), finely milled clay or material resembling pseudotachylite. **QTfb** thin sections do not show evidence of secondary mineral replacement along veins by either silica or calcite cement; brecciated rock fragments or crystals have no visible evidence of secondary alteration and are altogether identical to fresh samples obtained from outcrops outside the fault zone (**Figure 6-85c,d**, **Figure 6-86b,c**).

QTfb is assigned an early Miocene to Late Pleistocene age on the basis of displacement of units with variable stratigraphic age (**Figure 6-1**; Plates 1 and 2, cross sections). The North Fork Mill Creek fault zone and Chenoweth fault zone displace units as young as the late Miocene and early Pliocene-aged Dalles Formation (**Tmdl**), while the Hood River fault zone displaces units as young as late Pliocene (**Tpbs**, **Tpbrc**)(Plates 1, 2, and 3). Offset along some fault strands is likely to have occurred into the Pleistocene.

Figure 6-82. Fault breccia (QTfb) cropping out along North Fork Mill Creek. (a) QTfb in outcrop (45.53379, -121.40251). The iPad for scale is 25 cm (10 in) tall. View is looking southeast. (b) Closer view of QTfb from the outcrop in (a). Pen for scale is 15 cm (6 in) long. Photo credits: Jason McClaughry, 2015.

Figure 6-83. Fault breccia (QTfb) cropping out along Neal Creek. (a) QTfb cropping out along Neal Creek, north of the Chenoweth fault. View is looking southeast (45.58262, -121.48632). (b) Closer view of QTfb from the outcrop in (a)(45.58221, -121.48457). Hammer head for scale is 5 cm (2 in) long. Photo credits: Jason McClaughry, 2016.

Figure 6-84. Fault breccia (QTfb) evidence in CRBG lava flows. (a) A nontabular basalt breccia of no apparent measurable orientation, exposed along Chenoweth Road in the northern third of the map area (45.613611, -121.318525). (b) Close-up of a boulder of angular basalt breccia fragments (6 cm [2 in]) with a submicroscopic, pulverized basalt matrix (45.613611, -121.318525). (c) Shear zone with numerous slip surfaces bounding vertical breccia zones (45.610944, -121.330833). (d) Close-up slip surface bounding rotated breccia fragments in a granulated basalt matrix (45.610944, -121.330833). Hammer for scale in all four photographs is 30 cm (12 in) long; the hammer head is 10 cm (4 in) wide. Photo credits: Clark Niewendorp, 2016.

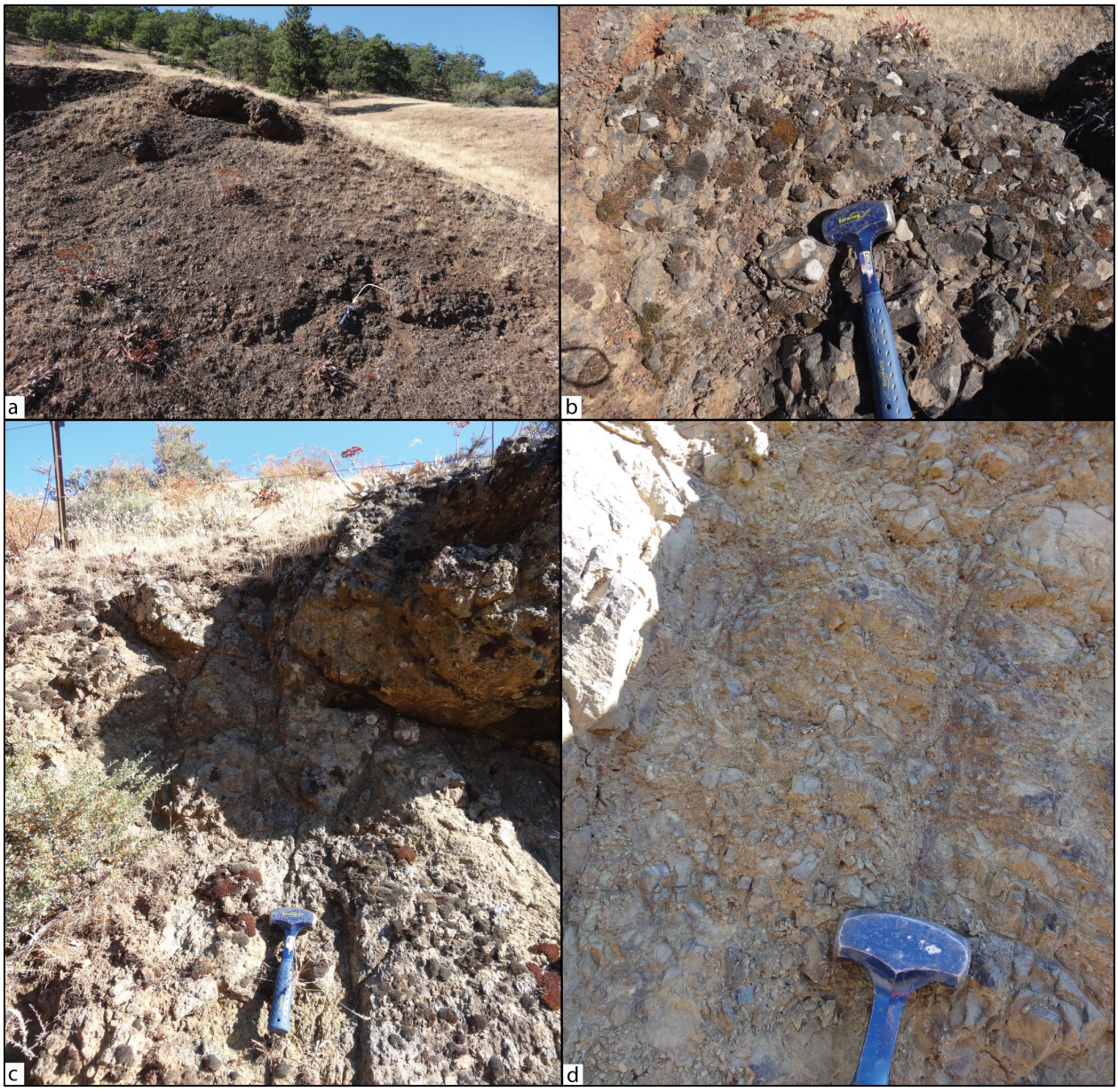

Figure 6-85. Hand sample and thin section photographs of North Fork Mill Creek fault zone breccia (QTfb). (a) Hand sample of QTfb. (b) Hand sample of QTfb. Scale bar in (a) and (b) is 2.5 cm (1 in). (c) Thin section under cross-polarized light. (d) Same view as in (c) under plane-polarized light. Scale bar in (c) and (d) is 7 mm (0.3 in). Photo credits: Jason McClaughry, 2017.

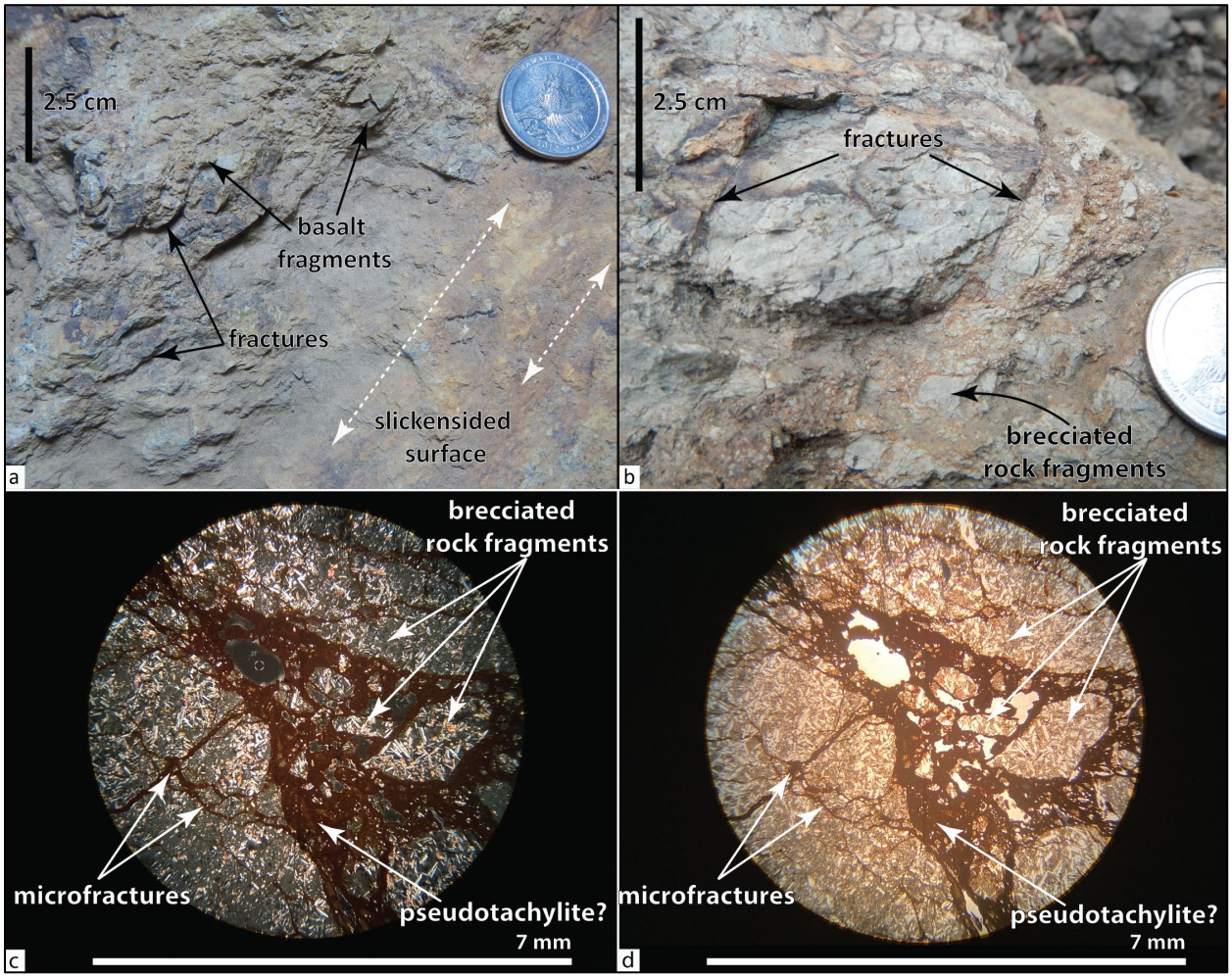

Figure 6-86. Hand sample and thin section photographs of Neal Creek Fault Breccia (QTfb). (a) Typical hand sample of QTfb. Scale bar is 2.5 cm (1 in). (b) Thin section under cross-polarized light. (c) Same view as in (b) under plane-polarized light. Scale bar in (b) and (c) is 7 mm (0.3 in). Photo credits: Jason McClaughry, 2017.

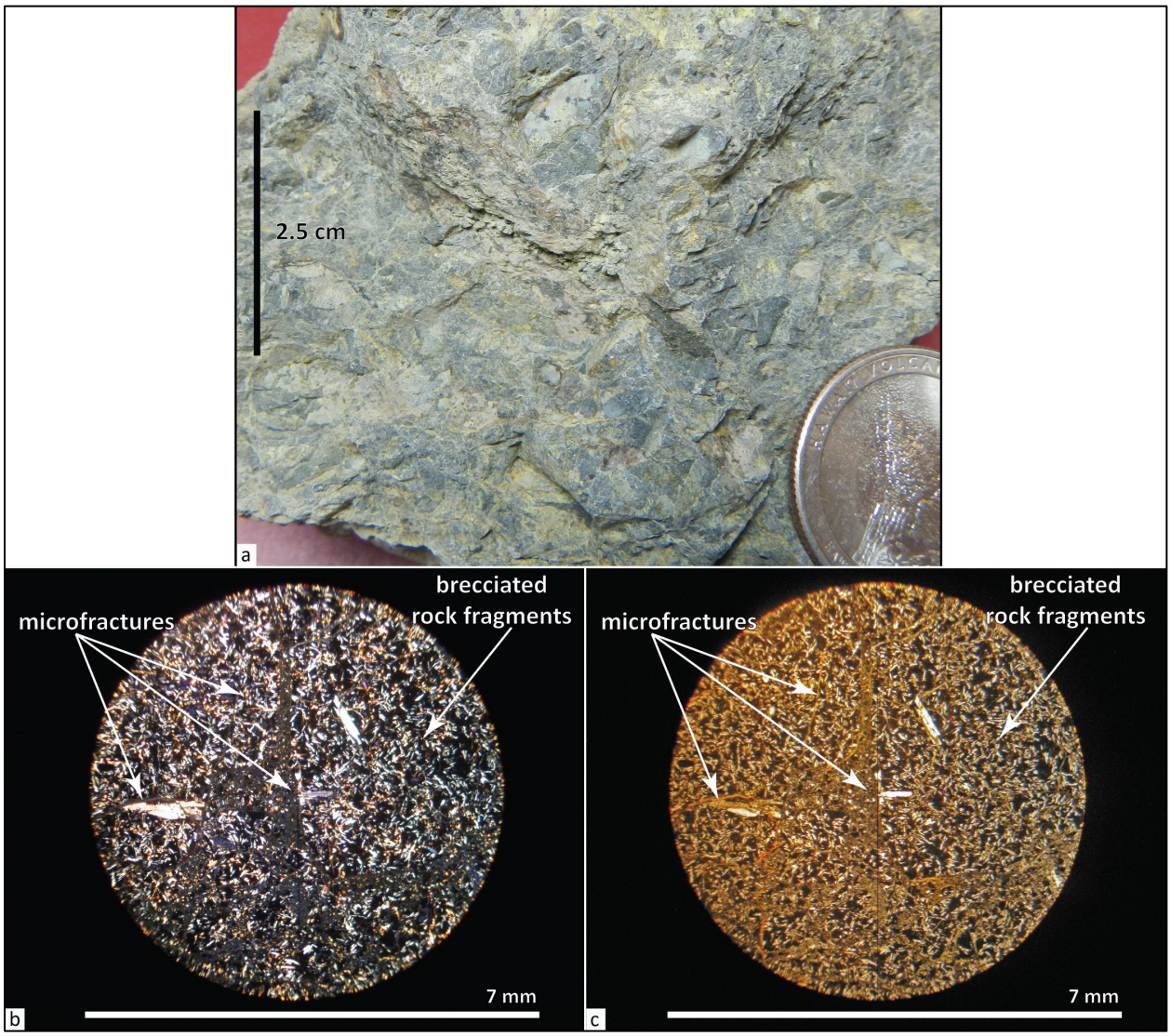

7.0 STRUCTURE

7.1 Introduction

Geologic structure in the Mill Creek area is defined by the mapped distribution of geologic units, offset geologic contacts, missing units, differences in the direction and amount of unit dip, broad zones of fault breccia, and topographic lineaments (as observed in 1-m lidar DEMs and 10-m DEMs), folds, and structural orientations (**Figure 5-3**; **Figure 5-4**; Plates 1, 2, and 3). The great thickness of relatively competent, brittle volcanic rocks of the CRBG and younger Cascade Range volcanic rocks results in a structural style that varies significantly in extensional and compressional regimes. Broad to narrow folds and locally steep dips are associated with propagating thrust and tear faults and define zones where shortening has been accommodated. In contrast, zones of extension are characterized by missing units and little changed or back-rotated bedding at varying elevations.

Several regional structural elements converge in the Mill Creek area, including the Yakima Fold Belt and the High Cascades Graben (**Figure 5-2**; see discussion in **Section 5.0** of this report). The salient structural features mapped in the Mill Creek area are 1) ENE- to WSW-trending fold axes, 2) ENE- to WSW-striking thrust faults segmenting anticlinal fold axes, 3) NW-striking strike-slip and oblique strike-slip faults, and 4) generally north-striking normal faults that are part of the Hood River fault zone. Complex interplay of these structures from the early-middle Miocene to recent times has resulted in the development of a variably folded and faulted stratigraphic succession in the Mill Creek area. Pliocene to Holocene faulting along the Hood River fault zone, in the northwestern part of the Ketchum Reservoir 7.5′ quadrangle, has led to subsidence of the Hood River Graben along the crest of the High Cascades (Plate 2).

7.2 Yakima Fold Belt

The CRBG, Dalles Formation, and to a much lesser extent, younger Late Pliocene sedimentary and volcanic rocks in the Mill Creek area are broadly folded into a series of ENE-trending folds. These structures are related to deformation occurring within the Yakima Fold Belt, a broad zone of regional east-west to NE-trending asymmetric folds covering much of the western and west-central Columbia Plateau and extending west beneath the Cascade Range (**Figure 5-2**; see discussion of the Yakima Fold Belt in **Section 5.1** ; Swanson and others, 1979b, 1981; Anderson, 1987; Watters, 1989; Reidel and Campbell, 1989; Tolan and Reidel, 1989; Tolan and others, 2009a; Anderson and others, 2013). Please refer to the detailed discussion of the Yakima Fold Belt in Section 5 of this report.

7.2.1 Folds

The CRBG and Dalles Formation in the Mill Creek area are deformed by parallel, characteristically open, broadly symmetrical folds, including the Mosier syncline, Ortley Segment of the Columbia Hills anticline, Mill Creek anticline, and Dalles syncline (Williams, 1916; Piper, 1932; Newcomb, 1966, 1967, 1969; Swanson and others 1979a, 1981; Bela, 1982; Korosec, 1987; Sherrod and Scott, 1995; McClaughry and others, 2012). The periodic spacing of folds observed in the Mill Creek area ranges between 7 and 10 km (4.4 and 6.3 mi), with up to 275 m (900 ft) of structural relief. Fold axes generally trend N20°E to N40°E across this part of the Middle Columbia Basin, curving to ~N70°E, north and east into Washington State (Newcomb, 1969; Korosec, 1987). Folds in the Mill Creek area are broadly symmetrical, but locally have dual, branching, faulted, or otherwise complex asymmetrical limbs. Secondary folds and undulations are superimposed on major folds throughout the map area (e.g., West Fork anticline, Badger Creek syncline;

Plates 1, 2, and 3). Synclines on top of the CRBG are filled by thick accumulations of volcaniclastic rocks of the Dalles Formation (**Tmdl;** Plates 1, 2, and 3, cross sections). Characteristic NE-directed river drainages in the map area flow parallel to major fold axes (**Figure 5-4**).

Mosier syncline — The Mosier syncline is a N20°E- to N50°E-trending, NE-plunging fold mapped parallel to Rock Creek, in the northwestern part of the Ketchum Reservoir 7.5′ quadrangle (Plate 2; Williams, 1916; Newcomb, 1966, 1967, 1969; Swanson and others 1979a, 1981; Bela, 1982; Korosec, 1987; McClaughry and others, 2012). The location of the fold lies between the gently dipping east limb of the Bingen anticline (~10 km; 6.2 mi) on the west (McClaughry and others, 2012) and the steeply dipping and faulted limb of the Ortley Segment of the Columbia Hills anticline (~8 km; 5 mi) on the east (**Figure 5-3**, **Figure 5-4**; Plates 1 and 2). The southwestern extent of the fold is mapped to the headwaters of Rock Creek, where it terminates against north- to NNW-striking normal faults in the Hood River fault zone (Plate 2). The Mosier syncline plunges NE to the city of Mosier where the fold forms a conspicuous trough followed by the Columbia River (Piper, 1932; Newcomb, 1967, 1969; McClaughry and others, 2012). Between the headwaters of Rock Creek and the city of Mosier, the structure is a characteristically tight fold, with beds dipping 10° and 20° toward the axis of the syncline. At Mosier, the southeastern limb to the Mosier syncline is faulted near its axis by a low-angle thrust fault, formed in front of the locally developed and tightly folded Rocky Prairie anticline (McClaughry and others, 2012). North of the Columbia River and eastward to Goldendale, WA, the mapped axial trace of the Mosier syncline curves to a N70°E-trend, becoming progressively broader and indistinct (Newcomb, 1967, 1969).

West Fork anticline — The West Fork anticline is a N-S-trending fold located east of the Mosier syncline in the northeastern part of the Ketchum Reservoir 7.5′ quadrangle (Plate 2; Newcomb, 1969; Swanson and others, 1981; Bela, 1982; Korosec, 1987). Erosion down through the fold reveals a section of Dalles Formation (**Tmdl**) underlin by CRBG lava flows including map units **Twpr**, **Twfs**, and **Twfh.** This north-plunging fold is asymmetric with CRBG lava flows on its western limb dipping 10–20°NW and those on its eastern limb dipping 4–9°NE. The southern part of the fold is cut by an E-W striking segment of the Chenoweth fault.

Ortley Segment of the Columbia Hills anticline — The Ortley Segment of the Columbia Hills anticline is a N50°E-trending fold located southeast of the Mosier syncline, in the northwestern part of the Brown Creek 7.5′ quadrangle (Plate 1; Williams, 1916; Piper, 1932; Newcomb, 1966, 1967, 1969; Swanson and others, 1981; Bela, 1982; Korosec, 1987). This anticline can be mapped east from the Maupin fault zone along a general N70°E trend until it exits the northern edge of the Brown Creek 7.5′ quadrangle. The fold is asymmetric and strata on its southern flank dip 10–15°S.; strata on the north flank dip 6–8°N. The steeper dipping southern limb of the fold is faulted in the Brown Creek 7.5′ quadrangle by the ~N70°E-striking, up-on-the-north, Chenoweth fault. Northeast of the map area, the Ortley Segment of the Columbia Hills anticline plunges NE to Rowena Gap along the Columbia River. At Rowena Gap, on the Washington side of the Columbia River, the fold is asymmetrical, with strata along its NE limb dipping nearly vertical near river level. Folding is accompanied by flexural slippage.

Mill Creek Ridge anticline — The Mill Creek Ridge anticline is a NE-trending fold mapped along Mill Creek Ridge in the southern part of the Ketchum Reservoir 7.5′ quadrangle and northern part of the Fivemile Butte 7.5′ quadrangle (Piper, 1932; Waters, 1968; Newcomb, 1966, 1967, 1969; Swanson and others, 1981; Bela, 1982; Korosec, 1987; Plate 2 cross sections C-C′ and D-D′; Plate 3 cross section A-A′). The

anticline is an upright and asymmetric box fold with a steeper dipping NW limb and a shallower dipping southeast limb. Bedding measurements taken on the CRBG and younger Dalles Formation reveal dips along the southern limb of the anticline ranging between 5° and 22°SE, whereas dips along the northern limb range between 7° and 70°NW. The fold axis across most of the structure trends ~N40°E. Vergence of the axial trace is to the southeast. As the deeply dissected fold enters the Brown Creek 7.5′ quadrangle (**Figure 1-2**) to the northeast, the axial trace becomes more northerly in trend (~N25°E) and lava flows of the CRBG plunge northeastward and disappear beneath the younger Dalles Formation. Continuation of the anticline further to the northeast is delineated in the Dalles Formation by a series of distinctive elliptical topographic features visible in 1-m lidar DEMs. These elliptical topographic features suggest the anticline continues NNE as a segmented string of doubly plunging anticlines, with segments ~0.5 km (0.3 mi) to 1.5 km (0.9 mi) long, extending up to the Maupin fault zone. On the east side of the Maupin fault zone, segmented anticlines continue, but trend in more northerly directions.

As the deeply dissected Mill Creek Ridge anticline trends into the Fivemile Butte 7.5′ quadrangles to the southwest, the fold is segmented and offset by the NNW-trending Mill Creek Ridge fault zone (discussed below). West of the Mill Creek Ridge fault zone, in the Ketchum Reservoir 7.5′ quadrangle, the axial trace of the Mill Creek Ridge anticline trends N50°E–N60°E and lava flows of the CRBG again disappear beneath the younger Dalles Formation, plunging ~4–6° to the southwest (plunge azimuth ~209–219°). At Gibson Prairie, along the northeastern edge of the Dog River 7.5′ quadrangle (**Figure 1-2**), the Mill Creek Ridge anticline is offset and terminated against the NNW-trending Gibson Prairie fault (McClaughry and others, 2020a)

Northeast, toward the city of The Dalles, the Mill Creek anticline projects generally in-line with the trace of the Columbia Hills anticline, a major structural uplift extending from the northwest corner of the Brown Creek 7.5′ to the northeast across the Columbia River (**Figure 1-2**). Although Newcomb (1969) indicates the two anticlinal uplifts to be "topographical equivalents", continuity between the two structures is uncertain due to several intervening major faults, including the Maupin and Chenoweth faults. Numerous smaller, more subtly expressed, unnamed, generally NE-SW-trending folds intervene between the major, named structures.

Differential relative uplift over the length of the axis of the Mill Creek Ridge anticline, along crosscutting, NW–SE-trending, right-lateral oblique-slip faults since the Middle Miocene, has controlled the distribution and depositional geometry of key units, or led to their omission from the typical stratigraphic section. Along Mill Creek Ridge, the Basalt of Ginkgo (**Twfg)** is notably missing from the CRBG stratigraphic section (Plate 2, cross sections C-C′ and D-D′; Plate 3, cross section A-A′). The Basalt of Ginkgo is a typically widespread and distinctive stratigraphic marker within the CRBG section across the Middle Columbia Basin. At Mill Creek Ridge, the younger Basalt of Sand Hollow (**Twfh**) lies directly on the older Sentinel Bluffs Member (**Tgsb; Figure 6-1**; Plates 2 and 3, cross sections). The area of stratigraphic omission of the Basalt of Ginkgo corresponds to the anticlinal axis of the Mill Creek Ridge anticline, implying deformation and localized relative uplift in the time between Grand Ronde and Frenchman Springs eruptions (ca. 16.1 to 15.9 Ma). This localized structural topography, generated concurrently with or closely following the end of Grande Ronde time, appears to have in part controlled the distribution of the Basalt of Ginkgo across this part of the Middle Columbia Basin.

Dalles syncline — The Columbia Hills and Mill Creek Ridge anticlines are paralleled by the Dalles syncline, a N50°E–N70°E-trending asymmetric fold mapped parallel to the North Fork Mill Creek and Main Fork Mill Creek in the middle part of the Brown Creek 7.5′ quadrangle (Plate 1; Piper, 1932; Newcomb, 1966, 1967, 1969; Swanson and others, 1981; Bela, 1982; Korosec, 1987). The Dalles syncline lies between the

Columbia Hills anticline (~8 km; 5 mi) on the north and Tygh Ridge anticline (~30 km; 20 mi) on the south. The western extent of the fold is mapped to the western edge of the Brown Creek 7.5′ quadrangle, but is not traced into the adjacent Ketchum Reservoir 7.5′ quadrangle. To the east, the Dalles syncline plunges NE to Dallesport, Washington (Piper, 1932; Newcomb, 1967, 1969). From Dallesport, the Dalles syncline swings east, continuing east to near Arlington, Oregon, where it merges with the Umatilla syncline (Newcomb, 1967, 1969). In the western part of the Brown Creek 7.5′ quadrangle, the strata on the northern limb of the syncline, where it is against the flank of the Mill Creek Ridge anticline, dip 10–40° SE The southern flank of the Dalles syncline is a regional north-dipping slope many tens of kilometers long (McClaughry and others, 2021). The amplitude of the Dalles syncline and the inclination along its northern flank diminish eastward and the fold becomes poorly defined.

7.2.2 Thrust and reverse faults

North Fork Mill Creek fault zone — At the deepest levels of exposure along the North Fork Mill Creek, in the Ketchum Reservoir 7.5′ quadrangle, the axis of the Mill Creek Ridge anticline is offset by a ~N50°E-striking, up-on-the-south, zone of blind to emergent thrust faults herein named the North Fork Mill Creek fault zone (**Figure 1-2**; **Figure 5-3**; Plate 2). The western part of the North Fork Mill Creek fault zone terminates or is offset by strands of the NW-striking Mill Creek fault zone, whereas the eastern part of the fault zone merges with an unnamed NW-striking fault, south of Thompson Point (Plate 2).

Along its mapped length, the North Fork Mill Creek fault zone offsets lava flows of the lower to middle Miocene CRBG and the upper Miocene to lower Pliocene Dalles Formation. The fault zone is often marked by meters-wide zones of fault-shattered basalt and imbricate fault strands that juxtapose separate blocks of CRBG lava flows (**Figure 6-85**). Three-point solutions for the main fault strand in the map area indicate a highly irregular fault trace striking ~N50°E and dipping 35°SE (Plate 2, cross sections C-C′ and D-D′). The mapped distribution of fault breccia, combined with cross section interpretation in the Ketchum Reservoir 7.5′ quadrangle (**Figure 1-2**), indicates a width (thickness) of the zone of ~91 m (300 ft). Vertical offset of CRBG units along the thrust fault is estimated to be about 140 m (460 ft), and up-on-the-south dip slip is estimated to be about 105 m (345 ft; Plate 2, cross sections C-C′ and D-D′). The North Fork Mill Creek fault zone displaces units as young as the upper Miocene and lower Pliocene Dalles Formation (**Tmd**; Plate 2, cross sections C-C′ and D-D′).

Chenoweth fault — The Chenoweth fault is a major zone of ~N70°E-striking, up-on-the-north, thrust fault first recognized and mapped by Piper (1932) and formally named by Newcomb (1969). The fault zone is mapped along the southern flank of the Ortley segment of the Columbia Hills anticline, across the northern parts of the Ketchum Reservoir (Plate 2), Brown Creek (Plate 1), and The Dalles North 7.5′ quadrangles, covering a distance of 36 km (~23 mi) between Neal Creek to the west (Plate 2) and the Columbia Hills (Washington) to the east (**Figure 5-3**; Newcomb 1969; Swanson and others, 1979a, 1981; Bela, 1982; Korosec, 1987; Burns and others, 2012). The western part of the Chenoweth fault terminates against strands of the Late Pliocene-Quaternary Hood River fault zone along the east side of Neal Creek (Plate 2), whereas the eastern part of the fault is mapped to the Columbia River by Burns and others (2012) (**Figure 7-1**). The Chenoweth fault may be part of the more regionally extensive Columbia Hills fault zone, a system of ~N70°E-striking, up-on-the-north thrust faults mapped for ~70 km (45 mi) east of the Laurel fault along the south flank of the Columbia Hills anticline (Reidel and others, 2013b; Woodring, 2020).

Figure 7-1. Complex intersection of fault zones along Neal Creek in the northwest part of the Ketchum Reservoir 7.5′ quadrangle. View is looking northwest. Photo credit: Jason McClaughry, 2015. See explanation of unit labels in the overview of map units section 6.1 . Labels are as follows: U – relative up across the fault; D relative down across the fault.

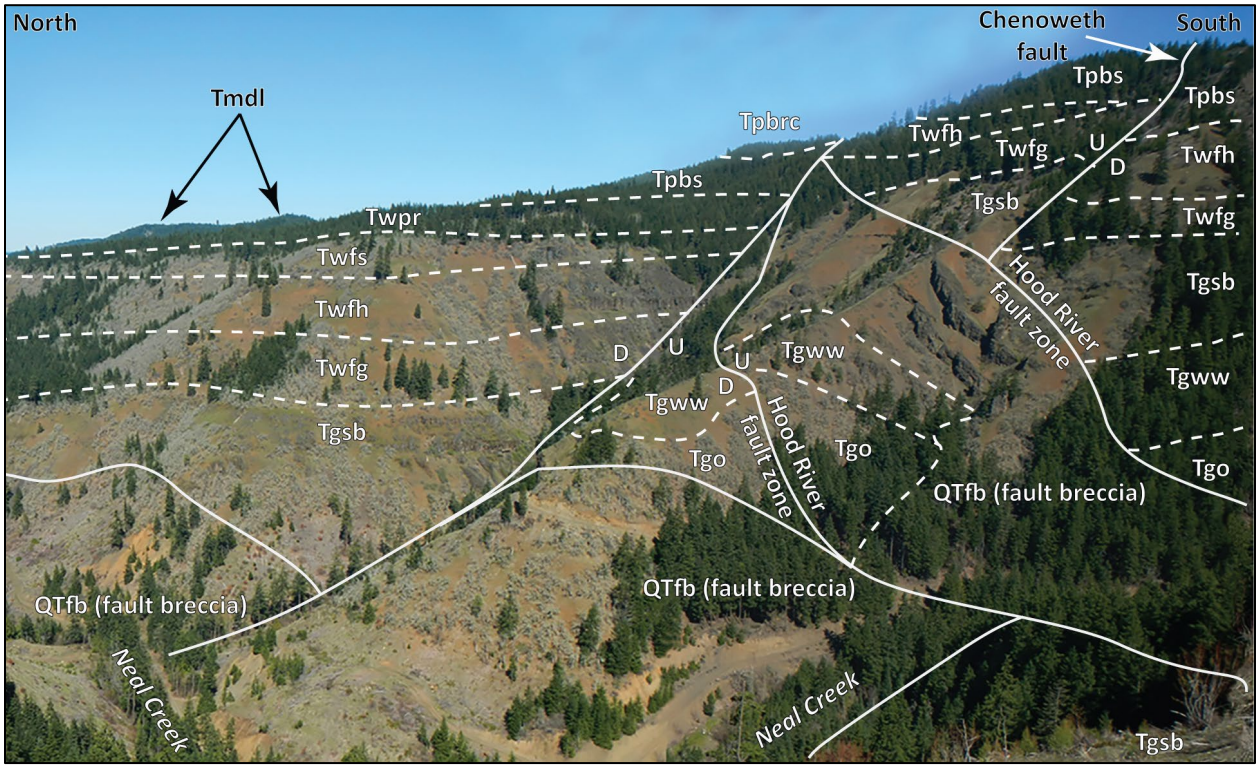

Along its mapped length in the Mill Creek area, the Chenoweth fault zone juxtaposes lava flows of the lower to middle Miocene CRBG on the north against the upper Miocene and lower Pliocene Dalles Formation on the south. The fault zone is often marked by meters-wide zones of fault-shattered basalt and imbricate fault strands that juxtapose and separate blocks of CRBG lava flows. Three-point solutions for the main fault strand in the map area indicate a highly irregular fault trace striking ~N70°E to N85°E and generally dipping 35–70°NW. Field observations of the fault plane in the map area are rare. Where the fault plane is exposed in a quarry in the headwaters area of Snyder Canyon in the Ketchum Reservoir 7.5′ quadrangle, it offsets the Basalt of Rosalia (**Twpr**), striking N85°W and dipping N45°E (**Figure 7-2**). Newcomb (1969) noted one outcrop example, where the Chenoweth fault was exposed in a test pit in the northeast corner of the Brown Creek 7.5′ quadrangle. There, the fault was a 68°N-dipping plane, characterized by 0.3 m (1 ft) of clayey gouge separating CRBG in the hanging wall to the north from conglomerate of the Dalles Formation in the footwall to the south.

Cross section interpretation of mapped traces of the Chenoweth fault in the Ketchum Reservoir 7.5′ quadrangle indicates vertical up-on-the-north separation of the top of the Basalt of Rosalia (**Twpr**) of ~165 m (540 ft) where cross section C-C′ intersects the southern, main strand (up-on-the-north dip slip equals 360 m [1180 ft]). Vertical up-on-the-north offset is ~45 m (150 ft) where cross section C-C intersects the northern strand of the Chenoweth fault along section C-C′ (up-on-the-north dip-slip = 85 m [280 ft])(Plate 2). Vertical up-on-the-north separation of ~ 259 m (850 ft) is estimated along the Chenoweth fault where cross section D-D′ intersects the fault trace (up-on-the-north dip-slip = 495 m; 1625 ft; Plate 2). Vertical up-on-the-north separation of ~535 m (1755 ft) is estimated along the Chenoweth fault where cross

section B-B′ intersects the fault trace in the Brown Creek 7.5′ quadrangle (Plate 1). Piper (1932) estimated a vertical, up-on-the-north, displacement of at least 305 m (1,000 ft) at the divide between Chenoweth and Mosier creeks. The Chenoweth fault displaces units as young as the Pliocene Basalt of Snakehead Creek (**Tpbs**) (**Figure 7-1**; Plate 2).

Figure 7-2. Chenoweth fault exposed in a rock pit in the headwaters of Snyder Canyon in the Ketchum Reservoir 7.5′ quadrangle (45.59243, -121.45308). Pillow basalt forming Twpr is segmented and offset by a strand of the Chenoweth fault at this location. Broken pillow basalt in the hanging wall of the Chenoweth fault lies above fault breccia within the footwall. The Chenoweth fault here strikes N85°W and dips N45°E. Dashed white lines within the hanging wall of the fault are anastomosing shear planes within pillow basalt. The height of the highwall is approximately 7 to 10 m (23 to 33 ft). View is looking southeast. Photo credit: Jason McClaughry, 2015.

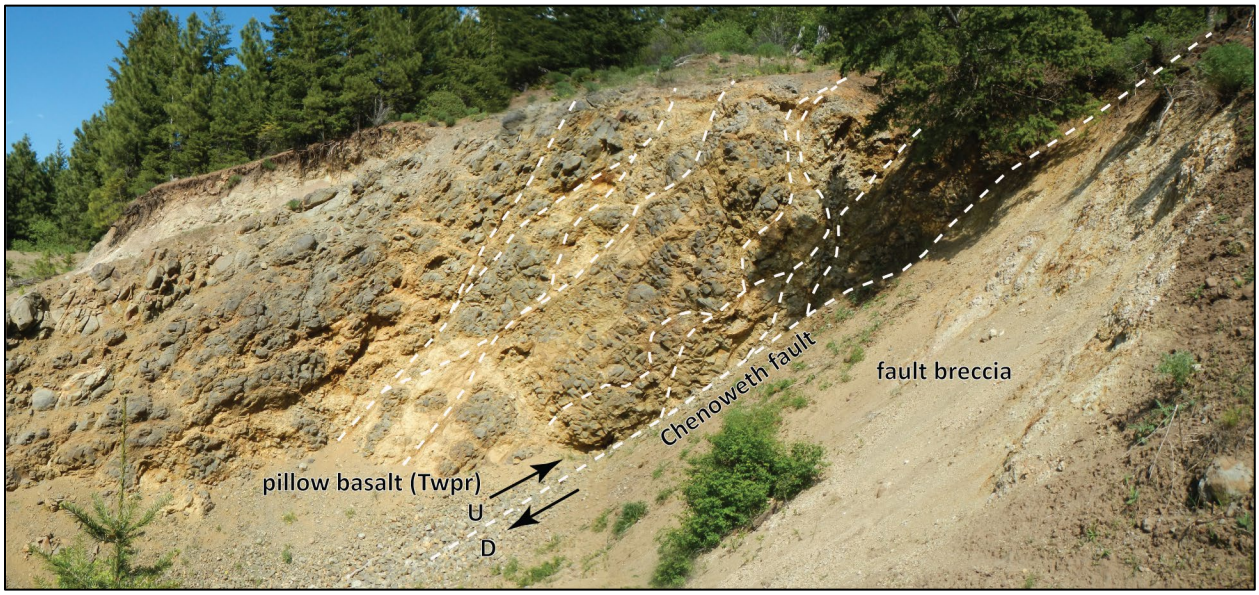

7.2.3 NNW-striking faults

ENE-trending folds in the area are locally crosscut by NNW-striking (N20°W to N30°W) strike-slip and oblique strike-slip faults (Plates 1, 2, and 3). Previous workers mapping the Columbia River Gorge (Anderson, 1987; Anderson and others, 2013) and the Columbia Plateau (Reidel and Campbell, 1989) have referred to these faults as wrench faults. The spatial relationships among folds, thrust faults, and strike-slip faults in the Mill Creek area indicate a mutual development of all three components during progressive deformational phases beginning in the middle Miocene and continuing into the Quaternary (Anderson, 1987; Anderson and others, 2013).

Maupin fault zone — The Maupin fault zone is a parallel set of N20°W to N30°W-striking, high-angle, right-lateral, oblique-slip faults mapped from NW to SE across the central part of the Brown Creek 7.5′ quadrangle (Plate 1; Swanson and others, 1981; Korosec, 1987). Collectively, these fault strands are part of the Maupin trend, a major NW-striking system of strike-slip faults discontinuously mapped over a length of ~100 km (62 mi) between the Columbia River, Tygh Ridge, and Maupin (**Figure 5-3**; **Figure 5-4**; Anderson, 1987; Anderson and others, 2013; Reidel and others, 2013b). We portray the Maupin fault zone in the map area as western and eastern, non-coplanar fault strands. The eastern strand of the Maupin fault

zone is mapped for ~4 km (2.5 mi) between Thousand Acre Pasture and the northwestern corner of the Brown Creek 7.5′ quadrangle (Plate 1). This eastern fault segment intersects and offsets the N70°E-striking Chenoweth fault north of Thousand Acre Pasture. The mapped fault traces indicate as much as 500 m (1,640 ft) of right-lateral strike-slip displacement of the Chenoweth fault has occurred along the eastern strand of the Maupin fault zone just north of Thousand Acre Pasture (Plate 1). Northwest of the Brown Creek 7.5′ quadrangle, the eastern fault strand links with right-lateral oblique-slip faults mapped for an additional 8 km (5 mi) on the west side of Eighteenmile Island on the Columbia River (McClaughry and others, 2012). The western strand of the Maupin fault zone is mapped for ~13 km (8 mi) in the Brown Creek 7.5′ quadrangle. Its northern tip terminates at the Chenoweth fault, northwest of Thousand Acre Pasture (Plate 1). Linear topographic features recognized in 1-m lidar DEMs, combined with field observations, trace the western fault strand south into the Wolf Run 7.5′ quadrangle (Plate 1; McClaughry and others, 2021). The western fault strand is linked with the eastern strand through several N30°E-striking, vertical to subvertical, left-lateral strike-slip faults including the Wasco Butte fault. The offset between the two fault segments is interpreted as an extensional en echelon stepover. The geometry of this stepover appears to be right-stepping. The linkage of these N30°E-striking faults is accommodated by the development of Riedel shear splay faults. The presence of topographic escarpments along both strands of the Maupin fault zone in the Brown Creek 7.5′ quadrangle suggest strike-slip faulting is coupled with oblique west-side-down displacement, consistent with the map interpretations of Swanson and others (1981) and Korosec (1987). Vertical, down-on-the-west displacement of the Sentinel Gap-Sand Hollow (**Twfs**-**Twfh**) contact along the eastern strand of the Maupin fault zone, north of Thousand Acre Pasture is on the order of 100 m (325 ft). Activity in the Maupin fault zone postdates the upper Miocene and lower Pliocene Dalles Formation. The age of the latest offset on the fault unknown.

Cherry Heights fault — The Cherry Heights fault is a N20°W to N30°W-striking, vertical to subvertical, right-lateral, strike-slip fault mapped east of and parallel to the Maupin fault in the Brown Creek 7.5′ quadrangle (Plate 1; Swanson and others, 1981; Korosec, 1987). Named the Cherry Heights fault by Burns and others (2012). The fault is mapped for a length of ~12 km (7.5 mi) between Dry Creek Road in the Lyle 7.5′ quadrangle (Burns and others, 2012), southeast nearly to Skyline Road (**Figure 1-2**; Plate 1). Between Chenoweth Creek and the northern part of the Brown Creek 7.5′ quadrangle (Plate 1), the Cherry Heights fault runs perpendicular to and intersects the N70°E-striking Chenoweth fault. This segment of the Cherry Heights fault forms the eastern boundary of a complex zone of imbricated thrust faults that characterize the Chenoweth fault system west to its intersection with the Wasco Butte fault (Plate 1). East of the Cherry Heights fault, CRBG lava flows are tightly folded into an asymmetric anticline with a steeply dipping (6–12°SE) forelimb in the hanging wall of the Chenoweth fault. South from Chenoweth Creek to Brown Creek, the Cherry Heights fault is concealed by a large landslide deposit (**Qls**) at the east end of Government Flat. There, the Cherry Heights fault runs approximately parallel to the east-facing, steep landslide head scarp, and is coincident with an ~1.2-km-long (0.75-mi), graben-like feature with an adjacent southwest facing block that reaches a height of 99 m (325 ft). The age of the latest offset on the fault unknown.

Wasco Butte fault — The NNW-striking Maupin and Cherry Heights faults are linked in the northern part of the Brown Creek 7.5′ quadrangle by the N30°E-striking, vertical to subvertical Wasco Butte fault, mapped over a length of 5.5 km (3.5 mi) between Thousand Acre Pasture in the southwest, to the northeast through Wasco Butte (Plate 1). The fault may be the southern extent of the Sevenmile fault as portrayed by Burns and others (2012). The Wasco Butte fault intersects the N70°E-striking Chenoweth

fault between Thousand Acre Pasture and Wasco Butte. Map patterns indicate Wasco Butte fault displaces the Chenoweth fault by as much as 760 m (2,500 ft) in a left-lateral, strike-slip sense. The segment of the Wasco Butte fault cutting through Wasco Butte, forms the western boundary of a complex zone of imbricated thrust faults that characterize the Chenoweth fault east to its intersection with the Cherry Heights fault (Plate 1). Activity on the Wasco Butte fault postdates the upper Miocene and lower Pliocene Dalles Formation. The age of the latest offset on the fault is unknown.

Rowena Creek fault — The Rowena Creek fault is a N20°W–N50°W-striking, vertical to subvertical fault mapped east of and roughly parallel to the Cherry Heights fault in the eastern part of the Brown Creek 7.5′ quadrangle (Plate 1; Korosec, 1987; Swanson and others, 1981). Swanson and others (1981) mapped the fault to extend from the Brown Creek area 6 mi (10 km) northwest through the Lyle 7.5′ quadrangle to the Columbia River. The fault was informally named the Rowena Creek fault by Lite and Grondin (1988) in the Lyle 7.5′ quadrangle, while southern strands of the Rowena Creek fault in the Brown Creek 7.5′ quadrangle were named as the Section 18 fault by Burns and others (2012). Herein referred to as the Rowena Creek fault following the precedent of Lite and Grondin (1988).

In the Brown Creek 7.5′ quadrangle, the northern part of the fault, mapped north of Chenoweth Creek, intersects the N70°E-striking Chenoweth fault. Map pattern in that area indicates the Brown Creek fault displaces both the Sentinel Gap-Sand Hollow (**Twfs-Twfh**) contact and the Chenoweth fault by ~30 m (100 ft) in a right-lateral, strike-slip sense. North into the Lyle 7.5′ quadrangle, Swanson and others (1981) indicated a component of horizontal right-lateral strike-slip movement and an apparent vertical offset of ~ 30 m (100 ft) across the fault. South of Chenoweth Creek, the Brown Creek fault is mapped as a narrow, NW-striking topographical lineament crossing NE-trending ridges underlain by Dalles Formation (**Tmdl**); the fault there also crosses and is concealed beneath extensive landslide deposits (**Qls**). Activity on the Brown Creek fault postdates the upper Miocene and lower Pliocene Dalles Formation. The age of the most recent offset on the fault unknown.

Mill Creek Ridge fault zone — The western mapped extent of the Mill Creek Ridge anticline, as it enters the northern part of the Fivemile Butte 7.5′ quadrangle, is segmented by a series of N20°W- to N30°W-striking, right-lateral, oblique-slip faults, together forming the Mill Creek Ridge fault zone (Plates 2 and 3). The Mill Creek Ridge fault zone cuts perpendicular across the Mill Creek Ridge anticline, representing a major discontinuity along the NE trend of the fold axis. Northeast of the Mill Creek Ridge fault zone, CRBG lava flows and the Dalles Formation are tightly folded in the Mill Creek Ridge anticline and displaced along the NE-striking, south-dipping North Fork Mill Creek Thrust fault zone (Plate 2, cross sections C-C′ and D-D′). Southwest of the Mill Creek Ridge fault zone, CRBG and Dalles strata dip generally to the south-southeast and are less deformed than counterparts mapped to the northeast. The North Fork Mill Creek Thrust fault zone is either offset by or terminates into the easternmost strand of the Mill Creek Ridge fault zone. It is nowhere mapped west of that location (Plate 2).

The Mill Creek Ridge fault zone is ~1.1 km (0.7 mi) wide as it crosses the Mill Creek Ridge anticline, and consists of at least four main fault strands, which separate and dismember intervening horst blocks of CRBG and Dalles Formation. The dominant sense of displacement in the Mill Creek Ridge fault zone is right-lateral strike-slip with a cumulative apparent horizontal offset of the Mill Creek Ridge anticline axis of at least 1.5 km (0.9 mi). Horizontal slip along faults is accompanied by normal, vertical offset of geologic units. Apparent relative vertical motion varies along strike, suggesting that individual strands act as oblique or scissor-type faults, accommodating an apparent rotation of intervening horst blocks. The westernmost fault strand in the Mill Creek Ridge fault zone has apparent strike-slip displacements of

geologic units ranging between 60 and 80 m (197 to 262 ft), with vertical offsets ranging between 15 and 31 m (50 to 100 ft). The easternmost fault strand in the Mill Creek Ridge fault zone shows the greatest strike-slip displacement of geologic units, with the Sentinel Bluffs-Winter Water (**Tgsb**-**Tgww**) contact displaced at least 1.5 km (0.9 mi) in a right-lateral sense. Apparent vertical offsets of geologic units of up to 45 m (150 ft) occur south of the North Fork Mill Creek. Overall, the oblique strike-slip offset of horst blocks and the geometry of fault strands suggests a series of negative flower structures occur within a right-lateral strike-slip duplex.

Northwest of Mill Creek Ridge in the Ketchum Reservoir 7.5′ quadrangle, individual NW-striking fault strands in the Mill Creek Ridge fault zone extend into and cut younger Quaternary lavas (**Qrbr** and **Qrbs**; **Figure 1-2**; Plate 2). Exposure southwest of Fir Mountain is poor, so the approximate location of fault strands is determined by parallel topographic lineaments and stream drainages observed in 1-m lidar DEMs, and association of these lineaments with Quaternary volcanic vents (Plate 2). Southeast of Mill Creek Ridge, the Mill Creek Ridge fault zone traverses large areas underlain by Dalles Formation, which largely lacks key stratigraphic markers (Plate 3). Two separate fault strands extending south-southeast across the Fivemile Butte 7.5′ quadrangle and into the headwaters areas of Fivemile Creek and Larch Creek (Wolf Run 7.5′ quadrangle) are interpreted in the map area based on subtle to more distinct topographic lineaments that cross ridges and offset the ledge-forming Dalles Formation and younger lavas. The southernmost strand of the Mill Creek Ridge fault zone, as it crosses into the Wolf Run 7.5′ quadrangle, forms a distinct NNW-trending lineament that offsets the 3.02 Ma dacite of Fifteenmile Creek (**Tpdf**) at least 75 m (246 ft) in a right-lateral strike-slip sense (**Figure 1-2**; Plate 3; McClaughry and others, 2021). Younger Quaternary basalt lava flows (**Qrbw**, **Qrbp**) may be offset by tens of meters in a right-lateral strike-slip sense along the fault as it crosses the area of Hesslan Canyon in the southeastern part of the Fivemile Butte 7.5′ (Plate 3).

Pine Flat fault — The Mill Creek Ridge fault zone is paralleled to the northeast by the N30°W-striking right-lateral, oblique-slip Pine Flat fault. The Pine Flat fault extends from Fir Mountain in the Ketchum Reservoir 7.5′ quadrangle in the northwest, to Mount Hood Flat in the Fivemile Butte 7.5′ quadrangle in the southeast (**Figure 1-2**; Plates 2 and 3). South of Mosier Creek and Pine Flat, the fault offsets Dalles Formation and CRBG strata as it cross-cuts the Mill Creek Ridge anticline (Plate 2). Apparent right-lateral strike-slip displacements of Dalles Formation and CRBG units range between ~200 and 250 m (650 to 820 ft) along the southern limb of the Mill Creek Ridge anticline. Vertical offset of units range between 43 and 76 m (140 to 250 ft). The southern extent of the Pine Flat fault is inferred to terminate into the eastern strand of the Mill Creek Ridge fault zone at Mount Hood Flat (Plate 3). North of the Mill Creek Ridge anticline, the Pine Flat fault zone offsets the lower Pleistocene basaltic andesite of Round Prairie (**Qrbr**) ~20 to 30 m (66 to 98 ft) in a right-lateral, strike-slip sense (Plate 2). The northern segment of this fault is inferred to continue northwest and to underlie the volcanic vent forming high ground at Fir Mountain, south of Beaver Spring (Plate 2).

Neal Creek fault zone — The Neal Creek fault zone is a N20°W- to N30°W-striking fault system mapped along Neal Creek in the northwest part of the Ketchum Reservoir 7.5′ quadrangle (Plate 2). Two parallel fault strands mapped along Neal Creek are separated by a 150- to 245-m-wide (490- to 800-ft) zone of pervasively brecciated CRBG (**Figure 6-86**; **Figure 7-1**). The Neal Creek fault zone is intersected and offset by a NE-striking southwest stepover fault of the Hood River fault zone, south of the mouth of Snakehead Creek (**Figure 7-1**). A single strand of the Neal Creek fault zone is mapped south of the Chenoweth fault, offsetting the CRBG with a right-lateral sense of displacement.

Puppy Creek fault — The Puppy Creek fault is a N20°W- to N30°W-striking normal or right-lateral, oblique-slip fault mapped for ~24 km (15 mi) from OR Highway 35 in the Dog River 7.5′ quadrangle (McClaughry and others, 2020a) in the northwest, southeast to Cold Point (Plate 3). The fault is best-defined between OR Highway 35 and Bottle Prairie in the Dog River 7.5′ quadrangle. Along lower Puppy Creek, three-point solutions on the fault indicate a ~N20°W-striking and ~60° to 70°SW-dipping fault plane (McClaughry and others, 2020a). Dalles Formation along lower Puppy Creek are vertically offset by more than 120 m (393 ft) (McClaughry and others, 2020a). West of Mill Creek Buttes, the fault offsets Quaternary basaltic lavas, including the ~2 Ma basalt of Cooks Meadow, in an apparent right-lateral, oblique-slip sense with down-on-the west vertical offset (McClaughry and others, 2020a). Vertical offset of the basalt of Cooks Meadow is ~30 m (100 ft), and right-lateral offset is ~100 m (328 ft). Southwest of Mill Creek Buttes, the fault forms a prominent lineament cutting across colluvium-mantled slopes (**Qc**) on the west side of the Dog River-Mill Creek divide before running beneath the cinder cone vent (**Qrbv**) for the 1.87 Ma basaltic andesite of Dog River (**Qr5dr**), which it does not appear to offset (McClaughry and others, 2020a). Southeast of this cinder cone, the fault bifurcates into two strands, forming a small graben. A continuation of the fault southeast into the Fivemile and Flag Point 7.5′ quadrangles is suggested by a N20°W- to N30°W-trending linear topographic feature evident in 10-m DEMs. Three-point solutions for southern strands of the fault in the Fivemile Butte and Flag Point 7.5′ quadrangles suggest a N20°W- to N30°W-striking, near vertical to slightly west-dipping fault plane. Relative offset of geologic units along this fault segment south into the Fivemile-Flag Point map area is not apparent, so the fault is therefore labeled as a generic fault in the map area (Plate 1). The Puppy Creek fault is inferred to extend an additional 9 km (5.6 mi) southeast from Cold Point to the east slope of Gordon Butte to Badger Creek, based on a significant N20°W-trending topographic lineament visible in USGS 10-m DEMs.

7.3 Hood River fault zone

The Hood River fault zone is a complex zone of generally north-south-striking, subparallel normal faults bounding the prominent west-facing eastern escarpment of the Hood River graben for ~50 km (31 mi) along the eastern flank of Mount Hood to the Columbia River (**Figure 5-3**, **Figure 5-4**; see discussion in **Section 5.3** of this report; McClaughry and others, 2012, 2013, 2020a, 2022). In the northwest part of the Ketchum Reservoir 7.5′ quadrangle, west-dipping to vertical, north-south- to ~N10°W-striking normal faults in the Hood River fault zone separate an east-dipping section of CRBG, Dalles Formation (**Tmdl**), and younger Pliocene basalt lava flows (**Tpbs**, **Tpbrc**, **Tpbh**) from their equivalents buried beneath the Hood River graben (Hood River Valley; Plate 2, cross sections A-A′ and B-B′). Characteristic north-south-striking faults in the Hood River fault zone are associated with sets of conjugate cross faults striking N30°E to N70°E At its southern extent in the Ketchum Reservoir 7.5′ quadrangle, the north-south-striking Hood River fault zone steps southwest to the west-facing eastern escarpment of the Hood River graben in the Upper Hood River Valley along a 7-km-long (4.5-mi), ~N50°E-striking normal fault zone mapped along and paralleling the northeast-flowing reach of Neal Creek (McClaughry and others, 2012). The fault zone, where exposed along Neal Creek, is characterized by an ~245-m-wide area (800 ft) of fault breccia hosted in brittle rocks of the CRBG (Plate 2). Both the NNW-striking Neal Creek fault zone and the east-northeast Chenoweth fault are offset by this NE-striking transfer fault south of the mouth of Snakehead Creek. To the southwest, the Hood River fault zone is associated with two notable features of the Hood River graben north and west of Neal Creek (west of the Ketchum Reservoir 7.5′ quadrangle). One feature is Middle Mountain, a structural block of CRBG, bounded by NNW-striking oblique-slip(?) faults. Middle Mountain

divides the graben into two rhombohedral-shaped segments known as the Hood River and Upper Hood River valleys. The other feature is the latest Pliocene and Quaternary Booth Hill and Lenz Butte volcanic fields lying across the floor of the Hood River graben (McClaughry and others, 2012).

Three-point solutions for north-south-striking fault strands in the Hood River fault zone in the map indicate vertical or west-facing fault planes dipping 45-75°W The cumulative displacement across multiple fault strands in the Hood River fault zone along cross sections A-A′ and C-C′, in the northwestern part of the Ketchum Reservoir 7.5′quadrangle, indicates that as much as 280 m (920 ft) of down-on-the-west normal vertical offset of the Dalles Formation-Basalt of Rosalia (**Tmdl**-**Twpr**) contact has occurred. Cumulative displacement across four fault strands in the Hood River fault zone along cross section B-B′ indicates ~105 m (345 ft) of down-on-the-west normal vertical offset of the basalt of Snakehead Creek-Dalles Formation (**Tpbs-Tmdl)** contact has occurred. Faults in the Hood River fault zone offset ca. 4.2 to 3 Ma Pliocene basalt lava flows east of Neal Creek. Therefore, local fault activity postdates those units. Field, map, and cross section evidence elsewhere along the eastern margin of the Hood River graben is consistent with this observation, with hundreds of meters of vertical offset Hood River fault zone margin developing after 3.7 Ma (McClaughry and others, 2012, 2020a, 2022). The age of latest offset in the Hood River fault zone is unknown in the Ketchum Reservoir 7.5′quadrangle, but faulting in the southern part of the Hood River fault zone along East Fork Hood River postdates 1.8 Ma (McClaughry and others 2020a).

8.0 GEOLOGIC RESOURCES

8.1 Aggregate materials and industrial minerals

Aggregate, in the form of crushed rock and gravel, is the major mineral resource now being mined in the map area. Accessible locations for aggregate resources in the area can be found in McClaughry and others (2020b; https://www.oregon.gov/dogami/milo/Pages/index.aspx). The Grande Ronde Basalt units of the CRBG (**Tgsb**, **Tgww**, **Tgo**, **Tggc**) are typically the most desirable geologic units for high-quality aggregate in this part of the Columbia Plateau. However, in the map area, quarries for aggregate are mainly developed within the Basalt of Lolo (**Twpl**), Basalt of Rosalia (**Twpr**), and Basalt of Ginkgo (**Twf**; McClaughry and others, 2020b; Plate 1). Late Miocene to Early Pliocene lava flows (**Tmdf**, **Tpdv**) are locally mined in small quarries on lands administered by the United States Forest Service for use as crushed rock and pit-run materials for forest road construction (e.g., Joes Point Quarry; McClaughry and others, 2020b; Plate 3). Sand and gravel, suitable for use as aggregate, is of limited supply in the map area, being restricted to small pits hosted in the Dalles Formation or unconsolidated alluvial deposits (**Qa**, **Qaf**). No industrial minerals are known to occur in the map area (McClaughry and others, 2020b).

8.2 Energy resources

Geothermal waters are not currently used in the map area and to the knowledge of the authors, no geothermal exploration has occurred. Localized deposits of siliceous sinter — the surface deposits remnant of past geothermal waters — do occur very locally along some fault strands (e.g., North Fork Mill Creek, Chenoweth, and Hood River fault zones). The map area also hosts several geologic characteristics (e.g., fault zone conduits, stratiform geologic units, Pleistocene volcanic centers) that may be favorable for the occurrence of localized geothermal reservoirs at depth (Plates 1, 2, and 3, cross sections). Additionally, the map area lies along the eastern structural margin of the Pleistocene–Holocene Hood River graben and

the axis of the High Cascades volcanic arc (Plates 2 and 3). The Hood River graben is an area characterized by Late Pleistocene volcanic heat source(s) and numerous fault zone conduits.

8.3 Water resources

A full discussion of the geologic controls on surface and groundwater resources in the map area is beyond the scope of this report. The reader is directed to previous water resource-specific reports published by Piper (1932), Sceva (1966), Newcomb (1969), Grady (1983), Lite and Grondin (1988), Lindsey and others (2009), Burns and others (2012), and Lite (2013) for a more thorough discussion of groundwater resources and hydrogeology in the Middle Columbia Basin. Groundwater resources are strongly influenced by permeability differences among stratigraphic units and geologic structures such as folds and faults. Several important hydrologic units have been identified in the area by the above-cited workers. The lowermost part of the groundwater flow systems in the map area lies within lava flows of the CRBG (Piper 1932; Newcomb, 1969). Overlying the CRBG are locally permeable epiclastic sedimentary and volcaniclastic rocks of the Dalles Formation, younger Pliocene and Pleistocene volcanics, and Quaternary surficial units.

8.3.1 CRBG aquifers

The extensive series of relatively stratiform units in the CRBG, many of which can be traced laterally from the Columbia Plateau west through the Columbia River Gorge, are a major host for groundwater in the Middle Columbia Basin (**Figure 5-6**). Most wells in the map area rely on groundwater from aquifers hosted within the CRBG (Piper, 1932; Newcomb, 1969; Grady, 1983). Wells producing from these units typically intercept aquifers residing at multiple levels within the CRBG flow succession (Newcomb, 1963). However, connecting aquifers in wells within the CRBG has elsewhere been shown to contribute to large water level declines in the aquifers (Lite and Grondin, 1988; Lindsey and others, 2009; Burns and others, 2012). Water-bearing horizons in the CRBG are generally associated with open framework interflow zones, including vesicular flow-top breccia, flow-foot breccia, pillow lavas, and hyaloclastite complexes occurring near the base of a unit (**Figure 8-1**; Newcomb, 1969; Lite and Grondin, 1988; Tolan and others, 2009a; Lindsey and others, 2009). These horizons serve as horizontal to subhorizontal pathways for groundwater flow. The interiors of thick flow complexes typically have extremely low permeability, and therefore act as confining units unless secondary permeability exists due to fractures created by faults or folds, flow-pinchouts, or erosional windows, or where vertical conductivity occurs through cross-connected wells (**Figure 8-1**). Sedimentary interbeds can act as either a confining unit or a porous media serving as a pathway for lateral transport of groundwater. Permeability contrasts created by heterogeneities in flow successions create a series of stacked confined aquifers in the CRBG aquifer system (**Figure 8-1**). Although some characteristics of CRBG flows are considered remarkably homogenous throughout their extent, hydrogeologic characteristics vary on local scales due to a difference in the environment of emplacement for each successive flow and the geologic setting of an area (Lite, 2013). Newcomb (1963) reported regional well yields from 300 gallons per minute (gpm) to 800 gpm from wells constructed in various formations of the CRBG in the nearby Mosier area (**Figure 1-1**). A recent well constructed in the Mosier area encountered a flow of 2,000 gpm coming from aquifers within the Sentinel Bluffs Member (Ken Lite, personal commun., 2022). Grady (1983) reported yields of a few hundred to a few thousand gpm to wells.

Faults and folds in the map area may act as flow boundaries within the CRBG aquifers (Plates 1, 2, and 3; e.g., Newcomb, 1969; Lite and Grondin, 1988; Burns and others, 2012; Lite, 2013). Faults in the map area, like many described within the Yakima Fold Belt, are roughly planar zones, composed of coarsely

shattered basalt that transitions outward into areas of fine rock flour. Variations in the type and severity of deformation and extent of alteration along fault traces affects their ability to convey groundwater flow. Variability in the alteration process along the fault trace may leave open breccia zones, which serve as high permeability groundwater pathways, or alternatively, may leave clay-altered or heavily cemented (calcite) gouge, which is likely to act as a low permeability zone. These low permeability fault zones inhibit lateral and vertical groundwater movement and create hydrologically isolated areas (Newcomb, 1969; Tolan and others, 2009a; Burns and others, 2012). Faults in the map area, such as the Chenoweth and North Fork Mill Creek thrust faults are characterized by areas of siliceous sinter and clay-altered rock (Plates 1 and 2).

The narrow anticlinal ridges and broad synclinal valleys that compose this part of the Yakima Fold Belt are also known to influence the occurrence and movement of groundwater through CRBG aquifers by affecting the hydraulic characteristics of interflow zones (Plates 1, 2, and 3; Newcomb, 1969; Lite and Grondin, 1988; Tolan and others, 2009a; Burns and others, 2012; Lite, 2013). Brittle folding in the Yakima Fold Belt has led to local flexural slippage parallel to layering in the basalt to accommodate structural shortening. Flexural slippage typically occurs along interflow zones, with results ranging from minor shearing to complete alteration, reducing or destroying the permeability of these features (**Figure 8-1**; Newcomb, 1969; Tolan and others, 2009a).

Figure 8-1. Schematic stratigraphic section of CRBG lava flows showing typical intraflow structures and vertical relationships of colonnade, entablature, and blocky columnar jointing, vesicular flow top, flow-top breccia, and pillow lava. K values represent the typical hydraulic conductivity ranges in meters per second (m/s) and feet per day (ft/day). Modified from Tolan and others (2009a).

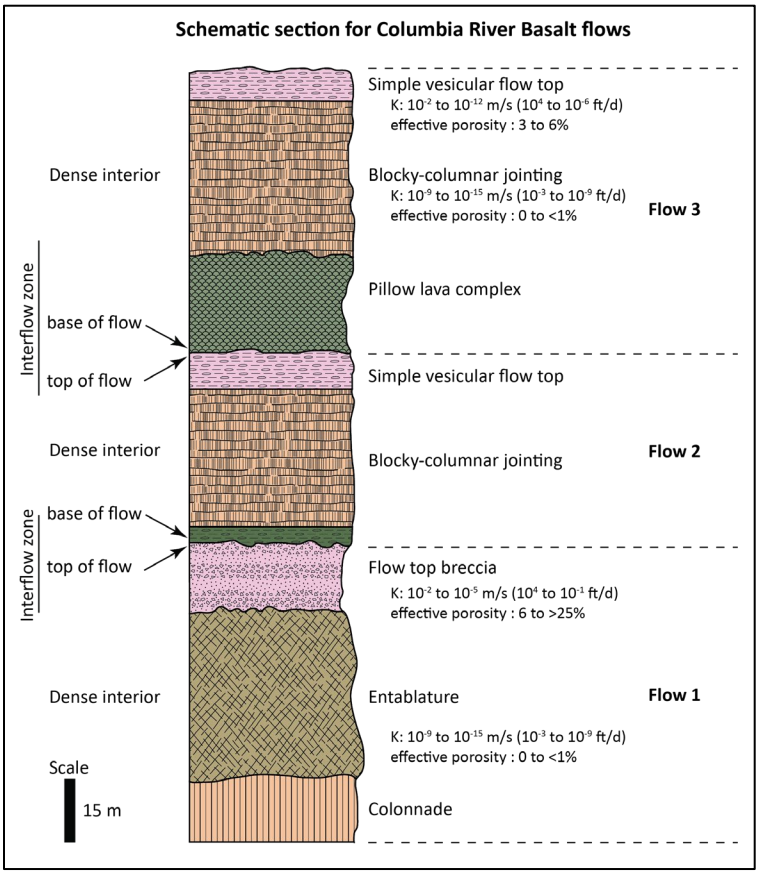

8.3.2 Dalles Formation aquifers

Permeability in the overlying Dalles Formation is generally very low due the presence of lenticular to laterally discontinuous beds of poorly sorted, clay-matrix breccia and conglomerate, fine-grained tuff, tuffaceous clay, and tuffaceous sandstone (**Figure 6-41**; Piper, 1932; Lite and Grondin, 1988). More permeable beds or lenses of well-sorted cobble conglomerate and sandstone are present locally, especially in the lower part of the unit near the axes of synclines. However, these permeable beds are laterally discontinuous and their permeabilities are starkly different from adjacent stratigraphic units, leading to several perched aquifers in the Dalles Formation (Piper, 1932). The catchment areas and recharge potential for permeable beds is also typically limited, as many Dalles beds lie far above the nearby drainages and below the crests of narrow ridges (**Figure 6-41e**; Plates 1, 2, and 3; Piper, 1932). Therefore, aquifers situated in more permeable layers within the formation may be suitable only for domestic use. Aquifers in the Dalles Formation may yield rates of 0.5 to 55 gpm, with larger production wells producing 150 to 250 gpm (Grady, 1983). Piper (1932) reported yields <20 gpm from the Dalles Formation in The Dalles and Dufur areas; where Dalles beds lie beneath perennial surface streams, wells in the formation may yield as much as 100 gpm.

8.3.3 Pliocene and Pleistocene volcanic aquifers

Pliocene and Pleistocene volcanics are not a significant source of groundwater in the map area. Physical properties of these units are similar to the older Dalles Formation. Wells drilled into tuff beds or unconsolidated volcaniclastic beds are likely to yield only small quantities of water.

8.3.4 Alluvial deposits along local streams

Unconsolidated to partly consolidated alluvial sand and gravel preserved in terraces and floodplains (**Qa**, **Qao**) and on fans (**Qaf**) contains groundwater that typically saturates sediments just above the underlying bedrock platform and is usually in hydraulic connection with nearby streams (Plates 1, 2, and 3; Piper, 1932). The deposits are typically thin (<15 m; 50 ft), but are very permeable, except where they contain large amounts of silt (Piper, 1932). Wells developed in permeable sand and gravel intervals may intermittently yield 10 to 100 gpm, depending on annual precipitation (Piper, 1932). Relatively impermeable silt-rich sedimentary intervals do not contain much recoverable groundwater (Piper, 1932).

8.4 Geologic hazards

8.4.1 Earthquakes and active faults

Numerous studies in the Pacific Northwest indicate that large, regional earthquakes have recently occurred and significant local events are possible (e.g., Atwater, 1987; McCaffrey and Goldfinger, 1995; Atwater and Hemphill-Haley, 1997; Clague, 1997; McCaffrey and others, 2007; Frankel and Peterson, 2008; Nelson and others, 2021). Few earthquakes have been recorded in the Mill Creek area (Goter, 1994; Niewendorp and Neuhaus, 2003; https://earthquake.usgs.gov/earthquakes/search/). Historic (1896 to 2002) earthquake epicenters in the area show events generally ranging in magnitude from M1.0 to 2.9 (Richter scale) with several larger events (M4.0–4.9) having occurred between Dufur and The Dalles in historic times (Beaulieu, 1977; Niewendorp and Neuhaus, 2003). Larger earthquake swarms are known to have occurred nearby, beneath the volcanic edifice at Mount Hood, 45 km (28 mi) to the WSW of the Mill Creek area, and near Maupin, 30 km (19 mi) to the SSE (Niewendorp and Neuhaus, 2003; Braunmiller and others, 2014; https://earthquake.usgs.gov/earthquakes/search/). The Mill Creek area may be at risk from four different types of earthquakes: 1) Cascadia subduction zone earthquakes, 2) crustal fault

earthquakes, 3) earthquakes related to volcanic activity, and 4) deeper intraplate earthquakes (**Figure 8-2**; Madin and Wang, 2000). A map of maximum earthquake shaking (peak ground acceleration) produced by Madin and Mabey (1996) predicted a probabilistic ground shaking estimate for the Mill Creek area of 8 percent g (i.e. shaking felt by all, heavy objects move, slight damage) for the peak ground acceleration with a 10 percent chance of exceedance in 50 years. The 2018 USGS National Seismic Hazard Model for the conterminous United States estimated that the peak ground acceleration for the area with a 2 percent chance of exceedance in 50 years is 0.14 to 0.30 g (Rukstales and Petersen, 2019; https://www.sciencebase.gov/catalog/item/5d5597d0e4b01d82ce8e3ff1). The probabilistic ground shaking is dominated by local crustal sources. Madin and others (2021) published seismic hazard data for Oregon and showed shaking probabilities based on the 2018 USGS National Seismic Hazard Model (Rukstales and Petersen, 2019), with local amplification of shaking added according to the updated National Earthquake Hazards Reduction Program site class map. The highest level of shaking expected with a 2 percent chance of occurring in the next 50 years from all earthquake sources is Modified Mercalli Intensity (MMI) VII (very strong) to MMI VI (strong), with corresponding moderate to light damage (Plate 1 in Madin and others, 2021b). The probability of the map area experiencing shaking of MMI VII in the next 50 years — the nominal threshold for structural damage to weak buildings — is generally low (6–10 percent) to very low (<5 percent) across the map area (Plate 3 in Madin and others, 2021b). There is a moderate (11–20 percent) chance of damaging shaking in valleys.

Figure 8-2. Schematic diagram showing the tectonic setting of the Pacific Northwest and idealized locations of the four earthquake types described in the text. Modified from Madin and Wang (2000). Asterisks show the generalized locations of the types of earthquakes described in the text.

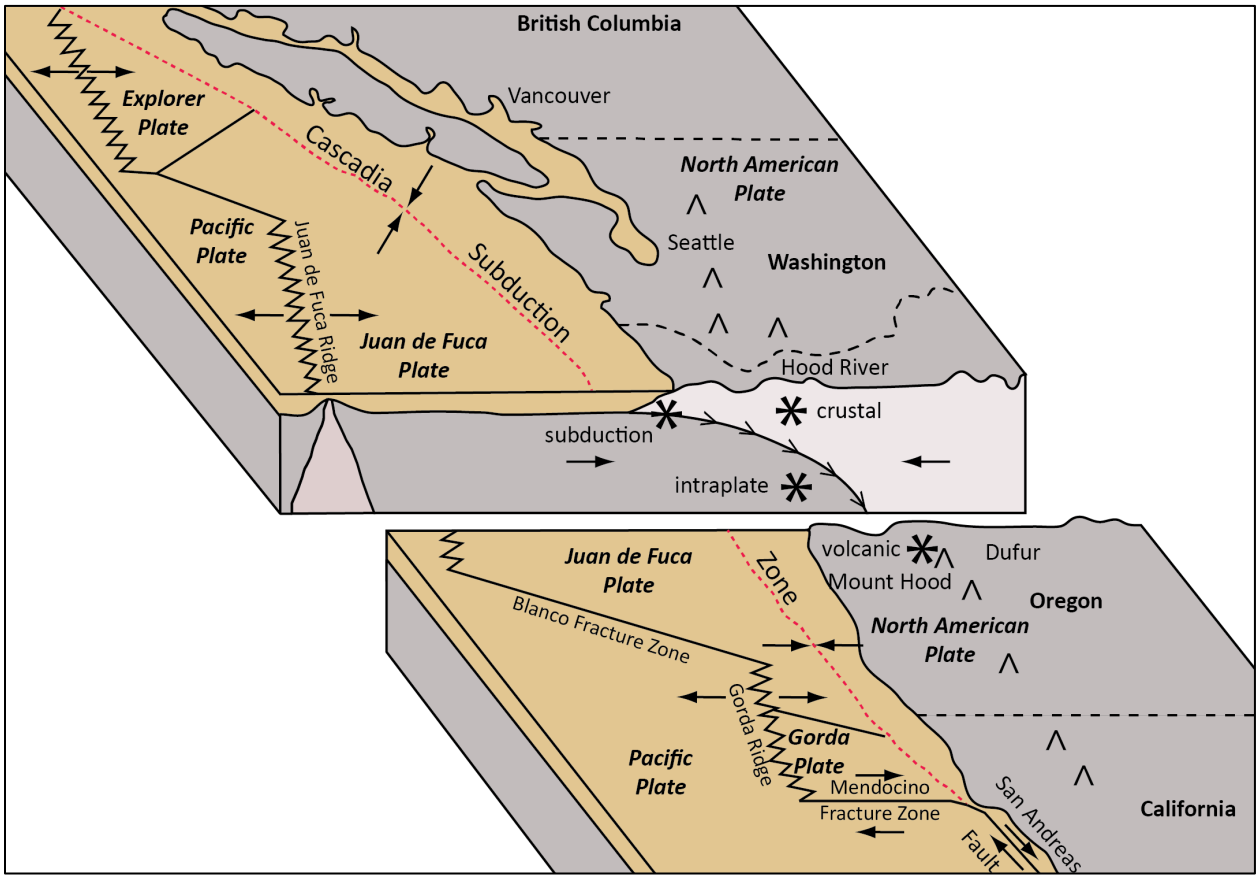

8.4.2 Subduction zone earthquakes

Subduction zone earthquakes occur where one crustal plate overrides an adjacent plate along a dipping interface, known as a subduction zone. The Mill Creek area sits ~280 km (174 mi) east of the Cascadia Subduction Zone, which marks the boundary between the North American Plate to the east and the underlying, smaller Juan de Fuca Plate to the west (**Figure 5-2**; **Figure 8-2**). Beneath the Earth's surface, this boundary extends eastward from the base of the continental slope, beneath western Oregon, and, as the lower plate continues to slide deeper into the Earth, it drives the processes that form the volcanoes in the Cascade Range. The Cascadia Subduction Zone is at high risk of large subduction zone earthquakes. Goldfinger and others (2003) and Nelson and others (2006) showed evidence of multiple great Cascadia subduction zone earthquakes, with the most recent occurring in 1700 A.D. (Satake and others, 1996). The Cascadia Subduction Zone is thought to produce earthquakes as large as M9.0 every 400 to 500 years (Frankel and Peterson, 2008). More recent work by Goldfinger and others (2012) indicated more frequent intervals of ~240 years along the southern margin (California-Gorda), with a 7–12 percent chance of a M9.0 Cascadia event in the next 50 years (**Figure 8-2**). Priest and others (2009) reported that at least 20 subduction earthquakes have occurred on the Cascadia Subduction Zone during the last ~10,000 years. These events, with magnitudes in the range of M8.0 to M9.0 likely caused long duration, moderately strong shaking throughout much of the region, with intensity decreasing eastward from the epicenter. Nelson and others (2021), working on the central and southern Cascadia subduction zone, indicated more frequent megathrust ruptures than previous coastal chronologies. These workers demonstrated 17 earthquakes in the past 6700 years, with a recurrence for all earthquakes of 370 to 420 years. Site effects from such an event, including earthquake induced liquefaction, landslides, and amplification of shaking by low-velocity surficial deposits could dramatically enhance damage in the area. Madin and Burns (2013) indicated that a M9.0 Cascadia event would result in light to very light damage in the Mill Creek area (see Plate 7 in Madin and Burns, 2013). Madin and others (2021) indicated MMI VI (strong) to V (moderate) perceived shaking, with corresponding light to very light damage potential for the map area based on a 2021 USGS M9 Cascadia ensemble shaking model (Wirth and others, 2021).

8.4.3 Crustal earthquakes

Crustal earthquakes result from shallow sources within the North American Plate (**Figure 8-2**). Epicenters are located at relatively shallow depths of 10–20 km (6–12 mi) below land surface. East of the Cascades, the majority of earthquake shaking hazard comes from crustal earthquakes (Madin and Mabey, 1996). In the western part of the Columbia River Flood Basalt Province, focal mechanisms of small magnitude (<M3) earthquakes are associated with some NW-striking wrench faults in the Yakima Fold Belt (**Figure 5-2**), providing direct evidence that some of these faults could remain active (Bela, 1982; USDOE, 1988; Yelin and Patton, 1991). The presence of other possibly Quaternary faults in north-central Oregon is also indicated by geologic mapping in the region (Geomatrix Consultants, Inc., 1995; Madin and Mabey, 1996; Weldon and others, 2003; Lidke and others, 2003; Personius and others, 2003; McClaughry and others, 2012; McClaughry and others, 2020a; Madin and others, 2021). No definitive evidence of Quaternary faulting has been found by the authors in the Mill Creek area. However, Holocene earthquake activity has been documented along the western margin of the Hood River graben along the Blue Ridge, Gate Creek, and Twin Lakes faults (Madin and others, 2017, 2021; A. Streig, Portland State University, oral communication, 2020; Bennett and others, 2021; **Figure 5-3**). These faults are all known to offset Late Pleistocene glacial till or post-glacial Holocene deposits. Madin and others (2017) reported radiocarbon ages (^{14}C) for a single earthquake event within the Blue Ridge fault zone between ~13,540 and 9,835 years before present.

8.4.4 Volcanic earthquakes

Volcanic earthquakes in the area are usually small in magnitude and occur over infrequent intervals; earthquakes of this type of ≥ M4.5 can occur around Mount Hood (**Figure 5-1**; **Figure 5-2**; **Figure 8-2**). During 2002 a swarm of earthquakes of M3.2–4.5 occurred on the southeast flank of Mount Hood (Burns and others, 2011). These types of earthquake swarms are known to occur periodically within the vicinity of the volcano; they do not necessarily indicate impending eruptions. The USGS Cascades Volcano Observatory (https://www.usgs.gov/observatories/cascades-volcano-observatory) continuously monitors earthquakes in the Cascades through a regional seismograph network and will provide warning, as possible, if activity suggests potential for volcanic eruptions.

8.4.5 Intraplate earthquakes

The Mill Creek area may also experience site effects from deeper intraplate earthquakes, which result from movement within the underlying Juan de Fuca Plate (**Figure 8-2**). These earthquakes could occur beneath much of the Pacific Northwest at depths of 40–60 km (25–37 mi). The large earthquakes that caused significant damage in the Puget Sound region in 1949 (Olympia), 1965 (Puget Sound), and 2001 (Nisqually) were deep intraplate earthquakes (Haugerud and others, 1999).

8.4.6 Site effects

Ground shaking, soil liquefaction, landslides, surface ruptures, and seiches are all possible causes of damage during an earthquake in the Mill Creek area. The damaging effects of earthquakes can be enhanced by proximity to epicenters, amplification of shaking in soft soils, liquefaction, or induced landslides. Detailed relative hazard maps that incorporate these hazards into single risk categories have not been compiled for the Mill Creek area, but Madin and Burns (2013) have produced regional seismic hazard maps generated on the basis of statewide geologic data. Liquefaction hazards occur where the shaking of a water-saturated soil causes its material properties to change from a solid to a liquid. Soils that liquefy tend to be loose, granular soils that are saturated with water. Unsaturated soils will not liquefy but may settle. Areas underlain by artificial fill (**Qf**), loess (**Qlo**), and alluvium (**Qa**, **Qao**), such as Fifteenmile Creek (Plates 1, 2, and 3) have a moderate liquefaction susceptibility (see liquefaction susceptibility map in Madin and Burns, 2013 and Figure 2-5 in Madin and others, 2021b). Where bedrock (volcanic rock or lithified sedimentary rock) is exposed at the surface, such as in uplands or in the bottoms of incised drainages, the liquefaction hazard is negligible (Madin and Burns, 2013).

8.5 Volcanic hazards

The Mill Creek area lies ~25 km (15 mi) east of the axis of the intermittently active volcanic zone along the Cascades volcanic arc, including Quaternary Mount Hood volcano (**Figure 5-1**; **Figure 5-2**). Unlike other geologic hazards discussed in this report (e.g., earthquakes), which may occur over several seconds to minutes, a volcanic episode can last days to decades and may include multiple syn- and inter-eruptive events. Volcanic hazards for the Mill Creek area, identified by the USGS and by DOGAMI are restricted to fallout of tephra and lava flows.

8.5.1 Tephra fall

Tephra (volcanic ash) generated by larger eruptions at Mount Hood or other nearby Cascade volcanoes may fall on areas up to several hundred kilometers downwind (**Figure 5-1**; **Figure 5-2**). Such events pose little risk to communities in the vicinity of Mount Hood (Scott and others, 1997). Based on Mount Hood's past tephra production, it is estimated that nearby communities such as Dufur and The Dalles would likely

receive a tephra thickness of up to 1.5 cm (0.6 in) in any one event (Scott and others, 1997). The 30-year probability of accumulation of 1 cm (0.4 in) or more tephra in the Mill Creek area from eruptions in the Cascade Range is 1 in 30. The 30-year probability of accumulation of 10 cm (4 in) or more tephra in the Mill Creek area from eruptions in the Cascade Range is 1 in 150 (Scott and others, 1997). However, no such thickness of a Quaternary tephra is known in the map area. Hazards associated with tephra falls include tens of minutes or more of darkness, paint damage, clogging of engine filters with fine particles, short circuiting of electric transformers and power lines, and disruption of air traffic (e.g., Mount St. Helens eruptions, May 1980). Larger events may include the possibility of roof collapse of structures.

8.5.2 Lava flows

Several basaltic and basaltic andesite shield volcanoes have erupted west of the Mill Creek area over the past three million years, sending lava flows down NE-directed stream channels. Remnants of the distal toes of several of these lava flows extend down the Threemile and Fivemile Creek drainages as far east as Mount Hood Flat (southwestern corner of The Dalles South 7.5′ quadrangle, northwest corner of the Wolf Run 7.5′ quadrangle; McClaughry and others, 2021) and Oak Flat (Brown Creek 7.5′ quadrangle; Plate 1; **Figure 1-2**). Corresponding vents for these lava flows are located along the eastern escarpment of the Hood River graben, along the western edge of the map area (**Figure 5-2**; McClaughry and others, 2020a). Far-traveled lava flows may extend down paleochannels more than 20–30 km (12.4–18.6 mi; e.g., basaltic andesite of Dog River; **Qr5dr**) from source volcanoes (Plate 1 and 3; McClaughry and others, 2020a). Future eruptions in the Mill Creek area are expected to occur within and marginal to the broad structural zone associated with the Hood River graben on the west (McClaughry and others, 2012, 2020a, 2022). Hazards associated with lava flow events include tephra falls proximal to vents, lava flows in more distal areas (probably ≥20 km; 12.4 mi) from the vent, and disruption of local stream drainages. Scott and others (1997) estimate the 30-year probability of such an eruption occurring in the area to be low, at 1 in 100,000.

8.6 Landslide hazards

The downslope movement of rock and soil, in the form of landslides, rockfalls, and debris flows may present a geologic hazard to residents, infrastructure, and transportation corridors in the Mill Creek area. Three general types of landslide processes are present in the map area, including (1) typical and colluvial landslides, (2) rockfall, and (3) debris flows.

8.6.1 Typical and colluvial landslides

A total of 212 landslide deposits (**Qls**) were mapped in the Mill Creek area. Those landslide deposits cover 0.05 percent of the map area (2347 total hectares; 5801 acres) The largest mapped landslide covers 539 hectares (1332 acres) and is located at the intersection of Chenoweth Creek and Brown Creek in the northeastern part of the Brown Creek 7.5′quadrangle. The smallest mapped landslide covers 0.04 hectares (0.01 acres) and is located at the intersection of Kellar Creek and Mosier Creek in the northeastern part of the Ketchum Reservoir 7.5′quadrangle. Most mapped landslide deposits are simple rotational or translational slides or shallow-seated earthflow-type features that occur along major drainages, originating on sparsely vegetated, moderately to steep slopes underlain by weakly consolidated rocks of the Dalles Formation or from lava flow contacts within the CRBG (Plates 1, 2, and 3; Beaulieu, 1977). Many of these simple slides can be attributed to the combined influences of parallel topographic slope and bedding dip, undercutting by streams, heavy precipitation, groundwater conditions, and rock type (Beaulieu, 1977). The generally weakly consolidated nature of the Dalles

Formation makes this unit especially prone to landslides on gently to steeply inclined slopes. Future landslides should be expected in this unit particularly in areas where infrastructure development (e.g., drain fields, septic tanks, modified runoff, and/or irrigation) may alter local groundwater conditions (Beaulieu, 1977).

A few slopes in the Mill Creek area are mantled by unstable colluvial wedges of soil and rock. These deposits, mapped as colluvium (**Qc**), typically form when weathered rock particles, ranging in size from clay to boulders, accumulate along a hillside contact (Plates 1, 2, and 3). When the mass of the accumulated material reaches a critical size, a triggering event such as heavy rainfall or earthquake may initiate the rapid down-slope movement of this mass. Areas denuded by fire or other vegetative removal can especially be at risk from such events.

8.6.2 Rockfall

Rockfall and rockslide hazards may be present in the Mill Creek area where very steep slopes are present. Potential natural triggering mechanisms for rockfall events may include freeze/thaw conditions, heavy rainfall, earthquakes, or extensive de-vegetation due to fire.

8.6.3 Debris flows

Many small-sized alluvial and debris fans (**Qaf**) in the Mill Creek area have been mapped along drainages (Plates 1, 2, and 3). Debris flows may be expected on both alluvial and debris fans (**Qaf**) lying at the mouth of steep-sided, colluvium-filled canyons and upland drainages. The potential for inundation of fan areas by debris flows is increased during episodes of intense rainfall that occur after soils have been saturated. Redirected drainage and poor construction practices are human activities that could initiate debris flows (Beaulieu, 1977). Debris flows have the potential to threaten life and may cause extensive damage to property and public lifelines.

9.0 ACKNOWLEDGMENTS

Geologic mapping in this part of the Middle Columbia Basin was supported through the STATEMAP component of the U.S. Geological Survey (USGS) National Cooperative Geologic Mapping Program under cooperative agreement numbers G15AC00180, G16AC00179, and G21AC00647. Additional funds were provided by the state of Oregon through DOGAMI and the OWRD. XRF geochemical analyses were prepared and analyzed by Dr. Scott Burroughs at the GeoAnalytical lab at Washington State University. The authors acknowledge many area landowners who provided local knowledge and graciously allowed access to private holdings. Larry McCollum, Water Quality Manager, granted access to lands administered by the City of The Dalles Municipal Watershed. We sincerely appreciate the gracious hospitality and support of Claire Sierra and Josiah Dean and the staff at the Historic Balch Hotel in Dufur. Cartography for the map plates was provided by Jon J. Franczyk; the geodatabase was constructed by Carlie Azzopardi. Gneiss Editing provided editing service for the manuscript and map plates. Critical and insightful reviews by Jim O'Connor (USGS), Charlie Cannon (USGS), Josh Hackett (OWRD), Ken Lite (formerly OWRD), Bob Houston (formerly DOGAMI), Lowell Anthony (DOGAMI), and Matt Williams (DOGAMI) greatly enriched the final manuscript, geodatabase, and geologic maps.

10.0 REFERENCES

Allen, J.E., 1966, The Cascade Range volcano-tectonic depression of Oregon, *in* Benson, G.T., ed., Transactions of the Lunar Geological Field Conference, Bend, Oregon, August 1965: Oregon Department of Geology and Mineral Industries Open-File Report O-66-01, p. 21-23. https://pubs.oregon.gov/dogami/ofr/O-66-01.pdf , accessed October 25, 2023.

Allison, I. S., 1935, Glacial erratics in the Willamette Valley: Geological Society of America Bulletin, v. 46, p. 615–632. https://pubs.geoscienceworld.org/gsa/gsabulletin/article-abstract/46/4/615/3444/Glacial-erratics-in-Willamette-Valley?redirectedFrom=fulltext, accessed October 25, 2023.

Anderson, J.L., 1987, The structure and ages of deformation of a portion of the southwest Columbia Plateau, Washington and Oregon: Los Angeles, University of Southern California, Ph.D. dissertation, 272 p.

Anderson, J.L., and Tolan, T.L., 1986, Ages of wrench faulting in interridge basins, southwest Columbia Plateau, Washington and Oregon: Geological Society of America Abstracts with Programs, v. 18, p. 82.

Anderson, J.L., and Vogt, B.F., 1987, Intracanyon flows of the Columbia River Basalt Group in the southwestern part of the Columbia Plateau and adjacent Cascade Range, Oregon and Washington, *in* Schuster, J.E., ed., Selected papers on the geology of Washington: Washington Division of Geology and Earth Resources Bulletin 77, p. 249-267. https://www.dnr.wa.gov/publications/ger_b77_papers_on_wa_geology_pt3of3.pdf, accessed October 25, 2023.

Anderson, J.L., Tolan, T.L., and Wells., R.E., 2013, Strike-slip faults in the western Columbia River flood basalt province, Oregon and Washington, *in* Reidel, S.P., Camp, V., Ross, M.E., Wolff, J.A., Martin, B.E., Tolan, T.L., and Wells, R.E., eds., The Columbia River Flood Basalt Province: Geological Society of America Special Paper 497, p. 325-347. https://pubs.geoscienceworld.org/books/book/661/chapter/3807302/Strike-slip-faults-in-the-western-Columbia-River, accessed October 25, 2023.

Atwater, B.F., 1987, Evidence for great Holocene earthquakes along the outer coast of Washington State: Science, v. 236, p. 942–944. http://activetectonics.asu.edu/lipi/Lecture24_Tsunami/Atwater_Science1987.pdf, accessed October 25, 2023.

Atwater, B.F., and Hemphill-Haley, E., 1997, Recurrence intervals for great earthquakes of the past 3,500 years at northeastern Willapa Bay, Washington: U.S. Geological Survey Professional Paper 1576, 108 p. https://pubs.er.usgs.gov/publication/pp1576, accessed October 25, 2023.

Baksi, A.K., 2013, Timing and duration of volcanism in the Columbia River Basalt Group: A review of existing radiometric data and new constraints on the age of the Steens through Wanapum Basalt extrusion, *in* Reidel, S.P., Camp, V., Ross, M.E., Wolff, J.A., Martin, B.E., Tolan, T.L., and Wells, R.E., eds., The Columbia River Flood Basalt Province: Geological Society of America Special Paper 497, p 67-86. https://pubs.geoscienceworld.org/books/book/661/chapter/3807126/Timing-and-duration-of-volcanism-in-the-Columbia, accessed October 25, 2023.

Baksi, A.K., 2022, New $^{40}Ar/^{39}Ar$ ages from the Grande Ronde and Wanapum Basalt, Columbia River Basalt Group (CRBG): Compilation of all ages and relationship to the geomagnetic polarity time scale for ˜17–15 Ma: Journal of Earth System Science, v. 131 158, p. 1-29. https://www.ias.ac.in/article/fulltext/jess/131/0158, accessed October 25, 2023.

Barry, T.L., Self, S., Kelley, S.P., Reidel, S., Hooper, P., and Widdowson, M., 2010, New $^{40}Ar/^{39}Ar$ dating of the Grande Ronde lavas, Columbia River Basalts, USA: implications for duration of flood basalt eruption episodes: Lithos, v. 118, p. 213–222. https://www.sciencedirect.com/science/article/abs/pii/S0024493710000897, accessed October 25, 2023.

Barry, T.L., Kelley, S.P., Reidel, S.P., Camp, V.E., Self, S., Jarboe, N.A., Duncan, R.A., and Renne, P.R., 2013, Eruption chronology of the Columbia River Basalt Group, *in* Reidel, S.P., Camp, V.E., Martin, M.E., Ross, M.E., Wolff, J.A., Martin, B.S., Tolan, T.L., and Wells, R.E., eds., The Columbia River Flood Basalt Province: Geological Society of America Special Paper 497, p. 45–66. https://pubs.geoscienceworld.org/books/book/661/chapter/3807104/Eruption-chronology-of-the-Columbia-River-Basalt, accessed October 25, 2023.

Beaulieu, J.D., 1977, Geologic hazards of parts of northern Hood River, Wasco, Sherman counties, Oregon: Oregon Department of Geology and Mineral Industries Bulletin 91, 95 p. 11 pl., scale 1:62,500. https://pubs.oregon.gov/dogami/B/B-091.pdf, accessed October 7, 2023.

Beeson, M.H., and Tolan, T.L., 1990, The Columbia River Basalt Group in the Cascade Range: A middle Miocene reference datum for structural analysis: Journal of Geophysical Research, v. 95, p. 19,547-19,559. https://agupubs.onlinelibrary.wiley.com/doi/abs/10.1029/JB095iB12p19547, accessed October 25, 2023.

Beeson, M.H., Fecht, K.R., Reidel, S.P., and Tolan, T.L., 1985, Regional correlations within the Frenchman Springs Member of the Columbia River Basalt Group: new insights into the middle Miocene tectonics of northwest Oregon: Oregon Geology, v. 47, no. 8, p. 87-96. https://pubs.oregon.gov/dogami/og/OGv47n08.pdf, accessed October 7, 2023.

Beeson, M.H., Tolan, T.L., and Anderson, J.L., 1989, The Columbia River Basalt Group in western Oregon: Geologic structures and other factors that controlled flow emplacement patterns, *in* Reidel, S. P., and Hooper, P. R., eds., Volcanism and tectonism in the Columbia River Flood-Basalt Province: Geological Society of America Special Paper 239, p. 223-246. https://pubs.geoscienceworld.org/books/book/375/chapter/3797037/The-Columbia-River-Basalt-Group-in-western-Oregon, accessed October 25, 2023.

Bela, J.L., 1982, Geologic and neotectonic evaluation of north-central Oregon: the Dalles 1° × 2° quadrangle: Oregon Department of Geology and Mineral Industries GMS 27, 2 pl., scale 1:250,000. https://pubs.oregon.gov/dogami/gms/GMS-027.pdf, accessed October 7, 2023.

Benito, G., and O'Connor, J. E., 2003, Number and size of last glacial Missoula floods in the Columbia River Valley between the Pasco Basin, Washington and Portland, Oregon: Geological Society of America Bulletin, v. 115, p. 624–638. https://pubs.geoscienceworld.org/gsa/gsabulletin/article-abstract/115/5/624/183988/Number-and-size-of-last-glacial-Missoula-floods-in, accessed October 25, 2023.

Bennett, S.E.K., Wells, R.E., Streig, A.R., Madin, I.P., and Stelten, M.E., 2019, Oblique slip history of active faults along the western margin of the Hood River graben, North-Central Oregon: Geological Society of America Abstracts with Programs., v. 51, no. 4. https://gsa.confex.com/gsa/2019CD/webprogram/Paper329235.html, accessed October 25, 2023.

Bennett, S.E.K., Streig, A.R., Levinson, R., Roberts, N., Dunning, A., Wells, R.E., Madin, I.P., O'Connor, J.E., Reynolds, N.D., Pringle, P., and Grant, A.R, 2021, The most recent earthquake on the Mount Hood fault zone, north-central Oregon: Implications for Cascading Earthquake, Landslide, And Flood Multi-Hazards In The Columbia River Gorge, Geological Society of America Abstracts with Programs. v. 53, no. 6. https://gsa.confex.com/gsa/2021AM/webprogram/Paper370262.html, accessed October 25, 2023.

Berger, G. W., and Busacca, A. J., 1995, Thermoluminescence dating of late Pleistocene loess and tephra from eastern Washington and southern Oregon and implications for the eruptive history of Mount St. Helens, Journal of Geophysical Research, v. 100(B11), p. 22361–22374. https://agupubs.onlinelibrary.wiley.com/doi/10.1029/95JB01686, accessed October 31, 2023.

Bond, J.G., 1963, Geology of the Clearwater embayment: Idaho Bureau of Mines and Geology Pamphlet 128, 83 p. https://www.idahogeology.org/pub/Pamphlets/P-128.pdf, accessed October 25, 2023.

Boyd, F.R., and Mertzman, S.A., 1987, Composition of structure of the Kaapvaal lithosphere, southern Africa, *in* Mysen, B.O., ed., Magmatic processes—physico-chemical principles: The Geochemical Society, Special Publication 1, p. 13–24. https://www.geochemsoc.org/files/8214/1258/3689/SP-1_013-024_Boyd.pdf, accessed October 25, 2023.

Braunmiller, J., Nabelek, J.L., and Trehu, A.M., 2014, A seasonally modulated earthquake swarm near Maupin, Oregon: Geophysical Journal International, v. 197, p. 1736-1743. https://ieeexplore.ieee.org/document/8144323, accessed October 25, 2023.

Bunker, R.C., Farooqui, S.M., and Thoms, R.E., 1982, K-Ar dates for volcanic rocks associated with Neogene sedimentary deposits in north-central and northeastern Oregon: Isochron/West, no. 33, p. 21-22, https://geoinfo.nmt.edu/publications/periodicals/isochronwest/33/iw_v33_p21.pdf, accessed October 25, 2023.

Burns, E.R., Morgan, D.S., Lee, K.K., Haynes, J.V., and Conlon, T.D., 2012, Evaluation of long-term water-level declines in basalt aquifers near Mosier, Oregon: U.S. Geological Survey Scientific Investigations Report 2012-5002, 134 p., GIS files. https://pubs.usgs.gov/sir/2012/5002/, accessed October 25, 2023.

Burns, W.J., Hughes, K.L.B., Olson, K.V., McClaughry, J.D., Mickelson, K.A., Coe, D.E., English, J.T., Roberts, J.T., Lyles Smith, R.R., and Madin, I.P., 2011, Multi-hazard and risk study for the Mount Hood region, Multnomah, Clackamas, and Hood River counties, Oregon: Oregon Department of Geology and Mineral Industries Open-File Report O-11-16, 179 p., 7 pl., scale 1:72,000, spreadsheets. https://pubs.oregon.gov/dogami/ofr/p-O-11-16.htm, accessed October 25, 2023.

Butler, R.F., 1992, Origins of natural remanent magnetism, *in* Paleomagnetism: Magnetic domains to geologic terranes: Boston, Blackwell Scientific Publications, p. 31-63.

Buwalda, J.P., and Moore, B.N., 1929, Age of Dalles Beds and "Satsop" Formation and history of Columbia River gorge (abs.): Geological Society of America Bulletin, v. 40, p. 176-177.

Buwalda, J.P., and Moore, B.N., 1930, The Dalles and Hood River Formations and the Columbia River Gorge: Washington, D.C., Carnegie Institution, Publications of the Carnegie Institution of Washington, no. 404, p. 11-26. https://babel.hathitrust.org/cgi/pt?id=mdp.39015024037213&seq=27, accessed October 25, 2023.

Cahoon, E.B., Streck, M.J., Koppers, A.A.P., and Miggins, D.P., 2020, Reshuffling the Columbia River Basalt chronology—Picture Gorge Basalt, the earliest- and longest-erupting formation: Geology, v. 48, p. 348-352. https://doi.org/10.1130/G47122.1, accessed October 25, 2023.

Cahoon, E.B., Streck, M.J., Koppers, A.A.P., 2023, Picture Gorge Basalt: Internal stratigraphy, eruptive patterns, and its importance for understanding Columbia River Basalt Group magmatism: Geosphere, v. 19, no. 2, p 406–430. https://pubs.geoscienceworld.org/gsa/geosphere/article/19/2/406/620369/Picture-Gorge-Basalt-Internal-stratigraphy, accessed October 25, 2023.

Camp, V.E., 1981, Geologic studies of the Columbia Plateau: Part II, Upper Miocene basalt distribution reflecting source locations, tectonism, and drainage history of the Clearwater embayment, Idaho: Geological Society of America Bulletin, v. 92, no. 9, p. 669-678. https://pubs.geoscienceworld.org/gsa/gsabulletin/article-abstract/92/9/669/202710/Geologic-studies-of-the-Columbia-Plateau-Part-II?redirectedFrom=fulltext, accessed October 25, 2023.

Cande, S.C., and Kent, D.V., 1992, A new geomagnetic polarity time scale for the Late Cretaceous and Cenozoic: Journal of Geophysical Research, v. 97, p. 13,917-13,951. https://onlinelibrary.wiley.com/doi/10.1029/92JB01202/abstract, accessed October 25, 2023.

Cannon, C.M., and O'Connor, J.E., 2019, New constraints on the timing of Neogene filling and incision of the Dalles Basin, Oregon and Washington: Geological Society of America Abstracts with Programs, v. 51, no. 4. https://gsa.confex.com/gsa/2017AM/webprogram/Paper303186.html, accessed October 25, 2023.

Chaney, R.W., 1944, The Dalles flora [Oregon], *in* Chaney, R.W., ed., Pliocene floras of California and Oregon: Washington, D.C., Carnegie Institution, Publications of the Carnegie Institution of Washington, no. 553, p. 285-320, 353-373. https://babel.hathitrust.org/cgi/pt?id=mdp.39015024038187&seq=9, accessed October 25, 2023.

Choiniere, S. R., and Swanson, D. A., 1979, Magnetostratigraphy and correlation of Miocene basalts of the northern Oregon coast and Columbia Plateau, southeast Washington: American Journal of Science, v. 279, no. 7, p. 755–777.

Clague, J. J., 1997, Evidence for large earthquakes at the Cascadia subduction zone: Reviews in Geophysics, v. 35, p. 439–460. https://agupubs.onlinelibrary.wiley.com/doi/epdf/10.1029/97RG00222, accessed October 25, 2023.

Cogliati, S., Sherlock, S. C., Halton, A. M., Ebinghaus, A., Kelley, S. P., Jolley, D. W., & Barry, T. L. 2021, Expanding the toolbox for dating basaltic lava sequences: $^{40}Ar^{39}Ar$ dating of silicic volcanic glass from interbeds. *Journal of the Geological Society*, v. 178, no 1, jgs2019-207, https://doi.org/10.1144/jgs2019-207, accessed October 24, 2023.

Cohen, K.M., Finney, S.C., Gibbard, P.L. and Fan, J.-X., 2013 (updated 2015), The ICS International Chronostratigraphic Chart: Episodes 36, p. 199-204. https://stratigraphy.org/ICSchart/Cohen2013_Episodes.pdf, accessed October 24, 2023.

Condon, T., 1874, Preliminary report of the State Geologist to the Legislative Assembly, 8th regular session: Salem, Oregon, 22 p. https://digital.osl.state.or.us/islandora/object/osl:7613, accessed October 25, 2023.

Conrey, R.M., Grunder, A., and Schmidt, M., 2004, State of the Cascade Arc: Stratocone persistence, mafic lava shields, and pyroclastic volcanism associated with intra-arc rift propagation: Oregon Department of Geology and Mineral Industries Open File Report O-04-04, 39 p. https://pubs.oregon.gov/dogami/ofr/O-04-04.pdf, accessed October 7, 2023.

Conrey, R.M., Sherrod, D.R., and McClaughry, J.D., 2019, Reconnaissance summary of High Cascades graben structures in central and northern Oregon: Geological Society of America Abstracts with Programs. v. 51, no. 4. https://gsa.confex.com/gsa/2019CD/webprogram/Paper329797.html, accessed October 25, 2023.

Conrey, R.M., Sherrod, D.R., Uto, K., and Uchiumi, S., 1996, Potassium-argon ages from Mount Hood area of Cascade Range, northern Oregon: Isochron/West, no. 63, p. 10-20. https://geoinfo.nmt.edu/publications/periodicals/isochronwest/63/iw_v63_p21.pdf, accessed October 25, 2023.

Conrey, R.M., Sherrod, D.R., Hooper, P.R., and Swanson, D.A., 1997, Diverse primitive magmas in the Cascade Arc, northern Oregon and southern Washington: The Canadian Mineralogist, v. 35, p. 367-396. https://pubs.geoscienceworld.org/canmin/article-abstract/35/2/367/12854/Diverse-primitive-magmas-in-the-Cascade-Arc?redirectedFrom=fulltext, accessed October 25, 2023.

Conrey, R.M., Taylor, EM., Donnelly-Nolan, J.M., and Sherrod, D.R., 2002, North-central Oregon Cascades: Exploring petrologic and tectonic intimacy in a propagating intra-arc rift, *in* Moore, G. W., ed., Field guide to geologic processes in Cascadia: Oregon Department of Geology and Mineral Industries Special Paper 36, p. 47-90. https://pubs.oregon.gov/dogami/sp/SP-36.pdf, accessed October 25, 2023.

Cope, ED., 1880, Corrections of the geological maps of Oregon: American Naturalist, v. 14, p. 457-458.

Cordero, D.I., 1997, Early to Middle Pleistocene catastrophic flood deposits, The Dalles, Oregon: Portland, Portland State University, M.S. thesis, 162 p. https://pdxscholar.library.pdx.edu/open_access_etds/6284/, accessed October 25, 2023.

Cox, K.G., Bell, J.D., and Pankhurst, R.J., 1979, The interpretation of igneous rocks: London, George Allen and Unwin, 450 p. https://link.springer.com/book/10.1007/978-94-017-3373-1, accessed October 25, 2023.

Dicken, S.N., 1965, Oregon geography: The people, the place, and the time, 4th ed: Ann Arbor, Mich., Edwards Brothers, 147 p.

Duda, C.J.M., McClaughry, J.D., Houston, R.A., and Niewendorp, C.A., 2018, Lidar and Structure from Motion-enhanced geologic mapping, examples from Oregon, *in* Thorleifson, L. H., ed., 2018, Geologic Mapping Forum 2018 Abstracts: Minnesota Geological Survey Open File Report OFR-18-1, 107 p. https://conservancy.umn.edu/handle/11299/194852, accessed October 25, 2023.

Duda, C.J.M., McClaughry, J.D., and Madin, I.P., 2019, Building the modern geologic map in Oregon: a multi-faceted field- and technology-based approach: Geological Society of America Abstracts with Programs. v. 51, no. 4. https://gsa.confex.com/gsa/2019CD/meetingapp.cgi/Paper/329552, accessed October 25, 2023.

Farooqui, S.M., Bunker, R.C., Thoms, R.E., and Clayton, D.C.; Bela, J.L., map comp., 1981a, Post-Columbia River Basalt Group stratigraphy and map compilation of the Columbia Plateau, Oregon: Oregon Department of Geology and Mineral Industries Open-File Report O-81-10, 79 p, 6 pl., scale 1:250,000. https://pubs.oregon.gov/dogami/ofr/O-81-10.pdf , accessed October 7, 2023.

Farooqui, S.M., Beaulieu, J.D., Bunker, R.C., Stensland, D.E., and Thoms, R.E., 1981b, Dalles Group: Neogene formations overlying the Columbia River Basalt Group in north-central Oregon: Oregon Geology, v. 43, no. 10, p. 131–140. https://pubs.oregon.gov/dogami/og/OGv43n10.pdf , accessed October 7, 2023.

Ferns, M.L., and McClaughry, J.D., 2013, Stratigraphy and volcanic evolution of the middle Miocene La Grande–Owyhee eruptive axis in eastern Oregon, *in* Reidel, S.P., Camp, V., Ross, M.E., Wolff, J.A., Martin, B.E., Tolan, T.L., and Wells, R.E., eds., The Columbia River Flood Basalt Province: Geological Society of America Special Paper 497, p. 401-427. https://pubs.geoscienceworld.org/books/book/661/chapter/3807352/Stratigraphy-and-volcanic-evolution-of-the-middle, accessed October 25, 2023.

Fiebelkorn, R. B., Walker, G. W., MacLeod, N. S., McKee, E. H., and Smith, J. G., 1983, Index to K/Ar age determinations for the state of Oregon: Isochron/West, no. 37, p. 3–60. https://geoinfo.nmt.edu/publications/periodicals/isochronwest/37/iw_v37_p03.pdf, accessed October 25, 2023.

Finn, D. R., Coe, R. S., Brown, E., Branney, M., Reichow, M., Knott, T., Storey, M., and Bonnichsen, B., 2016, Distinguishing and correlating deposits from large ignimbrite eruptions using paleomagnetism: The Cougar Point Tuffs (mid-Miocene), southern Snake River Plain, Idaho, USA: Journal of Geophysical Research Solid Earth, v. 121, p. 6293–6314. https://agupubs.onlinelibrary.wiley.com/doi/full/10.1002/2016JB012984, accessed October 24, 2023.

Fleck, R.J., Hagstrum, J.T., Calvert, A.T., Evarts, R.C., Conrey, R.M., 2014, $^{40}Ar/^{39}Ar$ geochronology, paleomagnetism, and evolution of the Boring volcanic field, Oregon and Washington, USA: Geosphere v. 10, no. 6, p. 1283–1314. https://doi.org/10.1130/GES00985.1, accessed October 23, 2023.

Frankel, A.D., and Peterson, M.D., 2008, Cascadia subduction zone, Appendix L in the Uniform California Earthquake Rupture Forecast, version 2 (UCERF2): U.S. Geological Survey Open File Report 2007-1437L and California Geological Survey Special Report 203L, 7 p. https://pubs.usgs.gov/of/2007/1437/, accessed October 25, 2023.

Gannett, M.W., 1982, A geochemical study of the Rhododendron and the Dalles Formations in the area of Mount Hood, Oregon: Portland, Oregon, Portland State University, M.S. thesis, 70 p. https://pdxscholar.library.pdx.edu/open_access_etds/3166/, accessed October 25, 2023.

Geological Society of America Rock-Color Chart Committee, 1991, Rock color chart, 7th printing: Boulder, Colorado.

Geomatrix Consultants, Inc., 1995, Seismic design mapping, State of Oregon: technical report to Oregon Department of Transportation, Salem, Oregon, under contract 11688, Jan. 1995, unpaginated, 5 pl., scale 1:1,250,000.

Gillespie, M.R., and Styles, M.T., 1999, BGS rock classification scheme, v. 1, Classification of igneous rocks: British Geological Survey Research Report (2nd ed.) RR99-06, 52 p. https://nora.nerc.ac.uk/id/eprint/3223/1/RR99006.pdf, accessed October 25, 2023.

Goldfinger, C., Nelson, C.H., Johnson, J.E., and the Shipboard Scientific Party, 2003, Deep-water turbidites as Holocene earthquake proxies: the Cascadia subduction zone and Northern San Andreas fault systems: Annuals of Geophysics, v. 46, no. 5, p. 1169-1194. https://www.annalsofgeophysics.eu/index.php/annals/article/view/3452, accessed October 25, 2023.

Goldfinger, C., Nelson, C.H., Morey, A.E., Johnson, J.E., Patton, J.R., Karabanov, E., Gutiérrez-Pastor, J., Eriksson, A.T., Gràcia, E., Dunhill, G., Enkin, R.J., Dallimore, A., and Vallier, T., 2012, Turbidite event history—methods and implications for Holocene paleoseismicity of the Cascadia subduction zone: U.S. Geological Survey Professional Paper 1661-F, 170 p. https://pubs.usgs.gov/publication/pp1661F, accessed October 25, 2023.

Goter, S.K., 1994, Earthquakes in Washington and Oregon: 1872–1993: U.S. Geological Survey Open-File Report 94-226-A, 1 p., 1 plate, scale 1:1,000,000. https://pubs.er.usgs.gov/publication/ofr94226A, accessed October 25, 2023.

Gradstein, F.M., and others, 2004, A geologic time scale 2004, Cambridge University Press, 589 p. https://www.cambridge.org/core/books/geologic-time-scale-2004/ACED6139A9320FC9CA982E316FFF3E38, accessed October 25, 2023.

Grady, S.J., 1983, Groundwater resources in the Hood Basin, Oregon: U.S. Geological Survey Water-Resources Investigations Report 81-1108, 68 p., 2 pl., scale 1:62,500. https://pubs.er.usgs.gov/publication/wri811108, accessed October 25, 2023.

Gray, L.B., Sherrod, D.R., and Conrey, R.M., 1996, Potassium-argon ages from the northern Oregon Cascade Range: Isochron/West, no. 63, p. 21-28. https://geoinfo.nmt.edu/publications/periodicals/isochronwest/63/iw_v63_p21.pdf, accessed October 25, 2023.

Green, G. L., 1981, Soil survey of Hood River County area, Oregon: Natural Resources Conservation Service Soil Conservation Survey 629, 66 p. https://archive.org/details/usda-soil-survey-of-hood-river-county-area-oregon-1981, accessed October 25, 2023.

Green, G.L., 1982, Soil survey of Wasco County, Oregon, northern part: Natural Resources Conservation Service Soil Conservation Survey 673, 83 p. https://archive.org/details/wascoOR1982 , accessed October 25, 2023.

Hallsworth, C.R., and Knox, R.W.O'B., 1999, BGS rock classification scheme, v. 3, Classification of sediments and sedimentary rocks: British Geological Survey Research Report 99-03, 44 p. https://nora.nerc.ac.uk/3227/1/RR99003.pdf, accessed October 25, 2023.

Haugerud, R.A., Ballantyne, D., Weaver, C.S., Meagher, K., and Barnett, E.A., 1999, Lifelines and earthquake hazards in the greater Seattle area: U.S. Geological Survey, Open-file Report, 10 p. https://pubs.usgs.gov/publication/ofr99387, accessed October 25, 2023.

Hildreth, W., 2007, Quaternary magmatism in the Cascades—Geologic perspectives: U.S. Geological Survey Professional Paper 1744, 125 p. https://pubs.usgs.gov/pp/pp1744/, accessed October 25, 2023.

Hildreth, W., and Fierstein, J., 1995, Geologic map of the Mount Adams volcanic field, Cascade Range of southern Washington: U.S. Geological Survey Map I–2460, scale 1:50,000, pamphlet 39 p. https://pubs.usgs.gov/publication/i2460, accessed October 25, 2023.

Hildreth, W., and Fierstein, J., 2015, Geologic Map of the Simcoe Mountains Volcanic Field, Main Central Segment, Yakama Nation, Washington: U.S. Geological Survey Scientific Investigations Map 3315, scale 1:50,000, pamphlet 76 p. https://pubs.usgs.gov/publication/sim3315, accessed October 25, 2023.

Hooper, P.R., 2000, Chemical discrimination of Columbia River Basalt flows: Geochemistry, Geophysics, and Geosystems, v. 1, no. 1, p. 1-14. https://onlinelibrary.wiley.com/doi/10.1029/2000GC000040/pdf, accessed October 25, 2023.

Hull, D.A., principal investigator, and Riccio, J.F., ed., 1979, Geothermal resource assessment of Mount Hood: Oregon Department of Geology and Mineral Industries Open-File Report O-79-8, part 1, 273 p. Compressed file available from https://pubs.oregon.gov/dogami/ofr/O-79-08.zip, accessed October 7, 2023.

Johnson, A.K., 2011, Dextral shear and north-directed crustal shortening defines the transition between extensional and contractional provinces in north-central Oregon: Corvallis, Oregon State University, M.S. thesis, 77 p., 3 pl., scale 1:24,000. http://ir.library.oregonstate.edu/xmlui/handle/1957/20928, accessed October 25, 2023.

Johnson, D.M., Hooper, P.R., and Conrey, R.M., 1999, XRF analysis of rocks and minerals for major and trace elements on a single low dilution Li-tetraborate fused bead: Advances in X-ray Analysis, v. 41, p. 843-867. https://environment.wsu.edu/facilities/geoanalytical-lab/technical-notes/xrf-method/, accessed October 25, 2023.

Kasbohm, J., and Schoene, B., 2018, Rapid eruption of the Columbia River flood basalt and correlation with mid-Miocene climate optimum; Science Advances, v. 4, no. 9. https://advances.sciencemag.org/content/4/9/eaat8223, accessed October 25, 2023.

Kasbohm, J., Schoene, B., Mark, D.F., Murray, J., Reidel, S., Szymanowski, D., Barfod, D., Barry, T., 2023, Eruption history of the Columbia River Basalt Group constrained by high-precision U-Pb and $^{40}Ar/^{39}Ar$ geochronology: Earth and Planetary Science Letters, Volume 617, p. 1-14. https://www.sciencedirect.com/science/article/abs/pii/S0012821X23002820, accessed October 25, 2023.

Keith, T.E.C., Donnelly-Nolan, J.M., Markman, J.L., and Beeson, M.H., 1985, K-Ar ages of rocks in the Mount Hood area, Oregon: Isochron/West, no. 42, p. 12-16. https://geoinfo.nmt.edu/publications/periodicals/isochronwest/42/iw_v42_p12.pdf, accessed October 25, 2023.

Korosec, M.A., 1987, Geologic map of the Hood River quadrangle, Washington and Oregon: Washington Division of Geology and Earth Resources Open File Report 87-6, 41 p., 1 pl., scale 1:100,000. https://ngmdb.usgs.gov/Prodesc/proddesc_30784.htm, accessed October 25, 2023.

Kuehn, S.C., 1995, The Olympic-Wallowa lineament, Hite fault system, and CRBG stratigraphy in northeast Umatilla County, Oregon: Pullman, Washington State University, M.S. thesis, 170 p.

Kuehn, S.C., Froese, D.G., Carrara, P.E., Foit, F.F., Pearce, N.J.G., and Rotheisler, P., 2009, Major- and trace-element characterization, expanded distribution, and a new chronology for the latest Pleistocene Glacier Peak tephras in western North America: Quaternary Research, v. 71, no. 2, p. 201-216. https://www.sciencedirect.com/science/article/abs/pii/S0033589408001373, accessed October 31, 2023

Le Bas, M.J., and Streckeisen, A.L., 1991, The IUGS systematics of igneous rocks: London, Journal of the Geological Society, v. 148, p. 825-833. https://www.lyellcollection.org/doi/10.1144/gsjgs.148.5.0825, accessed October 25, 2023.

Le Bas, M. J., Le Maitre, R. W., Streckeisen, A., and Zanettin, B., 1986, A chemical classification of volcanic rocks based on the total alkali-silica diagram: Journal of Petrology, v. 27, part 3, p. 745–750. https://academic.oup.com/petrology/article-abstract/27/3/745/1497841?redirectedFrom=fulltext, accessed October 25, 2023.

Le Maitre, R.W. (ed.), Bateman, P., Dudek, A., Keller, J., Lemeyre, J., Le Bas, M. J., Sabine, P. A., Schmid, R., Sorenson, H., Streckeisen, A., Wooley, A. R., and Zanettin, B., 1989, A classification of igneous rocks and glossary of terms: Oxford, Blackwell, 193 p.

Le Maitre, R.W. (ed.), Streckeisen, A., Zanettin, B., Le Bas, M.J,, Bonin, B., and Bateman, P., 2002, Igneous rocks: A classification and glossary of terms: Second Edition, Cambridge University Press, Recommendations of the International Union of Geological Sciences, Subcommission on the Systematics of Igneous Rocks, 236 p. https://doi.org/10.1017/CBO9780511535581, accessed October 23, 2023.

Lidke, D.J., Johnson, S.Y., McCrory, P.A., Personius, S.F., Nelson, A.R., Dart, R.L., Bradley, L., Haller, K.M., and Machette, M.N., 2003, Map and data for Quaternary faults and folds in Washington State: U.S. Geological Survey Open-File Report 03-428, 579 p., 1 pl., scale 1:750,000. https://pubs.usgs.gov/of/2003/428/, accessed October 25, 2023.

Lindsey, K., Morgan, D., Vlassopoulos, D., Tolan, T.L., and Burns, E., 2009, Hydrogeology of the CRBG in the Columbia Plateau: Road log and field trip stop descriptions, *in* O'Connor, J.E., Dorsey, R.J., and Madin, I.P., eds., Volcanoes to vineyards: Geologic field trips through the dynamic landscape of the Pacific Northwest: Geological Society of America Field Guide 15, p. 673-696. https://pubs.geoscienceworld.org/books/book/885/chapter/3931795/Hydrogeology-of-the-Columbia-River-Basalt-Group-in, accessed October 25, 2023.

Lite, K.E., 2013, The influence of depositional environment and landscape evolution on groundwater flow in Columbia River Basalt – examples from Mosier, Oregon, *in* Reidel, S.P., Camp, V.E., Martin, M.E., Ross, M.E., Wolff, J.A., Martin, B.S., Tolan, T.L., and Wells, R.E., eds., Geological Society of America Special Paper 497, p. 429-440. https://pubs.geoscienceworld.org/books/book/661/chapter/3807362/The-influence-of-depositional-environment-and, accessed October 25, 2023.

Lite, K.E., and Grondin, G.H., 1988, Hydrogeology of the basalt aquifers near Mosier, Oregon: A ground water resource assessment: Oregon Water Resources Department Ground Water Report 33, 119 p., 5 pl., scale 1:24,000. http://filepickup.wrd.state.or.us/files/for_Mike_Sloan/Lite%201988%20Hydrogeology%20basalt%20aqs%20mosier.pdf, accessed October 25, 2023.

Luttrell, G.W., Hubert, M.L., and Murdock, C.R., 1991, Lexicon of new formal geologic names of the United States1981-1985: U.S. Geological Survey Bulletin 1565, 376 p. http://pubs.er.usgs.gov/publication/b1565, accessed October 25, 2023.

Lux, D.R., 1982, K-Ar and $^{40}Ar/^{39}Ar$ ages of mid-Tertiary volcanic rocks from the West Cascades Range, Oregon: Isochron/West, no. 33, p. 27-32. https://geoinfo.nmt.edu/publications/periodicals/isochronwest/33/iw_v33_p27.pdf, accessed October 25, 2023.

Mackenzie, W.S., Donaldson, C.H., and Guilford, C., 1997, Atlas of igneous rocks and their textures: Addison Wesley Longman Ltd., 7th ed., 148 p.

Mackin, J.H., 1961, A stratigraphic section in the Yakima Basalt and Ellensburg Formation in south-central Washington: Washington Division of Mines and Geology Report of Investigations, 19, 45 p. https://pubs.usgs.gov/bul/1224g/report.pdf, accessed October 25, 2023.

Madin, I.P., and Burns, W.J., 2013, Ground motion, ground deformation, tsunami inundation, coseismic subsidence, and damage potential maps for the 2012 Oregon resilience plan for Cascadia subduction zone earthquakes: Oregon Department of Geology and Mineral Industries Open-File Report O-13-06, 39 p., 38 pl., various scales. https://pubs.oregon.gov/dogami/ofr/p-O-13-06.htm, accessed October 7, 2023.

Madin, I.P., and Mabey, M.A., 1996, Earthquake hazard maps for Oregon: Oregon Department of Geology and Mineral Industries Geological Map Series GMS-100, 1 pl., various scales. https://pubs.oregon.gov/dogami/gms/GMS-100.pdf, accessed October 7, 2023.

Madin, I.P., and McClaughry, J.D., 2019, Geologic map of the Biggs Junction and Rufus 7.5′ quadrangles, Wasco and Sherman counties, Oregon: Oregon Department of Geology and Mineral Industries Geological Map Series GMS 124, 105 p., 1 pl., scale 1:24,000, Esri™ format geodatabase; shapefiles, metadata; spreadsheet (4 sheets). https://pubs.oregon.gov/dogami/gms/p-GMS-124.htm, accessed October 7, 2023.

Madin, I.P., and Wang, Z., 2000, Relative earthquake hazard maps for selected areas in western Oregon: Oregon Department of Geology and Mineral Industries Interpretive Map Series IMS-7, scale 1:24,000. https://pubs.oregon.gov/dogami/ims/p-ims-007.htm, accessed October 7, 2023.

Madin, I.P., Streig, A.R., and Bennett, S.E.K., 2021a, The Mount Hood fault zone, active faulting at the crest of the dynamic Cascade Range, north-central Oregon, USA, *in* Booth, A.M., and Grunder, A.L., eds., From Terranes to Terrains: Geologic field guides on the construction and destruction of the Pacific Northwest: Geological Society of America Field Guide 62, p 49-71. https://pubs.geoscienceworld.org/gsa/books/book/2333/From-Terranes-to-Terrains-Geologic-Field-Guides-on, accessed October 25, 2023.

Madin, I.P., Franczyk, J.J., Bauer, J.M., and Azzopardi, C.J.M., 2021b, Oregon Seismic Hazard Database (OSHD), release 1.0 [OSHD-1], Oregon Department of Geology and Mineral Industries Digital Data Series OSHD-1, Esri™ geodatabase. https://pubs.oregon.gov/dogami/dds/p-OSHD-1.htm, accessed September 29, 2023.

Madin, I.P., Streig, A.R., Burns, W.J., and Ma, L., 2017, The Mount Hood fault zone—Late Quaternary and Holocene fault features newly mapped with high resolution lidar imagery: U.S. Geological Survey Scientific Investigations Report 2017-5022-G, p. 99-109. http://doi.org/10.3133/sir20175022G, accessed October 25, 2023.

Mahood, G.A., and Benson, T.R., 2017, Using $^{40}Ar^{39}Ar$ ages of intercalated silicic tuffs to date flood basalts: Precise ages for Steens Basalt Member of the Columbia River Basalt Group: Earth and Planetary Science Letters, v. 459, p. 340-351. https://www.sciencedirect.com/science/article/abs/pii/S0012821X16306720?via%3Dihub, accessed October 25, 2023.

Martin, B.S., Tolan, T.L., and Reidel, S.P., 2013, Revisions to the stratigraphy and distribution of the Frenchman Springs Member, Wanapum Basalt, *in* Reidel, S.P., Camp, V.E., Martin, M.E., Ross, M.E., Wolff, J.A., Martin, B.S., Tolan, T.L., and Wells, R.E., eds., Geological Society of America Special Paper 497, p. 155-180. https://pubs.geoscienceworld.org/books/book/661/chapter/3807169/Revisions-to-the-stratigraphy-and-distribution-of, accessed October 25, 2023.

McCaffrey, R., and Goldfinger, C., 1995, Forearc deformation and great subduction earthquakes: Implications for Cascadia offshore earthquake potential, Science, v. 267, p. 856-859. https://pubmed.ncbi.nlm.nih.gov/17813913/, accessed October 25, 2023.

McCaffrey, R., Qamar, A. I., King, R. W., Wells, R., Khazaradze, G., Williams, C. A., Stevens, C. W., Vollick, J. J., and Zwick, P. C., 2007, Fault locking, block rotation and crustal deformation in the Pacific Northwest: Geophysical Journal International, v. 169, no. 3, p. 1315-1340. https://pubs.er.usgs.gov/publication/70029869, accessed October 25, 2023.

McClaughry, J.D., Madin, I.P., Bennett, S.E.K., and Conrey, R.M., 2022, Volcano-tectonic history of the Hood River graben: a late Pliocene-Holocene intra-arc graben at the crest of the northern Oregon Cascade Range, USA, *in* Thorleifson, L. H., ed., 2022, Geologic Mapping Forum 21/22 Abstracts, Minnesota Geological Survey Open File Report OFR-22-2, 62 p. https://conservancy.umn.edu/handle/11299/228213, accessed October 25, 2023.

McClaughry, J.D., Scott, W.E., Duda, C.J.M., and Conrey, R.M., 2020a, Geologic map of the Dog River and northern part of the Badger Lake 7.5′ quadrangles, Hood River County, Oregon: Oregon Department of Geology and Mineral Industries Geological Map Series GMS-126, 145 p., 1 pl., scale 1:24,000, Esri™ format geodatabases; shapefiles, metadata; spreadsheet (5 sheets, https://pubs.oregon.gov/dogami/gms/p-GMS-126.htm, accessed October 7, 2023.

McClaughry, J.D., Niewendorp, C.A., Franczyk, J.J., Duda, C.J.M., and Madin, I.P., 2020b, Mineral Information Layer for Oregon, release 3 [MILO-3]: Oregon Department of Geology and Mineral Industries Digital Data Series MILO-3, Esri™ geodatabase. https://www.oregon.gov/dogami/milo/Pages/index.aspx, accessed October 7, 2023.

McClaughry, J.D., Herinckx, H.H., Niewendorp, C.A., Azzopardi, C.J.M., and Hackett, J.M, 2021, Geologic Map of the Dufur Area, Wasco County, Oregon: Oregon Department of Geology and Mineral Industries Geological Map Series GMS 127, 209 p., 3 plates, scale 1:24,000, Esri format geodatabases (3); shapefiles, metadata; spreadsheets (16 sheets). https://pubs.oregon.gov/dogami/gms/p-GMS-127.htm, accessed October 7, 2023.

McClaughry, J.D., Wiley, T.J., Conrey, R.C., Jones, C.B., and Lite, K.E., 2012, Digital geologic map of the Hood River Valley, Hood River and Wasco counties, Oregon: Oregon Department of Geology and Mineral Industries Open-File Report O-12-03, 142 p., 1 pl., scale 1:36,000, Esri ArcGIS™ geodatabase, GIS files, spreadsheets. https://pubs.oregon.gov/dogami/ofr/p-O-12-03.htm, accessed October 7, 2023.

McClaughry, J.D., Wiley, T.J., Conrey, R.C., Jones, C.B., and Lite, K.E., 2013, The Hood River graben: a late Pliocene and Quaternary intra-arc half graben in the northern Oregon Cascade Range: Geological Society of America Abstracts with Programs v. 45, no. 6, p. 14. https://gsa.confex.com/gsa/2013CD/webprogram/Paper219572.html, accessed October 25, 2023.

McDonald, E.V., Sweeney, M.R., and Busacca, A.J., 2012, Glacial outburst floods and loess sedimentation documented by Oxygen Isotope Stage 4 on the Columbia Plateau, Washington State: Quaternary Science Reviews, v. 45, p. 18-30. https://www.sciencedirect.com/science/article/abs/pii/S0277379112001412, accessed October 25, 2023.

McKee, E H., Swanson, D. A., and Wright, T. T., 1977, Duration and volume of Columbia River volcanism, Washington, Oregon, and Idaho [abs.]: Geological Society of America Abstracts with Programs, v. 9, no. 4, p. 463– 464.

Medley, E., 2012, Ancient cataclysmic floods in the Pacific Northwest: Ancestors to the Missoula Floods: Portland, Portland State University, M.S. thesis, 174 p. http://pdxscholar.library.pdx.edu/open_access_etds/581/, accessed October 25, 2023.

Mertzman, S.A., 2000, K-Ar results from the southern Oregon–northern California Cascade Range: Oregon Geology, v. 62, no. 4, p. 99-122. https://pubs.oregon.gov/dogami/og/OGv62n04.pdf, accessed October 7, 2023.

Miyashiro, A., 1974, Volcanic rock series in island arcs and active continental margins: American Journal of Science, v. 274, p. 321-355.

Moore, N.E., Grunder, A.L., and Bohrson, W.A., 2018, The three-stage petrochemical evolution of the Steens Basalt (southeast Oregon, USA) compared to large igneous provinces and layered mafic intrusions: Geosphere, v. 14, p. 2505-2532. https://pubs.geoscienceworld.org/gsa/geosphere/article/14/6/2505/548601/The-three-stage-petrochemical-evolution-of-the, accessed October 25, 2023.

Nash B.P., and Perkins, M.E. 2012, Neogene Fallout Tuffs from the Yellowstone Hotspot in the Columbia Plateau Region, Oregon, Washington and Idaho, USA: PLoS ONE v. 7, no. 10: e44205. https://journals.plos.org/plosone/article?id=10.1371/journal.pone.0044205, accessed October 24, 2023.

Nelson, A.R., Kelsey, H.M., and Witter, R.C., 2006, Great earthquakes of variable magnitude at the Cascadia subduction zone: Quaternary Research v. 65, p. 354-365. https://pubs.er.usgs.gov/publication/70030439, October 25, 2023.

Nelson, A.R., DuRoss, C.B., Witter, R.C., Kelsey, H.M., Engelhart, S.E., Mahan, S.A., Gray, H.J., Hawkes, A.D., Horton, B.P., and Padgett, J.S., 2021, A maximum rupture model for the central and southern Cascadia subduction zone—reassessing ages for coastal evidence of megathrust earthquakes and tsunamis: Quaternary Science Reviews, v. 261, 106922. https://www.sciencedirect.com/science/article/pii/S0277379121001293?via%3Dihub, accessed October 24, 2023.

Newcomb, R.C., 1963, Ground water in the Orchard Syncline, Wasco County, Oregon: The Ore Bin, v. 25, no. 8, p. 133-138. https://pubs.oregon.gov/dogami/og/OBv25n08.pdf , accessed October 7, 2023.

Newcomb, R.C., 1966, Lithology and eastward extension of The Dalles Formation, Oregon and Washington: U.S. Geological Survey Professional Paper 550-D, p. 059-063. https://pubs.er.usgs.gov/publication/pp550D, accessed October 24, 2023.

Newcomb, R.C., 1967, The Dalles-Umatilla syncline, Oregon and Washington, *in* Geological Survey Research 1967: U.S. Geol. Survey Professional Paper 575-B, p. B88-B93, 3 figs. https://pubs.usgs.gov/publication/pp575B, accessed October 25, 2023.

Newcomb, R.C., 1969, Effect of tectonic structure on the occurrence of groundwater in the basalt of the Columbia River Group of The Dalles area, Oregon and Washington: U.S. Geological Survey Professional Paper 383-C, 33 p., 1 pl., scale 1:62,500. https://pubs.er.usgs.gov/publication/pp383C, accessed October 25, 2023.

Niewendorp, C.A., and Neuhaus, M. E., 2003, Map of selected earthquakes for Oregon, 1841 through 2002: Oregon Department of Geology and Mineral Industries Open-File Report O-03-02, 1 pl. https://pubs.oregon.gov/dogami/ofr/p-O-03-02.htm, accessed October 7, 2023.

NOAA National Centers for Environmental Information, 2020, Data tools: 1981-2010 Normals: https://www.ncdc.noaa.gov/cdo-web/datatools/normals, accessed October 25, 2023.

O'Connor, J.E., Cannon, C.M., Schwid, M.F., Staisch, L., Engstrom, J., and Lee, S., 2021, 10,000 pebbles of the Columbia River basin—a provenance assessment, Geological Society of America Abstracts with Programs, v. 53, no. 6, https://doi.org/10.1130/abs/2021AM-369253, October 12, 2023.

O'Connor, J.E., Baker, V.R., Waitt, R.B., Smith, L.N., Cannon, C.M., George, D.L., Denlinger, R.P., 2020, The Missoula and Bonneville floods—A review of ice-age megafloods in the Columbia River basin: Earth-Science Reviews, v. 208, 103181, https://doi.org/10.1016/j.earscirev.2020.103181, accessed October 16, 2023.

O'Connor, J.E., Wells, R.E., Bennett, S.E.K., Cannon, C.M., Staisch, L.M., Anderson, J.L., Pivarunas, A.F., Gordon, G.W., Blakely, R.J., Stelten, M.E., and Evarts, R.C., 2021, Arc versus river—The geology of the Columbia River Gorge, *in* Booth, A.M., and Grunder, A.L., eds., From Terranes to Terrains: Geologic Field Guides on the Construction and Destruction of the Pacific Northwest: Geological Society of America Field Guide 62, p. 131–186, https://doi.org/10.1130/2021.0062(05), accessed October 25, 2023.

Ogg, J.G., Ogg, G., and Gradstein, F.M., 2008, Concise geologic time scale. Cambridge, University Press, 177. https://www.cambridge.org/core/journals/geological-magazine/article/abs/j-g-ogg-g-ogg-f-m-gradstein-2008-the-concise-geologic-time-scale-vi-177-pp-cambridge-new-york-melbourne-cambridge-university-press-price-2000-us-4000-hard-covers-isbn-9780-521-89849-2/FE9121A10C039AE3FA58D48B7E8D235A, accessed October 25, 2023.

Peccerillo, A., and Taylor, S.R., 1976, Geochemistry of Eocene calc-alkaline volcanic rocks from the Kastamonu area, northern Turkey: Contributions to Mineralogy and Petrology, v. 58, p. 63-81. https://link.springer.com/article/10.1007/BF00384745, accessed October 25, 2023.

Peck, D.L., Griggs, A.B., Schlicker, H.G., Well, F.G., and Dole, H.M., 1964, Geology of the central and northern parts of the Western Cascade Range in Oregon: U.S. Geological Survey Professional Paper 449, 56 p., 1 pl., scale 1:250,000. https://pubs.er.usgs.gov/publication/pp449, accessed October 25, 2023.

Perkins, M.E., Brown F.H., Nash, W.P., McIntosh, W., and Williams, S.K,, 1998, Sequence, age, and source of Silicic fallout tuffs in Middle to Late Miocene basins of the northern Basin and Range province: Geological Society of America Bulletin v. 110, no. 3, p. 344–360. https://pubs.geoscienceworld.org/gsa/gsabulletin/article-abstract/110/3/344/183363/Sequence-age-and-source-of-silicic-fallout-tuffs?redirectedFrom=fulltext, accessed October 25, 2023.

Personius, S.F., Dart, R.L., Bradley, L.-A., and Haller, K.M., 2003, Map and data for Quaternary faults and folds in Oregon: U.S. Geological Survey Open-File Report 03-095, 16 p., 1 pl., scale 1:750,000. https://pubs.usgs.gov/of/2003/ofr-03-095/, accessed October 25, 2023.

Phillips, W.M., Korosec, M.A., Schasse, H.W., Anderson, J.L., and Hagen, R.A., 1986, K-Ar ages of volcanic rocks in southwest Washington: Isochron/West, v. 47, p. 18-24. https://geoinfo.nmt.edu/publications/periodicals/isochronwest/47/iw_v47_p18.pdf, accessed October 25, 2023.

Piper, A.M., 1932, Geology and groundwater resources of The Dalles region, Oregon: U.S. Geological Survey Water-Supply Paper 659-B, p. 107–189, 2 pl., scale 1:62,500. https://pubs.er.usgs.gov/publication/wsp659B, accessed October 25, 2023.

Pluhar, C.J., Burns, S.F., Carpenter, B., Yazzie, K., and Melton, D., 2014, Paleomagnetism of Early and Middle Pleistocene cataclysmic flood deposits in the Pacific Northwest: American Geophysical Union, Fall Meeting 2014, abstract id. GP21A-3653. https://ui.adsabs.harvard.edu/abs/2014AGUFMGP21A3653P/abstract, accessed October 25, 2023.

Powell, J.E., 1982, Geology of the Columbia Hills, Klickitat County, Washington: Moscow, University of Idaho, M.S. thesis, 56 p., 4 pl.

Powell, L.V., 1978, The structure, stratigraphy, and correlation of Grande Ronde Basalt on Tygh Ridge, Wasco County, Oregon: Moscow, University of Idaho, M.S. thesis, 57 p.

Priest, G.R., 1990, Volcanic and tectonic evolution of the Cascade volcanic arc, central Oregon: Journal of Geophysical Research, v. 95, no. B12, p. 19,583–19,599. https://agupubs.onlinelibrary.wiley.com/doi/abs/10.1029/JB095iB12p19583, accessed October 25, 2023.

Priest, G.R., Woller, N.M., Black, G.L., and Evans, S.H., 1983, Overview of the geology of the central Oregon Cascade Range, *in* Priest, G. R., and Vogt, B. F., eds., Geology and geothermal resources of the central Oregon Cascade Range: Oregon Department of Geology and Mineral Industries Special Paper 15, 123 p., 3 pl., 1:24,000, 1:62,500. https://pubs.oregon.gov/dogami/sp/SP-15.pdf, accessed October 25, 2023.

Priest, G.R., Goldfinger, C., Wang, K., Witter, R.C., Zhang, Y., and Baptista, A.M., 2009, Tsunami hazard assessment of the northern Oregon coast: A multideterministic approach tested at Cannon Beach, Clatsop County, Oregon: Oregon Department of Geology and Mineral Industries Special Paper 41, 87 p., GIS files, time histories, animations, https://pubs.oregon.gov/dogami/sp/SP-41.zip, accessed October 25, 2023.

Reidel, S.P., 2005, A lava flow without a source: The Cohassett flow and its compositional components, Sentinel Bluffs Member, Columbia River Basalt Group: The Journal of Geology, v. 113, p. 1-21, https://www.journals.uchicago.edu/doi/10.1086/425966, accessed October 25, 2023.

Reidel, S.P., and Campbell, N.P., 1989, Structure of the Yakima Fold Belt, Central Washington, *in* Joseph, N.L. and others, eds., Geologic guidebook for Washington and adjacent areas: Washington Division of Geology and Earth Resources Information Circular 86, p. 275-303. https://www.dnr.wa.gov/Publications/ger_ic86_geol_guide_wa_area.pdf, accessed October 25, 2023.

Reidel, S.P., and Tolan, T.L., 2013, Grande Ronde Basalt, Columbia River Basalt Group, *in* Reidel, S.P., Camp, V.E., Martin, M.E., Ross, M.E., Wolff, J.A., Martin, B.S., Tolan, T.L., and Wells, R.E., eds., Geological Society of America Special Paper 497, p. 117-154. https://pubs.geoscienceworld.org/books/book/661/chapter/3807152/The-Grande-Ronde-Basalt-Columbia-River-Basalt, accessed October 25, 2023.

Reidel, S.P., Johnson, V.G., and Spane, F.A., 2002, Natural gas storage in basalt aquifers of the Columbia Basin, Pacific Northwest USA: a guide to site characterization: Richland, Wash., Pacific Northwest National Laboratory, 277 p. https://www.pnnl.gov/main/publications/external/technical_reports/PNNL-13962.pdf, accessed October 25, 2023.

Reidel, S.P., Camp, V.E., Tolan, T.L., and Martin, B.S., 2013a, The Columbia River flood basalt province: Stratigraphy, areal extent, volume, and physical volcanology, *in* Reidel, S.P., Camp, V.E., Martin, M.E., Ross, M.E., Wolff, J.A., Martin, B.S., Tolan, T.L., and Wells, R.E., eds., Geological Society of America Special Paper 497, p. 1-43. https://pubs.geoscienceworld.org/books/book/661/chapter/3807083/The-Columbia-River-flood-basalt-province, accessed October 25, 2023.

Reidel, S.P., Camp, V.E., Tolan, T,L., Kauffman, J.D., Garwood, D.L., 2013b, Tectonic evolution of the Columbia River flood basalt province, *in* Reidel, S.P., Camp, V.E., Martin, M.E., Ross, M.E., Wolff, J.A., Martin, B.S., Tolan, T.L., and Wells, R.E., eds., Geological Society of America Special Paper 497, p. 293-324, https://pubs.geoscienceworld.org/gsa/books/book/661/chapter-abstract/3807278/Tectonic-evolution-of-the-Columbia-River-flood?redirectedFrom=fulltext, accessed October 25, 2023.

Reidel, S.P., Tolan, T.L., Hooper, P.R., Beeson, M.H., Fecht, K.R., Bentley, R.D., and Anderson, J.L., 1989, The Grande Ronde Basalt, CRBG; Stratigraphic descriptions and correlations in Washington, Oregon, and Idaho, *in* Reidel, S. P., and Hooper, P. R., eds., Volcanism and tectonism in the Columbia River Flood-Basalt Province: Geological Society of America Special Paper 239, p. 21-53. https://pubs.geoscienceworld.org/books/book/375/chapter/3796997/The-Grande-Ronde-Basalt-Columbia-River-Basalt, accessed October 25, 2023.

Robertson, S., 1999, BGS rock classification scheme, v. 1, Classification of igneous rocks: British Geological Survey Research Report 99-06, 24 p. https://www.bgs.ac.uk/download/bgs-rock-classification-scheme-igneous/, accessed October 25, 2023.

Ross, M.E., 1978, Stratigraphy, structure, and petrology of Columbia River Basalt in a portion of the Grande Ronde River–Blue Mountains area of Oregon and Washington: Moscow, University of Idaho, Ph.D. dissertation, 407 p.

Rukstales, K.S., and Petersen, M.D., 2019, Data release for 2018 update of the U.S. National Seismic Hazard Model: U.S. Geological Survey data release. https://doi.org/10.5066/P9WT5OVB, accessed October 25, 2023.

Satake, K., Shimazaki, K., Tsuji, Y., and Ueda, K., 1996, Time and size of a giant earthquake in Cascadia inferred from Japanese tsunami records of January 1700: Nature, v. 379, p. 246-249. https://www.nature.com/nature/journal/v379/n6562/abs/379246a0.html, accessed July 25, 2023.

Sawlan, M.G., 2017, Alteration, mass analysis, and magmatic compositions of the Sentinel Bluffs Member, Columbia River flood basalt province: Geosphere, v.14, no. 1, p. 286–303. https://pubs.geoscienceworld.org/gsa/geosphere/article/14/1/286/524169/Alteration-mass-analysis-and-magmatic-compositions, accessed October 25, 2023.

Sceva, J.E., 1966, A reconnaissance of the groundwater resources of the Hood River Valley and the Cascade Locks area, Hood River County, Oregon: State of Oregon Groundwater Resources Report 10, 45 p, 1 pl. https://digital.osl.state.or.us/islandora/object/osl:14684, accessed October 25, 2023.

Scott, W.E., 1977, Quaternary glaciation and volcanism, Metolius River area, Oregon: Geological Society of America Bulletin, v. 88, p. 113-124. https://pubs.geoscienceworld.org/gsa/gsabulletin/article-abstract/88/1/113/202045/Quaternary-glaciation-and-volcanism-Metolius-River, accessed October 25, 2023.

Scott, W.E., and Gardner, C.A., 2017, Field-trip guide to Mount Hood, Oregon, highlighting eruptive history and hazards: U.S. Geological Survey Scientific Investigations Report 2017-5022-G, 115 p. https://doi.org/10.3133/sir20175022G, accessed October 16, 2023.

Scott, W.E., Pierson, T.C., Schilling, S.P., Costa, J.E., Gardner, C.A., Vallance, J.W., and Major, J.J., 1997, Volcano hazards in the Mount Hood region, Oregon: U.S. Geological Survey Open-File Report 97-89, 14 p. https://pubs.usgs.gov/of/1997/0089/, accessed October 25, 2023.

Seims, B.A., Bush, J.G., and Crosby, J.W., 1974, TiO_2 and geophysical logging criteria for Yakima Basalt correlation, Columbia Plateau: Geological Society of America Bulletin, v. 85, 1061-1068. https://pubs.geoscienceworld.org/gsa/gsabulletin/article-abstract/85/7/1061/201633/TiO2-and-Geophysical-Logging-Criteria-for-Yakima, accessed October 25, 2023.

Shannon and Wilson, 1973, Geologic studies of Columbia River basalt structures and age of deformation; the Dalles Umatilla region, Washington and Oregon; Boardman Nuclear Project: Portland General Electric Company.

Sherrod, D.R., 2019, Cascade Mountain Range in Oregon (essay): The Oregon Encyclopedia. https://oregonencyclopedia.org/articles/cascade_mountain_range/#.XuAE3UVKhaR, accessed October 25, 2023.

Sherrod, D.R., and Pickthorn, L.G., 1989, Some notes on the Neogene structural evolution of the Cascade Range in Oregon, *in* Muffler, L. J. P., Weaver, C. S., and Blackwell, D. D., eds., Geology, geophysics, and tectonic setting of the Cascade Range: U.S. Geological Survey Open-File Report 89-178, p. 351-368. https://pubs.usgs.gov/of/1989/0178/report.pdf, accessed October 25, 2023.

Sherrod, D.R., and Scott, W.E., 1995, Preliminary geologic map of the Mount Hood 30- by 60-minute quadrangle, Northern Cascade Range, Oregon: U.S. Geological Survey Open-File Report 95-219, 36 p., scale 1:100,000. https://pubs.usgs.gov/of/1995/of95-219/, accessed October 25, 2023.

Sherrod, D.R., and Smith, J.G., 2000, Geologic map of upper Eocene to Holocene volcanic and related rocks of the Cascade Range, Oregon: U.S. Geological Survey Map I-2569, 17 p., 2 pl., scale 1:500,000. https://pubs.usgs.gov/imap/i-2569/, accessed October 25, 2023.

Smith, G.A., and Fritz, W.J., 1989, Volcanic influences on terrestrial sedimentation: Geology, v.17, p. 375-376. https://pubs.geoscienceworld.org/gsa/geology/article-abstract/17/4/375/187791/Volcanic-influences-on-terrestrial-sedimentation?redirectedFrom=fulltext, accessed October 25, 2023.

Smith, G.A. and Taylor, E.M., 1983, The central Oregon High Cascade graben: What? Where? When?: Geothermal Resources Council Transactions, v. 7, p. 275-279.

Smith, G.A., Snee, L.W., and Taylor, E.M., 1987, Stratigraphic, sedimentologic, and petrologic record of late Miocene subsidence of the central Oregon High Cascades: Geology, v. 15, p. 389-392. https://pubs.geoscienceworld.org/gsa/geology/article-abstract/15/5/389/204381/Stratigraphic-sedimentologic-and-petrologic-record?redirectedFrom=fulltext, accessed October 25, 2023.

Smith, R.A., and Roe, W.P., compilers, 2015, Oregon Geologic Data Compilation [OGDC], release 6 (statewide): Oregon Department of Geology and Mineral Industries Digital Data Series OGDC-6, Esri™ geodatabase. https://pubs.oregon.gov/dogami/dds/p-OGDC-6.htm, accessed October 7, 2023.

Swanson, D.A., and Wright, T.L., 1978, Bedrock geology of the northern Columbia Plateau and adjacent areas, *in* Baker, V.R., and Nummedal, D., eds., The Channeled Scabland: A Guide to the Geomorphology of the Columbia Basin, Washington: Washington D.C., Planetary Geology Program, Office of Space Science, National Aeronautics and Space Administration, p. 37-57. https://ntrs.nasa.gov/citations/19780019524, accessed October 25, 2023.

Swanson, D.A., Anderson, J.L., Bentley, R.D., Byerly, G.R., Camo, V.E., Gardner, J.N., and Wright, T.L., 1979a, Reconnaissance geologic map of the Columbia River Basalt Group in parts of eastern Washington and northern Idaho: U.S. Geological Survey Open-File Report 79-1363, 44 p., 12 pl., scale 1:250,000. https://pubs.er.usgs.gov/publication/ofr791363, accessed October 25, 2023.

Swanson, D.A., Wright, T.L., Hooper, P.R., and Bentley, R.D., 1979b, Revisions in stratigraphic nomenclature of the Columbia River Basalt Group: U.S. Geological Survey Bulletin 1457-G, 59 p., 1 pl. https://pubs.er.usgs.gov/publication/b1457G, accessed October 25, 2023.

Swanson, D.A., Anderson, J.A., Camp, V.E., Hooper, P.R., Taubeneck, W.H., and Wright, T.L., 1981, Reconnaissance geologic map of the Columbia River Basalt Group, Northern Oregon and Western Idaho: U.S. Geological Survey Open-File Report 81-797, 35 p., 6 pl., scale 1:250,000. https://pubs.er.usgs.gov/publication/ofr81797, accessed October 25, 2023.

Taylor, E.M., 1981, Central High Cascade roadside geology—Bend, Sisters, McKenzie Pass, and Santiam Pass, Oregon, *in* Johnston, D.A., and Donnelly-Nolan, J., eds., Guides to some volcanic terranes in Washington, Idaho, Oregon, and northern California: U.S Geological Survey Circular 838, p. 55-83. https://pubs.er.usgs.gov/publication/cir838, accessed October 25, 2023.

Tolan, T.L., 1982, The stratigraphic relationships of the Columbia River Basalt Group in the lower Columbia River Gorge of Oregon and Washington: Portland, Portland State University, M.S. thesis, 169 p. https://doi.org/10.15760/etd.3232, accessed October 25, 2023.

Tolan, T.L., and Beeson, M.H., 1984, Intracanyon flows of the CRBG in the lower Columbia River Gorge and their relationship to the Troutdale Formation: Geological Society of America Bulletin, v. 95, no. 4, p. 463-477. https://pubs.geoscienceworld.org/gsa/gsabulletin/articleabstract/95/4/463/202924/Intracanyon-flows-of-the-Columbia-River-Basalt?redirectedFrom=fulltext, accessed October 25, 2023.

Tolan, T.L., and Reidel, S.P., compilers, 1989, Structure map of a portion the Columbia-River Flood-Basalt Province, *in* Reidel, S. P., and Hooper, P. R., eds., Volcanism and tectonism in the Columbia River Flood-Basalt Province: Geological Society of America Special Paper 239, scale 1:576,000, 1 pl. https://pubs.geoscienceworld.org/books/book/375/chapter/4697946/Map, accessed October 25, 2023.

Tolan, T.L., Beeson, M.H., and Lindsey, K.A., 2002, The effects of volcanism and tectonism on the evolution of the Columbia River System: a field guide to selected localities in the southwestern Columbia Plateau and Columbia River Gorge of Washington and Oregon State: Northwest Geological Society Field Trips in Pacific Northwest Geology, September 28-29, 2002, 74 p.

Tolan, T.L., Martin, B.S., Reidel, S.P., Anderson, J.L., Lindsey, K.A., and Burt, W., 2009a, An introduction to the stratigraphy, structural geology, and hydrogeology of the Columbia River flood-basalt province: A primer for the GSA CRBG field trips, *in* O'Connor, J. E., Dorsey, R. J., and Madin, I. P., eds., Volcanoes to vineyards: geologic field trips through the dynamic landscape of the Pacific Northwest: Geological Society of America Field Guide 15, p. 599-643. https://pubs.geoscienceworld.org/books/book/885/chapter/3931355/An-introduction-to-the-stratigraphy-structural, accessed October 25, 2023.

Tolan, T.L., Martin, B.S., Reidel, S.P., Kauffman, J.D., Garwood, D.L., and Anderson, J.L., 2009b, Stratigraphy and tectonics of the central and eastern portions of the Columbia River Flood-Basalt Province: An overview of our current state of knowledge, *in* O'Connor, J. E., Dorsey, R. J., and Madin, I. P., eds., Volcanoes to Vineyards: geologic field trips through the dynamic landscape of the Pacific Northwest: Geological Society of America Field Guide 15, p. 645-672. https://pubs.geoscienceworld.org/books/book/885/chapter/3931564/Stratigraphy-and-tectonics-of-the-central-and, accessed October 25, 2023.

Tolan, T.L., Reidel, S.P., Beeson, M.H., Anderson, J.L., Fecht, K.R., and Swanson, D.A., 1989, Revisions to the estimates of the areal extent and volume of the CRBG, *in* Reidel, S. P., and Hooper, P. R., eds., Volcanism and tectonism in the Columbia River Flood-Basalt Province: Geological Society of America Special Paper 239, p. 1-20. https://pubs.geoscienceworld.org/books/book/375/chapter/3796993/Revisions-to-the-estimates-of-the-areal-extent-and, accessed October 25, 2023.

USDOE (U.S. Department of Energy), 1988, Site characterization plan, Reference Repository Location, Hanford Site, Washington—consultation draft: Washington, D.C., Office of Civilian Radioactive Waste Management, DOE/RW-0164, v. 1 and 2, 1245 p.

U.S. Geological Survey National Cooperative Geologic Mapping Program, 2020, GeMS (Geologic Map Schema)—A standard format for the digital publication of geologic maps: U.S. Geological Survey Techniques and Methods, book 11, chap. B10, 74 p. https://doi.org//10.3133/tm11B10, accessed October 25, 2023.

Venkatakrishnan, R., Bond, J.G., and Kauffman, J.D., 1980, Geological linears of the northern part of the Cascade Range, Oregon: Oregon Department of Geology and Mineral Industries, Special Paper 12, 25 p., 5 pl., scale 1:250,000. https://pubs.oregon.gov/dogami/sp/SP-12.pdf, accessed October 7, 2023.

Verplanck, E.P., and Duncan, R.A., 1987, Temporal variations in plate convergence and eruption rates in the Western Cascades Oregon: Tectonics, v. 6, p. 197-209. https://agupubs.onlinelibrary.wiley.com/doi/abs/10.1029/TC006i002p00197, accessed October 25, 2023.

Vogt, B.F., 1981, The stratigraphy and structure of the Columbia River Basalt Group in the Bull Run Watershed, Oregon: Portland, Portland State University, M.S. thesis, 151 p. https://pdxscholar.library.pdx.edu/open_access_etds/3267/, accessed October 25, 2023.

Waters, A.C., 1968, Reconnaissance geologic map of the Dufur quadrangle, Hood River, Sherman, and Wasco counties, Oregon: U.S. Geological Survey Miscellaneous Geologic Investigations Map I-556, scale 1:125,000. https://pubs.er.usgs.gov/publication/i556, accessed October 25, 2023.

Watkins, N. D., and Baksi, A. K., 1974, Magnetostratigraphy and oroclinal folding of the Columbia River, Steens and Owyhee basalts in Oregon, Washington, and Idaho: America: Journal of Science, v. 274, p. 148–189.

Watters, T.R., 1989, Periodically spaced anticlines of the Columbia Plateau, *in* Reidel, S.P., and Hooper, P.R., eds., Volcanism and tectonism in the Columbia River flood-basalt province: Geological Society of America Special Paper 239, p. 283-292. https://pubs.geoscienceworld.org/books/book/375/chapter/3797045/Periodically-spaced-anticlines-of-the-Columbia, accessed October 25, 2023.

Weldon, R.J., II, Fletcher, D.K., Weldon, E.M., Scharer, K.M. and McCrory, P.A., 2003, An update of Quaternary faults of central and eastern Oregon: U.S. Geological Survey Open-File Report 2002-301, https://pubs.usgs.gov/of/2002/of02-301/, accessed October 25, 2023.

Wells, R.E., Niem, A.R., Evarts, R.C., and Hagstrum, J.T., 2009, The Columbia River Basalt Group—From the Gorge to the sea, *in* O'Connor, J.E., Dorsey, R.J., and Madin, I.P., eds., Volcanoes to vineyards: geologic field trips through the dynamic landscape of the Pacific Northwest: Geological Society of America Field Guide 15, p. 737-774. https://pubs.geoscienceworld.org/gsa/books/book/885/chapter-abstract/3932152/The-Columbia-River-Basalt-Group-From-the-gorge-to?redirectedFrom=fulltext, accessed October 25, 2023.

Wells, R.E., Simpson, R.W., Bentley, R.D., Beeson, M.H., Mangan, M.T., and Wright, T.L., 1989, Correlation of Miocene flows of the CRBG from the central Columbia River Plateau to the coast of Oregon and Washington, *in* Reidel, S. P., and Hooper, P. R., eds., Volcanism and tectonism in the Columbia River Flood-Basalt Province: Geological Society of America Special Paper 239, p. 113-129. https://pubs.geoscienceworld.org/books/book/375/chapter/3797019/Correlation-of-Miocene-flows-of-the-Columbia-River, accessed October 25, 2023.

Wentworth, C.K., 1922, A scale of grade and class terms of clastic sediments: Journal of Geology, v. 30, p. 377-392.

Westby, E.G., 2014, The geology and petrology of enigmatic rhyolites at Graveyard and Gordon Buttes, Mount Hood quadrangle, Oregon: Portland, Portland State University, M.S. thesis, 138 p. http://pdxscholar.library.pdx.edu/open_access_etds/2063/, accessed October 25, 2023.

Williams, I. A., 1916, The Columbia River Gorge — its geologic history interpreted from the Columbia River Highway: Oregon Bureau of Mines and Geology, Mineral Resources of Oregon, v. 2. no. 3, p. 7-130. https://pubs.oregon.gov/dogami/bomg/MineralResourcesofOregonVol2No3.pdf, accessed October 25, 2023.

Williams, D.L., Hull, D.A., Ackerman, H.D., and Beeson, M.H., 1982, The Mount Hood region: Volcanic history, structure, and geothermal potential: Journal of Geophysical Research, v. 87, p. 2767-2781. https://agupubs.onlinelibrary.wiley.com/doi/abs/10.1029/JB087iB04p02767, accessed October 25, 2023.

Wirth, E.A., Grant, A., Marafi, N.A., and Frankel, A.D., 2021, Ensemble ShakeMaps for magnitude 9 earthquakes on the Cascadia Subduction Zone: Seismol. Res. Lett., v. 92, no. 1, 99–211, https://doi.org/10.1785/0220200240, accessed October 25, 2023.

Wise, W.S., 1969, Geology and petrology of the Mt. Hood area: a study of High Cascade volcanism: Geological Society of America Bulletin, v. 80, no. 6, p. 969-1006. https://pubs.geoscienceworld.org/gsa/gsabulletin/article-abstract/80/6/969/6609/Geology-and-Petrology-of-the-Mt-Hood-Area-A-Study, accessed October 25, 2023.

Woodring, D, 2020, Kinematics of the Columbia Hills Anticline and the Warwick Strike-Slip fault, Yakima Fold and Thrust Belt, Washington, USA: Corvallis, Oregon State University, M.S. thesis, 108 p., 1 plate https://ir.library.oregonstate.edu/concern/graduate_thesis_or_dissertations/bv73c639j, accessed October 25, 2023.

Wright, T.L., Maurice, J.G., and Swanson, D.A., 1973, Chemical variation related to the stratigraphy of the Columbia River Basalt: Geological Society of America Bulletin, v. 84, p. 371-386. https://pubs.geoscienceworld.org/gsa/gsabulletin/article-abstract/84/2/371/201255/Chemical-Variation-Related-to-the-Stratigraphy-of?redirectedFrom=fulltext, accessed October 25, 2023.

Yelin, T.S., and Patton, H.J., 1991, Seismotectonics of the Portland, Oregon region: Seismological Society of America Bulletin, v. 81, p. 109-130. https://pubs.geoscienceworld.org/ssa/bssa/article-abstract/81/1/109/119420/Seismotectonics-of-the-Portland-Oregon-region?redirectedFrom=fulltext, accessed October 25, 2023.

Zakšek, K., Oštir, K., and Kokalj, Ž., 2011, Sky-View Factor as a relief visualization technique: Remote Sensing, v. 3, p. 398-415. https://iaps.zrc-sazu.si/en, accessed October 25, 2023.

11.0 APPENDIX

This **Appendix** contains a summary of the geodatabases along with a description of analytical and field methods and the list of attribute fields for spreadsheets (see page viii of this report). The **Appendix** is divided into two sections:

- Section 11.1 describes the digital databases included with this publication.
- Section 11.2 contains a summary of analytical and field methods. Accompanying tables explain the fields listed in spreadsheets.

11.1 Geographic Information Systems (GIS) database

Geodatabase specifications

Digital geologic data created for the Mill Creek area are stored in three Esri™ format geodatabases. The geodatabase structure of each follows that outlined by the U.S. Geological Survey (USGS) Geologic Map Schema (GeMS), version 2.7 (U.S. Geological Survey National Cooperative Geologic Mapping Program, 2020). The following information describes the overall database structure, the feature classes, and supplemental tables (**Figure 11-1**, **Figure 11-2**, **Table 11-1**, **Table 11-2**).

The data are stored in a file geodatabase feature dataset (GeologicMap). Accessory file geodatabase tables (DataSources, DescriptionOfMapUnits, GeoMaterialDict, and Glossary) were created by using ArcGIS version 10.7 (SP 1). The GeologicMap feature dataset contains all the spatially oriented data (feature classes) (**Figure 11-1**). The file geodatabase tables are used to hold additional geologic attributes (**Figure 11-2**). Each feature class within the GeologicMap feature dataset in the geodatabase contains detailed metadata (**Figure 11-1**). Please see the embedded metadata for detailed information such as process descriptions, accuracy specifications, and entity attribute descriptions. Additional information and complete descriptions of the GeMS can be found at https://doi.org//10.3133/tm11B10.

All spatial data are stored in the Oregon Statewide Lambert Conformal Conic projection. The datum is NAD83 HARN. The linear unit is international feet. See detailed projection parameters below:

Projection: Lambert_Conformal_Conic
False_Easting: 1312335.958005
False_Northing: 0.0
Central_Meridian: -120.5
Standard_Parallel_1: 43.0
Standard_Parallel_2: 45.5
Latitude_Of_Origin: 41.75
Linear Unit: Foot (0.3048)

Geographic Coordinate System: GCS_North_American_1983_HARN
Angular Unit: Degree (0.0174532925199433)
Prime Meridian: Greenwich (0.0)
Datum: D_North_American_1983_HARN

Spheroid: GRS_1980
Semimajor Axis: 6378137.0
Semiminor Axis: 6356752.314140356
Inverse Flattening: 298.257222101

Figure 11-1. Mill Creek area feature datasets and data tables contained in geodatabases BC2024.gdb, KR2024.gdb, and FBFP2024.gdb.

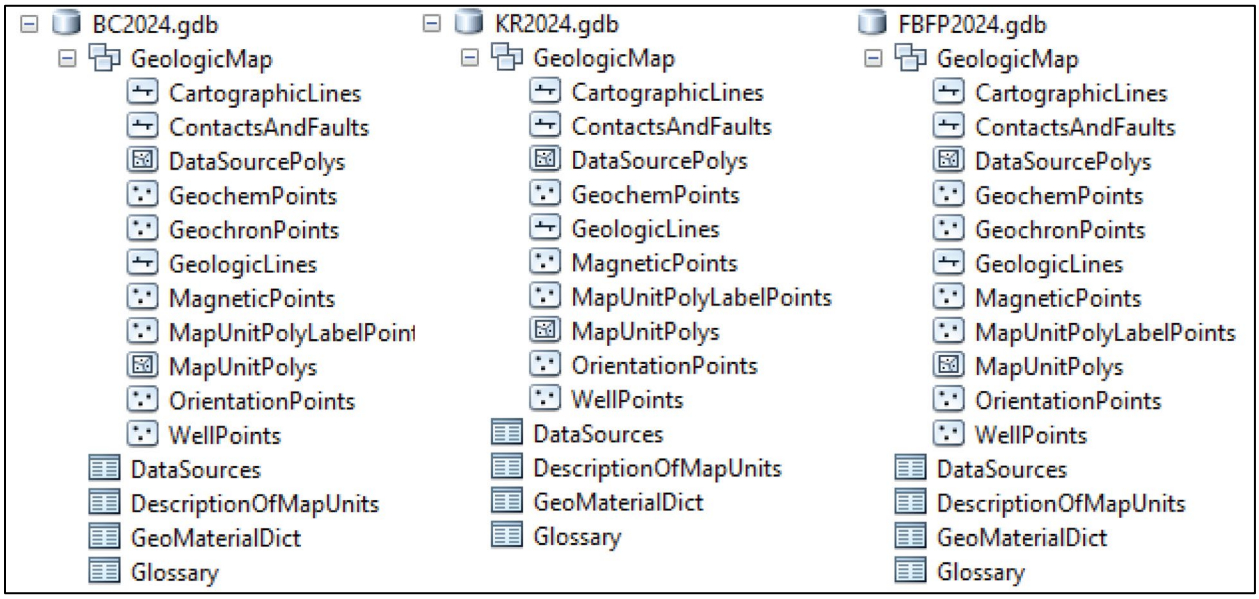

Figure 11-2. Mill Creek area geodatabase data tables.

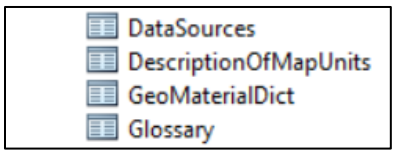

Table 11-1. Feature class descriptions.

Name	Description
CartographicLines	Vector lines that have no real-world physical existence and do not participate in map unit topology. The feature class includes cross section lines used for cartography.
ContactsAndFaults	The vector lines in this feature class contain geologic content including contacts and fault locations used to create the map unit polygon boundaries. The existence and location confidence values for the contacts and faults are provided in the feature class attribute table.
DataSourcePolys	This feature class contains polygons that delineate data sources for all parts of the geologic map. These sources may be a previously published map, new mapping, or mapping with a certain technique. For a map with one data source, for example all new mapping, this feature class contains one polygon that encompasses the map area.
GeochemPoints	This feature class represents point locations where whole-rock samples have been analyzed by X-ray fluorescence (XRF) techniques. Includes data collected by the authors during this study or compiled from previous studies. These data are also contained in the geochemistry spreadsheet.
GeochronPoints	This feature class represents point locations where isotopic ages have been obtained for rock samples in the map area. Data collected by the authors or compiled during the course of this study. These data are also contained in the geochronology spreadsheet.
GeologicLines	These vector lines represent known fold axis locations in the quadrangle. The existence and location confidence for the fold axes are provided in the feature class attribute table.
MagneticPoints	This feature class represents point locations where measurements of natural remanent magnetization have been obtained for strongly magnetized lava flows. Includes data collected by the authors during the course of this study. These data are also contained in the magnetic polarity spreadsheet.
MapUnitPolyLabelPoints	This feature class represents points used to generate the MapUnitPolys feature class from the ContactsAndFaults feature class.
MapUnitPolys	This polygon feature class represents the geologic map units as defined by the authors.
OrientationPoints	This feature class represents point locations in the quadrangle where structural measurements were made or were compiled from previous studies. These data are also contained in the bedding (strike and dip) spreadsheet described in more detail below.
WellPoints	This feature class represents point locations of water wells in the quadrangle. Includes data obtained by the authors from the Oregon Department of Water Resources (OWRD). These data are also contained in the Wells Points spreadsheet.

Table 11-2. Geodatabase tables.

Name	Description
DataSources	Data table that contains information about data sources used to compile the geology of the area.
DescriptionOfMapUnits	Data table that captures the content of the Description of Map Units, or equivalent List of Map Units and associated pamphlet text, included in a geologic map.
GeoMaterialDict	Data table providing definitions and hierarchy for GeoMaterial names prescribed by the GeMS database schema.
Glossary	Data table that contains information about the definitions of terms used in the geodatabase.

Geologic maps

This report is accompanied by three map plates displaying the geology for the Mill Creek area at a scale of 1:24,000 and geologic cross sections (**Figure 11-3**, **Figure 11-4**, **Figure 11-5**). The map plates were generated from detailed geologic data (scale of 1:8,000 or better) contained in the accompanying Esri™ format geodatabases.

Figure 11-3. Reproduction of the geologic map of the Brown Creek 7.5' quadrangle, Wasco County, Oregon (Plate 1). Plate dimensions are 36 by 42 inches, scale 1;24,000. See digital folder for map plate.

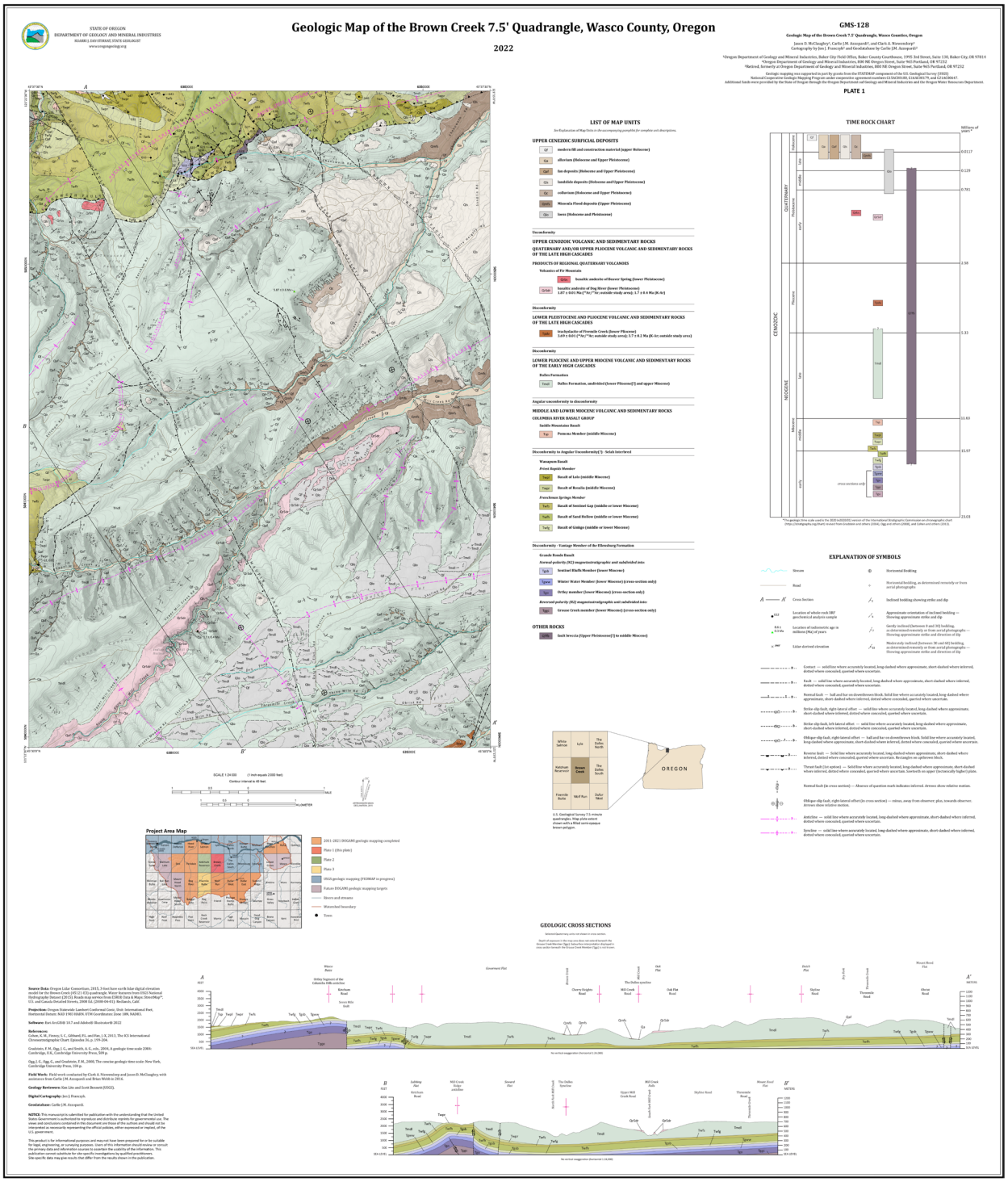

Figure 11-4. Reproduction of the geologic map of the Ketchum Reservoir 7.5' quadrangle, Hood River and Wasco counties, Oregon (Plate 2). Plate dimensions are 36 by 46 inches, scale 1;24,000. See digital folder for map plate.

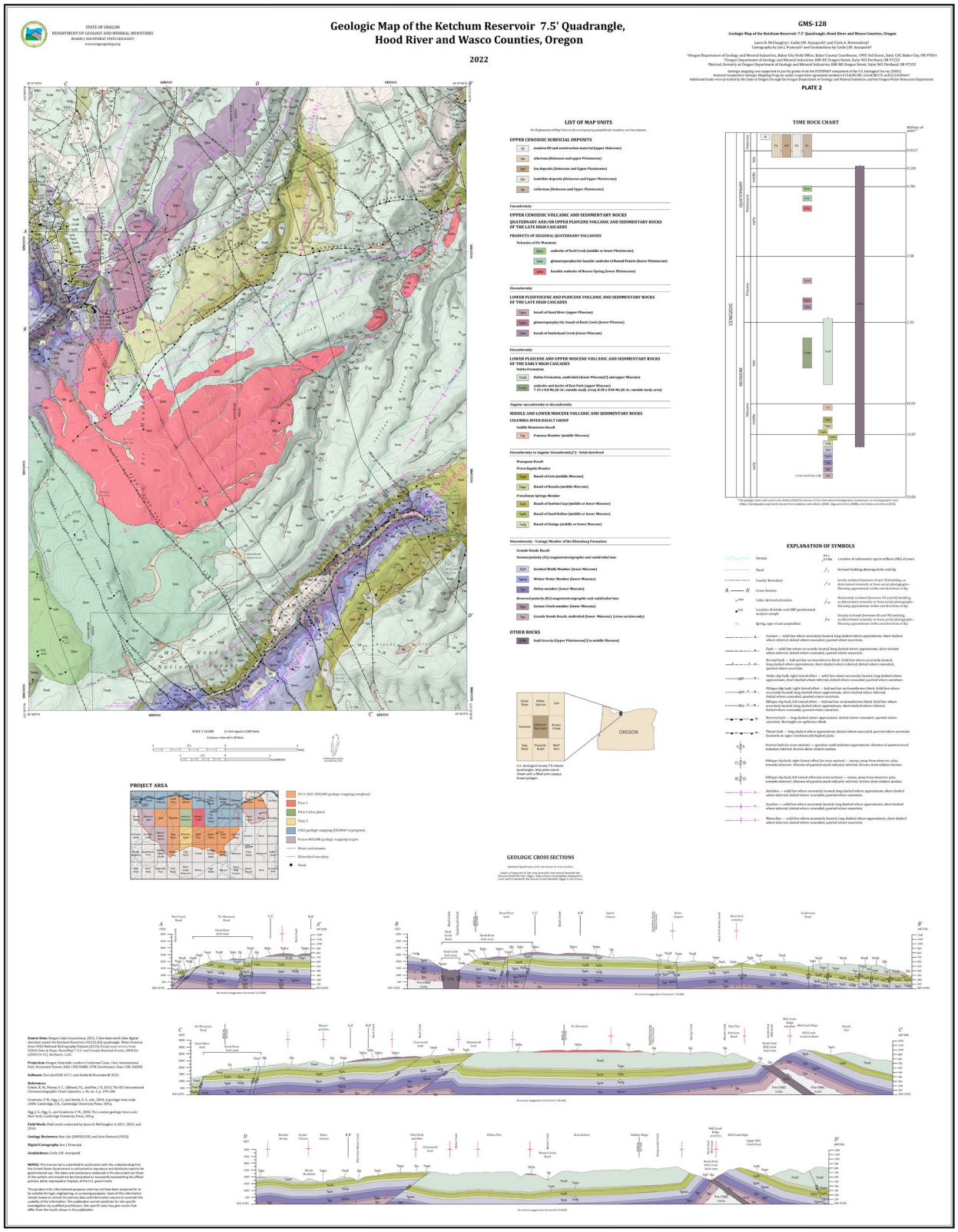

Figure 11-5. Reproduction of the geologic map of the Fivemile Butte and northern part of the Flag Point 7.5' quadrangles, Hood River and Wasco counties, Oregon (Plate 3). Plate dimensions are 37 by 44 inches, scale 1;24,000. See digital folder for map plate.

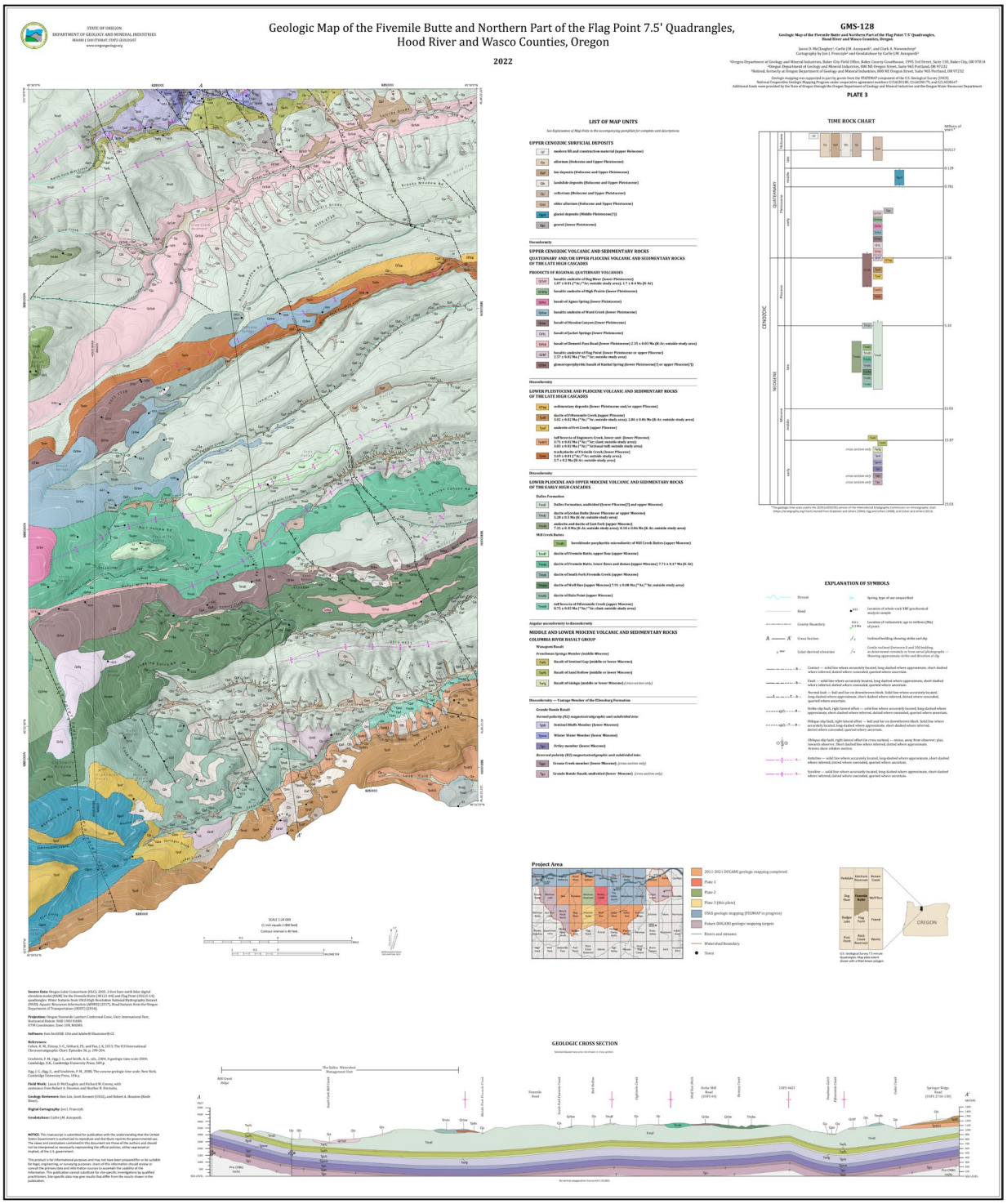

11.2 Methods

Geochemical analytical methods

Geologic mapping in the Mill Creek area was supported by 273 X-ray fluorescence (XRF) geochemical analyses of whole-rock samples. Whole-rock geochemical samples were prepared and analyzed by XRF at the Washington State University GeoAnalytical Lab, Pullman, Washington, and at the Franklin and Marshall X-ray laboratory, Lancaster Pennsylvania. Analytical procedures for the Washington State University GeoAnalytical Lab are described by Johnson and others (1999) and are available online at https://environment.wsu.edu/facilities/geoanalytical-lab/technical-notes/; analytical procedures for the Franklin and Marshall X-ray laboratory are described by Boyd and Mertzman (1987) and Mertzman (2000), and are available online at https://www.fandm.edu/earth-environment/laboratory-facilities/xrf-and-xrd-lab. Samples denoted by lab abbreviation WSU were analyzed at Washington State University; samples denoted by lab abbreviation FM were analyzed at Franklin and Marshall College. Descriptive rock unit names for igneous rocks are based on normalized major element analyses plotted on the total alkalis ($Na_2O + K_2O$) versus silica (SiO_2) diagram (TAS) of Le Bas and others (1986), Le Bas and Streckeisen (1991), and Le Maitre and others (1989, 2002). New and compiled XRF geochemical analyses are included in each of the geodatabases:

- BC2024.gdb,
- KR2024.gdb,
- FBFP2024.gdb,

and in separate open file formats.

Table 11-3 describes the fields listed in the databases. The locations of all geochemical samples are given in five coordinate systems: UTM Zone 10 (datum = NAD 27, NAD 83, units =meters), Geographic (datum = NAD 27, NAD 83, units = decimal degrees), and Oregon Lambert (datum = NAD 83, HARN, units = international feet). Notes for spreadsheet: -9 equals no data for numerical fields for analytical data; nd equals no data in text fields; na equals information not applicable for text fields; samples shown with an "R" (e.g., 356 MCBJ 16R) are a repeat analysis of a single sample.

Table 11-3. Geochemical database spreadsheet columns.

Field	Description
Type	The geochemical method used by laboratory that analyzed the sample – e.g., XRF, ICP-MS
FieldSampleID	Unique alpha-numeric id applied to the sample – e.g., 21 MCBJ 16.
AlternateSampleID	Unique alpha-numeric id applied to the sample – e.g., 21 MCBJ 16.
Symbol	References a symbol in the GeMS style file – e.g., 31.21.
Label	A unique number assigned to the sample for cartographic purposes – e.g., G1.
LocationConfidenceMeters	Radius in meters of positional uncertainty envelope for the observation locale. Null values not permitted. Recommended value is -9 if value is not otherwise available.
PlotAtScale	Cartographic map scale or larger that the observation or analysis should be plotted at. Value is scale denominator.
Quadrangle	The USGS 7.5' quadrangle in which the sample is located – e.g., Brown Creek.
Elevation	Elevation of data location in feet – e.g., 22.
MapUnit	Map unit from which the analyzed sample was collected – e.g., Tpdv.
MaterialAnalyzed	Type of material analyzed – e.g., whole rock.
TASLithology	Rock name assigned based on the total alkalis ($Na_2O + K_2O$) versus silica (SiO_2) diagram (TAS) of Le Bas and others (1986), Le Bas and Streckeisen (1991), and Le Maitre and others (1989) – e.g., basalt.
MajorElements	SiO_2, Al_2O_3, TiO_2, FeOTotal, MnO, CaO, MgO, K_2O, Na_2O, P_2O_5. as oxides in wt. percent.
TraceElements	Ni, Cr, Sc, V, Ba, Rb, Sr, Zr, Y, Nb, Ga, Cu, Zn, Pb, La, Ce, Th, Nd, U, Cs, Co, Hf, Sm, Eu, Yb, Lu. In ppm.
TotalInitial	Original analytical total as reported by the lab.
LossOnIgnition	Value for loss on ignition as reported by the laboratory.
FE2O3	Iron (III) oxide or ferric oxide reported in original analysis.
FeO	Iron (II) oxide or ferrous oxide reported in original analysis.
UTMNorthingNAD27	Meters north in NAD 27 UTM projection, zone 10.
UTMEastingNAD27	Meters east in NAD 27 UTM projection, zone 10.
LatitudeNAD27	Latitude in NAD 27 geographic coordinates.
LongitudeNAD27	Longitude in NAD 27 geographic coordinates.
UTMNorthingNAD83	Meters north in NAD 83 UTM projection, zone 10.
UTMEastingNAD83	Meters east in NAD 83 UTM projection, zone 10.
LatitudeNAD83	Latitude in NAD 83 geographic coordinates.
LongitudeNAD83	Longitude in NAD 83 geographic coordinates.
Northing83HARN	Feet north in Oregon Lambert NAD 83, HARN, international feet.
Easting83HARN	Feet east in Oregon Lambert NAD 83, HARN, international feet.
LocationSourceID	Unique data source from which the data were obtained – e.g., McClJD2022.
AnalysisSourceID	Foreign key to DataSources. Identifies source of analytical data for this sample. Null values not permitted – e.g., WSU.
Notes	Special information about certain samples – e.g., alteration.
GeochemPoints_ID	e.g., GCM01
Display	This is a flag for points displayed on the plate.

Geochronology analytical methods

Six K-Ar ages, originally published by Bela (1982), Bunker and others (1982), Fiebelkorn and others (1983), Anderson (1987), Sherrod and Scott (1995), Conrey and others (1996), and Gray and others (1996) are included with the publication. No new radiometric ages were obtained in the map area. Geochronological data are included in the geodatabases:

- BC2024.gdb,
- FBFP2024.gdb,

and in separate open file formats.

Table 11-4 describes the fields listed in the databases. The location of each radiometric age is given in five coordinate systems: UTM Zone 10 (datum = NAD 27, NAD 83, units = meters), Geographic (datum = NAD 27, NAD 83, units = decimal degrees), and Oregon Lambert (datum = NAD 83, HARN, units = international feet). Notes for spreadsheet: -9 equals no data for numerical fields for analytical data; nd equals no data in text fields; na equals information not applicable for text fields.

Table 11-4. Geochronology database spreadsheet columns.

Field	Description
Type	The geochronological method – e.g., $^{40}Ar^{39}Ar$, K-Ar, radiocarbon, mineral - whole-rock Rb-Sr isochron, etc.) used to estimate the age.
FieldSampleID	Unique alpha-numeric id applied to the sample – e.g., 383 MCBJ 16.
AlternateSampleID	Unique alpha-numeric id applied to the sample – e.g., 383 MCBJ 16.
MapUnit	Map unit from which the analyzed sample was collected.
Symbol	References a symbol in the GeMS style file.
Label	Radiometric age of sample with error – e.g., 3.83 ± 0.02 Ma
LocationConfidenceMeters	Radius in meters of positional uncertainty envelope for the observation locale. Null values not permitted. Recommended value is -9 if value is not otherwise available.
PlotAtScale	Cartographic map scale or larger that the observation or analysis should be plotted at. Value is scale denominator.
MaterialAnalyzed	Type of material analyzed – e.g., amphiboles, plagioclase.
NumericAge	Interpreted (preferred) age calculated from geochronological analysis, not necessarily the date calculated from a single set of measurements.
AgePlusError	Plus error in age determination in thousands of years.
AgeMinusError	Minus error in age determination in thousands of years.
ErrorMeasure	Measure of error whose values are recorded in AgePlusError and AgeMinusError fields.
AgeUnits	Values = years, Ma, ka, radiocarbon ka, calibrated ka, etc.
UTMNorthingNAD27	Meters north in NAD 27 UTM projection, zone 10.
UTMEastingNAD27	Meters east in NAD 27 UTM projection, zone 10.
LatitudeNAD27	Latitude in NAD 27 geographic coordinates.
LongitudeNAD27	Longitude in NAD 27 geographic coordinates.
UTMNorthingNAD83	Meters north in NAD 83 UTM projection, zone 10.
UTMEastingNAD83	Meters east in NAD 83 UTM projection, zone 10.
LatitudeNAD83	Latitude in NAD 83 geographic coordinates.
LongitudeNAD83	Longitude in NAD 83 geographic coordinates.
Northing83HARN	Feet north in Oregon Lambert NAD 83, HARN, international feet.
Easting83HARN	Feet east in Oregon Lambert NAD 83, HARN, international feet.
StationsID	Foreign key to Stations point feature class.
LocationSourceID	Unique data source from which the data were obtained; e.g., McClJD2022.
AnalysisSourceID	Foreign key to DataSources. Identifies source of analytical data for this sample. Null values not permitted – e.g., OSU.
Notes	Special information about certain samples – e.g., alteration.
GeochronPoints_ID	e.g., GCR1

Natural remanent magnetization (magnetic polarity) methods

Field measurements of natural remanent magnetization (the magnetic field of a sample measured when induced magnetic fields are absent or zeroed out by probe; Butler, 1992) were determined from strongly magnetized lava flows exposed in the Mill Creek area during the course of this study in order to distinguish between flow units with normal and reversed magnetic polarity. Magnetic polarity also serves as a check on the permissible age of isotopically dated samples, when compared to the paleomagnetic time scale of Cande and Kent (1992). This method of constraining isotopic ages by magnetic polarity determinations is most effective when the analytical error is less than 0.20 million years. Larger errors reported for isotopic ages may overlap so many polarity subchrons that no constraint is provided by knowing a samples magnetic polarity. Magnetic polarity values reported were determined using a MEDA, Inc. μMag handheld digital fluxgate magnetometer (**Figure 11-6**). The measured point data are included in the geodatabases:

- BC2024.gdb,
- KR2024.gdb,
- FBFP2024.gdb,

and in separate open file formats.

Table 11-5 describes the fields listed in the databases. The locations of magnetics data are given in five coordinate systems: UTM Zone 10 (datum = NAD 27, NAD 83, units = meters), Geographic (datum = NAD 27, NAD 83, units = decimal degrees), and Oregon Lambert (datum = NAD 83, HARN, units = international feet). Notes for spreadsheet: -9 equals no data for numerical fields for analytical data; nd equals no data in text fields; na equals information not applicable for text fields.

The natural remanent magnetization (magnetic polarity) of strongly magnetized lavas was determined using the following method:

- A north-pointing arrow and near horizontal line were drawn on and around (to the extent possible) an approximately fist-sized equidimensional sample that was then removed from the outcrop (**Figure 11-6a**). Next, a line is drawn from the south end of the sample to the north end at an angle approximating the magnetic inclination (approximately equivalent to the latitude). For the study area, a line was drawn inclined at approximately 45° down to the north. This line gives the approximate orientation of the magnetic pole of the sample.
- The magnetometer was placed on the most level ground available in a relatively magnetically clean area (**Figure 11-6b**). The probe was then placed in a fixed position in the horizontal plane and rotated to null the local magnetic field (μMag reads zero). This procedure was done incrementally beginning with minimum range sensitivity (2,000 mG [milliGauss]), increasing the sensitivity (20 mG) and re-rotating the probe until maximum sensitivity was reached. Magnetic polarity was then checked with the north end of a locked compass needle. Total field value will decrease when the compass needle is moved horizontally toward and remains parallel to the probe.
- The polarity of a sample was determined by placing the oriented sample in a path parallel to the probe. The inclined north-directed line drawn to represent the approximate magnetic pole of the sample was held horizontally (approximately) with the north end facing toward the probe at a distance of at least 10 times further than the measurement distance. A reading was then determined with the sample absent from the probe. The sample was then moved to a point (typically within 1 to 2 cm) toward the probe in order to cause a change of at least several times greater than the minimum resolution of the magnetometer (**Figure 11-6b**). A decrease

in the total field value indicated normal-polarity (N); an increase in total field value indicated reversed-polarity (R).

- The sample was then rotated backward (top away from the probe) about a horizontal axis approximately 45° to see if field strength increased as the sample's inclined magnetic field was rotated into parallel with the probe.
- The polarity of two to ten representative samples from different portions of an outcrop or from different outcrops was determined to verify the repeatability of results. Erratic results, due to re-magnetization resulting from lighting strikes, obscure post-emplacement alteration, or aberrant declination and inclination are reported as indeterminate (I). Reversed readings should take precedence over normal readings in assigning polarity. Re-magnetization will more likely reset the remnant magnetism to the present-day normal polarity.

Figure 11-6. **Procedure for determining natural remanent magnetism of lavas. (a) Ideal sample is selected and oriented in outcrop. North arrow is drawn on upper surface; horizontal lines are drawn around the exposed edges of the sample. Fist-sized sample is then removed. (b) Magnetometer probe is placed in a fixed position in the horizontal plane and rotated to null the local magnetic field. Sample polarity is determined by moving the oriented sample into the path of the probe. Photo credits: Jason McClaughry, 2011.**

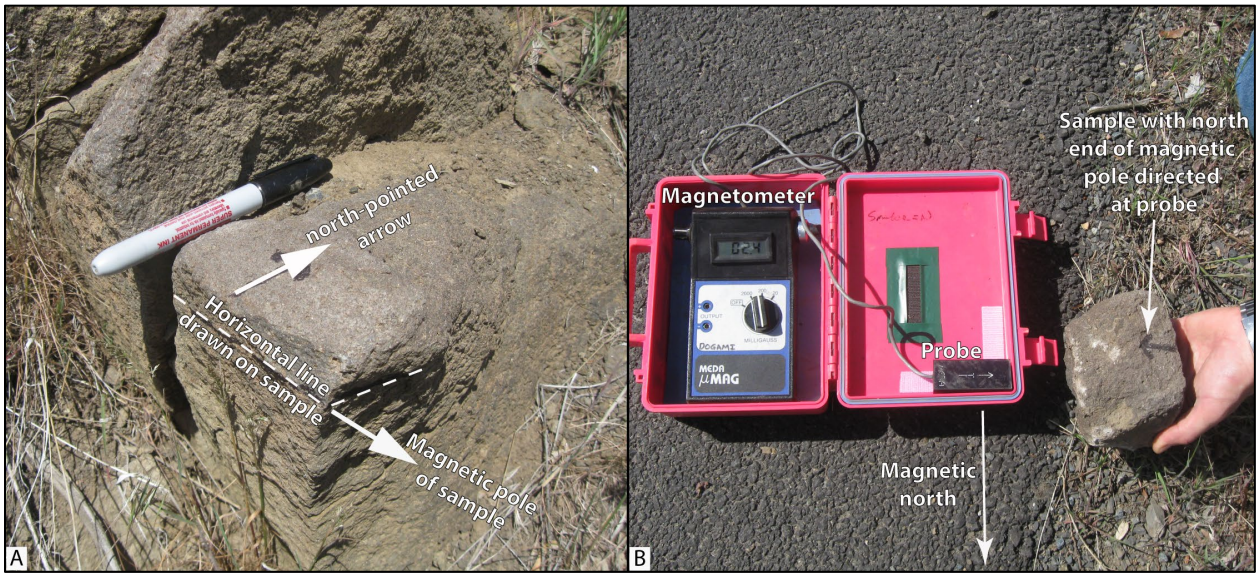

Table 11-5. Magnetic polarity database spreadsheet columns.

Field	Description
Type	The method of measurement – e.g., Digital Portable Fluxgate
FieldSampleID	Unique alpha-numeric id applied to the sample – e.g., 18 MCBJ 16.
AlternateSampleID	
NaturalRemanentMagnetization	Natural remanent magnetization of sample as determined from a portable fluxgate magnetometer. Normal, reversed, indeterminate.
MapUnit	Map unit from which the analyzed sample was collected.
Symbol	References a symbol in the GeMS style file.
Label	<Null>
LocationConfidenceMeters	Radius in meters of positional uncertainty envelope for the observation locale. Null values not permitted. Recommended value is -9 if value is not otherwise available.
PlotAtScale	Cartographic map scale or larger that the observation or analysis should be plotted at. Value is scale denominator.
Quadrangle	The USGS 7.5' quadrangle in which the sample is located – e.g., Brown Creek.
Elevation	Elevation of sample location in feet – e.g., 1928.
UTMNorthingNAD27	Meters north in NAD 27 UTM projection, zone 10.
UTMEastingNAD27	Meters east in NAD 27 UTM projection, zone 10.
LatitudeNAD27	Latitude in NAD 27 geographic coordinates.
LongitudeNAD27	Longitude in NAD 27 geographic coordinates.
UTMNorthingNAD83	Meters north in NAD 83 UTM projection, zone 10.
UTMEastingNAD83	Meters east in NAD 83 UTM projection, zone 10.
LatitudeNAD83	Latitude in NAD 83 geographic coordinates.
LongitudeNAD83	Longitude in NAD 83 geographic coordinates.
Northing83HARN	Feet north in Oregon Lambert NAD 83, HARN, international feet.
Easting83HARN	Feet east in Oregon Lambert NAD 83, HARN, international feet.
LocationSourceID	Unique data source from which the data were obtained; e.g., McClJD2022.
AnalysisSourceID	Foreign key to DataSources. Identifies source of analytical data for this sample. Null values not permitted – e.g., OSU.
Notes	Special information about certain samples – e.g., alteration.
MagneticPoints_ID	e.g., MGP001

Orientation Points

Orientation measurements of inclined bedding were taken in the Mill Creek area during the course of this study by traditional compass and clinometer methods. Additional structural measurements were determined from interpretation of lidar imagery. DOGAMI has developed a routine and model in Esri ArcGIS™ Model Builder to calculate three-point solutions for lidar-derived bedding (Duda and others, 2018, 2019). The modeling process incorporates the use of 1) a 1-m lidar-derived DEM (digital elevation model); 2) the registration of three non-collinear points picked along the trace of a geological plane or contact discernible from a 1-m lidar DEM; 3) updating these points with their lidar-derived elevation values; and 4) creating a TIN (triangular irregular network) facet of the three points. The aspect of the TIN facet is equivalent to the dip direction, and the slope corresponds to the dip (0 to 90 degrees). The strike is then determined from the dip direction, subtracting or adding 90 degrees on the basis of the right-hand rule (described in below).

The factors influencing the certainty of lidar-derived bedding are the subjectivity of the digitizer and the clarity of the feature presumed to be indicative of bedding. To improve the clarity of lidar visualization, lidar-derived bedding was compiled using both a hillshade and slopeshade image, each at 50 percent transparency, draped over a Sky-View Factor (SVF) image. Sky-View Factor images are enhanced 1-m lidar DEMs, processed using the Sky-View Factor computation tool. The Sky-View Factor computation tool is part of the RVT, open-source processing software produced by the Institute of Anthropological and Spatial Studies (http://iaps.zrc-sazu.si/en) at the Research Centre of the Slovenian Academy of Sciences and Arts (ZRCSAZU), to help visualize raster elevation model datasets. Sky-View visualizes hillshade models using diffuse illumination, overcoming the common problem of direct illumination, which can obscure linear objects that lie parallel to the direction of the light source and saturation of shadow areas. This brings improvements in detection of linear structures because the method exposes edges and holes (Zakšek and others, 2011). DOGAMI's visualization routine, combining a lidar-derived hillshade, slopeshade, and SVF imagery, helps illuminate shadows and amplifies the edges/ridges related to bedding features. Where possible, aerial photography, combined with a contextual knowledge of the geology of the area, was used to verify bedding features interpreted from lidar.

Orientation points are reported in both quadrant format (e.g., N30°W, 15°NE) and azimuthal format using the right-hand rule (e.g., 330°, 15°NE, American convention). Field-measured bedding is coded by its appropriate Federal Geographic Data Committee reference number for geologic map symbolization. The measured point data are included in the geodatabases:

- BC2024.gdb,
- KR2024.gdb,
- FBFP2024.gdb,

and in separate open file formats.

Table 11-6 describes the fields listed in the databases. The locations of these point data are given in five coordinate systems: UTM Zone 10 (datum = NAD 27, NAD 83, units = meters), Geographic (datum = NAD 27, NAD 83, units = decimal degrees), and Oregon Lambert (datum = NAD 83, HARN, units = international feet). Strike and dip symbols can be properly drawn by the Esri ArcMap™ product by opening the layer properties, categorizing by type, choosing the appropriate symbol, and rotating the symbol based on the "Strike_Azi" field. (The Advanced button allows you to select the rotation field.) The rotation style should be set to geographic in order to maintain the right-hand rule property. Azimuths are given in true north; an additional clockwise correction of about 1.6 degrees is needed to plot strikes and dips properly on the Oregon Lambert conformal conic projection in this area. Notes for spreadsheet: nd, no data.

Table 11-6. Orientation points database spreadsheet columns.

Field	Description
Type	Type of geologic structure from which feature was determined – e.g., Inclined bedding.
Azimuth	Strike or trend, measured in degrees clockwise from geographic North. Values limited to range 0-360. Use right-hand rule (dip is to right of azimuth direction). Horizontal planar features may have any azimuth – e.g., 20.
Inclination	Dip or plunge, measured in degrees down from horizontal. Values limited to range -90 to 90. Types defined as horizontal (e.g., horizontal bedding) have Inclination = 0. Null values not Data type=float – e.g., 45.
StrikeQuadrant	Strike direction of the inclined plane, stated in a north-directed quadrant format – e.g., N35E
DipQuadrant	Amount of dip, degrees from horizontal, with direction – e.g., 45SE
Symbol	References a symbol in the GeMS style file – e.g., 6.40.
Label	Amount of dip, degrees from horizontal – e.g., 45.
LocationConfidenceMeters	Radius in meters of positional uncertainty envelope for the observation locale. Null values not permitted. Recommended value is -9 if value is not otherwise available.
IdentityConfidence	Specifies confidence that observed structure is of the type specified; e.g., 'certain', 'questionable', 'unspecified'.
OrientationConfidenceDegrees	Estimated circular error, in degrees – e.g., 20.
PlotAtScale	Cartographic map scale or larger that the observation or analysis should be plotted at. Value is scale denominator.
Quadrangle	The USGS 7.5' quadrangle in which the sample is located – e.g., Brown Creek.
Elevation	Elevation of data location in feet – e.g., 22.
MapUnit	Map unit from which the analyzed sample was collected.
UTMNorthingNAD27	Meters north in NAD 27 UTM projection, zone 10.
UTMEastingNAD27	Meters east in NAD 27 UTM projection, zone 10.
LatitudeNAD27	Latitude in NAD 27 geographic coordinates.
LongitudeNAD27	Longitude in NAD 27 geographic coordinates.
UTMNorthingNAD83	Meters north in NAD 83 UTM projection, zone 10.
UTMEastingNAD83	Meters east in NAD 83 UTM projection, zone 10.
LatitudeNAD83	Latitude in NAD 83 geographic coordinates.
LongitudeNAD83	Longitude in NAD 83 geographic coordinates.
Northing83HARN	Feet north in Oregon Lambert NAD 83, HARN, international feet.
Easting83HARN	Feet east in Oregon Lambert NAD 83, HARN, international feet.
LocationSourceID	Unique data source from which the data were obtained – e.g., McClJD2022.
OrientationSourceID	Unique data source from which the data were obtained – e.g., McClJD2022.
Notes	Special information about the point – e.g., lidar derived.
OrientationPoints_ID	Primary key – e.g., ORP001.
Display	This is a flag for points displayed on the plate.
PTTYPE	e.g., Bedding
RuleID1	Rule ID used for cartographic representation – e.g., 6.40.

Well Points

The well points database is derived from written drillers' logs provided by Oregon Department of Water Resources (OWRD). Well logs vary greatly in completeness and accuracy, therefore locally limiting the utility of subsurface interpretations based upon these data. Water-well logs, compiled and used for interpretation during the course of this study were not field located. The approximate locations were estimated using tax lot maps, street addresses (coordinates obtained from Google Earth™), and aerial photographs to plot locations on the map. The accuracy of the locations ranges widely, from errors of one-half mile possible for wells located only by section and plotted at the section centroid to a few tens of feet for wells located by address or tax lot number on a city lot with bearing and distance from a corner. At each mapped location the number of the well log is indicated. This number can be combined with the first four letters of the county name (e.g., WASC 5473), to retrieve an image of the well log from the OWRD website. The point data are included in the geodatabases:

- BC2024.gdb,
- KR2024.gdb,
- FBFP2024.gdb,

and in separate open file formats.

Table 11-7 and **Table 11-8** explain the fields in the databases. The locations of water-well point data are given in six coordinate systems: UTM Zone 10 (datum = WGS 84, NAD 27, NAD 83, units = meters), Geographic (datum = NAD 27, NAD 83, units = decimal degrees), and Oregon Lambert (datum = NAD 83, HARN, units = international feet).

Well intervals listed in the well log database sometimes alternate between consolidated and unconsolidated lithologies and may be listed as alternating between bedrock and surficial geologic units. This may occur where bedrock units are soft, where paleosols or weak zones lie within bedrock, or where cemented or partly cemented zones alternate with unconsolidated zones in surficial deposits.

Table 11-7. Well log database lithologic abbreviations.

Lithologic abbreviations (alphabetical by group)

UNCONSOLIDATED SURFICIAL UNITS	
Abbreviation	**Description**
a	ash
bd	boulders
c	clay
ch	clay, hard (often logged as claystone but probably not bedrock)
g	gravel
gc	cemented gravel
gs	gravel and sand (also sandy gravel)
m	mud
s	sand
sg	sand and gravel (also gravelly sand)
st	silt
Rock, sedimentary	
bc	breccia
cg	conglomerate
cs	claystone
sh	shale
ss	sandstone
Rock, igneous	
an	andesite
b	basalt
ba	basaltic andesite
cd	cinders
da	dacite
pu	pumice
gr	granite
l	lava
r	rhyolite
sc	scoria
t	tuff
v	volcanic, undivided
vb	volcanic breccia
Other	
af	artificial fill
cl	coal (lignite)
dg	decomposed granite
o	other (drillers unit listed in notes column of spreadsheet)
rk	rock
sl	soil
u	unknown (typically used where a well has been deepened)

Table 11-8. Well log database spreadsheet columns.

Field	*Description and Example
Type	Type of well located; e.g., well used for domestic-water supply, well used for irrigation-water supply, drill hole for hydrocarbon exploration or exploitation- Showing name and number.
Symbol	References a symbol in the GeMS style file – e.g., 26.1.25.
Label	A unique label identifying the well, if applicable – e.g., Federal 1-10.
IdentityConfidence	Specifies confidence that observed structure is of the type specified; e.g., 'certain', 'questionable', 'unspecified'.
LocationConfidenceMeters	Radius in meters of positional uncertainty envelope for the observation locale. Null values not permitted. Recommended value is -9 if value is not otherwise available.
PlotAtScale	Cartographic map scale or larger that the observation or analysis should be plotted at. Value is scale denominator.
TownshipRangeSection	Two digits for township, two digits for range, and two for section; negative if township is south of Willamette baseline. Exception for township and range if they contain a decimal – e.g., −2132.503.
County	Wasco County – e.g., WASC.
Grid	Well log number for wells. Wells in Wasco County preceded by acronym WASC – e.g., WASC53799.
WellElevation	Wellhead elevation in feet as given by Google Earth™ at corresponding WGS 84 location. e.g., 1978.
LocatedBy	Google Earth™ elevation for cursor location at a given address – e.g., Google. Google Earth™ elevation at house in vicinity of given address – e.g., House. Pad identifying approximate well location, visible in air photo – e.g., Pad. Approximate tax lot centroid or other best guess for well location using a combination of tax lot maps and aerial photographs – e.g., Tax lot. Owner name – e.g., Owner. Address of well listed on OWRD Startcard. Wells located by OWRD using handheld GPS – e.g., OWRD. GPS coordinates of wellhead included with well log – e.g., GPS. Approximate quarter-quarter-quarter-section centroid – e.g., QQQ. Approximate quarter-quarter-section centroid – e.g., QQ. Approximate quarter-section centroid – e.g., Q. Approximate fit to sketch map included with well log – e.g., map.
Lithology	Best interpretation of driller's log using abbreviations above – e.g., g.
Base	Record base of driller's interval or, if lithology abbreviation would not change, similar intervals, in feet below wellhead – e.g., 17.
Top	Calculated top of driller's interval or similar intervals, in feet below wellhead – e.g., 14.
TopElevation	Calculated elevation at top of driller's interval, or similar intervals, in feet above sea level – e.g., 86.
BaseElevation	Calculated elevation at base of driller's interval, or similar intervals, in feet above sea level – e.g., 83.
BedrockLithology	Lists bedrock lithologies, when encountered, abbreviations listed above – e.g., b.
BedrockElevation	Calculated elevation at which bedrock or soil over bedrock was first encountered, in feet above sea level – e.g., 1924.
Tax lot	Tax lot number. Where it is determined that a tax lot number is used more than once in the section then the appropriate subdivision of the section is indicated in the notes field – e.g., 800.
Color	Color of interval as reported by the well driller – e.g., green.
MapUnit	Geologic unit interpreted in subsurface based on drillers log and designated by map unit label used in accompanying geodatabase. Intervals labeled "suna" (surface unit not applicable) are those where the lithology as interpreted by the original drillers' log do not correspond; also denotes intervals in the subsurface where a precise unit label cannot be applied – e.g., Tb.
Quadrangle	The USGS 7.5' quadrangle in which the sample is located – e.g., Fivemile Butte.
UTMNorthingWGS84	Meters north in WGS84 UTM projection, zone 10.
UTMEastingWGS84	Meters east in WGS84 UTM projection, zone 10.
UTMNorthingNAD27	Meters north in NAD 27 UTM projection, zone 10.
UTMEastingNAD27	Meters east in NAD 27 UTM projection, zone 10.
LatitudeNAD27	Latitude in NAD 27 geographic coordinates.
LongitudeNAD27	Longitude in NAD 27 geographic coordinates.
UTMNorthingNAD83	Meters north in NAD 83 UTM projection, zone 10.
UTMEastingNAD83	Meters east in NAD 83 UTM projection, zone 10.

LatitudeNAD83	Latitude in NAD 83 geographic coordinates.
LongitudeNAD83	Longitude in NAD 83 geographic coordinates.
Northing83HARN	Feet north in Oregon Lambert NAD 83, HARN, international feet.
Easting83HARN	Feet east in Oregon Lambert NAD 83, HARN, international feet.
LocationSourceID	Unique data source from which the data were obtained – e.g., OWRD2020.
WellSourceID	Unique data source from which the data were obtained – e.g., OWRD2020.
Notes	Notes about the stratigraphic interval as originally described by the well driller or observer.
WellPoints_ID	Primary key – e.g., WLP593
PTTYPE	e.g., Water Well, Oil and Gas.

*Well location given in six coordinate systems calculated by reprojecting original WGS 84 UTM, zone 10 locations.